UNIVERSITÀ DEGLI STUDI DI UDINE

Dottorato di Ricerca in Scienze e Biotecnologie Agrarie

Ciclo XXVIII

Coordinatore: prof. Mauro Spanghero

TESI DI DOTTORATO DI RICERCA

EFFECT OF WATER DEFICIT ON FRUIT METABOLISM IN WHITE AND RED GRAPE VARIETIES

DOTTORANDO

Stefania Savoi

SUPERVISORI

Prof. Enrico Peterlunger

Dr. Fulvio Mattivi

Dr. Simone Diego Castellarin

ANNO ACCADEMICO 2014/2015

EFFECT OF WATER DEFICIT ON FRUIT METABOLISM IN WHITE AND RED GRAPE VARIETIES

Stefania Savoi

Prof. Enrico Peterlunger

Department of Agrifood, Environmental and Animal Sciences
Università degli Studi di Udine, Udine, Italy

Dr. Fulvio Mattivi

Department of Food Quality and Nutrition
Research and Innovation Center
Fondazione Edmund Mach, San Michele all'Adige, Italy

Dr. Simone Diego Castellarin

Wine Research Center
The University of British Columbia, Vancouver, Canada

With Wings And Roots

CONTENT

Abstract

Plants are sessile organisms and often they have to cope with environmental stresses (abiotic factors) such as drought, cold, heat, extreme light, excessive soil salinity, or several combinations of them. The genotype x environment (GxE) interaction is the source of the main variability in the responses to these constrains. Among the abiotic factors that can influence plant physiology, drought is the most relevant because it can influence plant growth and yield, and affects fruits composition. Secondary metabolism contributes to the adaptation of a plant to its environment. In fruit crops such as grapevine (*Vitis vinifera* L.), secondary metabolism also largely determines fruit quality. Grapevine is considered a drought-tolerant plant and traditionally is not irrigated, especially in Europe. Mediterranean climate, with warm and dry summers and cold and wet winters, is considered optimal for viticulture. Climate change is predicted to exacerbate drought events in several viticultural areas, potentially affecting the accumulation of secondary metabolites in the grapes, thus affecting wine quality.

We adopted a multidisciplinary approach that considered a two-years field trial, high-throughput transcripts profiling (RNA-sequencing) and large-scale targeted metabolite analyses to investigate the effect of drought events on the berry metabolism during fruit development and ripening in white and red grape varieties. An open field experiment was therefore conducted on Tocai friulano (white grape variety) and Merlot (red grape variety) vines in 2011 and 2012, in a North Italian viticultural area characterized by transient drought events during the summer. Two irrigation treatments were applied to the vines: (i) control vines were weekly irrigated, in order to keep their stem water potential (a sensitive indicator of grapevine water status) between -0.4 and -0.6 MPa; (ii) deficit irrigated vines were not irrigated from fruit set to harvest except in case of acute water deficit. Merlot vines were sheltered with an open-sided transparent cover at the beginning of the seasons, while Tocai friulano vines were cultivated without any cover and hence subjected to the natural precipitations. In Merlot, deficit irrigated vines experienced water deficit from 40-50 days after anthesis in both seasons. In Tocai friulano, deficit irrigated vines manifested a late deficit (from 80-90 days after anthesis) in 2011, and a prolonged water deficit from early stages of fruit development (from 30-40 days after anthesis) to harvest in 2012. For both varieties, berries were sampled for transcript and metabolite analyses during berry development and ripening. Furthermore, at harvest, grapes were microvinificated and wines composition was evaluated focusing on the secondary metabolites that largely contribute to the final color, taste, and aromatic features.

A large effect of water deficit on fruit secondary metabolism of the white grape variety Tocai friulano was observed in the season when the deficit occurred from early stages of berry development to harvest. In this particularly season, increased concentrations of phenylpropanoids, monoterpenes, and tocopherols were observed, while carotenoid and flavonoid accumulations were differentially modulated by water deficit accordingly to the berry developmental stage. In parallel, RNA sequencing analysis revealed that many key genes of the phenylpropanoid, flavonoid, and terpenoid pathways were modulated by water deficit indicating a transcriptional regulation of these specific pathways in the berry under drought.

The higher co-regulation of several terpenoid transcripts with monoterpene accumulation under water deficit and the enrichment of drought-responsive elements in the promoter region of many terpenoid genes highlight that drought can enhance the production of these flavour components in grapes with potential effects on wine composition and sensory features. The wines produced from grapes subjected to water deficit revealed a more pronounced accumulation of monoterpenes and C_{13}-norisoprenoids, and especially glycosidically-bound compounds. However, differences in the metabolic response between seasons suggest that the endurance of water deficit and the timing of application strongly impact this response.

In Merlot berries, the drought stress response encompassed both ABA-dependent and ABA-independent signal transduction pathways with several *VviAREB/ABFs*, *VvibZIP*, and *VviAP2/ERF-DREB* transcription factors that were up-regulated by water deficit at one or more developmental stages. These transcription factors can play critical roles in the drought response by modulating a large suite of genes. Analyses of the central and specialized berry metabolism was conducted both at the transcript and metabolite levels by investigating several metabolic pathways (glycolysis and sugar accumulation, tricarboxylic acid cycle and amino acid biosynthesis, phenylpropanoid, flavonoid, terpenes, carotenoids, and fatty acid degradation pathways). The study revealed that water deficit enhanced the accumulation of several osmoprotectants (proline, sucrose, and raffinose) and of secondary metabolites such as anthocyanins and C_5, C_7, C_8, and C_9 volatile organic compounds. Furthermore, a weighted gene co-expression network analysis clustered in a module several genes involved in the branched chain amino acids biosynthesis, phenylpropanoid and flavonoid pathways, and sugar derivative metabolism together with the transcription factors mentioned above involved in the drought-stress signal, indicating a putative role of these transcription factors on the regulation of the response of the fruit metabolism to drought in Merlot berries. The wines produced from grapes subjected to water deficit revealed a higher concentration of anthocyanins that determined higher color intensity and a bluer coloration of the wines.

A comparison between the two genotypes can be done only for the 2012 season, when levels and endurances of water deficit were similar between Tocai friulano and Merlot deficit irrigated vines. The data indicate that water deficit modulated the accumulation of several secondary compounds; however, the modulation of the secondary metabolism varied between cultivars indicating a genotype x environment interaction. In the Tocai friulano berry, water deficit specifically stimulated the synthesis of phenolic acids, such as gallic acid, ellagic acid, and caftaric acid, tocopherols, and monoterpenes, such as linalool, α-terpineol, nerol, and hotrienol. In Merlot, the response included an overproduction of anthocyanins, such as the tri-substituted delphinidin, petunidin, and malvidin both in the glycosylated and acylated form, and C_5, C_7, C_8 and C_9 volatile organic, such as 1-penten-3-ol, *(E)*-2-heptenal, *(E)*-2-octenal, 1-octen-3-ol, and nonanol. A common response between the two varieties included a higher accumulation of gallic acid, zeaxanthin, *(E)*-2-heptenal, *(E)*-2-octenal, 1-octen-3-ol, and nonanol in the berry. Furthermore, these results indicate that drought events can affect the composition and sensory features of white and red wines by increasing the accumulation of benzoic and cinnamic acids, pigments in the red grape variety and monoterpenes in the white grape variety.

Chapter 1

INTRODUCTION

Grapevine (*Vitis vinifera* L.) is one of the major fruit crop cultivated in the world with 7573 thousands of hectares of vineyards worldwide and a production of 73,7 million tons of grapes in 2014 of which 55% were used for wine-making, 35% as fresh grapes, 8% for raisin production and the remaining 2% for juices and other products. It is also economically relevant considering that the international trade in volume amounted to 104 million hectoliters along with a value of 26 billion Euros in 2014 with top world producer and exporter countries like, Italy France and Spain (from 'OIV Statistical Report on World Vitiviniculture' – 2015 release).

Grapevine is member of the *Vitaceae* family, genus *Vitis* that consists of ~ 60-70 species. Among them, predominantly *Vitis vinifera* L. gained, over time, agronomic characteristics like good fruit quality that made it suitable for fresh consumption and for wine production even though other species such as for example *Vitis labrusca* had some popularity in the US and it is used for the production of rather important grapes (Concord, Catawba, Niagara) and in several hybrids (Isabella, etc.). Other species such as the American *Vitis berlandieri*, *Vitis riparia* and *Vitis rupestris* were selected in viticulture as rootstock due to their resistance to the phylloxera and fungal diseases and as genes reservoir for inter-breeding purposes (Keller, 2015). The beginning of the domestication process of *Vitis vinifera* subsp. *vinifera*, from its wild ancestor *Vitis vinifera* subsp. *sylvestris*, finds archaeological records in the Near East dated back to the Neolithic Era. Evidences based on chloroplastic microsatellite polymorphisms analysis report a second independent domestication center in the western Mediterranean basin from local wild *Vitis vinifera* subsp. *sylvestris*. In both ways the major advantages of the domestication process were the switch from dioecy to self-pollinating hermaphroditism, an increase in seed and berry size and a higher sugar accumulation (Arroyo-García et al., 2006; This et al., 2006; Myles et al., 2011). Nowadays, numerous grapevine varieties (or cultivars) exist. Many of them were obtained through sexual reproduction by crossing (mainly intraspecific hybrids) and then perpetuated through vegetative propagation by cuttings preserving in this way the selected traits and the high level of heterozygosity of grapevine. Somatic mutations greatly added variability within clones of a variety and contributed to the development of new phenotypes (Pelsy, 2010). Examples can be found in the variations of berry color. It is thought that berry grape was in the first place black-skinned. An insertion of a jumping gene in the promoter region of a gene, *VviMybA1* (*VIT_02s0033g00410*), plus a two non-consecutive mutation in the neighboring one, *VviMybA2* (*VIT_02s0033g00390*), which both trigger the anthocyanin biosynthesis, led to the white-skinned phenotype (Walker et al., 2007).

Grapevine genome has been sequenced in 2007 by the French-Italian Public Consortium (Jaillon et al., 2007) and by the Italian-American Collaboration (Velasco et al., 2007). The first plant genome sequenced was the genome of the model *Arabidopsis thaliana* (Arabidopsis Genome Initiative, 2000), followed by rice, *Oryza sativa* subsp. *indica* and subsp.

japonica (Goff et al., 2002; Yu et al., 2002) and poplar, *Populus trichocarpa*, (Tuskan et al., 2006). The grapevine genome was therefore the fourth among flowering plants, the second for woody plants and the first one as a fruit crop. The French-Italian Consortium selected the nearly homozygote (93%) PN40024 genotype derived from inbreeding cycle of Pinot noir while the Italian-American Collaboration opted for a cultivated clone of Pinot noir (heterozygous genotype). The genome size is approximately 487 Mb with 19 pairs of chromosomes and the last updated sequence currently available online is the 12X coverage of PN40024, that became the reference genome for *Vitis vinifera*. Gene predictions identified 31922 protein-coding genes in the recently released V2 version (Vitulo et al., 2014) whereas the previous one (V1) annotated 29970 protein-coding genes (Grimplet et al., 2012) with on average 5 exons per gene which in total account for the 7% of the genome and 140 miRNA classified in 28 conserved families (Mica et al., 2010). Moreover, 41.4% of the genome is composed of repetitive/transposable elements.
(download data: http://genomes.cribi.unipd.it/DATA/
browse genome: http://genomes.cribi.unipd.it/gb2/gbrowse/public/vitis_vinifera_v2/)
Effort has been made to elaborate guidelines and protocols for gene functional and structural annotation and their nomenclature (Grimplet et al., 2014) following what has been done in the *Arabidopsis Information Resources* (TAIR, http://www.arabidopsis.org/) and for tomato in the *Sol Genomics Network* (SGN, http://solgenomics.net/). At present, the *International Grape Genome Program* (IGGP, http://www.vitaceae.org/) is the reference for the grapevine community.

With the availability of the genome sequence and the development of high-throughput analyses such as the microarray (i.e. NimbleGen 12x135K 090918_Vitus_exp_HX12 microarray) and the next-generation sequencing technique such as the RNA sequencing (i.e. Illumina technology), it is possible to profile the entire grape transcriptome and perform study on gene expression during development and/or in response to biotic and environmental conditions. Moreover, with the progression of the techniques based on liquid and gas chromatography coupled to mass spectrometry, it is now possible perform large-scale analyses on metabolite changes with targeted or untargeted approaches. However, due to the chemical complexity of the metabolome that differs from the four nucleotides with similar chemical properties that characterize the transcriptome, it not feasible at the moment profile the entire grape metabolome using a single protocol extraction and a single analytical technique. Moreover, there is not a correspondence gene-metabolite. A single gene can produce multiple metabolites, and cultivar specific metabolites are the result of the fine-tuning of enzymes and/or transcription factors governed by specific alleles in highly heterozygous specie. Therefore, several important information needs to be extracted from the genome of heterozygous cultivars (see Drew et al., 2015). In this direction, the genome of the cultivar Tannat has been recently sequenced and de-novo assembled (Da Silva et al., 2013). This allowed the definition of 5901 unannotated or unassembled genes and the discovery of 1873 genes that were not shared with PN40024. Currently, many sequencing projects of several grape cultivars are underway. A partial list can be seen here (http://www.vitaceae.org/index.php/Current_Sequencing_Projects).

1.1 Grapevine physiology

The annual growth cycle of grapevine is described with a series of well-defined developmental stages (Fig. 1). The timing and the duration of each of them is variable. Grapevine feels time in day-length (photoperiodism) and hence seasonal succession by means of internal clocks. This circadian rhythm allows the plant to cope with environment conditions and biotic factors.

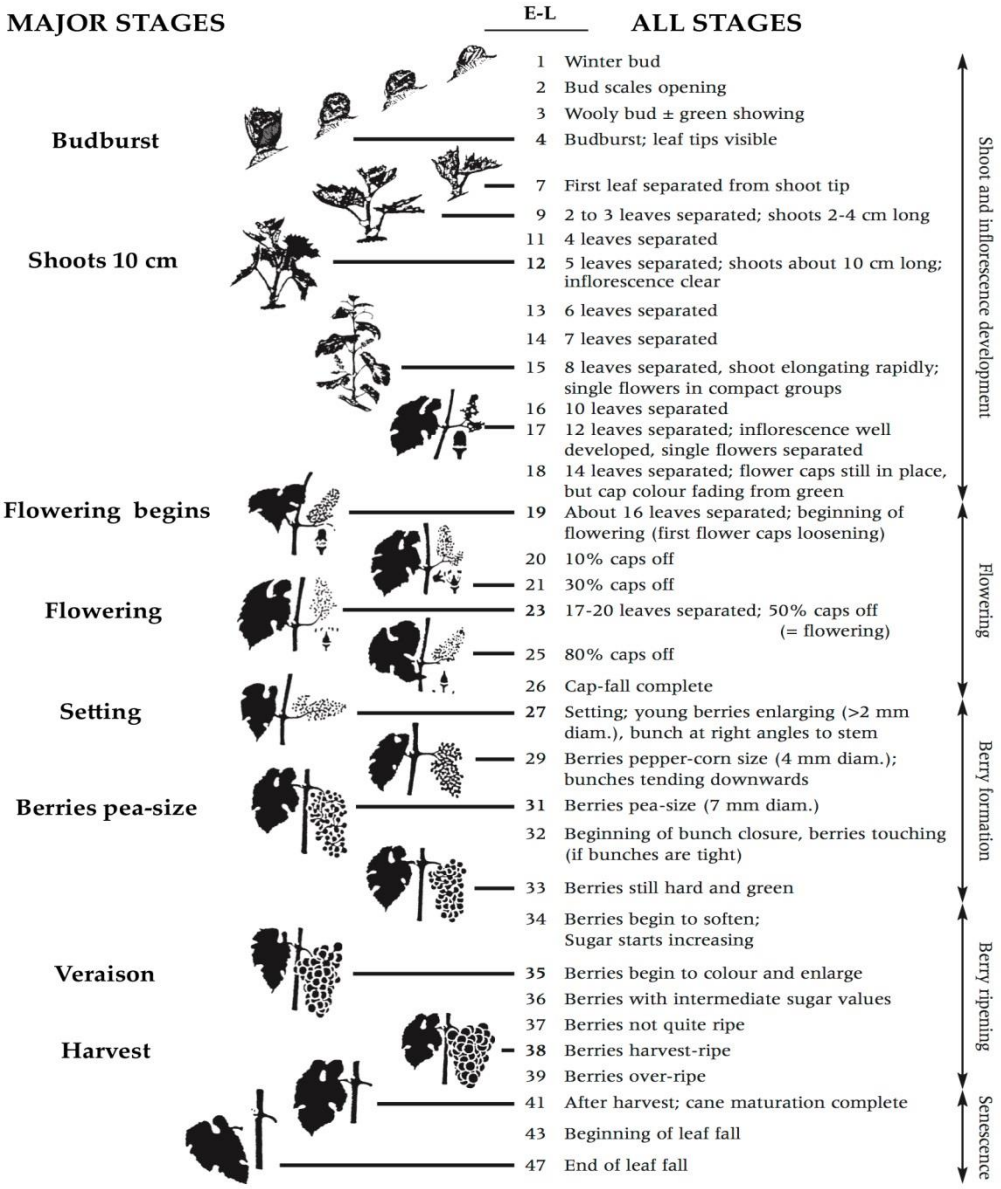

Figure 1. Growth stages of *Vitis vinifera* according to Eichhorn and Lorenz (modified by B.G. Coombe, 1995).

On the left, there are listed the major stages that take place during the growth cycle of grapevine. In the middle, a graphical representation of them. On the right, a detailed list of all stages with the respective E-L number.

In spring, nutrient reserves, stored in the roots and in the trunk during winter dormancy, begin to be metabolized and relocated through the xylem. The root pressure starts one month before budburst and causes the exudation of the xylem sap from pruned canes (a process also called "bleeding") restoring thus the xylem system functionality and furthermore buds swell. Budburst marks the beginning of shoot growth. Leaves are arising every few days alternating on the two sides of the shoot with a single leaf at each node. Grapevine leaves are palmate with five lobes, partly separated from each other with differences in shape varying among cultivars. The rate of new leaves and the length of internodes is directly proportional to day length and temperature. Buds formed during the previous growing season give rise to a shoot bearing fruits in the following one. Inflorescences arise opposite to a leaf, typically at the third to sixth node from the shoot base. Grapevine flower shows a calyx with five fused sepals, the calyptra (corolla or cap) with five joined petals, five stamens and the pistil with a bicarpellary ovary with two ovules each carpellary leaf. Anthesis marks the beginning of bloom with the shed of the calyptra or capfall. Blooming can last two to three weeks depending on the weather conditions. Pollen is released from the anthers and falls on the stigma of the pistil, allowing thus pollination. The fusion of the male and female gametes in the ovule is named fertilization. The ovule together with the zygotic embryo develops into the seed whereas the ovary becomes the fruit. There are four ovules in the grapevine flower but rarely all reach the same stage of development simultaneously and hence berries seldom have four seeds. (Vasconcelos et al., 2009; Keller, 2015). Grapevine berry is a non-climacteric fleshy fruit and has three major type of tissue: skin, pulp and seed. The curve of growth of the berry (Fig. 2) is characterized by a double sigmoidal pattern and can be divided in three stages with two phases of growth (stage I and III) separated by a lag phase (stage II). During berry development there are changes in weight, volume, texture, composition, color and flavour (Coombe, 1976). Stage I is characterized by berry growth through cell division and cell expansion. Seeds are green. Berries are firm and dark green, and they are accumulating organic acids while sugar content is constantly low. Stage II is a lag phase. Seeds are reaching their final size, maximum weight, and tannin content; the embryo is completed and concurrently a thick cuticle coats the seeds. Berries are switching from immature/green to mature/ripe developmental program (Fasoli et al., 2012). The onset of stage III is called veraison. Seeds turn from green to brown due to oxidation of the tannins in the outer layer. Berries start to soften and vacuoles expand, mostly due to water import and retention, resulting also in a decline in the berry turgor pressure. Organic acids are metabolized. Sugar content increases and there is a change in skin color from green to red/blue in dark-skinned cultivars and to light green/yellow in white cultivars. Aroma and flavour compounds accumulate in the berries. Ripening starts in the cell of the pulp and then proceeds outward to skin cells (Castellarin et al., 2011). A vascular system, which consists of xylem and phloem, links each berry to the shoot and hence to the vine. Xylem sap is the main source of water, minerals and nutrients before veraison; the flux is coming from the roots upward. Evidences indicate that the functionality of the xylem after veraison is reduced (Keller et al., 2006; Choat et al., 2009). From veraison onward, phloem sap becomes the primary source of berry water and photosynthate: the flux is coming from the leaves downward. The average grape berry weight ranges from 0.5 to 10 g among *Vitis vinifera* cultivars (Dai et al., 2011). The potential size/weight is managed by three factors: cell number, cell density and cell volume.

Cell division is primarily under genetic control (i.e. fruits from the same cultivar should have the same cell numbers) and is settled during the first weeks after anthesis. At that time there are on average per berry 200,000 cells while at harvest this number rise up to 600,000. That means that there are around 17 doublings during the first phases of growth, and twice afterward (Harris et al., 1968). On the other hand, cell expansion is influenced by environmental factors. On average the volume of cells, in particular the volume of the cell of the pulp, increases 300-fold from anthesis to harvest (Coombe, 1976). The grape is considered ripe when sugars, acidity, phenolic and volatile compounds are well balanced. Climate influences most the harvest date. Growth, development and ripening are hastened with high temperature with an optimum of 25-30 °C. If temperature is lower or higher, it is delayed. Average heat units or growing degree days (GDD) alias Winkler scale is a beneficial tool that can be used for comparing different vine growing regions, seasons and foreseeing important grapevine developmental stages. Developed in the 1944 by Amerine and Winkler, it is based on the cumulative sum of daily mean temperature from April 1 to October 31 in the northern hemisphere (or October 1 to April 30 in the southern hemisphere) considering only those days with a mean temperature above 10 °C. Accordingly, grape production is suitable between 850 and 2700 GDD. After the grapes have been harvested, the vine growth cycle ends with leaf senescence and abscission. The nutrients (starch, proteins, lipids and minerals) are recycled to the canes, trunk and roots and they will be used in the start of the following growing season. Lastly, grapevine enters dormancy acclimating to cold weather.

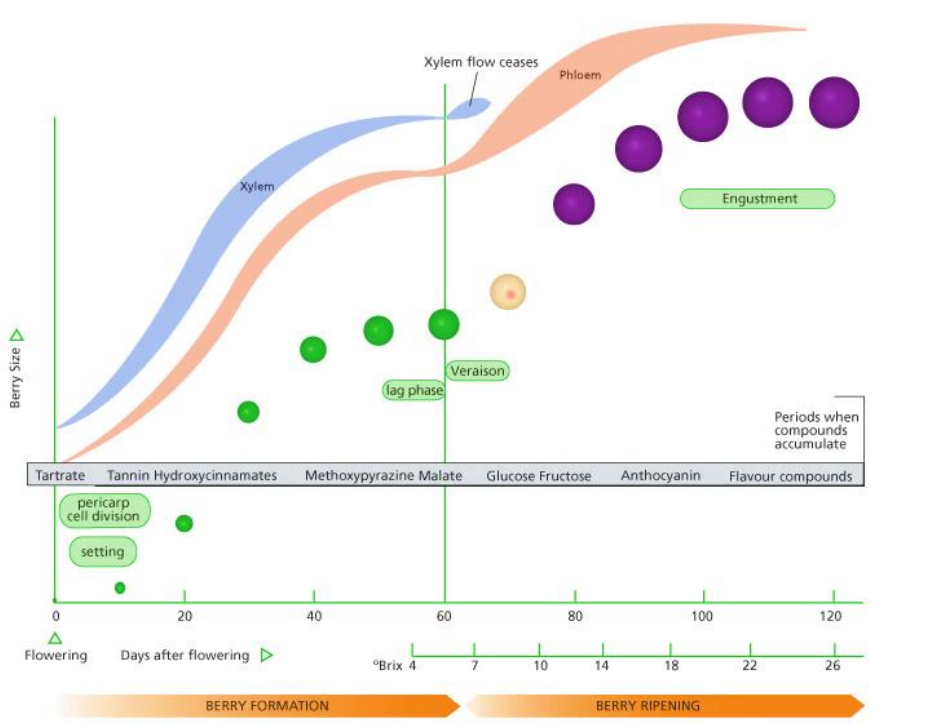

Figure 2. Development of a grape berry.

The scheme shows the main phases of berry development in 10-day intervals from flowering to harvest with details on the berry size and color. It shows also the various compounds accumulated during each stage, the °Brix level and the activity of the vascular system. Illustration by Jordan Koutroumanidis.

1.2 Grape berry composition

1.2.1 Organic acids

Differently from most fruit species, the main organic acids that grapes accumulate during development and ripening are tartrate and malate, which together comprise 70-90 % of the total acidity and contribute largely to the pH of the juice, must and wine (Dai et al., 2011). They are diprotic acids with first dissociation pKa of 3 and 3.5 for tartrate and malate respectively that means tartrate is a stronger acid than malate. Despite they share a close structure (tartrate: 2,3-dihydroxybutanedioic acid, $C_4H_6O_6$; malate: hydroxybutanedioic acid, $C_4H_6O_5$), they are formed through different metabolic pathways (Ford, 2012).

Tartrate is produced by the breakdown of the ascorbate (vitamin C) through a five-step pathway with the rate-limiting step the conversion of L-idonate to 5-keto-D-gluconate. The enzyme responsible of this reaction was identified and encodes for a L-idonate dehydrogenase (*VviL-IdnDN*: *VIT_16s0100g00290*) (DeBolt et al., 2006). Tartrate biosynthesis occurs during the early stages of berry development, from post-anthesis to the onset of ripening, and then declines (Deluc et al., 2007). Tartrate, stored in the vacuoles, is not metabolized neither in the berry nor by microorganisms during must fermentation and hence after veraison its concentration in the berry decrease due to dilution from water import; it is found in the wine, where often it is added to the must with the aim to control and adjust the pH.

Malate is produced from phosphoenolpyruvate (PEP), the second last compound of glycolysis, through the activity of the cytoplasmatic enzymes phosphoenolpyruvate carboxylase (PEPC) (*VviPEPC*: *VIT_01s0011g02740, VIT_12s0028g02180, VIT_19s0014g01390*), which converts phosphoenolpyruvate in oxalacetate, and malate dehydrogenase (*VvicytMDH: VIT_07s0005g03350, VIT_07s0005g03360, VIT_15s0021g02410*) that reversibly converts oxalacetate in malate. PEPC activity is higher during the early stages of development as the concentration of malate. From veraison on, the activity of two of them (*VIT_01s0011g02740, VIT_12s0028g02180*) is decreasing. Malate, once formed, can be transported and stored in the vacuole and therefore the activity of the cytosolic malate dehydrogenases is enhanced until there is equilibrium between malate and oxalacetate. However, since this reaction is reversible, in situations of high amount of malate (i.e. after veraison, during malate catabolism) this reaction is in favor of oxalacetate. Another route of malate production is from the mitochondrial enzyme fumarase (*VIT_07s0005g00880, VIT_14s0060g01690, VIT_14s0060g01700*) that converts fumarate to malate as part of the TCA cycle. Part of the malate exits the mitochondrion and it is stored in the vacuole. Furthermore, in the glyoxysome, malate synthase (*VIT_17s0000g01820*) converts glyoxylate to malate as part of the glyoxylate cycle (Sweetman et al., 2009). Contrary to tartrate, malate is a metabolic substrate and it is catabolized during berry ripening starting at veraison when glycolysis is inhibited in favor of sugars accumulation. Hence, there is an efflux of malate from the vacuole with a simultaneously influx of sugars in it and malate is used in the respiration process as a carbon source in the TCA cycle; it is also used in gluconeogenesis and ethanol fermentation. Mitochondrial malate dehydrogenases (*VvimMDH*: *VIT_10s0003g01000, VIT_14s0108g00870, VIT_17s0000g06270, VIT_19s0014g01640*) are enhanced at veraison together with the aforementioned cytosolic malate dehydrogenase, which convert malate to oxalacetate. Moreover, also the mitochondrial NAD dependent malic enzyme

(*VvimNAD-ME*: *VIT_15s0021g00500, VIT_15s0046g03670*) and the cytosolic NADP dependent malic enzyme (*VvicytNADP-ME*: *VIT_04s0008g00180, VIT_09s0002g03620, VIT_11s0016g03210*), that are converting malate to pyruvate, are enhanced at veraison (Sweetman et al., 2009). Recently, two carriers involved in malate transport into the mitochondria have been identified in grapevine berry (*VviDTC*: *VIT_06s0004g00470, VIT_08s0007g07270*) and they showed an up-regulation at the onset of ripening (Regalado et al., 2012). Other organic acids are present in the berry in a lower amount and include those of the TCA cycle (i.e. citrate, succinate, fumarate and oxalacetate).

To conclude, fruit acidity peaks immediately before veraison and then sharply decreases. Fruit acidity is inversely correlated with temperature: as the temperature increases, the total acidity decreases. On average, juice from mature grape contains between 5 and 10 g/L of organic acids and a titratable acidity of 6.5 - 8.5 g/L is considered optimal.

1.2.2 Sugars

Carbohydrates, produced by photosynthesis in the leaves, are imported to the berry as sucrose via the phloem. Before veraison, sucrose (broken in its hexose components, glucose and fructose) is quickly used in the respiration process through glycolysis, TCA and oxidative phosphorylation. At the onset of ripening, the concentration of sugars stored in the berry's vacuole strongly increases with approximately an equal amount of glucose and fructose found in a ripe berry. At harvest, they represent 90 % of the soluble solids. Moreover, during must fermentation, they are converted in ethanol by yeast. After veraison, it is observed a shift in the phloem unloading: from symplastic to apoplastic (Zhang et al., 2006) where in the first case there is a passive movement through plasmodesmata and in the second one there is an active movement with the assimilates crossing the membranes by means of transporters.

Sucrose is sugar that is transported over long distance in the phloem sap from source (leaves) to sink (berries). Up to now, two routes are known. Firstly, it can be directly imported through sucrose transporters and through the activity of sucrose synthase or cytosolic (neutral) invertase be cleaved into UDP-glucose and fructose, and glucose and fructose respectively; alternatively, it can be cleaved by cell wall invertase into monosaccharides and then transported by means of hexose transporters (Davies et al., 2012). In the grapevine genome, a small gene family with four members encodes for sucrose transporters (*VviSUC11/SUT1*: *VIT_18s0001g08210*, *VviSUC12*: *VIT_01s0026g01960*, *VviSUC27*: *VIT_18s0076g00250*, *VviSUC28/SUT2*: *VIT_18s0076g00220*). The transcripts of *VviSUC11* and *VviSUC12* are increasing after veraison, whereas *VviSUC27* shows a different behavior and it is described as a low-affinity/high capacity (LAHC) transporter (Zhang et al., 2007). Instead *VviSUC28* seems not to be expressed in the berry (Afoufa-Bastien et al., 2010). The activity of the cell wall invertase (*VvicwINV*: *VIT_09s0002g02320*) shows a peak at veraison and during late ripening (Hayes et al., 2007) indicating a role in the sugar accumulation process. Several hexose transporters have been identified in grapevine (Afoufa-Bastien et al., 2010). Five of them got particular attention namely *VviHT1-VviHT5* (*VIT_00s0181g00010, VIT_18s0001g05570, VIT_11s0149g00050, VIT_16s0013g01950, VIT_05s0020g03140*). They are H^+ dependent glucose and fructose transporters of the plasma membrane showing different levels of affinity. Among them, *VviHT2* and *VviHT3* seem apt to carry out this role having a peak at veraison and during ripening

(Lecourieux et al., 2014). Lastly, hexoses reach their storage location by tonoplast monosaccharide transporters (*VviTM1-VviTM2*:*VIT_18s0122g00850, VIT_03s0038g03940*).

Many other sugars are present in the berry. Polysaccharides are the major components of the cell wall. In particular, cell wall is composed of a framework of cellulose (a linear polysaccharide of β 1-> 4 linked glucose units) embedded in a matrix of pectins (a complex polymer composed of homogalacturonan, rhamnogalacturonan I and II, xylogalacturonan and apiogalacturonan with various degrees of ramifications) and hemicellulose (a branched polymer composed mainly of xyloglucan) (Nunan et al., 1997; Vidal et al., 2001). Pectin and hemicellulose demethylation and depolymerization through the activity of pectin methylesterase (PME) and polygalacturonase (PG) is the driving force of berry softening during ripening and post-harvest dehydration (Zoccatelli et al., 2013). Recently it was also discovered that sugars and polyols, in particular mannitol, sorbitol, myo-inositol, dulcitol, galactinol and the raffinose family oligosaccharides (RFO), namely raffinose and stachyose, may have a role in abiotic stress tolerance as osmoprotectants (Pillet et al., 2012; Conde et al., 2015).

1.2.3 Phenolics

Phenolic compounds contribute significantly to fruit and wine quality. They are belonging to different classes showing various responses to biotic and abiotic stresses. Phenolics are produced in the berry strongly under the control of transcription factors that regulate their biosynthetic pathway. The starting point of the phenylpropanoid and flavonoid pathways is the aromatic amino acid phenylalanine. Phenylalanine biosynthesis is linked with the shikimate pathway, which converts phosphoenolpyruvate (from glycolysis) and erythrose-4-phosphate (from the pentose phosphate pathway) into the production of the aromatic amino acids.

The phenylpropanoid pathway (Fig. 3) leads to the production of *p*-coumaryl-CoA from phenylalanine in three steps. Firstly phenylalanine ammonia lyase (*VviPAL*: *VIT_06s0004g02620, VIT_08s0040g01710, VIT_13s0019g04460*) catalyze the deamination of the phenylalanine in cinnamic acid. Cinnamic acid is further hydroxylated by cinnamate-4-hydroxylase (*VviC4H*: *VIT_06s0004g08150, VIT_11s0065g00350, VIT_11s0078g00290*) into *p*-coumaric acid. Lastly, *p*-coumaric acid is esterificated with CoA producing *p*-coumaryl-CoA by means of 4-coumarate-CoA ligase (*Vvi4CL*: *VIT_01s0010g02740, VIT_02s0025g03660, VIT_02s0109g00250, VIT_04s0008g02550, VIT_06s0061g00450, VIT_11s0052g01090, VIT_16s0039g02040, VIT_16s0050g00390, VIT_17s0000g01790*). This is a branching point of the pathway: *p*-coumaryl-CoA (plus three molecules of malonyl-CoA) is the substrate of both chalcone synthase and stilbene synthase starting the flavonoid and stilbene pathway, respectively (Castellarin et al., 2012).

Modifications of the intermediates of the phenylpropanoid pathway by means of *VviCOMT* and *VviCCoAOMT* give rise to phenolic acids, like *p*-coumaric, caffeic and ferulic acids with different type and number of substituents on the aromatic ring. They can be esterificated with tartaric acid and are named caftaric, coutaric and fertaric respectively. They are the major phenolic acids present in the berry flesh and their synthesis is promoted before veraison. Recently, two negative transcription factors (*VviMYB4a-b*: *VIT_03s0038g02310,*

VIT_04s0023g03710) were characterized in grapevine, leading to the repression of this pathway, in particular affecting *VviCOMT* and *VviCCoAOMT* (Cavallini et al., 2015).

Stilbenes are phytoalexins produced by the activity of the enzymes stilbene synthases. Their synthesis is constitutive in healthy berries from veraison onward, varying in composition among varieties. Their synthesis is furthermore enhanced by biotic and abiotic stresses (Gatto et al., 2008) especially upon *Botrytis cinerea* infections (Bavaresco et al., 1997). In the genome of *Vitis vinifera*, there are forty-five stilbene synthases with at least 33 encoding full-length proteins (*VviSTS: VIT_10s0042g00840, VIT_10s0042g00850, VIT_10s0042g00860, VIT_10s0042g00870, VIT_10s0042g00880, VIT_10s0042g00890, VIT_10s0042g00910, VIT_10s0042g00920, VIT_10s0042g00930, VIT_16s0100g00750, VIT_16s0100g00760, VIT_16s0100g00770, VIT_16s0100g00780, VIT_16s0100g00800, VIT_16s0100g00810, VIT_16s0100g00830, VIT_16s0100g00840, VIT_16s0100g00850, VIT_16s0100g00860, VIT_16s0100g00880, VIT_16s0100g00900, VIT_16s0100g00910, VIT_16s0100g00920, VIT_16s0100g00930, VIT_16s0100g00940, VIT_16s0100g00950, VIT_16s0100g00960, VIT_16s0100g00990, VIT_16s0100g01000, VIT_16s0100g01010, VIT_16s0100g01020, VIT_16s0100g01030, VIT_16s0100g01040, VIT_16s0100g01060, VIT_16s0100g01070, VIT_16s0100g01100, VIT_16s0100g01110, VIT_16s0100g01120, VIT_16s0100g01130, VIT_16s0100g01140, VIT_16s0100g01150, VIT_16s0100g01160, VIT_16s0100g01170, VIT_16s0100g01190, VIT_16s0100g01200*) (Vannozzi et al., 2012). Two R2R3 MYB transcription factors, namely *VviMYB14* (*VIT_07s0005g03340*) and *VviMYB15* (*VIT_05s0049g01020*) regulates stilbene biosynthesis well correlating with the expression of *VviSTSs* both under biotic and abiotic stresses and in healthy grapes (Höll et al., 2013). The main stilbenes found in grape are *cis*- and *trans*-resveratrol, piceatannol, *cis*- and *trans*-piceid, astringin, pallidol and α-, β-, γ-, δ-, ε-viniferin.

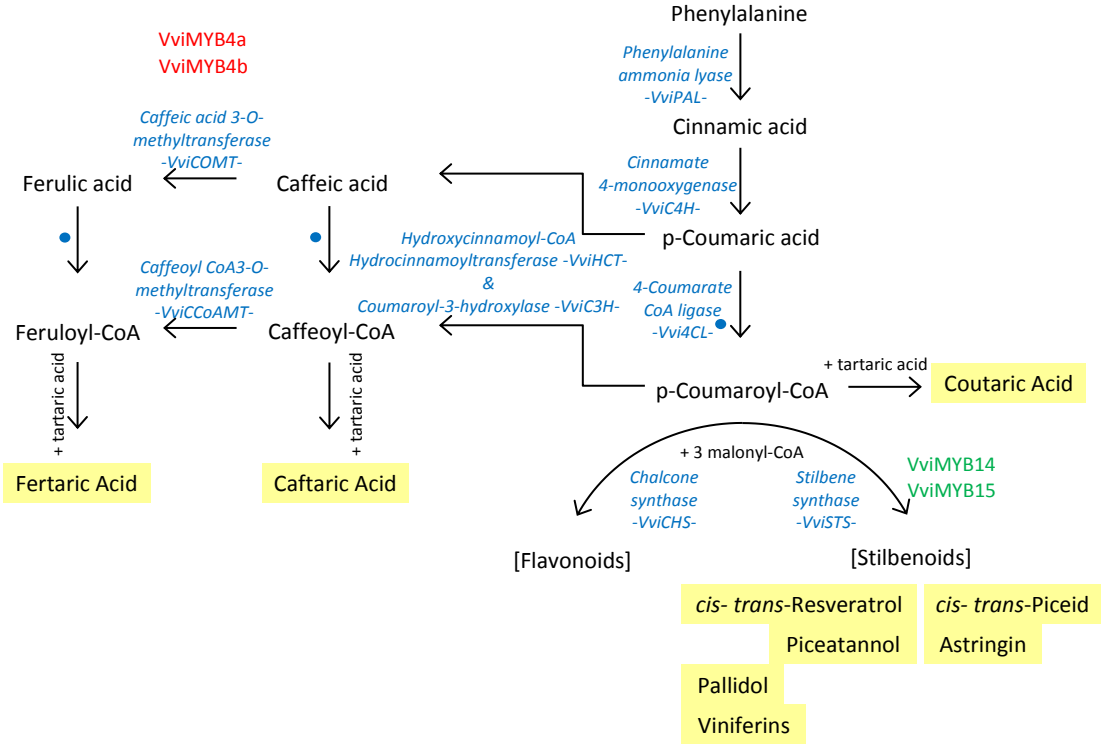

Figure 3. Schematic representation of the phenylpropanoids pathway of grapevine.

The main compounds of the phenylpropanoid pathway are represented in black color with important metabolites highlighted in yellow. The enzymes involved in the reactions are written in blue. Positive and negative regulators of the pathway are written in green or red, respectively. Drawing of the author.

The flavonoid pathway (Fig. 4) leads to the production of flavonols, flavan-3-ols and anthocyanins. Through the activity of the enzymes chalcone synthases (*VviCHS*: *VIT_05s0136g00260, VIT_14s0068g00920, VIT_14s0068g00930*) (Goto-Yamamoto et al., 2002) and chalcone isomerases (*VviCHI*: *VIT_13s0067g02870, VIT_13s0067g03820*) there is the production of naringenin. Naringenin can be hydroxylated at different positions: at the 3 position thanks to flavanone-3-hydroxylases (*VviF3H VIT_04s0023g03370, VIT_18s0001g14310*), forming dihydrokämpferol; at the 3′ or 3′,5′ positions by the activity of flavonoid-3′-hydroxylase (*VviF3′H*: *VIT_17s0000g07200, VIT_17s0000g07210*) and flavonoid-3′,5′-hydroxylase (*VviF3′5′H*: *VIT_06s0009g02810, VIT_06s0009g02830, VIT_06s0009g02840, VIT_06s0009g02860, VIT_06s0009g02880, VIT_06s0009g02920, VIT_06s0009g02970, VIT_06s0009g03010, VIT_06s0009g03040, VIT_06s0009g03050, VIT_06s0009g03110, VIT_06s0009g03140, VIT_08s0007g05160*) (Falginella et al., 2010), which catalyze the conversion into eriodictyol and pentahydroxyflavanone, respectively. Eriodictyol and pentahydroxyflavanone are then converted into dihydroquercetin or dihydromyricetin by *VviF3H*, respectively. Dihydrokämpferol is also a substrate for *VviF3′H* and *VviF3′5′H*, which catalyze the hydroxylation into dihydromyricetin or dihydroquercetin (Castellarin et al., 2012).

Flavonol synthases (*VviFLS*: *VIT_18s0001g03430, VIT_18s0001g03470, VIT_18s0001g03490, VIT_18s0001g03510*) are key enzymes for flavonols production: they convert dihydrokämpferol, dihydroquercetin, and dihydromyricetin in kämpferol, quercetin, and myricetin. Moreover in grape, it is found isorhamnetin, the methylated form of quercetin, and laricitrin and syringetin, the methylated forms of myricetin Two flavonol synthases are mainly expressed in the berry (*VIT_18s0001g03430, VIT_18s0001g03470*) and they are transcribed in the skin after veraison (Fujita et al., 2006). Their expression is under the control of a light-induced transcription factor (*VviMYBF1*/*VviMYB12*: *VIT_07s0005g01210*) (Czemmel et al., 2009). Flavonols are normally glycosylated at the 3 position of the C ring and hence they are present as glucosides, galactosides, rhamnosides, rutinosides and glucuronides. Recently, two specific flavonol-3-*O*-glycosyltransferases have been characterized (*VviGT5-6*: *VIT_11s0052g01600, VIT_11s0052g01630*) showing the same pattern of expression of *VviFLS* (Ono et al., 2010). Flavonols are yellow pigments that contribute to the color of white wines. In red cultivars, flavonols can conjugate to anthocyanins reinforcing the stability of wine color. In white grapes, the main flavonol are the mono- and di-hydroxylated quercetin, kämpferol and isorhamnetin whereas in red grapes, beside them, there are the tri-hydroxylated, myricetin, laricitrin and syringetin (Mattivi et al., 2006). They have a role as UV-protectants.

Dihydroflavonols can lead to the production of flavan-3-ols and anthocyanins. Firstly, the enzyme dihydroflavonol 4-reductase (*VviDFR*: *VIT_18s0001g12800*) reduces them to leucoanthocyanidins namely leucocyanidin, leucopelargonin and leucodelphinidin. Then, the enzymes leucoanthocyanidin dioxygenases (*VviLDOX VIT_02s0025g04720, VIT_08s0105g00380*) form the anthocyanidins cyanidin, pelargonin and delphinidin (Castellarin et al., 2012).

Flavan-3-ols can thus be formed either from the leucoanthocyanidins by means of leucoanthocyanidin reductase (*VviLAR1-2*: *VIT_01s0011g02960, VIT_17s0000g04150*) or from anthocyanidins by means of anthocyanidin reductase (*VviANR*: *VIT_00s0361g00040*) (Bogs et al., 2005). Their synthesis is promoted from anthesis to veraison and is regulated by multiple transcription factors of the Myb family. In particular *VviLAR1* and *VviANR* are under the control of *VviMYBPA1* (*VIT_15s0046g00170*) and *VviMYBPA2* (*VIT_11s0016g01320*) (Bogs et al., 2007;

Terrier et al., 2009) whereas *VviLAR2* is under the control of *VviMYBPAR* (*VIT_11s0016g01300*) (Koyama et al., 2014). The monomeric flavan-3-ols present in grape are (+)-catechin, (-)-epicatechin, (-)-epicatechin-3-*O*-gallate and in lesser amount (+)-gallocatechin and (-)-epigallocatechin. They differ according to the stereochemistry, the level of hydroxylation and the acylation by gallic acid. Oligomeric and polymeric proanthocyanidin (condensed tannins), are the most abundant class of phenolics. They are formed by multiple subunit of monomers with different mean degree of polymerization (mDP) and level of galloylation (Mattivi et al., 2009). Up to now, the mechanisms involved in either polymerization or galloylation and their transport into the vacuole, is not well understood (Zhao et al., 2010). Only recently, three glycosyltransferases (*VvigGT1-3*: *VIT_03s0091g00040, VIT_03s0180g00200, VIT_03s0180g00320*) were putatively described to be involved in the production of hydroxycinnamic esters and proanthocyanidins galloylation (Khater et al., 2012) and two specific transporters of proanthocyanidin were identified (*VviPAMATE1-2*: *VIT_12s0028g01160, VIT_12s0028g01150*) (Pérez-Díaz et al., 2014) but further analyses toward a fully characterization are necessary.

Anthocyanins are responsible for red, purple and blue pigmentation of the grape berries. They are normally glycosylated at the 3' position of the C ring by the addition of a glucose moiety through the activity of the enzyme UDP-glucose: flavonoid-3-*O*-glucosyltransferase (*VviUFGT*: *VIT_16s0039g02230*) which make them more stable than the corresponding aglycones. The anthocyanins synthetized by *VviUFGT* are the di-hydroxylated cyanidin-3-*O*-glucoside and the tri-hydroxylated delphinidin-3-*O*-glucoside. From them, through the activity of an *O*-methyltransferase (*VviAOMT1-3*: *VIT_01s0010g03510, VIT_01s0010g03490, VIT_01s0010g03470*) (Fournier-Level et al., 2011), there is the formation of the di-hydroxylated peonidin-3-*O*-glucoside and the tri-hydroxylated petunidin-3-*O*-glucoside and malvidin-3-*O*-glucoside. *Vitis vinifera* is able to glycosylate only in 3' position and not in 5', such as other grapevine species, due to two disruptive mutations in the anthocyanin 5-*O*-glucosyltransferase genes (Jánváry et al., 2009). Moreover, anthocyanins can also be acylated to the 6'' position of the glucose bonded to the 3' position of the C ring producing 3-*O*-6''-acetyl-, 3-*O*-6''-coumaroyl- and 3-*O*-6''-caffeoyl-monoglucosides. Recently, an anthocyanin-3-*O*-glucoside-6''-*O*-acyltransferase was characterized (*Vvi3AT: VIT_03s0017g00870*) (Rinaldo et al., 2015). The gene *VviUFGT* is under the control of the transcription factors of the MYBA cluster (*VviMYBA1-2*: *VIT_02s0033g00410, VIT_02s0033g00390*) which triggers the synthesis of anthocyanins at veraison. These genes play a pivotal role in determining the anthocyanin content of grape. Inactivation of these two functional genes, through the insertion of the Gret1 retrotransposon in the promoter of *VviMybA1* and through a two disruptive mutations present in the *VviMybA2* coding region, gave rise to the white berry phenotype (Walker et al., 2007). Anthocyanins are synthetized in the skin of red cultivars from veraison onward and then stored in the vacuole. Anthocyanin-acylglucosides can be translocated into the vacuole by means of MATE-type transporters H^+ dependent localized to the tonoplast (*VviAnthoMATE1-3 VIT_16s0050g00930, VIT_16s0050g00910 VIT_16s0050g00900*) (Gomez et al., 2009), whereas the glycosylated ones are translocated by means of ATP-binding cassette (ABC) proteins glutathione-S-transferase (GST) dependent (*VviABCC1: VIT_16s0050g02480*) (Francisco et al., 2013).

Two transcription factors (*VviMYB5a-b: VIT_08s0007g07230, VIT_06s0004g00570*) are general regulators of the flavonoids pathway and in particular they can activate the promoters of structural and proanthocyanidin genes (*VviCHI*, *VviF3'5'H*, *VviLDOX*, *VviLAR*, and *VviANR*) displaying different expression profiles during berry development and ripening, but they do not influence anthocyanin synthesis, i.e. *VviUFGT* (Deluc et al., 2006; Deluc et al., 2008; Cavallini et al., 2014). Recently, two negative transcription factors (*VviMYBC2-L1* and *L3*: *VIT_01s0011g04760, VIT_14s0006g01620*) were characterized, leading to the repression of both proanthocyanidin and anthocyanins biosynthesis (Huang et al., 2014; Cavallini et al., 2015). Moreover, a basic Helix-Loop-Helix protein (bHLH) (*VviMYC1, VIT_07s0104g00090*) was, for the first time, functional characterized in grapevine: it physically interact with *VviMYB5a-b*, *VviMYBPA1* and *VviMYBA1-A2* taking thus part of the transcriptional cascade controlling proanthocyanidin and anthocyanins biosynthesis in grapevine (Hichri et al., 2010).

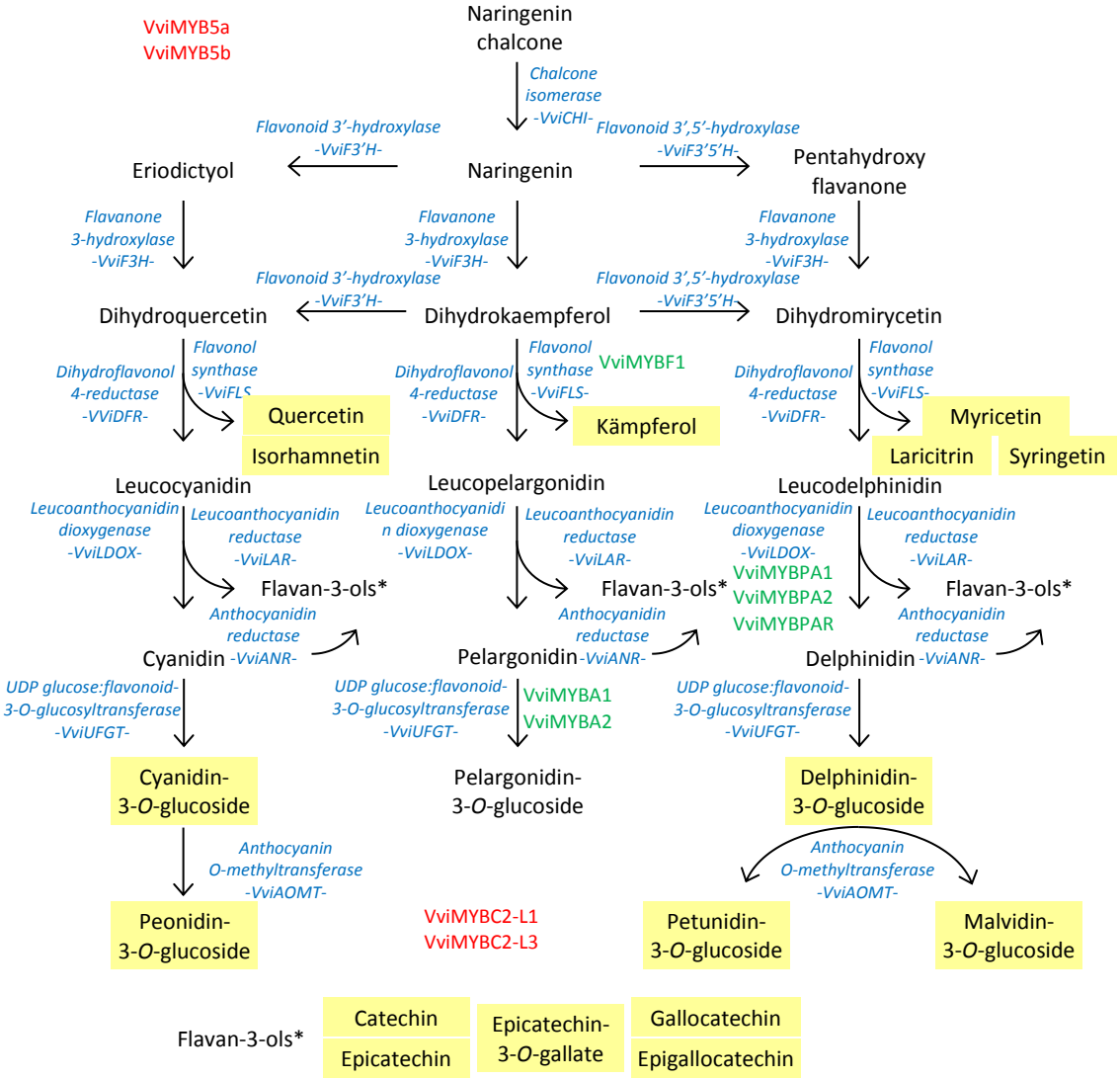

Figure 4. Schematic representation of the flavonoid pathway of grapevine.

The main compounds of the flavonoid pathway are represented in black color with important metabolites highlighted in yellow. The enzymes involved in the reactions are written in blue. Positive and negative regulators of the pathway are written in green or red, respectively. Drawing of the author.

Taken together, the synthesis of phenolic acids, stilbenes, flavonols, flavan-3-ols and anthocyanins is spatiotemporally separated during grape berry development and ripening and tightly regulated by positive and/or negative regulators (Czemmel et al., 2012). Specifically, transcription factors are complexes of a R2R3-MYB protein, a basic Helix-Loop-Helix protein (bHLH) and a tryptophan-aspartic acid repeat protein (WDR or WD40). The MYB/bHLH/WDR complexes (MBW) recognize and bind to responsive elements found in the promoters of specific genes, resulting in the activation or repression of their expression (Matus et al., 2010). Moreover, there are evidences that (i) the activators induce repressors, (ii) repressors repress activators, and (iii) repressors repress repressors indicating the complexity and the fine tuning of the biosynthesis of secondary metabolites during berry development and ripening (Cavallini et al., 2015). To further gain knowledge into the regulation of the biosynthesis of flavonols, flavan-3-ols and anthocyanins, quantitative trait loci (QTL) mapping analysis with the consequent identification of new candidate genes is a promising tool (Huang et al., 2012; Costantini et al., 2015; Malacarne et al., 2015).

1.2.4 Terpenoids and fatty acid derivatives

Two independent pathways lead to the production of the vast group of terpenoids in plants: the plastidial 2C-methyl-D-erythritol-4-phosphate (MEP) pathway starting from pyruvate and glyceraldehyde-3-phosphate and the cytosolic mevalonate (MVA) pathway starting from three molecules of acetyl-CoA. Both provide the initial building blocks, the five-carbon unit isopentenyl pyrophosphate (IPP) and its isomer dimethylallyl pyrophosphate (DMAPP). Through the activity of specific prenyltransferases, there is the formation of terpenoid precursors. Geranyl pyrophosphate synthase (*VviGPPS*) in plastids give rise to monoterpenes (C_{10}) and geranylgeranyl pyrophosphate synthase (*VviGGPPS*) still in plastids give rise to diterpenes (C_{20}) and carotenoids (C_{40}) while in the cytosol, farnesyl pyrophosphate synthase (VviFPPS) give rise to sesquiterpenes (C_{15}) and triterpenoids (C_{30}) by means of terpene synthases (Fig. 5) (Rodríguez-Concepción and Boronat, 2002; Bohlmann and Keeling, 2008).

In the genome of *Vitis vinifera* there are sixty putatively terpene synthases with 39 of them already functional characterized (*VviTPS: VIT_00s0266g00010, VIT_00s0266g00020, VIT_00s0266g00070, VIT_00s0271g00010, VIT_00s0271g00030, VIT_00s0271g00060, VIT_00s0361g00060, VIT_00s0372g00030, VIT_00s0372g00040, VIT_00s0372g00070, VIT_00s0385g00010, VIT_00s0385g00020, VIT_00s0392g00060, VIT_00s0572g00010, VIT_00s0572g00020, VIT_00s0724g00010, VIT_00s0847g00020, VIT_00s2271g00010, VIT_07s0151g01040, VIT_07s0151g01070, VIT_08s0007g06860, VIT_12s0059g02710, VIT_12s0059g02720, VIT_12s0134g00020, VIT_12s0134g00030, VIT_12s0134g00040, VIT_12s0134g00090, VIT_12s0134g00140, VIT_13s0067g03700, VIT_13s0067g03770, VIT_13s0067g03790, VIT_13s0084g00010, VIT_18s0001g04050, VIT_18s0001g04110, VIT_18s0001g04120, VIT_18s0001g04170, VIT_18s0001g04220, VIT_18s0001g04280, VIT_18s0001g04530, VIT_18s0001g04870, VIT_18s0001g04990, VIT_18s0001g05230, VIT_18s0001g05240, VIT_18s0001g05290, VIT_18s0001g05360, VIT_18s0001g05430, VIT_18s0001g05450, VIT_18s0001g05470, VIT_18s0001g05520, VIT_19s0014g01060, VIT_19s0014g01070, VIT_19s0014g02550, VIT_19s0014g02580, VIT_19s0014g02590, VIT_19s0014g04800, VIT_19s0014g04810, VIT_19s0014g04900, VIT_19s0014g04930, VIT_19s0015g02070, VIT_19s0085g00830*) (Martin et al., 2010). Recently, terpene synthases were divided into seven clades: TPS-a, TPS-b, TPS-c, TPS-d, TPS-e/f, TPS-g and TPS-h (Chen et al., 2011). TPS-a, TPS-b and TPS-g are angiosperm-specific clades: TPS-a subfamily with 27 genes in grapevine, located on chr 18 and 19, contains mostly sesquiterpene and possibly diterpene synthases,

whereas the TPS-b subfamily, with 14 genes in grapevine located on chr 8, 12 and 13, and TPS-g subfamily, with 16 genes with unknown location, consist mostly of monoterpene synthases. TPS-c subfamily, with two genes in grapevine, contains the copalyl diphosphate synthases, whereas TPS-e/f subfamily with only one copy in grapevine contains kaurene synthase genes. No genes belonging to TPS-d and TPS-h were recorded in grapevine.

Through quantitative trait loci (QTL) mapping analysis, the gene 1-deoxy-D-xylulose 5-phosphate synthase (*VviDXS: VIT_05s0020g02130*), a structural gene of the MEP pathway, was identified as the responsible of the total monoterpenes content in grapevine (Battilana et al., 2008; Emanuelli et al., 2010; Battilana et al., 2011). Monoterpenes (C_{10}) are highly aromatic compounds and among them the most aromatic are linalool, geraniol, nerol, citronellol, hotrienol, α-terpineol and rose oxides which develop floral aromas with reminiscent of rose, lilac, citrus to cite a few (Darriet et al., 2012). Sesquiterpenes (C_{15}) contribute less to grape flavour as their concentrations are usually below the olfactory threshold. The most studied sesquiterpenes is the rotundone which gives peppery character in some red and white varieties (Siebert et al., 2008; Wood et al., 2008; Caputi et al., 2011; Mattivi et al., 2011) and recently its biosynthetic pathway was elucidated (Drew et al., 2015; Takase et al., 2015). A major fraction of monoterpenes and sesquiterpenes are present in grapevine as nonvolatile terpene glycosides, i.e. chemically bound to sugars. Some of the bound terpenes are converted to their free form by either acid or enzymatic hydrolysis, usually both, during must fermentation and wine maturation. Glycosides are formed by the action of glycosyltransferases that catalyze the transfer of a sugar moiety from an activated sugar donor, usually UDP-Glc, to acceptor molecules. In grapevine, three glycosyltransferases were recently characterized (*VviGT7-14-15*: *VIT_16s0050g01580, VIT_18s0001g06060, VIT_06s0004g05780*) (Bönisch et al., 2014a; Bönisch et al., 2014b).

The diterpenes (C_{20}) include the side chain of chlorophyll, phylloquinones and tocopherol, gibberellins, phytoalexins, and taxol. The triterpenes (C_{30}), such as phytosterols, brassinosteroids, and some phytoalexins, toxins, and waxes, are generated by the joining of two C_{15} chains (Rodríguez-Concepción and Boronat, 2002).

The most prevalent tetraterpenes (C_{40}) are carotenoids, which are pigments in many flowers and fruits, contribute to light harvesting, and protect the photosynthetic apparatus from photooxidation (Rodríguez-Concepción and Boronat, 2002). Recently, the genes involved in the biosynthetic pathway were identified in grapevine (Young et al., 2012) (Fig. 5). From two molecules of geranylgeranyl diphosphate there is the formation of phytoene by means of phytoene synthase and it is the rate-liming step of the pathway (*VviPSY1-2*: *VIT_04s0079g00680* and *VIT_12s0028g00960*). Phytoene undergoes a series of four desaturation reactions that result in the formation of 9,15,9′-tri-*cis*-ζ-carotene, then 9,9′-di-*cis*-ζ-carotene, 7,9,7′,9′-tetra-*cis*-licopene and finally lycopene by means of respectively phytoene desaturase (*VviPDH1-2* and *VviPDS1*: *VIT_04s0023g01790, VIT_04s0023g01780* and *VIT_09s0002g00100*), 15-*cis*-ζ-carotene isomerase (*VviZISO1*: *VIT_05s0062g01110*), ζ-carotene desaturase (*VviZDS1*: *VIT_14s0030g01740*) and carotenoid isomerase (*VvCISO1-2*: *VIT_08s0032g00800* and *VIT_12s0035g01080*). The lycopene-β-cyclase (*VviLBCY1-2*: *VIT_06s0080g00810* and *VIT_08s0007g05690*), catalyzes the formation of the β-carotene from lycopene whereas the lycopene ε-cyclase (*VviLECY1*: *VIT_11s0016g01880*) catalyze the formation of α-carotene. α -Carotene and β -carotene are further hydroxylated to produce the xanthophylls lutein and

zeaxanthin respectively by means of carotene hydroxylase (*VviLUT1-5*: *VIT_08s0007g04530* and *VIT_04s0023g00080*) and β-carotene hydroxylase (*VvBCH1-2*: *VIT_02s0025g00240* and *VIT_16s0050g01090*). Zeaxanthin epoxidase (*VviZEP1-2*: *VIT_07s0031g00620* and *VIT_13s0156g00350*) hydroxylates the rings of zeaxanthin in two consecutive steps to yield antheraxanthin and then violaxanthin. Violaxanthin can be de-epoxidated by means of violaxanthin de-epoxidase (*VviVDE1-2*: *VIT_04s0043g01010* and *VIT_07s0031g01770*) regenerating zeaxanthin. These genes are also responsible for the interconversion of lutein to lutein 5,6-epoxide. This process, also called xanthophyll cycle, has a role in photoprotection rapidly converting violaxanthin to zeaxanthin because zeaxanthin helps thermal dissipation of excess light energy in the light-harvesting complex and thus plays a key role in protecting the photosynthetic apparatus (Havaux et al., 2007). Violaxanthin is also converted to neoxanthin by neoxanthin synthase (*VviNSY1*: *VIT_14s0006g02880*), which represents the final step in the core carotenoid biosynthetic pathway. Carotenoids during berry development and ripening are decreasing with the lowest level at harvest. Only the concentration of zeaxanthin and antheraxanthin increased during berry ripening with a peak at harvest. (Cunningham and Gantt, 1998; Cazzonelli and Pogson, 2010; Nisar et al., 2015). Both neoxanthin and violaxanthin can be cleaved by 9-cis-epoxycarotenoid dioxygenases (*VviNCED1-2-3*: *VIT_05s0051g00670, VIT_10s0003g03750, VIT_19s0093g00550*) and further modified to produce the plant hormone abscisic acid (ABA). Carotenoids can also be cleaved by means of carotenoid cleavage dioxygenases (*VviCCD7-8a/b: VIT_15s0021g02190, VIT_04s0008g03510, VIT_04s0008g03380*) to form the phytohormone strigolactone and finally carotenoids can be cleaved by means of other families of carotenoid cleavage dioxygenases (*VviCCD1a/b, VvCCD4a/b/c*: *VIT_13s0064g00840* and *VIT_13s0064g00810*; *VIT_02s0087g00910, VIT_02s0087g00930* and *VIT_16s0039g01370*) (Lashbrooke et al., 2013) to form volatile flavour and aroma-related compounds, such as the C_{13}-norisoprenoids with the major compounds β-ionone, β-damascenone which contribute to floral and fruity aroma. The majority of them are glycosylated in grape (Robinson et al., 2014).

The unsaturated C_{18} fatty acids linoleic acid and linolenic acid are the precursor of the volatile organic compounds (VOCs) such as the C_6-compounds, C_9-compounds and recently it was hypothesized in tomato also a role in the production of the C_5 .compounds (Shen et al., 2014), although the major aroma compounds derived from fatty acids in grapes are the C_6-aldehydes and alcohols. They are formed by the activity of lipoxygenases (*Vvi9LOX*: *VIT_05s0020g03170, VIT_14s0128g00780, VIT_14s0128g00790*; *Vvi13LOX*: *VIT_00s0265g00170, VIT_01s0010g02750, VIT_06s0004g01450, VIT_06s0004g01460, VIT_06s0004g01470, VIT_06s0004g01480, VIT_06s0004g01500, VIT_06s0004g01510, VIT_09s0002g01080, VIT_13s0064g01480*) (Podolyan et al., 2010), hydroperoxide lyase (*VviHPL1-2: VIT_12s0059g01060, VIT_03s0063g01830*) (Zhu et al., 2012), *(3Z)-(2E)* enal isomerase and alcohol dehydrogenase. These C_6 aldehydes and alcohols are responsible of the green-grassy aroma even though considering their detection threshold they rarely contribute to the herbaceous character of musts and wines (Darriet et al., 2012; Robinson et al., 2014).

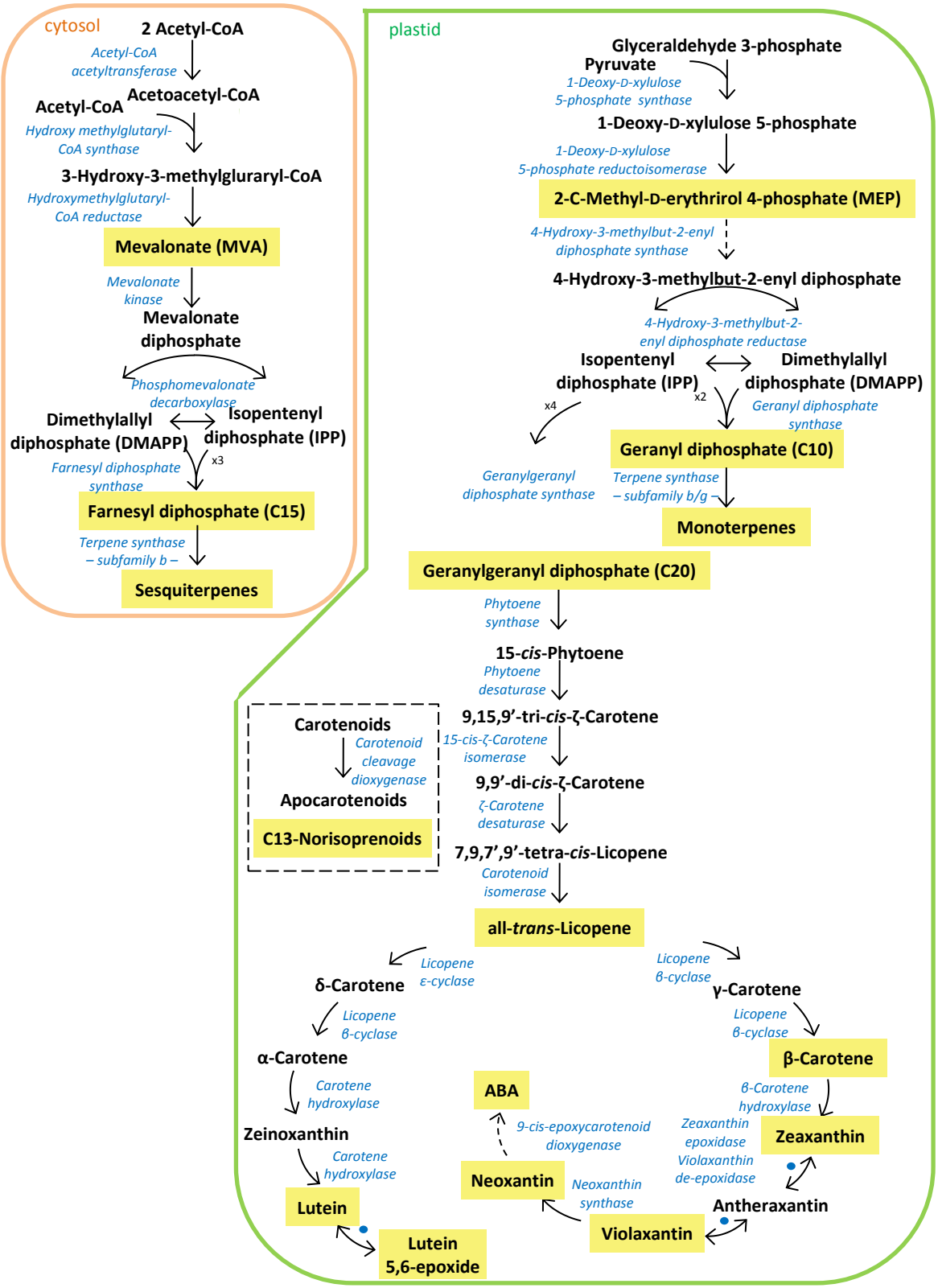

Figure 5. Schematic representation of the terpenoid pathway of grapevine.

The main compounds of the terpenoid pathway are represented in black color with important metabolites highlighted in yellow. The enzymes involved in the reactions are written in blue. Drawing of the author.

1.3 Vineyard deficit irrigation

Grapevine is considered a drought tolerant plant and traditionally is not irrigated, especially in Europe. In Spain, law forbade grapevine irrigation until 1996; then new guidelines came into force and irrigation increased dramatically. In France, irrigation is forbidden for the '*Appellation d'Origine Contrôlée*' while in the other zones is allowed from 15 June until 15 August. In Italy, irrigation was mainly refused by grape growers also because dry seasons were uncommon and often corresponded with high-quality vintages. Only recently in the areas of production of several DOC/DOCG/IGP wines is not possible to irrigate unless as an emergency procedure. Mediterranean climate, with warm and dry summers and cool and wet winters, is indeed considered optimal for viticulture. However, recent heat waves and heavy rainfalls in a short timespan have led to situations of water shortages, in particular in summer, with transient drought events more or less long lasting with serious repercussions on grapevine physiology. Moreover, these phenomena may decrease sustainability of viticulture in regions where grapes have been traditionally cultivated and shift the grape production to new regions (Hannah et al., 2013). Thus, the ongoing climate changes might lead to having to irrigate the vines to ensure an appropriate yield and in extreme cases plants survival. For this purpose, it is suitable to adopt a proper and better managing of the irrigation in the vineyards in order to maximize the efficiency of water use (WUE) in circumstances of water scarcity. Several deficit irrigation strategies have been implemented and in all of them the amount of water supplied is lower than the crop evapotranspiration (ETc) (Fereres and Soriano, 2007). The main techniques used in viticulture for the control of the irrigation are the *regulated deficit irrigation* (RDI) where plant water status is kept in a situation of mild deficit in specific developmental stages and the *partial rootzone drying* (PRD) where, alternatively, half roots are exposed to drying state while the other half is irrigated (Chaves et al., 2007) with a shifting rhythm of 10-15 days. Nevertheless, the management of the irrigation is still wholly in the hands of the grape growers. To help them in this difficult task, as an example, the Italian Ministry of Agricultural, Food and Forestry Policies (MiPAAF) in collaboration with the National Association of Land Reclamation of Irrigation and Land Improvements (ANBI) launched an app called IRRIFRAME. It gives all the information for a cautious and efficient water usage while maintaining high, or even improving, productivity of crops. Moreover, it provides functional services that indicate to the farmers when irrigate and the amount of water to use based on data that include the water balance of the soil, the crop developmental stage, the air temperature, rainfall and evaporative demand. For the specific case of the Italian region where these experiments have been conducted, i.e. Friuli Venezia Giulia, the Consortium Ledra-Tagliamento provides this kind of information together with the regional government agricultural services (ERSA).

Generally, the water demand increases during the season. From bud-burst to flowering, there is a low water use assessed at less than the 5% of the annual water usage; from flowering to fruit set this percentage rise up to 15%. From fruit set to veraison vines need a higher amount of water evaluate as the 60% of the total water usage. Then from veraison to harvest the water required for ripening is about 20%. Finally from harvest to leaf fall, vines need little amount of water evaluate at 3-5% (Wample and Smithyman, 2002).

1.4 Grapevine responses to water deficit

The genotype x environment (GxE) interaction is the source of the main variability in the responses to abiotic stresses. The phenotypic plasticity showed by a specific cultivar is indeed the ability to change the phenotype in response to the environmental conditions (Nicotra et al., 2010) in order to avoid or tolerate the stress, namely adaptation and acclimation process (Levitt, 1980). Among the abiotic factors that can influence plant physiology, water availability, in particular water deficit, is the most relevant: it can influence plant growth, plant yield and fruit quality. Moreover, different cultivars show different physiologic, genetic and metabolic responses to water deficit.

Water deficit limits the vegetative development of the vines. The first visible symptoms on grapevine morphology are the inhibition of the shoot and internode growth, a decrease in the angle formed by the axis of the leaf petiole and the plane of the lamina. With the progression of the deficit, there is necrosis of the shoot apex and eventually leaf abscission (Williams and Matthews, 1990). In addition, there is a reduction in the stomatal conductance, in the xylem conductivity together with a reduction of the vessel size, thus avoiding embolism and limiting transpiration (Lovisolo and Schubert, 1998). Consequently leaf water potential drops. However different genotypes showed different responses to the water potential decrement. Precisely vines can be classified as isohydric and anisohydric. Isohydric varieties, also called 'pessimists', tend to keep the leaf water potential constant preserving their hydric resources, promptly closing the stomata, thus reducing transpiration and water loss under the control of the hormone abscisic acid. To the other hand, anisohydric, called also 'optimists', reduce their water potential as the water availability decrease with a soft stomatal closure management (Schultz, 2003). This is not a strict classification because further studies showed that the same varieties can act as iso- or anisohydric depending on the timing and the severity of the deficit and therefore they can be collocated as near iso/anisohydric (Lovisolo et al., 2010). Roots, in response to water deficit, acidify the apoplast by protons pumped from the cytoplasm, stimulating thus the action of expansins and leading to the initiation of new roots (Lovisolo et al., 2010). Moreover, in the roots of vines under water deficit it is observed a process of suberization of the endodermal and exodermal cell walls (Vandeleur et al., 2009). Furthermore, water deficit stimulate the expression of genes encoding for aquaporins, which control the radial movement of water through the roots.

Water deficit limits the photosynthesis rate and hence the photooxidative damages. Depending on the magnitude of the deficit (mild, moderate or severe), different responses can happen linked with stomatal conductance. Under mild to moderate stress, the activity of the enzymes involved in the Calvin cycle are maintained constant and there is no reduction in the maximum rates of carboxylation (V_{cmax}) and electron transport (J_{max}) and moreover it is not observed an increase in photoprotection mechanics or heat energy dissipation, indicating that photosynthesis is quite resilient to water deficit. Only in cases of severe deficit (i.e. when stomatal conductance drops below 50 mmol H_2O m^{-2} s^{-1}), there is a reduction of these parameters and the enzymes involved in the Calvin cycle, in particular the RuBisCo, are impaired (Chaves et al., 2010; Lovisolo et al., 2010).

Water deficit reduces berry size, hence cluster weight, clusters per vine and vine yield in the current season and also in the following one affecting bud flower differentiation (Matthews and Anderson, 1989). The extent of this reduction varies depending on when deficit is imposed. If water deficit is imposed in phase I during berry development the reduction is greater than if water deficit is imposed in phase III during berry ripening (Matthews et al., 1987; McCarthy, 1997).

Water deficit affects both the primary and the secondary metabolism of the berry.

The effect of water deficit on the accumulation and subsequently degradation of the organic acids is not univocal. However, no differences in titratable acidity are recorded in the fully ripe berry of Merlot (Sivilotti et al., 2005; Bucchetti et al., 2011; Herrera et al., 2015), although Deluc et al. (2009) reported a reduction in TA in Chardonnay but not in Cabernet Sauvignon. Moreover, the malate/tartrate ratio is reduced under water deficit due to malate catabolism enhanced by warm temperature (Conde et al., 2007) when the clusters are unsheltered by leaves which abscission is promoted by deficit.

The effect of the water deficit on the sugar accumulation is variable and is cultivar dependent (Gaudillère et al., 2002). A moderate water deficit promotes the accumulation of sugar as a results of the inhibited lateral shoot growth, inducing thus a reallocation of carbohydrates to fruits, or as a direct effect of the abscisic acid signaling on fruit ripening (Chaves et al., 2010). Several study showed that water deficit increased the sugar concentration of berry under water deficit at harvest (Castellarin et al., 2007a; Castellarin et al., 2007b; Deluc et al., 2009)

The effect of water deficit on the amino acid affected several biosynthetic and catabolic routes. Among them, proline is the most abundant amino acid and acts as a osmoprotectants and is enhanced by water deficit especially after veraison (Matthews and Anderson, 1988; Deluc et al., 2009).

The effect of water deficit on the phenylpropanoid and flavonoid pathway is well studied. The class of phenolics most influenced by water deficit, in the red varieties, is the anthocyanins which synthesis is enhanced by water deficit (Castellarin et al., 2007a; Castellarin et al., 2007b; Deluc et al., 2009; Bucchetti et al., 2011; Herrera et al., 2015) together with the promotion of structural genes of the flavonoid pathway and in particular the transcription factors *MYBA1-2* and the gene under their regulation, the *UFGT*. Moreover, water deficit affects not only the concentration of anthocyanins but also their composition. Water deficit increases the concentration of tri-hydroxylated anthocyanins, which shifted the anthocyanin profile of grapes under water deficit towards an enrichment of purple/blue pigments, up-regulating the expression of the flavonoid-3',5'-hydroxylase genes (Castellarin et al., 2007a; Castellarin et al., 2007b; Ollé et al., 2011). Proanthocyanidins are in general less affected by water deficit resulting in a slight increase of their concentration or in a null effect (Ojeda et al., 2002; Roby et al., 2004; Bucchetti et al., 2011; Herrera et al., 2015). Water deficit affected also flavonols synthesis increasing their concentration especially in white cultivars compared to the red (Deluc et al., 2009). Moreover, synthesis of stilbenes is enhanced under water deficit, with a higher effect in the red variety Cabernet Sauvignon where there are present 12 single nucleotide

polymorphisms causing eight modifications in the promoter region make that genotype more susceptible to water deficit (Deluc et al., 2011).

The effect of water deficit on the aroma production is less studied compared to the other compounds previously mentioned and more studies are dedicated to the effect of water deficit on the aromatic composition and sensory properties of wine rather than the concentration of volatile precursors in grape berries. Song et al. (2012) and Ou et al. (2010) analyzed respectively the aromatic composition of Merlot grapes and wines under water deficit. In grapes, there is a reduction of C_6 compounds (hexanal, 2-hexenal, hexanol) and an increase of glycosylated terpenoid, mainly nerol and geraniol. No differences were found on the free terpenoids, which are present in small amount. Moreover, water deficit increased the concentration of the C_{13}-norisoprenoids β-damascenone both in the free and glycosylated form. Wines produced from vines under water stress had higher concentrations of terpenoids together with higher concentration of β-damascenone. However, no effect on the concentration of terpenoids was detected by Qian et al. (2009) in Merlot wines produced from plants under water deficit. Moreover, descriptive sensory analysis on Cabernet Sauvignon produced with vines under water deficit revealed a higher presence of red/blackberry aroma, jam/cooked berry aroma, dried fruit/raisin aroma and fruity by mouth compared to the wines produce from fully irrigated vines (Chapman et al., 2005).

The role of the hormone abscisic acid (ABA) in response to abiotic stresses, in particular to water deficit, is largely recognized. Firstly, ABA is the long signal produced in the roots after sensing soil water deficit, it is transported via xylem to the shoot and it is involved in stomatal regulation in vines under water deficit even though ABA is also synthetized in situ in the leaves maybe stimulated by a second root to shoot signal such as phaseic acid or cytokinins and it could be the major responsible of stomata closure (Lovisolo et al., 2010). Moreover, ABA is the hormone that promotes berry ripening and its concentration increase at the onset of ripening when sugars start to accumulate in the vacuole of the berries (Gambetta et al., 2010). Deluc et al. (2009) reported that genes involved in ABA biosynthesis, namely 9-cis-epoxycarotenoid dioxygenases (*NCED*), are enhanced by water deficit in the berry as it is enhanced the concentration of ABA.

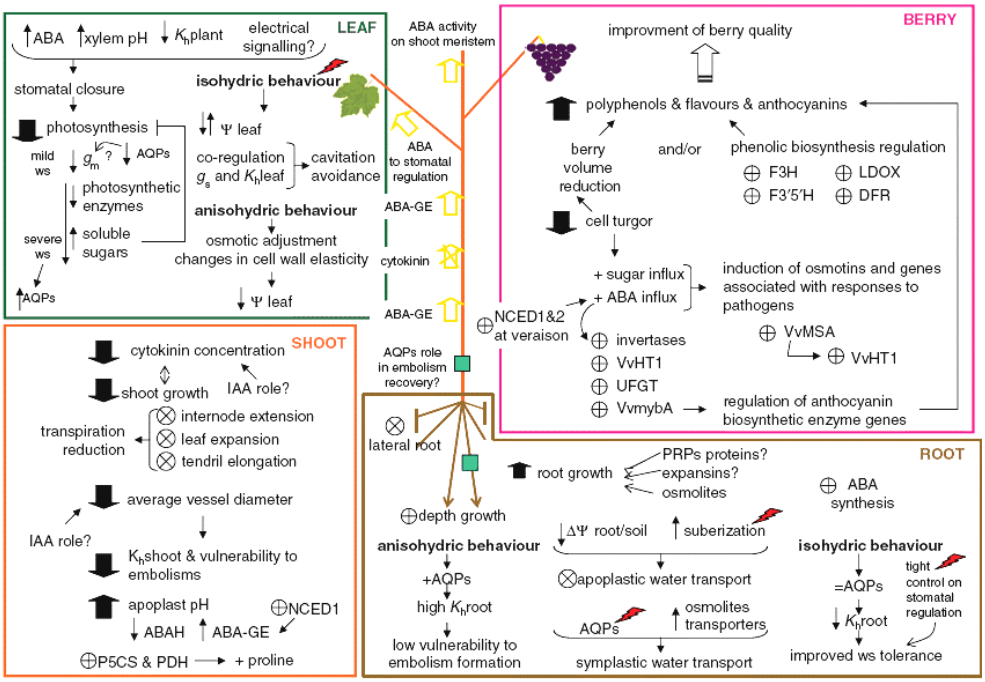

Figure 6. Schematic representation of the effect of water deficit on grapevine (Lovisolo et al., 2010).

In the four panels are outlined the major effects of water deficit on the grapevine root, shoot, leaf and berry.

References

Afoufa-Bastien D, Medici A, Jeauffre J, Coutos-Thévenot P, Lemoine R, Atanassova R, Laloi M (2010) The *Vitis vinifera* sugar transporter gene family: phylogenetic overview and macroarray expression profiling. BMC Plant Biol **10**: 245

Arabidopsis Genome Initiative (2000) Analysis of the genome sequence of the flowering plant *Arabidopsis thaliana*. Nature **408**: 796–815

Arroyo-García R, Ruiz-García L, Bolling L, Ocete R, López MA, Arnold C, Ergul A, Söylemezolu G, Uzun HI, Cabello F, et al (2006) Multiple origins of cultivated grapevine (*Vitis vinifera* L. ssp. sativa) based on chloroplast DNA polymorphisms. Mol Ecol **15**: 3707–3714

Battilana J, Costantini L, Emanuelli F, Sevini F, Segala C, Moser S, Velasco R, Versini G, Grando MS (2008) The 1-deoxy-d-xylulose 5-phosphate synthase gene co-localizes with a major QTL affecting monoterpene content in grapevine. Theor Appl Genet **118**: 653–669

Battilana J, Emanuelli F, Gambino G, Gribaudo I, Gasperi F, Boss PK, Grando MS (2011) Functional effect of grapevine 1-deoxy-D-xylulose 5-phosphate synthase substitution K284N on Muscat flavour formation. J Exp Bot **62**: 5497–5508

Bavaresco L, Petegolli D, Cantù E, Fergoni M, Chiusa G, Trevisan M (1997) Elicitation and accumulation of stilbene phytoalexins in grapevine berries infected by *Botrytis cinerea*. VITIS - J Grapevine Res **36**: 77–83

Bogs J, Downey MO, Harvey JS, Ashton AR, Tanner GJ, Robinson SP (2005) Proanthocyanidin synthesis and expression of genes encoding leucoanthocyanidin reductase and anthocyanidin reductase in developing grape berries and grapevine leaves. Plant Physiol **139**: 652–663

Bogs J, Jaffé FW, Takos AM, Walker AR, Robinson SP (2007) The grapevine transcription factor VvMYBPA1 regulates proanthocyanidin synthesis during fruit development. Plant Physiol **143**: 1347–1361

Bohlmann J, Keeling CI (2008) Terpenoid biomaterials. Plant J **54**: 656–669

Bönisch F, Frotscher J, Stanitzek S, Rühl E, Wüst M, Bitz O, Schwab W (2014a) Activity-based profiling of a physiologic aglycone library reveals sugar acceptor promiscuity of family 1 UDP-glucosyltransferases from grape. Plant Physiol **166**: 23–39

Bönisch F, Frotscher J, Stanitzek S, Rühl E, Wüst M, Bitz O, Schwab W (2014b) A UDP-glucose:monoterpenol glucosyltransferase adds to the chemical diversity of the grapevine metabolome. Plant Physiol **165**: 561–581

Bucchetti B, Matthews MA, Falginella L, Peterlunger E, Castellarin SD (2011) Effect of water deficit on Merlot grape tannins and anthocyanins across four seasons. Sci Hortic **128**: 297–305

Caputi L, Carlin S, Ghiglieno I, Stefanini M, Valenti L, Vrhovsek U, Mattivi F (2011) Relationship of changes in rotundone content during grape ripening and winemaking to manipulation of the "peppery" character of wine. J Agric Food Chem **59**: 5565–5571

Castellarin SD, Matthews MA, Di Gaspero G, Gambetta GA (2007a) Water deficits accelerate ripening and induce changes in gene expression regulating flavonoid biosynthesis in grape berries. Planta **227**: 101–112

Castellarin SD, Pfeiffer A, Sivilotti P, Degan M, Peterlunger E, Di Gaspero G (2007b) Transcriptional regulation of anthocyanin biosynthesis in ripening fruits of grapevine under seasonal water deficit. Plant Cell Environ **30**: 1381–1399

Castellarin SD, Gambetta GA, Wada H, Shackel KA, Matthews MA (2011) Fruit ripening in *Vitis vinifera*: spatiotemporal relationships among turgor, sugar accumulation, and anthocyanin biosynthesis. J Exp Bot **62**: 4345–4354

Castellarin SD, Bavaresco L, Falginella L, Gonçalves MIVZ, Di Gaspero G (2012) Phenolics in grape berry and key antioxidants. In: The Biochemistry of the Grape Berry, edited by Gerós H, Chavez MM, and Delrot S. Bentham Science Publishers. pp: 89–110

Cavallini E, Zenoni S, Finezzo L, Guzzo F, Zamboni A, Avesani L, Tornielli GB (2014) Functional diversification of grapevine MYB5a and MYB5b in the control of flavonoid biosynthesis in a Petunia anthocyanin regulatory mutant. Plant Cell Physiol **55**: 517–534

Cavallini E, Matus JT, Finezzo L, Zenoni S, Loyola R, Guzzo F, Schlechter R, Ageorges A, Arce-Johnson P, Tornielli GB (2015) The phenylpropanoid pathway is controlled at different branches by a set of R2R3-MYB C2 repressors in grapevine. Plant Physiol **167**: 1448–1470

Cazzonelli CI, Pogson BJ (2010) Source to sink: regulation of carotenoid biosynthesis in plants. Trends Plant Sci **15**: 266–274

Chapman DM, Roby G, Ebeler SE, Guinard J-X, Matthews MA (2005) Sensory attributes of Cabernet Sauvignon wines made from vines with different water status. Aust J Grape Wine Res **11**: 339–347

Chaves MM, Santos TP, Souza CR, Ortuño MF, Rodrigues ML, Lopes CM, Maroco JP, Pereira JS (2007) Deficit irrigation in grapevine improves water-use efficiency while controlling vigour and production quality. Ann Appl Biol **150**: 237–252

Chaves MM, Zarrouk O, Francisco R, Costa JM, Santos T, Regalado AP, Rodrigues ML, Lopes CM (2010) Grapevine under deficit irrigation: hints from physiological and molecular data. Ann Bot **105**: 661–676

Chen F, Tholl D, Bohlmann J, Pichersky E (2011) The family of terpene synthases in plants: a mid-size family of genes for specialized metabolism that is highly diversified throughout the kingdom. Plant J **66**: 212–229

Choat B, Gambetta GA, Shackel KA, Matthews MA (2009) Vascular function in grape berries across development and its relevance to apparent hydraulic isolation. Plant Physiol **151**: 1677–1687

Conde C, Silva P, Fontes N, Dias ACP, Tavares RM, Sousa MJ, Agasse A, Delrot S, Gerós H (2007) Biochemical changes throughout grape berry development and fruit and wine quality. Food **1**: 1–22

Conde A, Regalado A, Rodrigues D, Costa JM, Blumwald E, Chaves MM, Gerós H (2015) Polyols in grape berry: transport and metabolic adjustments as a physiological strategy for water-deficit stress tolerance in grapevine. J Exp Bot **66**: 889–906

Coombe BG (1976) The development of fleshy fruits. Annu Rev Plant Physiol **27**: 207–228

Coombe BG (1995) Growth stages of the grapevine: adoption of a system for identifying grapevine growth stages. Aust J Grape Wine Res **1**: 104–110

Costantini L, Malacarne G, Lorenzi S, Troggio M, Mattivi F, Moser C, Grando MS (2015) New candidate genes for the fine regulation of the colour of grapes. J Exp Bot **66**: 4427–4440

Cunningham FX, Gantt E (1998) Genes and enzymes of carotenoid biosynthesis in plants. Annu Rev Plant Physiol Plant Mol Biol **49**: 557–583

Czemmel S, Stracke R, Weisshaar B, Cordon N, Harris NN, Walker AR, Robinson SP, Bogs J (2009) The grapevine R2R3-MYB transcription factor VvMYBF1 regulates flavonol synthesis in developing grape berries. Plant Physiol **151**: 1513–1530

Czemmel S, Heppel SC, Bogs J (2012) R2R3 MYB transcription factors: key regulators of the flavonoid biosynthetic pathway in grapevine. Protoplasma **249**: 109–118

Da Silva C, Zamperin G, Ferrarini A, Minio A, Molin AD, Venturini L, Buson G, Tononi P, Avanzato C, Zago E, et al (2013) The high polyphenol content of grapevine cultivar Tannat berries is conferred primarily by genes that are not shared with the reference genome. Plant Cell **25**: 4777–4788

Dai ZW, Ollat N, Gomès E, Decroocq S, Tandonnet JP, Bordenave L, Pieri P, Hilbert G, Kappel C, Van Leeuwen C, et al (2011) Ecophysiological, genetic, and molecular causes of variation in grape berry weight and composition: a review. Am J Enol Vitic **62**: 413–425

Darriet P, Thibon C and Dubourdieu D (2012) Aroma and aroma precursors in grape berry. In: The Biochemistry of the Grape Berry, edited by Gerós H, Chavez MM, and Delrot S. Bentham Science Publishers. pp: 111–136

Davies C, Boss PK, Gerós H, Lecourieux F and Delrot S (2012) Source/Sink relationships and molecular biology of sugar accumulation in grape berries. In: The Biochemistry of the Grape Berry, edited by Gerós H, Chavez MM, and Delrot S. Bentham Science Publishers. pp: 44–66

DeBolt S, Cook DR, Ford CM (2006) l-Tartaric acid synthesis from vitamin C in higher plants. Proc Natl Acad Sci **103**: 5608–5613

Deluc L, Barrieu F, Marchive C, Lauvergeat V, Decendit A, Richard T, Carde J-P, Mérillon J-M, Hamdi S (2006) Characterization of a grapevine R2R3-MYB transcription factor that regulates the phenylpropanoid pathway. Plant Physiol **140**: 499–511

Deluc LG, Grimplet J, Wheatley MD, Tillett RL, Quilici DR, Osborne C, Schooley DA, Schlauch KA, Cushman JC, Cramer GR (2007) Transcriptomic and metabolite analyses of Cabernet Sauvignon grape berry development. BMC Genomics **8**: 1–42

Deluc L, Bogs J, Walker AR, Ferrier T, Decendit A, Merillon J-M, Robinson SP, Barrieu F (2008) The transcription factor VvMYB5b contributes to the regulation of anthocyanin and proanthocyanidin biosynthesis in developing grape berries. Plant Physiol **147**: 2041–2053

Deluc LG, Quilici DR, Decendit A, Grimplet J, Wheatley MD, Schlauch KA, Mérillon JM, Cushman JC, Cramer GR (2009) Water deficit alters differentially metabolic pathways affecting important flavor and quality traits in grape berries of Cabernet Sauvignon and Chardonnay. BMC Genomics **10**: 212

Deluc LG, Decendit A, Papastamoulis Y, Mérillon J-M, Cushman JC, Cramer GR (2011) Water deficit increases stilbene metabolism in Cabernet Sauvignon berries. J Agric Food Chem **59**: 289–297

Drew DP, Andersen TB, Sweetman C, Møller BL, Ford C, Simonsen HT (2015) Two key polymorphisms in a newly discovered allele of the *Vitis vinifera* TPS24 gene are responsible for the production of the rotundone precursor α-guaiene. J Exp Bot erv491

Emanuelli F, Battilana J, Costantini L, Cunff LL, Boursiquot JM, This P, Grando MS (2010) A candidate gene association study on muscat flavor in grapevine (*Vitis vinifera* L.). BMC Plant Biol **10**: 241

Falginella L, Castellarin SD, Testolin R, Gambetta GA, Morgante M, Di Gaspero G (2010) Expansion and subfunctionalisation of flavonoid 3′,5′-hydroxylases in the grapevine lineage. BMC Genomics **11**: 562

Fasoli M, Santo SD, Zenoni S, Tornielli GB, Farina L, Zamboni A, Porceddu A, Venturini L, Bicego M, Murino V, et al (2012) The grapevine expression atlas reveals a deep transcriptome shift driving the entire plant into a maturation program. Plant Cell **24**: 3489–3505

Fereres E, Soriano MA (2007) Deficit irrigation for reducing agricultural water use. J Exp Bot **58**: 147–159

Ford CM (2012) The biochemistry of organic acids in the grape. In: The Biochemistry of the Grape Berry, edited by Gerós H, Chavez MM, and Delrot S. Bentham Science Publishers. pp: 67–88

Fournier-Level A, Hugueney P, Verriès C, This P, Ageorges A (2011) Genetic mechanisms underlying the methylation level of anthocyanins in grape (*Vitis vinifera* L.). BMC Plant Biol **11**: 179

Francisco RM, Regalado A, Ageorges A, Burla BJ, Bassin B, Eisenach C, Zarrouk O, Vialet S, Marlin T, Chaves MM, et al (2013) ABCC1, an ATP Binding Cassette protein from grape berry, transports anthocyanidin 3-*O*-glucosides. Plant Cell **25**: 1840–1854

Fujita A, Goto-Yamamoto N, Aramaki I, Hashizume K (2006) Organ-specific transcription of putative flavonol synthase genes of grapevine and effects of plant hormones and shading on flavonol biosynthesis in grape berry skins. Biosci Biotechnol Biochem **70**: 632–638

Gambetta GA, Matthews MA, Shaghasi TH, McElrone AJ, Castellarin SD (2010) Sugar and abscisic acid signaling orthologs are activated at the onset of ripening in grape. Planta **232**: 219–234

Gatto P, Vrhovsek U, Muth J, Segala C, Romualdi C, Fontana P, Pruefer D, Stefanini M, Moser C, Mattivi F, et al (2008) Ripening and genotype control stilbene accumulation in healthy grapes. J Agric Food Chem **56**: 11773–11785

Gaudillère JP, Van Leeuwen C, Ollat N (2002) Carbon isotope composition of sugars in grapevine, an integrated indicator of vineyard water status. J Exp Bot **53**: 757–763

Goff SA, Ricke D, Lan TH, Presting G, Wang R, Dunn M, Glazebrook J, Sessions A, Oeller P, Varma H, et al (2002) A draft sequence of the rice genome (*Oryza sativa* l. ssp. japonica). Science **296**: 92–100

Gomez C, Terrier N, Torregrosa L, Vialet S, Fournier-Level A, Verriès C, Souquet JM, Mazauric JP, Klein M, Cheynier V, et al (2009) Grapevine MATE-Type proteins act as vacuolar H+-dependent acylated anthocyanin transporters. Plant Physiol **150**: 402–415

Goto-Yamamoto N, Wan GH, Masaki K, Kobayashi S (2002) Structure and transcription of three chalcone synthase genes of grapevine (*Vitis vinifera*). Plant Sci **162**: 867–872

Grimplet J, Hemert JV, Carbonell-Bejerano P, Díaz-Riquelme J, Dickerson J, Fennell A, Pezzotti M, Martínez-Zapater JM (2012) Comparative analysis of grapevine whole-genome gene predictions, functional annotation, categorization and integration of the predicted gene sequences. BMC Res Notes **5**: 213

Grimplet J, Adam-Blondon AF, Bert PF, Bitz O, Cantu D, Davies C, Delrot S, Pezzotti M, Rombauts S, Cramer GR (2014) The grapevine gene nomenclature system. BMC Genomics **15**: 1077

Hannah L, Roehrdanz PR, Ikegami M, Shepard AV, Shaw MR, Tabor G, Zhi L, Marquet PA, Hijmans RJ (2013) Climate change, wine, and conservation. Proc Natl Acad Sci **110**: 6907–6912

Harris JM, Kriedemann PE, Possingham JV (1968) Anatomical aspects of grape berry development. Vitis **7**: 106–109

Havaux M, Dall'Osto L, Bassi R (2007) Zeaxanthin has enhanced antioxidant capacity with respect to all other xanthophylls in *Arabidopsis* leaves and functions independent of binding to PSII antennae. Plant Physiol **145**: 1506–1520

Hayes MA, Davies C, Dry IB (2007) Isolation, functional characterization, and expression analysis of grapevine (*Vitis vinifera* L.) hexose transporters: differential roles in sink and source tissues. J Exp Bot **58**: 1985–1997

Herrera JC, Bucchetti B, Sabbatini P, Comuzzo P, Zulini L, Vecchione A, Peterlunger E, Castellarin SD (2015) Effect of water deficit and severe shoot trimming on the composition of *Vitis vinifera* L. Merlot grapes and wines. Aust J Grape Wine Res **21**: 254–265

Hichri I, Heppel SC, Pillet J, Léon C, Czemmel S, Delrot S, Lauvergeat V, Bogs J (2010) The basic Helix-Loop-Helix transcription factor MYC1 Is involved in the regulation of the flavonoid biosynthesis pathway in grapevine. Mol Plant **3**: 509–523

Hochberg U, Degu A, Toubiana D, Gendler T, Nikoloski Z, Rachmilevitch S, Fait A (2013) Metabolite profiling and network analysis reveal coordinated changes in grapevine water stress response. BMC Plant Biol **13**: 184

Höll J, Vannozzi A, Czemmel S, D'Onofrio C, Walker AR, Rausch T, Lucchin M, Boss PK, Dry IB, Bogs J (2013) The R2R3-MYB transcription factors MYB14 and MYB15 regulate stilbene biosynthesis in *Vitis vinifera*. Plant Cell **25**: 4135–4149

Huang YF, Doligez A, Fournier-Level A, Cunff LL, Bertrand Y, Canaguier A, Morel C, Miralles V, Veran F, Souquet JM, et al (2012) Dissecting genetic architecture of grape proanthocyanidin composition through quantitative trait locus mapping. BMC Plant Biol **12**: 30

Huang YF, Vialet S, Guiraud JL, Torregrosa L, Bertrand Y, Cheynier V, This P, Terrier N (2014) A negative MYB regulator of proanthocyanidin accumulation, identified through expression quantitative locus mapping in the grape berry. New Phytol **201**: 795–809

Jaillon O, Aury JM, Noel B, Policriti A, Clepet C, Casagrande A, Choisne N, Aubourg S, Vitulo N, Jubin C, et al (2007) The grapevine genome sequence suggests ancestral hexaploidization in major angiosperm phyla. Nature **449**: 463–467

Jánváry L, Hoffmann T, Pfeiffer J, Hausmann L, Töpfer R, Fischer TC, Schwab W (2009) A double mutation in the anthocyanin 5-*O*-glucosyltransferase gene disrupts enzymatic activity in *Vitis vinifera* L. J Agric Food Chem **57**: 3512–3518

Keller M, Smith JP, Bondada BR (2006) Ripening grape berries remain hydraulically connected to the shoot. J Exp Bot **57**: 2577–2587

Keller M (2015) The science of grapevines: anatomy and physiology. Academic Press

Khater F, Fournand D, Vialet S, Meudec E, Cheynier V, Terrier N (2012) Identification and functional characterization of cDNAs coding for hydroxybenzoate/hydroxycinnamate glucosyltransferases co-expressed with genes related to proanthocyanidin biosynthesis. J Exp Bot **63**: 1201–1214

Koyama K, Numata M, Nakajima I, Goto-Yamamoto N, Matsumura H, Tanaka N (2014) Functional characterization of a new grapevine MYB transcription factor and regulation of proanthocyanidin biosynthesis in grapes. J Exp Bot **65**: 4433–4449

Lashbrooke JG, Young PR, Dockrall SJ, Vasanth K, Vivier MA (2013) Functional characterisation of three members of the *Vitis vinifera* L. carotenoid cleavage dioxygenase gene family. BMC Plant Biol **13**: 156

Lecourieux F, Kappel C, Lecourieux D, Serrano A, Torres E, Arce-Johnson P, Delrot S (2014) An update on sugar transport and signalling in grapevine. J Exp Bot **65**: 821–832

Levitt J (1980) Responses of plants to environmental stresses. Chilling, freezing, and high temperature stresses. New York Academic Press

Lovisolo C, Schubert A (1998) Effects of water stress on vessel size and xylem hydraulic conductivity in *Vitis vinifera* L. J Exp Bot **49**: 693–700

Lovisolo C, Perrone I, Carra A, Ferrandino A, Flexas J, Medrano H, Schubert A (2010) Drought-induced changes in development and function of grapevine (*Vitis* spp.) organs and in their hydraulic and non-hydraulic interactions at the whole-plant level: a physiological and molecular update. Funct Plant Biol **37**: 98–116

Malacarne G, Costantini L, Coller E, Battilana J, Velasco R, Vrhovsek U, Grando MS, Moser C (2015) Regulation of flavonol content and composition in (Syrah×Pinot Noir) mature grapes: integration of transcriptional profiling and metabolic quantitative trait locus analyses. J Exp Bot **66**: 4441–4453

Martin DM, Aubourg S, Schouwey MB, Daviet L, Schalk M, Toub O, Lund ST, Bohlmann J (2010) Functional annotation, genome organization and phylogeny of the grapevine (*Vitis vinifera*) terpene synthase gene family based on genome assembly, flcdna cloning, and enzyme assays. BMC Plant Biol **10**: 226

Matthews MA, Anderson MM, Schultz HR (1987) Phenologic and growth responses to early and late season water deficits in Cabernet Franc. Vitis **26**: 147–160

Matthews MA, Anderson MM (1988) Fruit ripening in *Vitis Vinifera* L.: responses to seasonal water deficits. Am J Enol Vitic **39**: 313–320

Matthews MA, Anderson MM (1989) Reproductive development in grape (*Vitis vinifera* L.): Responses to seasonal water deficits. Am J Enol Vitic **40**: 52–60

Mattivi F, Guzzon R, Vrhovsek U, Stefanini M, Velasco R (2006) Metabolite profiling of grape: flavonols and anthocyanins. J Agric Food Chem **54**: 7692–7702

Mattivi F, Vrhovsek U, Masuero D, Trainotti D (2009) Differences in the amount and structure of extractable skin and seed tannins amongst red grape varieties. Aust J Grape Wine Res **15**: 27–35

Mattivi F, Caputi L, Carlin S, Lanza T, Minozzi M, Nanni D, Valenti L, Vrhovsek U (2011) Effective analysis of rotundone at below-threshold levels in red and white wines using solid-phase microextraction gas chromatography/tandem mass spectrometry. Rapid Commun Mass Spectrom **25**: 483–488

Matus JT, Poupin MJ, Cañón P, Bordeu E, Alcalde JA, Arce-Johnson P (2010) Isolation of WDR and bHLH genes related to flavonoid synthesis in grapevine (*Vitis vinifera* L.). Plant Mol Biol **72**: 607–620

McCarthy MG (1997) The effect of transient water deficit on berry development of cv. Shiraz (*Vitis vinifera* L.). Aust J Grape Wine Res **3**: 2–8

Mica E, Piccolo V, Delledonne M, Ferrarini A, Pezzotti M, Casati C, Fabbro CD, Valle G, Policriti A, Morgante M, et al (2010) Correction: High throughput approaches reveal splicing of primary microRNA transcripts and tissue specific expression of mature microRNAs in *Vitis vinifera*. BMC Genomics **11**: 109

Myles S, Boyko AR, Owens CL, Brown PJ, Grassi F, Aradhya MK, Prins B, Reynolds A, Chia J-M, Ware D, et al (2011) Genetic structure and domestication history of the grape. Proc Natl Acad Sci **108**: 3530–3535

Nicotra AB, Atkin OK, Bonser SP, Davidson AM, Finnegan EJ, Mathesius U, Poot P, Purugganan MD, Richards CL, Valladares F, et al (2010) Plant phenotypic plasticity in a changing climate. Trends Plant Sci **15**: 684–692

Nisar N, Li L, Lu S, Khin NC, Pogson BJ (2015) Carotenoid metabolism in plants. Mol Plant **8**: 68–82

Nunan KJ, Sims IM, Bacic A, Robinson SP, Fincher GB (1997) Isolation and characterization of cell walls from the mesocarp of mature grape berries (*Vitis vinifera*). Planta **203**: 93–100

Ojeda H, Andary C, Kraeva E, Carbonneau A, Deloire A (2002) Influence of pre- and post-veraison water deficit on synthesis and concentration of skin phenolic compounds during berry growth of *Vitis vinifera* cv. Shiraz. Am J Enol Vitic **53**: 261–267

Ollé D, Guiraud JL, Souquet JM, Terrier N, Ageorges A, Cheynier V, Verries C (2011) Effect of pre- and post-veraison water deficit on proanthocyanidin and anthocyanin accumulation during Shiraz berry development. Aust J Grape Wine Res **17**: 90–100

Ono E, Homma Y, Horikawa M, Kunikane-Doi S, Imai H, Takahashi S, Kawai Y, Ishiguro M, Fukui Y, Nakayama T (2010) Functional differentiation of the glycosyltransferases that contribute to the chemical diversity of bioactive flavonol glycosides in grapevines (*Vitis vinifera*). Plant Cell **22**: 2856–2871

Ou C, Du X, Shellie K, Ross C, Qian MC (2010) Volatile compounds and sensory attributes of wine from cv. Merlot (*Vitis vinifera* L.) grown under differential levels of water deficit with or without a kaolin-based, foliar reflectant particle film. J Agric Food Chem **58**: 12890–12898

Pelsy F (2010) Molecular and cellular mechanisms of diversity within grapevine varieties. Heredity **104**: 331–340

Pérez-Díaz R, Ryngajllo M, Pérez-Díaz J, Peña-Cortés H, Casaretto JA, González-Villanueva E, Ruiz-Lara S (2014) VvMATE1 and VvMATE2 encode putative proanthocyanidin transporters expressed during berry development in *Vitis vinifera* L. Plant Cell Rep **33**: 1147–1159

Pillet J, Egert A, Pieri P, Lecourieux F, Kappel C, Charon J, Gomès E, Keller F, Delrot S, Lecourieux D (2012) VvGOLS1 and VvHsfA2 are involved in the heat stress responses in grapevine berries. Plant Cell Physiol **53**: 1776–1792

Podolyan A, White J, Jordan B, Winefield C (2010) Identification of the lipoxygenase gene family from *Vitis vinifera* and biochemical characterisation of two 13-lipoxygenases expressed in grape berries of Sauvignon Blanc. Funct Plant Biol **37**: 767–784

Qian MC, Fang Y, Shellie K (2009) Volatile composition of Merlot wine from different vine water status. J Agric Food Chem **57**: 7459–7463

Regalado A, Pierri CL, Bitetto M, Laera VL, Pimentel C, Francisco R, Passarinho J, Chaves MM, Agrimi G (2012) Characterization of mitochondrial dicarboxylate/tricarboxylate transporters from grape berries. Planta **237**: 693–703

Rinaldo A, Cavallini E, Jia Y, Moss SMA, McDavid DAJ, Hooper LC, Robinson SP, Tornielli GB, Zenoni S, Ford CM, et al (2015) A grapevine anthocyanin acyltransferase, transcriptionally regulated by VvMYBA, can produce most acylated anthocyanins present in grape skins. Plant Physiol pp.01255.2015

Robinson AL, Boss PK, Solomon PS, Trengove RD, Heymann H, Ebeler SE (2014) Origins of grape and wine aroma. Part 1. Chemical components and viticultural impacts. Am J Enol Vitic **65**: 1–24

Roby G, Harbertson JF, Adams DA, Matthews MA (2004) Berry size and vine water deficits as factors in winegrape composition: Anthocyanins and tannins. Aust J Grape Wine Res **10**: 100–107

Rodríguez-Concepción M, Boronat A (2002) Elucidation of the methylerythritol phosphate pathway for isoprenoid biosynthesis in bacteria and plastids. a metabolic milestone achieved through genomics. Plant Physiol **130**: 1079–1089

Schultz HR (2003) Differences in hydraulic architecture account for near-isohydric and anisohydric behaviour of two field-grown *Vitis vinifera* L. cultivars during drought. Plant Cell Environ **26**: 1393–1405

Shen J, Tieman D, Jones JB, Taylor MG, Schmelz E, Huffaker A, Bies D, Chen K, Klee HJ (2014) A 13-lipoxygenase, TomloxC, is essential for synthesis of C_5 flavour volatiles in tomato. J Exp Bot **65**: 419–428

Siebert TE, Wood C, Elsey GM, Pollnitz AP (2008) Determination of rotundone, the pepper aroma impact compound, in grapes and wine. J Agric Food Chem **56**: 3745–3748

Sivilotti P, Bonetto C, Paladin M, Peterlunger E (2005) Effect of soil moisture availability on Merlot: from leaf water potential to grape composition. Am J Enol Vitic **56**: 9–18

Song J, Shellie KC, Wang H, Qian MC (2012) Influence of deficit irrigation and kaolin particle film on grape composition and volatile compounds in Merlot grape (*Vitis vinifera* L.). Food Chem **134**: 841–850

Sweetman C, Deluc LG, Cramer GR, Ford CM, Soole KL (2009) Regulation of malate metabolism in grape berry and other developing fruits. Phytochemistry **70**: 1329–1344

Takase H, Sasaki K, Shinmori H, Shinohara A, Mochizuki C, Kobayashi H, Ikoma G, Saito H, Matsuo H, Suzuki S, et al (2015) Cytochrome P450 CYP71BE5 in grapevine (*Vitis vinifera*) catalyzes the formation of the spicy aroma compound (−)-rotundone. J Exp Bot erv496

Terrier N, Torregrosa L, Ageorges A, Vialet S, Verriès C, Cheynier V, Romieu C (2009) Ectopic expression of VvMYBPA2 promotes proanthocyanidin biosynthesis in grapevine and suggests additional targets in the pathway. Plant Physiol **149**: 1028–1041

This P, Lacombe T, Thomas MR (2006) Historical origins and genetic diversity of wine grapes. Trends Genet **22**: 511–519

Tuskan GA, DiFazio S, Jansson S, Bohlmann J, Grigoriev I, Hellsten U, Putnam N, Ralph S, Rombauts S, Salamov A, et al (2006) The genome of black cottonwood, *Populus trichocarpa* (Torr. & Gray). Science **313**: 1596–1604

Vandeleur RK, Mayo G, Shelden MC, Gilliham M, Kaiser BN, Tyerman SD (2009) The role of plasma membrane intrinsic protein aquaporins in water transport through roots: diurnal and drought stress responses reveal different strategies between isohydric and anisohydric cultivars of grapevine. Plant Physiol **149**: 445–460

Vannozzi A, Dry IB, Fasoli M, Zenoni S, Lucchin M (2012) Genome-wide analysis of the grapevine stilbene synthase multigenic family: genomic organization and expression profiles upon biotic and abiotic stresses. BMC Plant Biol **12**: 130

Vasconcelos MC, Greven M, Winefield CS, Trought MCT, Raw V (2009) The flowering process of *Vitis vinifera*: a review. Am J Enol Vitic **60**: 411–434

Velasco R, Zharkikh A, Troggio M, Cartwright DA, Cestaro A, Pruss D, Pindo M, FitzGerald LM, Vezzulli S, Reid J, et al (2007) A high quality draft consensus sequence of the genome of a heterozygous grapevine variety. PLoS ONE **2**: e1326

Vidal S, Williams P, O'Neill MA, Pellerin P (2001) Polysaccharides from grape berry cell walls. Part I: tissue distribution and structural characterization of the pectic polysaccharides. Carbohydr Polym **45**: 315–323

Vitulo N, Forcato C, Carpinelli EC, Telatin A, Campagna D, D'Angelo M, Zimbello R, Corso M, Vannozzi A, Bonghi C, et al (2014) A deep survey of alternative splicing in grape reveals changes in the splicing machinery related to tissue, stress condition and genotype. BMC Plant Biol **14**: 99

Walker AR, Lee E, Bogs J, McDavid DAJ, Thomas MR, Robinson SP (2007) White grapes arose through the mutation of two similar and adjacent regulatory genes. Plant J **49**: 772–785

Wample RL, Smithyman R (2002) Regulated deficit irrigation as a water management strategy in *Vitis vinifera* production.

Williams LE, Matthews MA (1990) Grapevine. Irrig Agric Crops **30**: 1019–1055

Wood C, Siebert TE, Parker M, Capone DL, Elsey GM, Pollnitz AP, Eggers M, Meier M, Vössing T, Widder S, et al (2008) From wine to pepper: rotundone, an obscure sesquiterpene, is a potent spicy aroma compound. J Agric Food Chem **56**: 3738–3744

Young PR, Lashbrooke JG, Alexandersson E, Jacobson D, Moser C, Velasco R, Vivier MA (2012) The genes and enzymes of the carotenoid metabolic pathway in *Vitis vinifera* L. BMC Genomics **13**: 243

Yu J, Hu S, Wang J, Wong GKS, Li S, Liu B, Deng Y, Dai L, Zhou Y, Zhang X, et al (2002) A draft sequence of the rice genome (*Oryza sativa* l. ssp. indica). Science **296**: 79–92

Zhang XY, Wang XL, Wang XF, Xia GH, Pan QH, Fan RC, Wu FQ, Yu XC, Zhang DP (2006) A shift of phloem unloading from symplasmic to apoplasmic pathway is involved in developmental onset of ripening in grape berry. Plant Physiol **142**: 220–232

Zhang YL, Meng QY, Zhu HL, Guo Y, Gao HY, Luo YB, Lu J (2007) Functional characterization of a LAHC sucrose transporter isolated from grape berries in yeast. Plant Growth Regul **54**: 71–79

Zhao J, Pang Y, Dixon RA (2010) The mysteries of proanthocyanidin transport and polymerization. Plant Physiol **153**: 437–443

Zhu BQ, Xu XQ, Wu YW, Duan CQ, Pan QH (2012) Isolation and characterization of two hydroperoxide lyase genes from grape berries. Mol Biol Rep **39**: 7443–7455

Zoccatelli G, Zenoni S, Savoi S, Dal Santo S, Tononi P, Zandonà V, Dal Cin A, Guantieri V, Pezzotti M, Tornielli GB (2013) Skin pectin metabolism during the postharvest dehydration of berries from three distinct grapevine cultivars. Aust J Grape Wine Res **19**: 171–179

Preface to Chapter 2: Tocai friulano

Tocai friulano was considered a cultivar adapted since a long time in the territory of Friuli Venezia Giulia (Italy). Recently, its identity has been linked to the French cultivar *Sauvignonasse* or *Sauvignon vert*. It has been confirmed that *Tocai friulano* has no similarity with the Hungarian cultivars *Furmint* or *Harslevelü* used to produce the wine *Tokay*.

The ampelographic features of the vine can be summarized in an expanded, velvety, golden-green in color shoot apex, in a medium-large mature leaf with three lobes and a smooth lamina, glabrous underside.

The vine has a good and regular yield although it may suffer from excessive humidity. Furthermore, excessive water supply can lead to high vigor, causing the clusters to tighten too much and hence making the vine extremely sensitive to *Botrytis cinerea*. It is also sensitive to downy and powdery mildew.

The grape cluster is medium in size, with a truncated-pyramidal shape with two wings; the grape berry is spheroid with pruinose skin and it is yellow-green in color.

Its grapes produce pale straw yellow with greenish reflections wine with elegant hints of white flowers. With evolution, it develops typical scent of dried fruits. Smooth on the palate, sometimes structured and often scarcely sapid.

Information was retrieved from the *Vitis Rauscedo Catalogue – Variety Description Cards*.

Images of Tocai friulano grape bunch and adaxial and abaxial leaf surfaces were retrieved from the *Vitis International Variety Catalogue – VIVC*.

The following chapter is part of a manuscript that has been submitted to BMC Plant Biology.

Chapter 2

TRANSCRIPTOME AND METABOLITE PROFILING REVEALS THAT PROLONGED DROUGHT MODULATES THE PHENYLPROPANOID AND TERPENOID PATHWAY IN WHITE GRAPES (VITIS VINIFERA L.)

Introduction

Plant secondary metabolites include more than 200,000 compounds that display a large chemical diversity while accumulating in specific organs tissues and cells (Hartmann, 2007). They ensure a plant's survival in the environment by performing a multitude of functions, such as defending plant tissues from pathogens or herbivorous attacks, and aiding reproduction by attracting pollinators or seed dispersers (Kliebenstein, 2004). Fruits, generally accumulate a variety of secondary metabolites such as polyphenols, stilbenoids, carotenoids, and free and bound volatile organic compounds (VOCs) (Lund and Bohlmann, 2006; Klee and Giovannoni, 2011). These metabolites affect fruit pigmentation and flavour, and confer to the fruit well-known health benefits. In several fruit crops, the concentration of these metabolites significantly impacts the quality of the fruit and, indeed, the economic value of production. As part of the adaptation mechanism of a plant to its environment, secondary metabolism is sensitive to biotic and abiotic cues (Hartmann, 2007). Hence, in agricultural settings, environmental factors generally impact the accumulation of secondary metabolites in fruits. The effect of climatic constraints on the accumulation of these metabolites should be taken into consideration for developing cultivation strategies that optimize fruit composition and crop economic value.

Grapes are one of the major fruit crops in the world (Ferrandino and Lovisolo, 2014). Dry and warm Mediterranean climates are considered optimal for wine grape production; in these climates, grapes are often produced without artificial irrigation. However, limited water availability results in reduced vine vigor and fruit growth, significant losses in crop yield, and changes in fruit composition (Chaves et al., 2010). Moreover, climate change is predicted to exacerbate drought events in several viticultural areas, and Hannah et al. (2013) postulate that these phenomena may reduce the viability of viticulture in regions where grapes have been traditionally cultivated.

Grapevine berry secondary metabolism is under strong genetic control, and varies among varieties (Mattivi et al., 2006; Degu et al., 2015). Hence, the task of understanding the response of this metabolism to environmental cues is complicated. Several studies have investigated the impact of drought and deficit irrigation strategies on berry secondary metabolism in red grape varieties, focusing specifically on the accumulation of phenolics. Recently, Hochberg et al. (2015) employed large-scale metabolite analyses to investigate the impact of deficit irrigation in Cabernet Sauvignon and Shiraz grapes, and showed cultivar specificity in the magnitude of response. In general, it is recognized that moderate and severe

water deficits promote the synthesis and increased concentration of flavonoids in the berry (Teixeira et al., 2013), often resulting into better sensory attributes of wines (Chapman et al., 2005; Herrera et al., 2015). Besides phenolics, many other secondary metabolites accumulate in the grape berry. These include carotenoids (Young et al., 2012) and VOCs such as C_{13}-norisoprenoids, terpenes, aldehydes, ketones, esters, and alcohols (Robinson et al., 2014). The information on the effect of water deficit on the accumulation of these metabolites is scant. Deluc et al. (2009) adopted a microarray platform to investigate differences in the transcriptome response to water deficit between Cabernet Sauvignon, a red grape variety, and Chardonnay, a white grape variety. The study revealed that genes of several secondary metabolic pathways were modulated by water deficit and this metabolic response varied with the cultivar considered. In Chardonnay grapes, water deficit increased the level of expression of one terpene synthase, indicating that terpenoids might be part of the metabolic response to water deficit. The effect of water deficit on secondary metabolism remains largely unexplored in fruits; particularly, very little information is available on the effect of this deficit on the concentration of VOCs, key determinants of fruit economic value, and in the case of wine grapes, of the wine sensory features.

In this study, we employed large-scale metabolite and transcript profiling to evaluate the impact of water deficit on berry secondary metabolite composition in white grapes. We hypothesize that water deficit may activate the terpenoid pathway and the production of monoterpenes. An open field experiment was conducted in a North Italian viticultural area characterized by transient drought events during the summer. Two different water regimes were applied to Tocai friulano vines for two consecutive seasons, and the effect of water deficit on phenolic, carotenoid, tocopherol, and free VOC accumulation was investigated at different stages of berry development. Finally, an integrated network analysis was undertaken to investigate the impact of the water deficit on metabolite-metabolite and metabolite-transcript interactions in developing grapes.

Results

Impact of irrigation treatment on plant water status, yield, berry growth, soluble solids, and titratable acidity

Two water treatments were applied to vines during the seasons. Irrigated vines (defined as C henceforward) were weekly irrigated in order to keep their stem water potential (Ψ_{Stem}) above -0.8 MPa, whereas vines subjected to deficit irrigation (defined as D henceforward) were not irrigated from fruit set until harvest, unless they displayed signs of extreme water deficit: Ψ_{Stem} lower than -1.4 MPa and fading of the canopy.

In 2011, abundant rainfalls occurred during the first part of the season (Fig. 1a) and during the week preceding the onset of fruit ripening (called "veraison"). Hence, Ψ_{Stem} was similar between treatments until 89 days after anthesis (DAA), except at 49 and 60 DAA when Ψ_{Stem} was slightly lower in D vines (Fig. 1c). The prolonged drought event associated with high mean temperatures recorded from 65 DAA to harvest induced a progressive decrease of Ψ_{Stem} from about 70 DAA. This decrease was buffered by irrigation in C vines, while it was steep in D vines. In 2012, rainfalls during the summer were very limited (Fig. 1b) and mean temperatures peaked just before veraison. Ψ_{Stem} of D vines decreased from early stages of fruit development (Fig. 1d) while Ψ_{Stem} of C vines generally remained above -0.8 MPa. Ψ_{Stem} of D vines reached the seasonal minimum (-1.5 MPa) at 67 DAA. Three irrigations together with some rainfalls initiated a partial recovery of Ψ_{Stem} values in D vines during the last part of the season.

Irrigation treatments significantly affected vine productivity only in 2012, when D reduced both cluster weight and yield per vine (Table 1). In 2011, D reduced berry weight at 62 DAA and at harvest (Fig. 1e), while in 2012, D severely reduced berry weight during most part of the season (Fig. 1f). Water deficit did not affect total soluble solids (a good indicator of sugar concentration) in 2011 (Fig. 1g), but produced increased soluble solids before veraison (41 and 54 DAA) and at harvest (93 DAA) in 2012 (Fig. 1h). Titratable acidity (Fig 1g,h) was increased before veraison (46 and 41 DAA in 2011 and 2012 respectively) and decreased during berry ripening (105 DAA in 2011 and 68 and 82 DAA in 2012).

Table 1. Effect of water deficit on crop production. Cluster per vine, cluster weight and yield per vine of fully irrigated (C, controls) and deficit irrigated (D, water deficit) grapevines in 2011 and 2012. Values are averages ± the standard error. Differences between treatments ($P<0.05$) were assessed with a one-way ANOVA. The level of significance is reported within the columns: * or ns, $P < 0.05$ or not significant, respectively

	Tocai friulano			
Year	2011		2012	
Treatment	C	D	C	D
Cluster per Vine	13.9 ± 2.2	14.9 ± 2.3	20.1 ± 2.6	18.4 ± 2.0
	ns		ns	
Cluster Weight (g)	228.1 ± 24.5	210.3 ± 27.3	170.5 ± 10.8	139.4 ± 15.5
	ns		*	
Yield per Vine (Kg)	3.18 ± 0.60	3.08 ± 0.48	3.27 ± 0.25	2.52 ± 0.26
	ns		*	

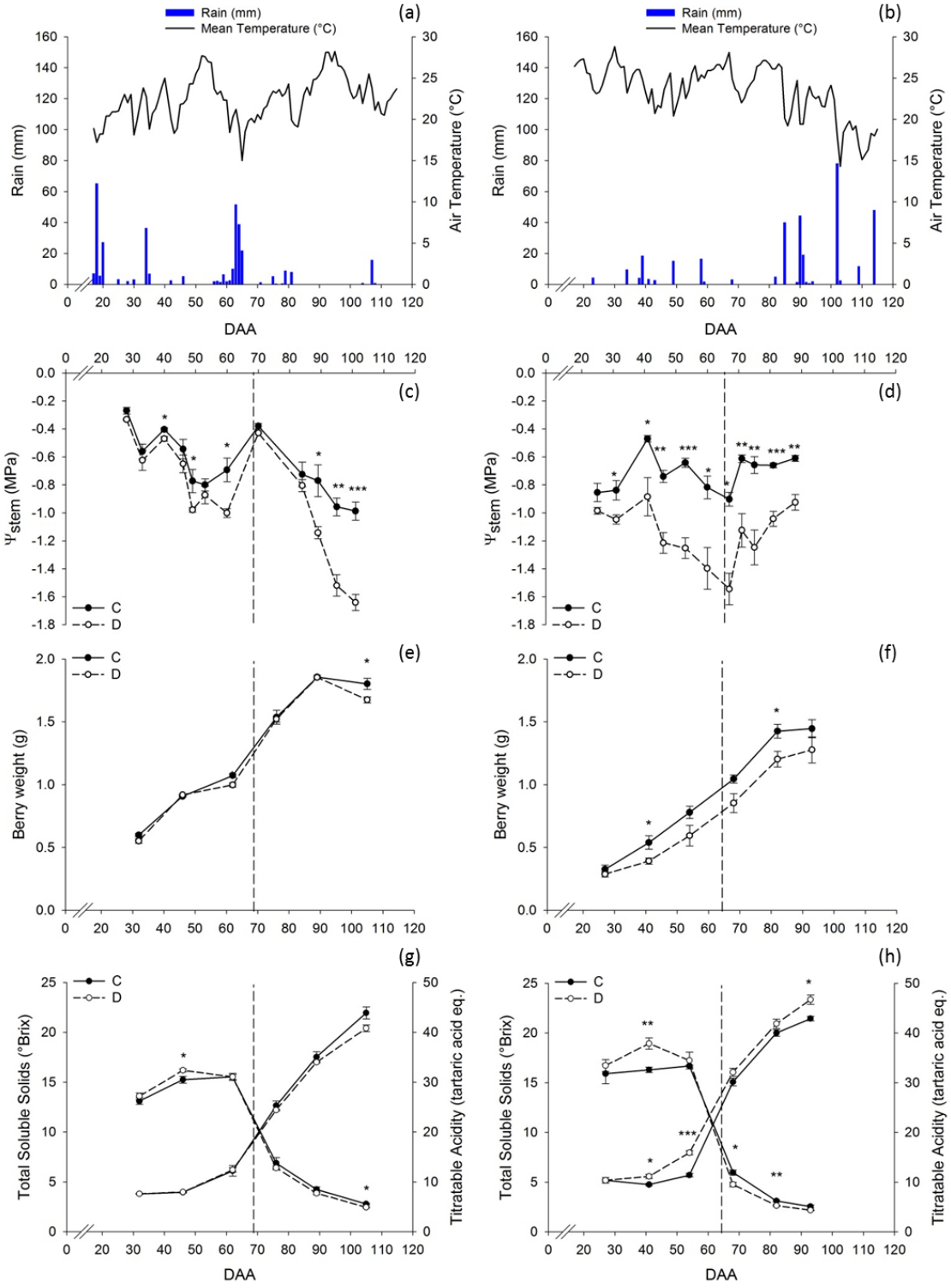

Figure 1. Weather conditions at the experimental site and impact of irrigation treatments on plant and fruit physiology. Daily rainfall and average temperature in 2011 (a) and 2012 (b). Progress of (c, d) stem water potential (ΨStem), (e, f) berry weight, and (g, h) sugar accumulation and titratable acidity in fully irrigated (C) and deficit irrigated (D) vines in 2011 (left hand panels) and 2012 (right hand panels). Dotted lines indicate the onset of ripening (veraison). Bars represent ±SE. Asterisks indicate significant differences between treatments at P<0.05 (*), P<0.01 (**), P<0.001 (***) evaluated by one-way ANOVA.

Impact of water deficit on secondary metabolites

Berries were sampled for secondary metabolite analyses six times during the seasons: three times before veraison (32, 46, and 62 DAA in 2011 and 27, 41, and 54 DAA 2012), one at the onset of ripening (76 DAA in 2011 and 68 DAA in 2012), one at mid-ripening (89 DAA in 2011 and 82 DAA in 2012), and one at the end of ripening (105 DAA in 2011 and 93 DAA in 2012) that coincided with the harvest date of the vineyard.

In 2011, water deficit reduced the concentration of several phenolics in the berry (Fig. 2a, Figure S1) – procyanidin B2+B4, epicatechin, pallidol, gallic acid, catechin, procyanidin B3, epigallocatechin gallate, phlorizin, procyanidin B1, caffeic acid-catechin condensation product, and rutin – but the differences were observed mostly at the latest developmental stages. Only one phenolic compound, astringin, was more concentrated in D than in C berries, and only at one early stage. D also decreased carotenoid and tocopherol concentration at specific developmental stages (Fig. 2b, Figure S2); however, there were no big differences in their concentration between treatments. Only four VOCs (hotrienol, nerol, 1-octen-3-ol, and 1-octen-3-one) were transiently affected by water deficit during berry development; all of them but nerol were reduced in D (Fig. 2c, Figure S3).

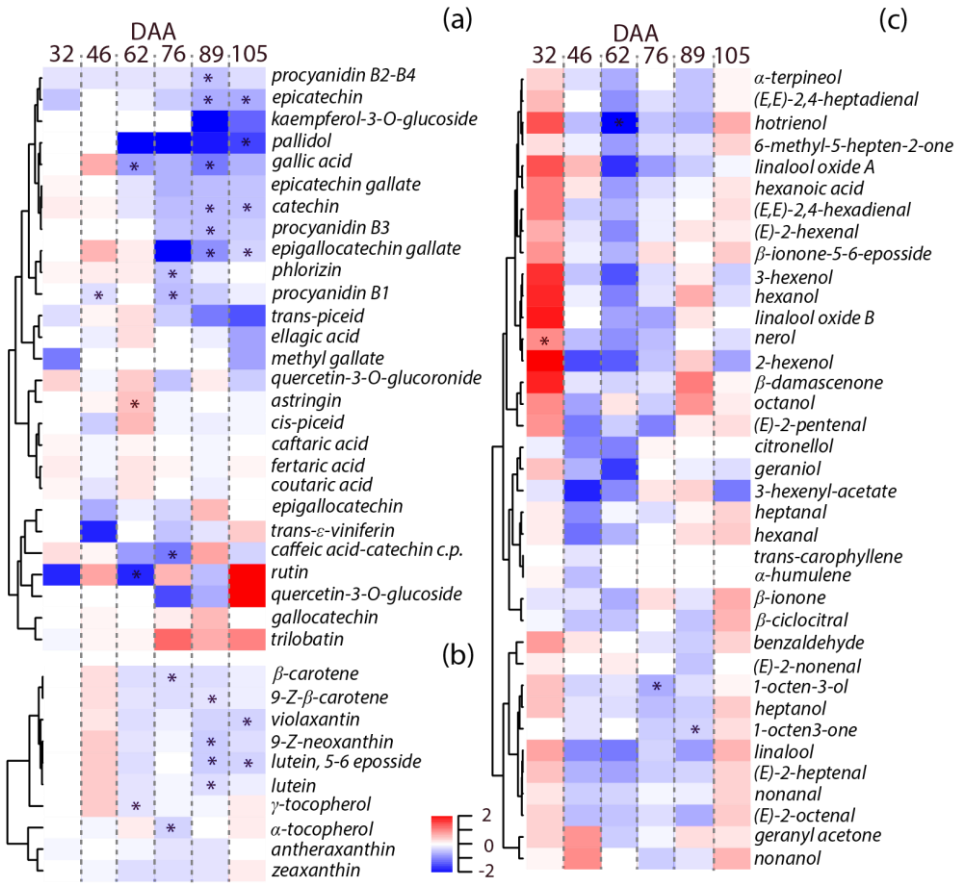

Figure 2. Effect of water deficit on secondary metabolites during fruit development in 2011. Heatmaps represent $\log_2$ fold change (D/C) of the (a) phenolic, (b) carotenoid and tocopherol, and (c) VOC concentration under water deficit conditions at 32, 46, 62, 76, 89, 105 DAA. Blue and red boxes indicate lower and higher concentration in D, respectively. Asterisks indicate significant differences ($P<0.05$) between treatments. Metabolites were hierarchically clustered based on their response to water deficit.

In 2012, water deficit affected the concentration of 20 out of 27 phenolics at one or more developmental stages (Fig. 3a, Figure S1). Water deficit generally increased the concentration of benzoic and cinnamic acids and modulated the accumulation of flavan-3-ols and proanthocyanidins. Their concentration was increased and decreased by water deficit before (27, 41, and 54 DAA) and after (68, 82, and 93 DAA) veraison, respectively. Limited effects of water deficit on stilbenoid accumulation were observed. In contrast, D largely affected the accumulation of carotenoid and tocopherols in the berry (Fig. 3b, Figure S2). The concentration of most carotenoids was increased and decreased in D before and after veraison, respectively. Zeaxanthin, α-tocopherol, and γ-tocopherol concentrations were higher in D than in C after veraison. Water deficit also increased the concentration of 12 VOCs (Fig. 3c, Figure S3) late during fruit development (93 DAA). At this stage, D promoted the accumulation of monoterpenes such as hotrienol, linalool, nerol, and α-terpineol.

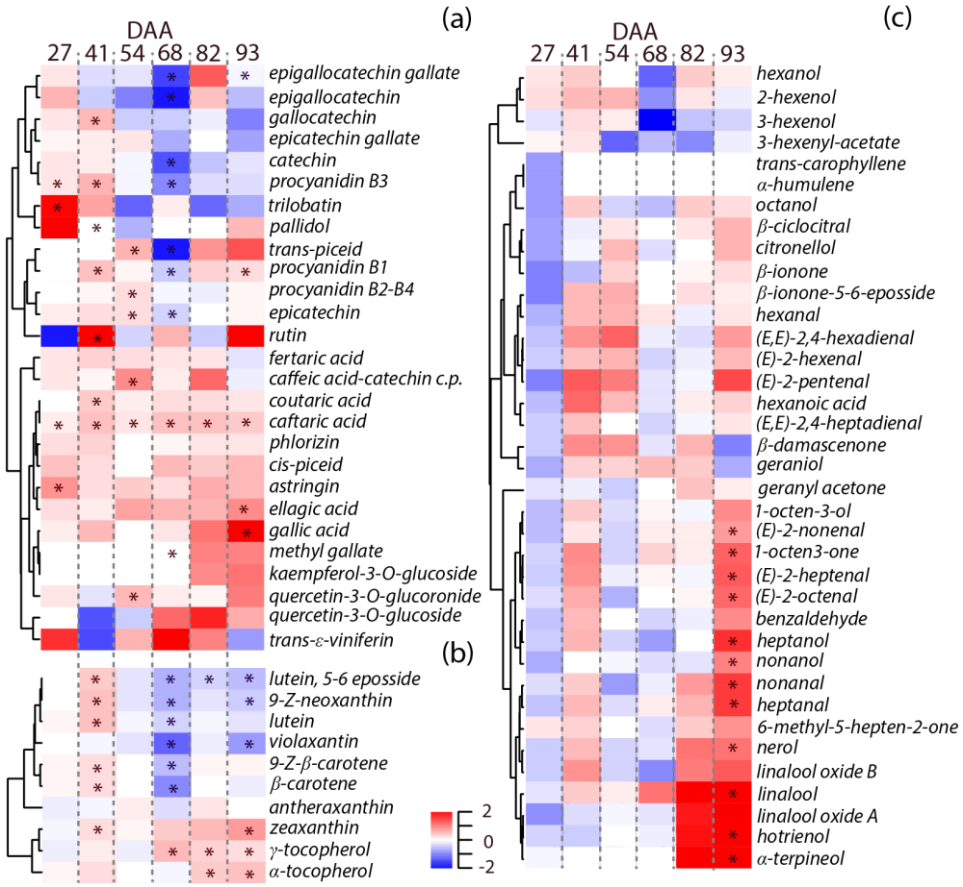

Figure 3. Effect of water deficit on secondary metabolites during fruit development in 2012. Heatmaps represent $\log_2$ fold change (D/C) of the (a) phenolic, (b) carotenoid and tocopherol, and (c) VOC concentration under water deficit conditions at 27, 41, 51, 68, 82, 93 DAA. Blue and red boxes indicate lower and higher concentration in D, respectively. Asterisks indicate significant differences ($P<0.05$) between treatments. Metabolites were hierarchically clustered based on their response to water deficit.

Impact of water deficit on berry transcriptome

To investigate the molecular changes that take place in the berry under water deficit, and to relate these changes to the observed changes in the berry metabolite profile, we compared the transcriptome of C and D berries at three selected developmental stages, 41 DAA (before veraison), 68 DAA (onset of ripening), 93 DAA (end of ripening) in 2012—the year when a major response of berry secondary metabolism to water deficit was observed.

After filtering for organelles contamination and quality trimming, the average number of unique reads that mapped the V1 version of the grape genome (Jaillon et al., 2007) was 25.4M (Table 2). Among the 29,971 genes of the grapevine genome, 23,603 (78.8%) were expressed at 41 DAA, 22,259 (74.4%) at 68 DAA, and 22,349 (74.7%) at 93 DAA. At harvest, the number of expressed genes was significantly higher in D (22,655) than in C (22,042).

Table 2. RNA sequencing analysis metrics. From 2012 samples, transcriptome analyses were performed in C and D berries at three selected berry developmental stages (41 DAA, before veraison; 68 DAA, beginning of ripening; 93 DAA, end of ripening) using an Illumina HiSeq platform.

Sampling (DAA)	Treatment	Biol. Rep.	Sequenced Reads	Trimmed and Filtered Reads	Mapped Reads	Unique Reads	Expressed Genes
41	C	1	28,142,936	27,754,632	25,988,030	24,755,747	23,610
41	C	2	30,305,610	29,876,940	27,973,973	26,562,085	23,599
41	C	3	28,671,516	28,222,582	26,091,160	24,772,968	23,540
41	D	1	28,149,289	27,778,718	26,187,110	24,902,068	23,514
41	D	2	33,830,303	33,405,718	31,568,524	30,062,254	23,674
41	D	3	32,599,088	32,104,203	30,020,648	28,489,098	23,680
68	C	1	28,782,803	28,323,977	26,348,993	25,223,216	22,237
68	C	2	25,079,582	24,669,614	22,976,645	21,995,680	22,390
68	C	3	28,125,993	27,686,829	25,741,134	24,643,657	22,791
68	D	1	26,901,387	26,446,179	24,543,406	23,239,648	21,956
68	D	2	30,338,107	29,825,731	27,814,720	26,486,281	22,100
68	D	3	28,142,082	27,663,249	25,648,895	24,384,788	22,077
93	C	1	23,482,080	23,170,055	21,908,218	21,010,267	21,799
93	C	2	28,620,256	28,210,433	26,438,882	25,361,424	22,073
93	C	3	27,093,095	26,687,888	24,966,036	23,949,887	22,254
93	D	1	32,448,861	32,030,568	30,407,000	29,224,179	22,774
93	D	2	32,234,615	31,726,941	29,721,915	28,544,263	22,783
93	D	3	27,177,622	26,846,929	25,470,062	24,417,385	22,408

A strong relationship was found between the RNA-seq and qPCRs gene expression values of 15 genes selected for validating the transcriptomic dataset (Table 3). Coefficient of correlation between RNA-seq and qPCR gene expression ranged between 0.765 and 0.998, indicating the reliability of the whole transcriptome assays.

Table 3. List of genes assayed for expression by qPCR. For each, the coefficient of correlation between RNA-Seq data and qPCR data, forward and reverse primers used, and literature references are shown.

Gene ID	Correlation Coefficient	p-Value	Forward / Reverse primer sequence	Reference
VviPAL2 (VIT_13s0019g04460)	0.849	0.032	atgaggtgaagcggatggtg / gcctttactccctctctcgc	Newly designed
VviCHS1 (VIT_14s0068g00930)	0.84	0.037	agccagtgaagcaggtagcc / gtgatccggaagtagtaat	Goto-Yamamoto et al. 2002 Plant Science
VviCHS2 (VIT_14s0068g00920)	0.834	0.039	tctgagcgagtatgggaaca / agggtagctgcgtaggttgg	Goto-Yamamoto et al. 2002 Plant Science
VviCHS3 (VIT_05s0136g00260)	0.9	0.015	gtttcggaccagggctcact / ggcaagtaaagtggaaacag	Goto-Yamamoto et al. 2002 Plant Science
VviF3H_2 (VIT_18s0001g14310)	0.819	0.046	ctgtggtgaactccgactgc / caaatgttatgggctcctcc	Jeong et al. 2004 Plant Science
VviLDOX (VIT_02s0025g04720)	0.765	0.076	agggaagggaaaacaagtag / actctttggggattgactgg	Jeong et al. 2004 Plant Science
VviLAR1 (VIT_01s0011g02960)	0.977	0.001	caggaggctatggagaagatac / acgcttctctctgtacatgttg	Bogs et al. 2005 Plant Physiology
VviANR (VIT_00s0361g00040)	0.95	0.004	agcaggttgcgactttgtct / accagacctgtcccatcaag	Castellarin et al. 2007 Planta
VviMybPA1 (VIT_15s0046g00170)	0.95	0.004	ttgacggggttgacttcttc / gagtagtgattcggcgaagg	Terrier et al. 2009 Plant Physiology
VviFLS (VIT_18s0001g03470)	0.975	0.001	tggggttaggtctgggagag / aacctgcaagccctgaactt	Newly designed
VviTPS_15 (VIT_18s0001g05290)	0.948	0.004	ggaatgcctcaaacctactgc / ggttaatgaagaaagccgcaatg	Newly designed
VviTPS_28 (VIT_19s0014g04930)	0.996	1.89 e-05	cgggtggtggaatgctactt / acctctcaactgcttcggtg	Newly designed
VviTPS_35 (VIT_12s0134g00030)	0.998	5.14 e-06	ctctgaggaaagtgctcgtga / ccttgatctagcgtccggag	Newly designed
VviNCED3 (VIT_19s0093g00550)	0.833	0.039	tttgtgcacgacgagaagac / agggaactcgtgagggaagt	Newly designed
VviCCD4b (VIT_02s0087g00930)	0.966	0.002	atctgaaaacggggacagtg / acgtccagcttcacaattcc	Newly designed

A principal component analysis over the transcriptome profiles of the 18 samples analyzed (two treatments x three developmental stages x three biological replicates) was performed (Fig. 4a). The first three principal components explain 52.9%, 26.5%, 7.1% of the variance among samples, respectively. Similarities and differences among berry transcriptomes were mostly driven by the developmental stage when berries were sampled. C and D samples were mixed within the group of the samples harvested at 41 DAA, but were clearly separated at 68 and 93 DAA, with the majority of the variance explained by the second principal component.

The total number of differentially expressed genes between C and D was 4,889 (Table S1a,b,c). The number of DE genes changed during fruit development. D modulated the expression of 1,016 genes (316 up-regulated; 700 down-regulated) at 41 DAA, 2,448 genes (1,119 up-regulated; 1,329 down-regulated) at 68 DAA, and 2,446 genes (1,142 up-regulated; 1,304 down-regulated) at 93 DAA. Some genes were differentially regulated in unison among two or three developmental stages (Fig. 4b). Several transcription factors were modulated by water deficit, in particular, of a possible 2,211 *VviTFs* encoded in the grapevine genome 91, 230 and 201 were DE in response to water deficit at 41, 68 and 93 DAA, respectively (Table S1d).

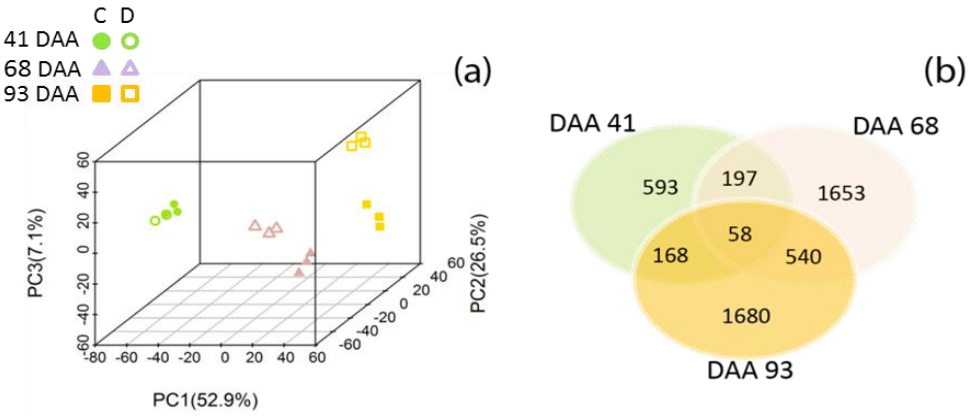

Figure 4. Analysis of the berry transcriptome in fully irrigated (C) and deficit irrigated (D) vines in 2012. (a) Principal component analysis (PCA) of the berry transcriptome of 18 independent samples collected from C and D vines at 41, 68, and 93 DAA. Circles, triangles and squares represent berries at 41, 68, and 93 DAA, respectively. Full and open symbols identify C and D berries, respectively. (b) Common and unique DE genes at 41, 68, and 93 DAA are represented in the Venn diagram.

Seventeen plant GO categories (slim biological processes) were significantly overrepresented among DE genes (Table S1e). Before veraison, *carbohydrate metabolic process*, *development*, and *response to biotic stress* were the three major GO categories within up-regulated genes, while *response to stress*, *transport*, and *response to abiotic stress* within down-regulated genes. At the beginning of ripening, *response to stress*, *carbohydrate metabolic process*, and *response to abiotic stress* were the three major GO categories within up-regulated genes, and *response to stress*, *transport*, and *development* within down-regulated genes. At the end of ripening, *response to stress*, *development*, and *response to abiotic stress* were the three major GO categories within up-regulated genes, and *response to stress*, *transport*, and *carbohydrate metabolic process* within down-regulated genes. The GO category *secondary metabolic process* was overrepresented within up-regulated genes at all the stages of fruit development considered, and within down-regulated genes at 41 DAA.

Impact of water deficit on phenylpropanoid, flavonoid, carotenoid, and terpenoid pathway

Because this study focuses on the impact of water deficit on secondary metabolism, we did identify the DE genes that belonged to the major secondary metabolic pathways in the grapevine berry during development and ripening. The impact of water deficit on the expression of these genes was expressed as the log_2 fold change of the transcript level in D compared to C and the genes were mapped into the related metabolic pathways (Fig. 5, 6, 7).

Water deficit modulated the expression of many genes that codify for structural enzymes of the phenylpropanoid and flavonoid pathway (Fig. 5). Most of these genes were up-regulated under D, particularly at 41 and 93 DAA.

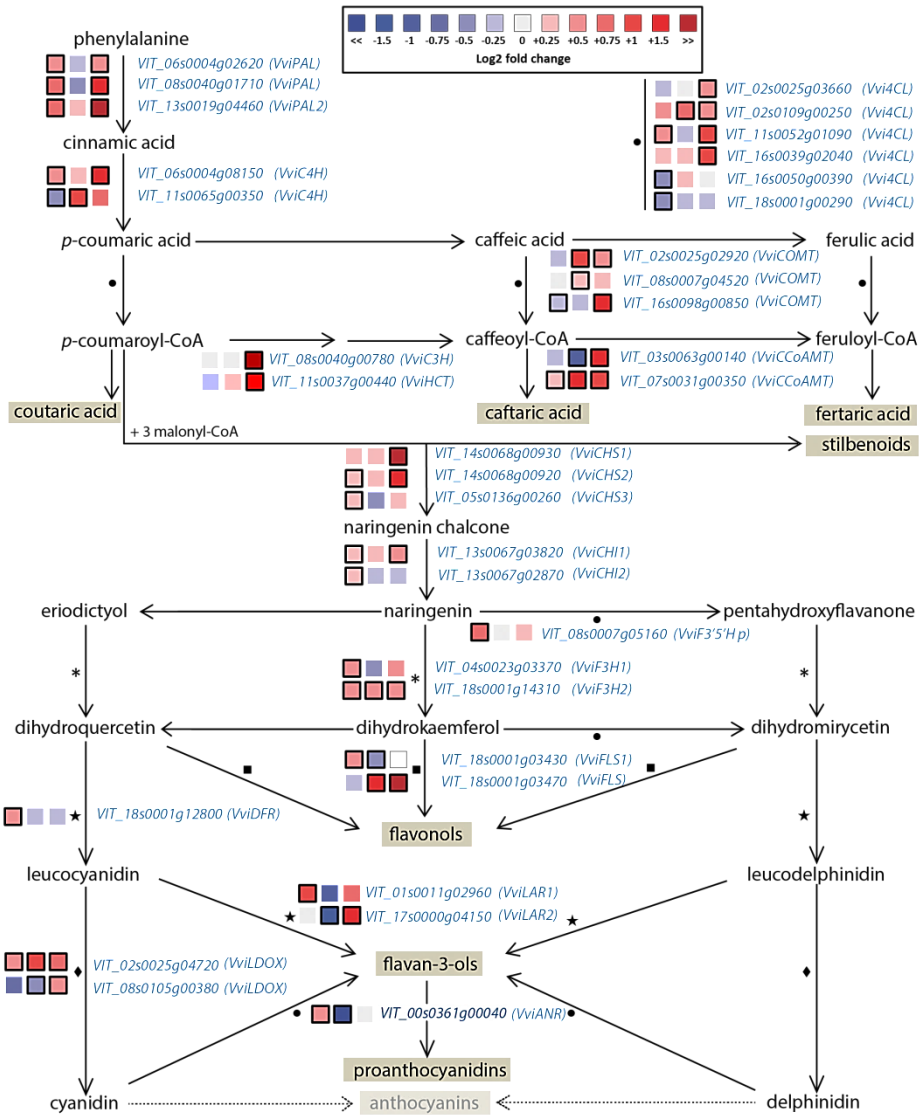

Figure 5. Modulation of phenylpropanoid and flavonoid pathway under water deficit in 2012. Log_2FC (D/C) levels of differential gene expression are presented at 41 (left box), 68 (central box), and 93 (right box) DAA. Blue and red boxes indicate down- or up-regulation of the gene under water deficit, respectively. Bold margins identify significant differences ($P<0.05$) between treatments. Symbols identify commonly regulated steps of the pathway.

Among the DE genes, three genes annotated as phenylalanine ammonia lyases (*VviPALs*), two trans-cinnamate 4-monooxygenase (*VviC4H*), six 4-coumarate-CoA ligase (*Vvi4CL*), one p-coumaroyl shikimate 3'-hydroxylase (*VviC3H*), one hydroxycinnamoyl-CoA:shikimate/quinate hydroxycinnamoyltransferase (*VviHCT*), three caffeic acid 3-*O*-metyltransferase (*VviCOMT*), and two caffeoyl-CoA 3-*O*-methyltransferase (*VviCCoAMT*) were differentially regulated under water deficit; most of them were up-regulated.

In parallel, water deficit modulated the expression of most structural flavonoid genes; particularly three chalcone synthases (*VviCHSs*), two chalcone isomerases (*VviCHIs*), one flavonoid-3'5'-hydroxylase (*VviF3'5'H*), two flavanone-3-hydroxylases (*VviF3Hs*), one dihydroflavonol reductase (*VviDFR*), and two leucoanthocyanidin dioxygenases (*VviLDOX*). All the above genes except one *VviLDOX* (*VIT_08s0105g00380*) were up-regulated by D. The flavonol synthase (*VviFLS*) is a key enzyme for flavonol production. Water deficit significantly promoted the expression of one *VviFLS* (*VIT_18s0001g03470*) at 68 and 93 DAA while down-regulating the expression of another *VviFLS* (*VIT_18s0001g03430*) at 68 DAA. The leucoanthocyanidin reductase (*VviLAR*) and anthocyanidin reductase (*VviANR*) are key regulators of the flavan-3-ol and proanthocyanidin biosynthesis. *VviLAR1* was up-regulated by water deficit at 41 DAA, while *VviLAR2* was down-regulated in the same condition at 68 DAA and upregulated at 93 DAA. *VviANR* was up-regulated by water deficit at 41 DAA and down-regulated at 68 DAA.

Despite the fact that *VviMyb14* (*VIT_07s0005g03340*) and *VviMyb15* (*VIT_05s0049g01020*) – transcription factors that regulate stilbene synthesis in grapevine (Höll et al., 2013) – were differentially expressed in D at 68 DAA (Table S1b), transcript levels of the 48 annotated *VviSTSs* (Vannozzi et al., 2012) were never affected by water deficit.

The effect of water deficit on the carotenoid pathway (Fig. 6) was analyzed bearing in mind the *Vitis vinifera* L. carotenoid genes identified by Young et al. (2012).

A phytoene synthase gene (*VviPSY2*) was upregulated under water deficit but only at 68 DAA. The same was observed for a ζ-carotene desaturase (*VviZDS1*). On the contrary, water deficit down-regulated the expression of a lycopene β-cyclase (*VviLBCY*), a β-carotene hydroxylase (*VviBCH2*), and a carotene hydroxylase (*VviLUT5*) at 68 DAA, and of a carotenoid isomerase (*VviCISO1*) at 93 DAA. The expression of a lycopene ε-cyclase (*VviLECY1*) was down-regulated by D at 41 and up-regulated at 93 DAA.

In plants, carotenoids are also the substrate for the production of C_{13}-norisoprenoids. Some C_{13}-norisoprenoids such as β-ionone and β-damascenone are important determinants of the grape and wine aroma (Robinson et al., 2014) contributing mainly to violet and rose scent, respectively. The enzymes (9,10) (9`,10`) cleavage dioxygenase (CCD4) and (5,6) (5',6') (9,10) (9',10') cleavage dioxygenase (CCD1) are key regulators of this conversions. In this study, D up-regulated the expression of *VviCCD4b* at 68 DAA and down-regulated the expression of *VviCCD4a* at 93 DAA.

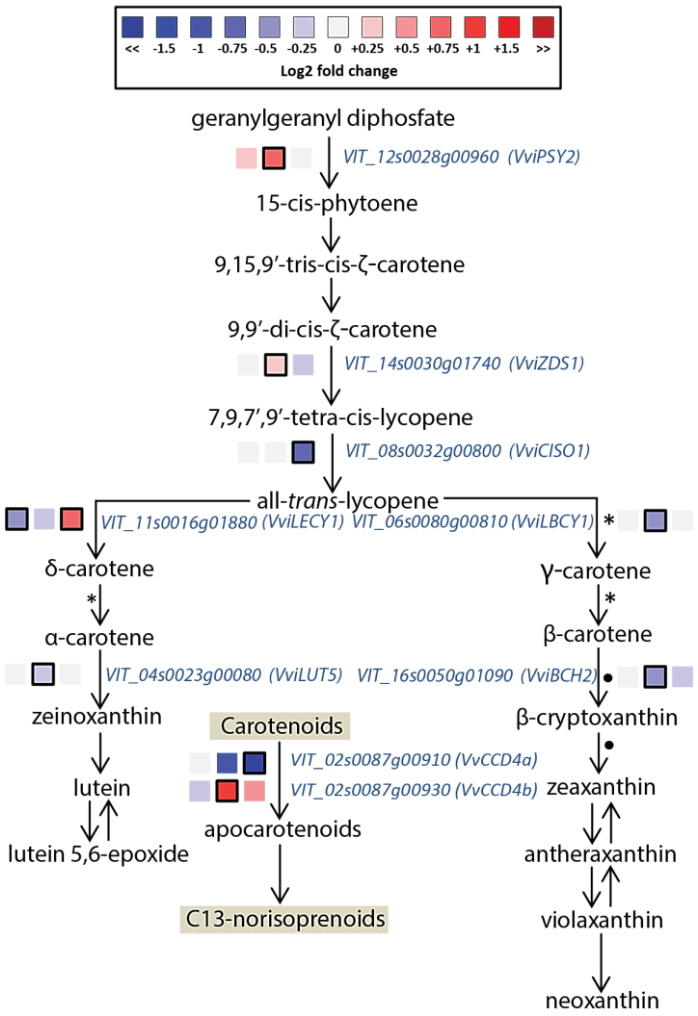

Figure 6. Modulation of carotenoid pathway under water deficit in 2012. Log_2FC (D/C) levels of differential gene expression are presented at 41 (left box), 68 (central box), and 93 (right box) DAA. Blue and red boxes indicate down- or up-regulation of the gene under water deficit, respectively. Bold margins identify significant differences ($P<0.05$) between treatments. Symbols identify commonly regulated steps of the pathway.

Plant terpenes are synthesized in the plastids through the 2C-methyl-D-erythritol-4-phosphate pathway (MEP), and in the cytosol through the mevalonate (MVA) pathway (Lund and Bohlmann, 2006). Water deficit modulated the expression of several genes of the two pathways (Fig. 7). Genes regulating early steps of the MEP pathway, such as one 1-deoxy-D-xylulose-5-phosphate synthase (*VviDXS1*) and the 1-deoxy-D-xylulose-5-phosphate reductoisomerase (*VviDXR*), were down-regulated by D at 41 DAA, while another *VviDXS* was down-regulated at 68 DAA and upregulated at 93 DAA. Terpene synthases (*VviTPSs*) were generally up-regulated under water deficit, particularly at 93 DAA. The terpene synthases gene family was recently characterized in Vitis vinifera (Martin et al., 2010). Water deficit modulated the expression of seven terpene synthases of the TPS-a family (*VIT_18s0001g04280*, *VIT_18s0001g04530*, *VIT_18s0001g05240*, *VIT_18s0001g05290*, *VIT_18s0001g05430*, *VIT_19s0014g04810*, *VIT_19s0014g04930*), one of the TPS-b family (*VIT_12s0134g00030*), and one of the TPS-g family (*VIT_00s0266g00070*).

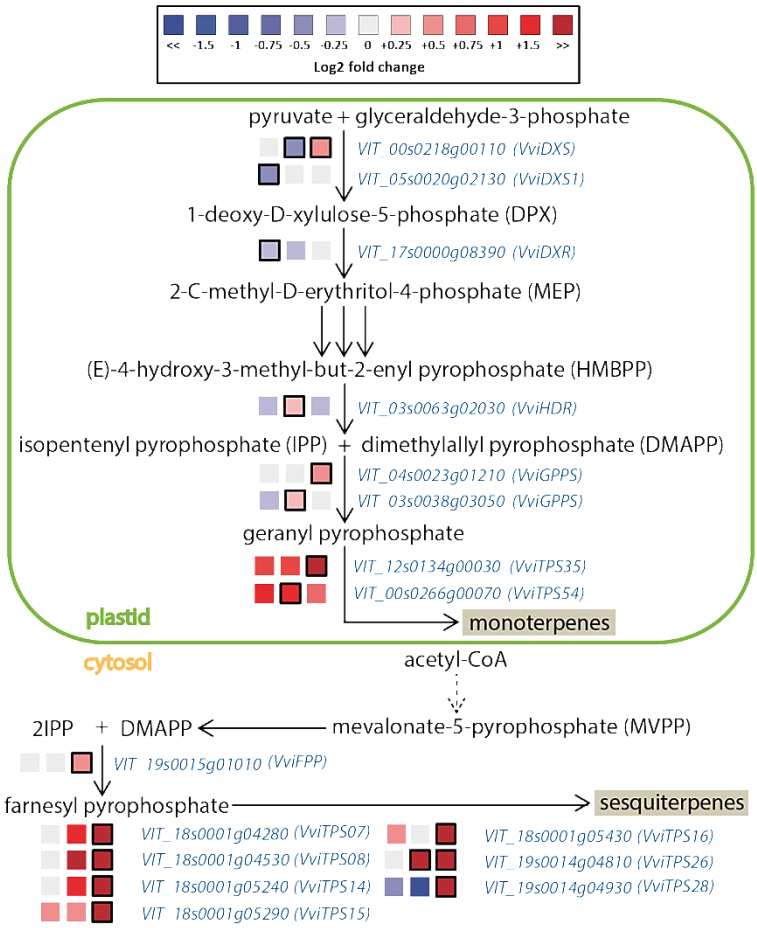

Figure 7. Modulation of terpenoid pathway under water deficit in 2012. Log_2FC (D/C) levels of differential gene expression are presented at 41 (left box), 68 (central box), and 93 (right box) DAA. Blue and red boxes indicate down- or up-regulation of the gene under water deficit, respectively. Bold margins identify significant differences ($P<0.05$) between treatments.

Differences in the impact of water deficit on the expression of key genes in the phenylpropanoid, flavonoid, and terpenoid pathway were observed between seasons (Fig. 8). Water deficit had no effect on the expression of *VviPAL2*, *VviCHS1*, *VviFLS*, and *VviANR* in 2011, consistently with the limited effect of D on the phenolic accumulation observed that season (Fig. 2a); while the same genes were up-regulated by water deficit at several developmental stages in 2012, in parallel with the observed increase of phenolic concentration under the same conditions. Similarly, the expression profile of two *VviTPSs* (*VIT_12s0134g00030* and *VIT_19s0014g04930*) confirmed that in 2011 monoterpenes synthesis was not modulated by water deficit at late stages of development; while, in 2012, water deficit stimulated their synthesis from 82 DAA.

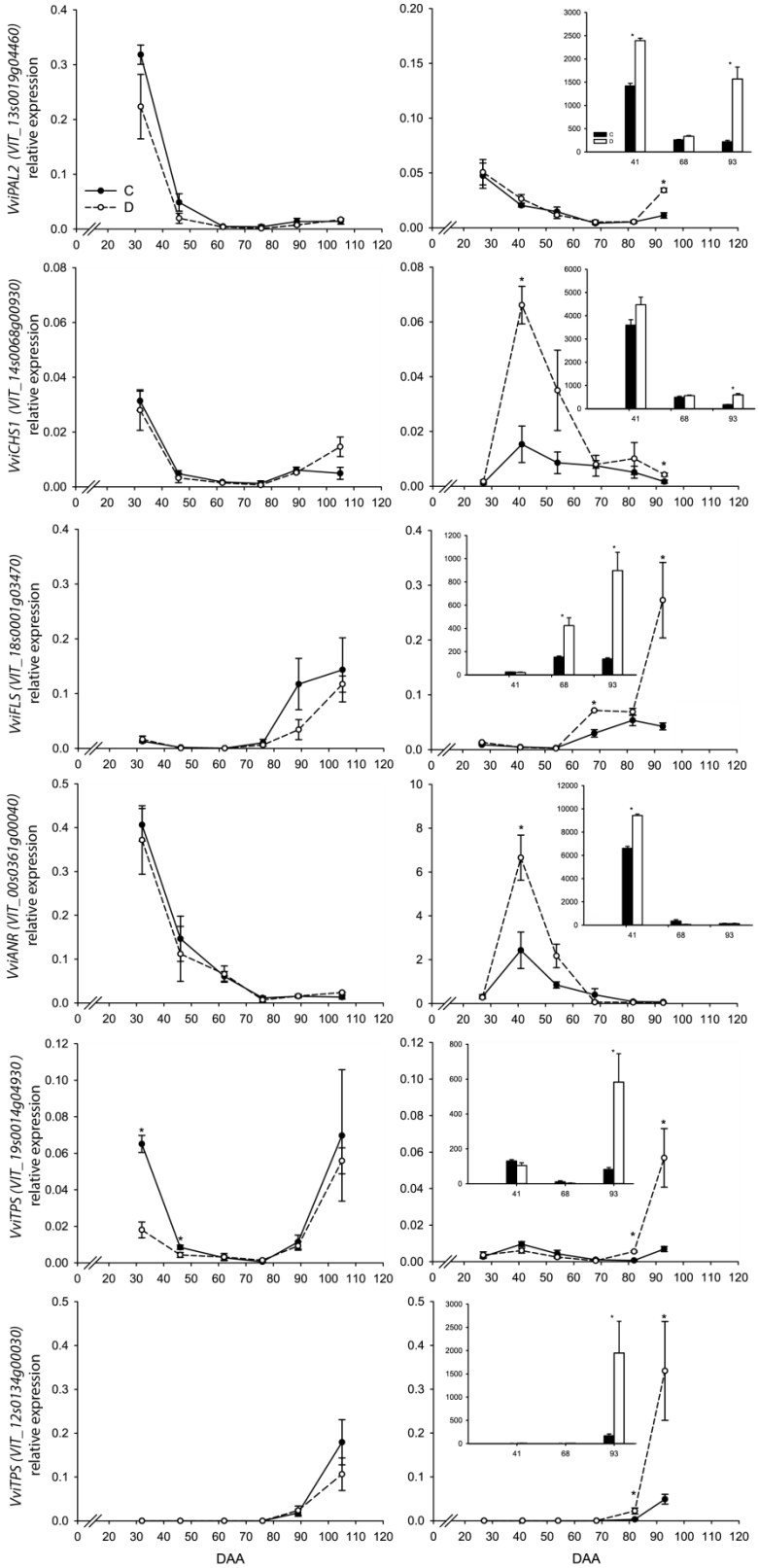

Figure 8. Impact of water deficit on transcript abundance of selected genes of the phenylpropanoid, flavonoid, and terpenoid pathway. Using qPCR, gene expression was analyzed at each sampling point in 2011 (left hand panel) and in 2012 (right hand panel). Gene expression levels analyzed in 2012 with RNA-sequencing at 41, 68, and 93 DAA are reported in inset graphs for comparison. Bars represent ±SE. Asterisks indicate significant differences between treatments at $P<0.05$ (*).

Impact of water deficit on integrated networks of metabolites and transcripts

Differences in metabolic network properties could be observed between C and D for the phenolic (Fig. 9a, b) and VOC (Fig. 9c, d) networks but not for the carotenoid and tocopherol ones (Fig. 9e, f). Water deficit affected the phenolic and VOC network topology by increasing the network connectedness in comparison with the controls. In general, the majority of both C and D metabolite-metabolite correlations are based on positive interactions among nodes, but negative correlations were observed especially under D, in particular for gallic acid. We observed two highly interconnected clusters within the VOC network of D berries; one of these clusters contained many of the VOCs that were significantly modulated under D, with two nodes namely nerol and *(E)*-2-octenal that had the highest degree of connections.

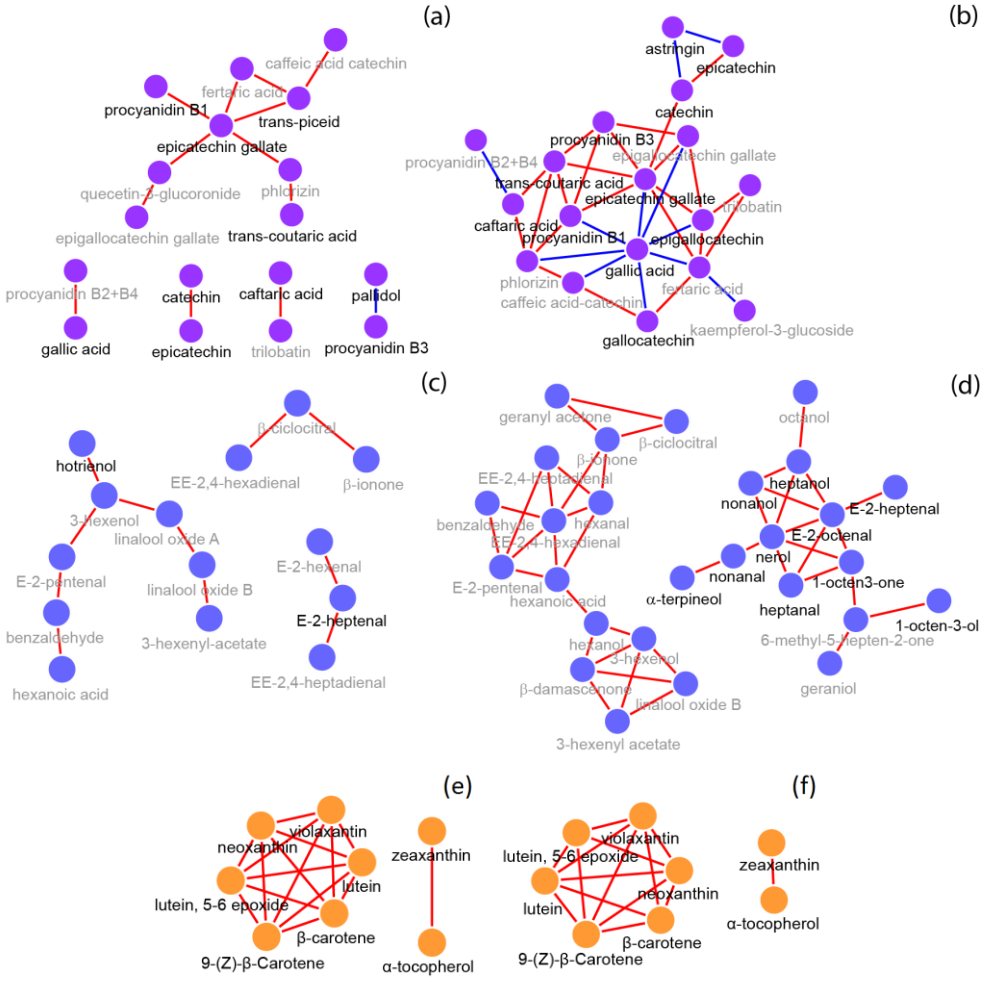

Figure 9. Network representation of phenolics VOCs and carotenoids in C (a, c, e) and D (b, d, f) berries during development. Nodes represent 'metabolites' and edges represent 'relationships' between any two metabolites. Edges colored in 'red' and 'blue' represent positive and negative correlations (P<0.001), respectively. Metabolites in bold indicate a significant effect (P<0.05) of water deficit on the concentration of that metabolite at one or more developmental stages. Number of correlating edges were 13, 35, 11, 42 in a, b, c, and d, respectively. The average node neighborhood was 1.53, 3.89, 1.57, and 3.11 in a, b, c, and d, respectively. The clustering coefficient was 0.08, 0.53, 0.00, and 0.49 in a, b, c, and d, respectively.

The increased average node degree, clustering coefficient, and network density between the C and D metabolite-metabolite networks prompted us to perform an association study between metabolites and transcripts in order to reveal the major transcripts that were associated with changes in metabolite networks. Emphasis was given on biosynthetic genes of the metabolite pathways considered. Generally, the number of positive correlations between phenolic compounds and phenolic biosynthetic genes slightly increased under D particularly because of an increase in the number of correlations within benzoic and cinnamic acid pathway elements (Table S1h,i). VOC-transcript links were also affected by water deficit. Correlations between geraniol, citronellol and hotrienol levels and terpenoid transcripts were observed in controls only (Table S1g). In contrast, correlations between nerol and α-terpineol and terpenoid transcripts were observed only in water deficit (Table S1h). Water deficit also modulated the correlations between the non-terpenoid VOCs and the fatty acid related transcripts: reducing them for *(EE)*-2,4-hexadienal and *(E)*-2-pentenal, and increasing them for nonanal, hexanol, and 3-hexenol. The number of carotenoid-transcript correlations was not affected by water deficit.

The knowledge of the regulation of monoterpene biosynthesis is scant. Because of the remarkable effect of water deficit on the VOC networks, we furthered our analysis into gene-metabolite relationship focusing on ripening-related monoterpenes induced by water deficit. These included linalool, nerol, and α-terpineol. The gene-metabolite network included the top 100 gene correlators for each monoterpene (Fig. 10a). Among the 222 genes present in the network, 116 genes (52%) were differentially expressed under water deficit. There were 49, 48 and 64 gene-metabolite relationship that were specific for α-terpineol, nerol, and linalool, respectively. Inspection of the overall network showed that a large proportion of these correlated genes were involved in terpenoid (18), lipid (10), and hormone (7) metabolism, as well as various transport (11) and signaling (13) mechanisms (Table S1j). Eleven gene-metabolite interactions were found for all the three metabolites and a large subset of 29 interactions was in common between α-terpineol and nerol. We highlight several potential transcriptional regulators annotated as *MYB24* (*VIT_14s0066g01090*), *C2H2 Zinc finger* (*VIT_07s0005g02190*) and *Constans-like 11* (*VIT_19s0014g05120*), which significantly correlated with these monoterpenes. Promoter enrichment analysis of the top 100 correlated transcripts for each metabolite further revealed that many of the genes within each network contain significantly enriched ($P<0.01$) MYB recognition (such as *MYBZM*, *MYBCOREATCYCB1*, *MYB1AT*, *MYBPLANT*, *MYBCORE*, *MYB2CONSENSUSAT*) and various drought-responsive (*RYREPEATBNNAPA*, *LTRECOREATCOR15*, *DRECRTCOREAT*, *MYCCONSENSUSAT*, *MYCATRD22*) motif elements (Fig. 10b, Table S1k).

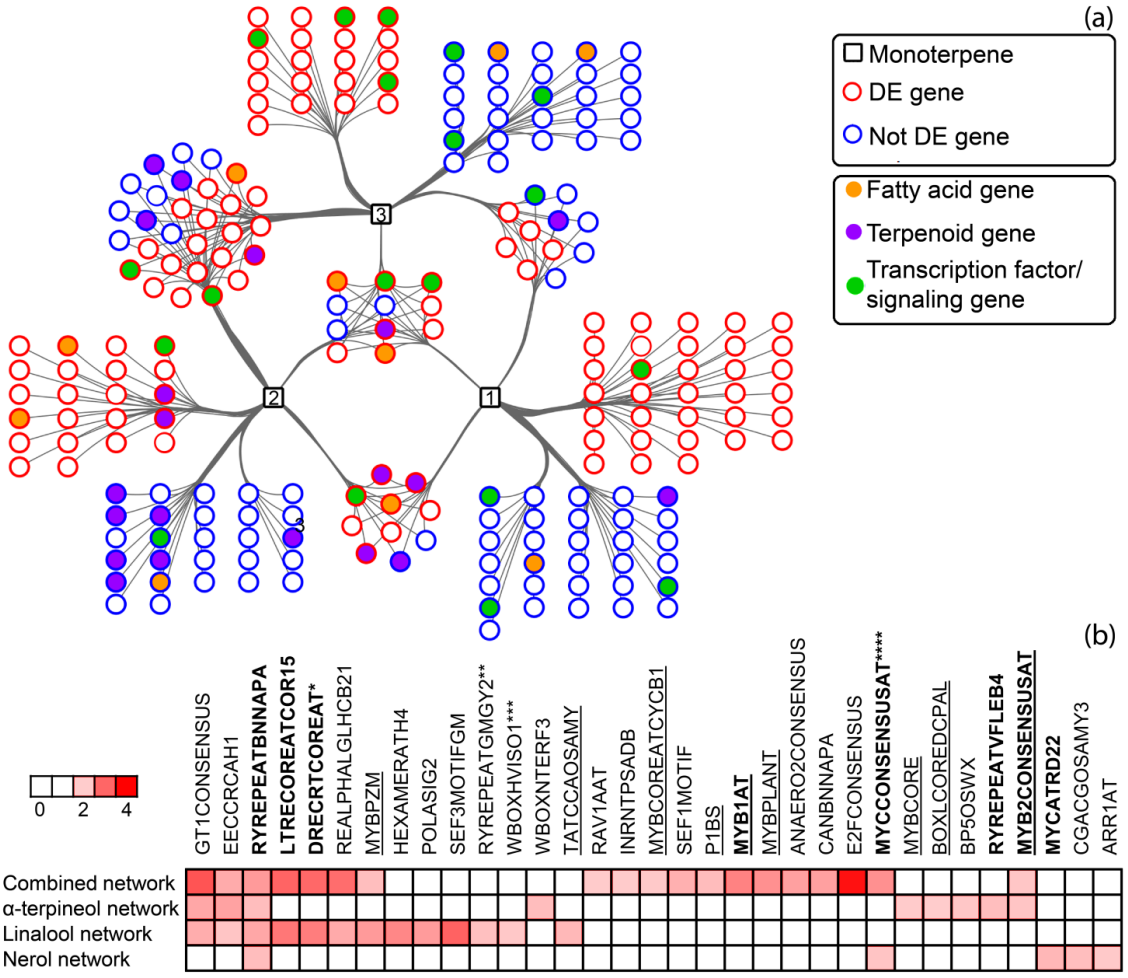

Figure 10. Predicted gene-metabolite networks related to linalool (1), α-terpineol (2), and nerol (3) in grapevine berries during development. (a) Genes and metabolites are represented by circle and square nodes respectively. Edges represent associations (P<0.001) between transcripts and metabolites. The top 100 correlators for each metabolite are shown. Node borders in red represent DE transcripts. Node colors indicate the pathway of the transcripts. (b) Heatmap of cis-regulatory elements enriched (P<0.01) within the networks in a. *Cis*-regulatory elements in bold and underlined are associated with ABA/drought response and MYB binding, respectively. Light and dark red color denotes enrichment scores between 2 (P<0.01) and 4 (P<0.0001) respectively. White color represents no significant enrichment. *, **, ***, and **** denotes other PLACE cis-regulatory motifs sharing similar consensus sequence with the associated motif (Table S1k).

Discussion

Water deficit modulated the accumulation of phenylpropanoids, flavonoids, carotenoids, and several VOCs in the berry; however the response of this berry secondary metabolism varied between seasons, indicating that the phase when drought is manifested and/or the length of the drought period impacts this response.

At present, little information is available on the effect of water deficit on phenolic accumulation in white grapes. Our study indicates that the phenylpropanoid and the flavonoid pathway respond to water deficit at the transcript and metabolite level. In 2011, when the deficit was limited to late developmental stages, it correlated with a general decrease in the concentration of several phenolics, particularly flavan-3-ols and proanthocyanidins. Vice versa, when the water deficit occurred from early stages of development to harvest in 2012, it mostly correlated with increases in phenolic concentrations. In red grape varieties, water deficit strongly promotes accumulation of flavonoids, particularly anthocyanin (Castellarin et al., 2007a,b; Deluc et al., 2009). Anthocyanin biosynthesis is limited in white grapes; however, these grapes do accumulate other major flavonoids such as flavonols, flavan-3-ols, and proanthocyanidins. Recent studies reported that water deficit increases the concentration of flavonols in grapes (Deluc et al., 2009; Degu et al., 2015) and reduces (Hochberg et al., 2015) or does not affect proanthocyanidin concentration (Castellarin et al., 2007a). Our gene expression analysis indicated that many phenylpropanoid and flavonoid genes were upregulated under water deficit, and the modulation of these pathways increased the concentration of benzoic and cinnamic acids and of several flavonoids. Interestingly, key structural genes for the flavonol and flavan-3-ol biosynthesis such as flavonol synthases (*VviFLSs*) and leucoanthocyanidin reductases (*VviLARs*) were upregulated at late stages of development, while flavonols, flavan-3-ols, and proanthocyanidin increased in concentration under water deficit only at early stages of development (except procyanidin B1, which was also higher at harvest). Similarly, in the red berries of Cabernet Sauvignon vines exposed to water deficit, *VviLAR*, *VviANR*, and *VviFLS* were upregulated after the onset of fruit ripening, but no differences in flavonol and proanthocyanidin concentration were observed (Castellarin et al., 2007a). Our combined transcript and metabolite data suggest that a competition for precursors between enzymes of the flavonoid and phenylpropanoid pathways is occurring, with phenylpropanoid enzymes being more efficient in directing the substrates into the production of benzoic and cinnamic acid than the flavonoid enzymes in sequestrating these precursors for the productions of flavonoids, particularly after the onset of fruit ripening when the accumulation of flavan-3-ols and proanthocyanidins decreases dramatically (Teixeira et al., 2013).

Water deficit affected the concentration of carotenoids and tocopherols – key antioxidants in plants (Munné-Bosch and Alegre, 2002; Nisar et al., 2015) – in the berry, but the modulation of carotenoid genes was much lower than for the phenylpropanoid and flavonoid genes. Carotenoids are normally degraded after the onset of fruit ripening (Young et al., 2012), and our data indicate that this degradation is increased under water deficit. However, in 2012, water deficit increased the concentration of zeaxanthin—the only carotenoid synthesized after the onset of berry ripening (Figure S2). Zeaxanthin's role in drought tolerance has been already

hypothesized in plants. *Nerium oleander* increased zeaxanthin content in the leaf under water deficit (Demmig et al., 1988), and the enhancement of zeaxanthin levels in the transgenic tobacco lines made plants more tolerant to drought stress (Zhao et al., 2013). As in our work with berries, previous studies have shown a positive correlation between tocopherol accumulation and water deficit in photosynthesizing tissues (Munné-Bosch et al., 1999; Cela et al., 2011). However, we did not observe a consistent upregulation of key genes of the tocopherol pathway under water deficit and, at late stages of ripening (93 DAA), the gene *VviHPT* (*VIT_11s0052g00610*) that encodes one key enzyme of the pathway was actually down-regulated in D berries (Table S1c). This result agrees with previous findings in Arabidopsis, where wild-type plants subjected to water deficit increased the accumulation of the same tocopherols in the leaves without a parallel modulation of tocopherol biosynthetic genes (Cela et al., 2011).

The VOC profiling indicated that in Tocai Friulano, VOCs are primarily accumulated at early stages of development (Figure S3), but that water deficit imposed from early stages of development can stimulate the accumulation of several VOCs at late stages of development. Among these VOCs, four monoterpenes – key aromatics of several white grapes (Lund and Bohlmann, 2006) – were largely increased under water deficit, in parallel with an up-regulation of key structural genes of the MEP pathway. In particular, key genes for monoterpene production in the grapes such as *VviDXS* and two *VviTPSs* (Martin et al., 2010; Battilana et al., 2011) were up-regulated. The induction of monoterpene production under water deficit has been reported in several plants (reviewed in Selmar and Kleinwächter (2013)), including the recent studies in grapevine leaves (Alonso et al., 2015; Griesser et al., 2015) but the information on the effect of drought on monoterpene biosynthesis in fruits (where monoterpenes impact the quality and value of production) is scant (Ripoll et al., 2014). Besides monoterpene synthases, water deficit also up-regulated seven sesquiterpene synthases (Martin et al., 2010). We identified only two sesquiterpenes, α-humulene and *trans*-caryophyllene, which were accumulated in the berry only at early stages, and were not affected by water deficit. However, the molecular data indicate that a more detailed profiling of the sesquiterpene accumulated in the berry is necessary to investigate the role of these compounds in the response to water deficit. Other key odorants of grapes and wines are the carotenoid degradation products C_{13}-norisoprenoids that were observed to increase in red grapes subjected to a limiting irrigation regime (reviewed in Robinson et al., (2014). Interestingly, despite the higher degradation of carotenoids observed under water deficit, no clear modulation in the concentration of C_{13}-norisoprenoids such as β-damascenone and β-ionone, and of β-cyclocitral – a 7,8 cleavage product of β-carotene were observed (Sánchez and Winterhalter, 2013) in either seasons.

Metabolomic studies coupled with network analysis comparing contrasting genotypes, stress perturbations, and tissues have been useful for understanding the mechanism of genotype-environment interactions of plants (Stitt et al., 2010). Deficit irrigation increased the metabolite network connectivity for primary metabolites in grapevine leaf, but the effect was genotype-dependent for phenolic networks (Hochberg et al., 2013). Network-based analysis conducted here on secondary metabolism revealed that water deficit contributed significantly to restructuring the underlying network properties of fruit metabolites. The higher network connectivity of secondary metabolites observed under water deficit also coincided with the

modulation of several genes of the related biosynthetic pathway. It is therefore likely that the observed differential network connectivity between irrigation treatments may be determined by regulation at the transcript level (Zamboni et al., 2010; Degu et al., 2014). In support of this hypothesis, we have observed strong gene-metabolite correlations with phenolic and VOC pathway genes. Our results also showed that this observation could be extended to other pathways, such as that for terpenoid biosynthesis. The higher number of positive metabolite-transcript correlations for phenolics and terpenoids further strengthens our finding that those metabolic pathways take part of the grape response to water deficit, producing secondary metabolites that potentially enhance grapevine fitness under this abiotic stress.

In grapes, correlation network analysis (Wong et al., 2013) has been used recently to ascribe functions to candidate genes potentially involved in the regulation of color development (Costantini et al., 2015) and flavonol content/composition (Malacarne et al., 2015). Ma et al. (2015) recently adopted a metabolite-transcript network approach to identify key regulators of the terpenoid pathway in *Artemisia annua*. Similarly, we aimed to identify new genes potentially involved in the regulation of terpenoid metabolism during development and under water deficit. The comprehensive metabolite-transcript network constructed with three key monoterpenes whose synthesis was promoted under water deficit showed strong positive association of these metabolites with terpenoid transcripts. Interestingly, transcripts related to hormone synthesis (salicylic and jasmonic acid) and signaling (auxin and brassinosteroid) were also highly correlated. Terpene levels were significantly increased with the application of BTH (a salicylic acid analog) and methyljasmonate to berries (Gómez-Plaza et al., 2012) in grapevine. Additionally, our analysis allowed us to identify a transcription factor annotated as *VviMYB24* (*VIT_14s0066g01090*) as a promising regulatory candidate for monoterpene and fatty acid biosynthetic pathways in grapevine. Closer inspection of the annotated MYB gene showed high homology towards Arabidopsis *MYB24*, *MYB21*, and *MYB57*, all of which are involved in regulating terpenoid biosynthesis (Reeves et al., 2012). Recently *MYB24* was found to be strongly up-regulated under solar UV radiation in grape skins, in parallel with the up-regulation of three terpenoid structural genes (Carbonell-Bejerano et al., 2014), suggesting a major role in the grapevine berry response to abiotic factors. Previous studies have shown that terpenoid metabolism responds to light and UV stimuli in berry and leaf tissues (Reynolds and Wardle, 1989; Gil et al., 2012; Carbonell-Bejerano et al., 2014) and we discovered that light-responsive motif elements were significantly enriched throughout the monoterpene gene network (Table S1k). This data also indicates that the effects of water limitation on berry terpenes may be indirect, in part owing to changes in the fruit microclimate due to a reduction in canopy density. However, recent studies showed that water deficit and ABA treatments significantly increased the monoterpene and sesquiterpene concentration in grapevine leaves (Alonso et al., 2015; Griesser et al., 2015) even in the absence of UV radiation (Alonso et al., 2015). Moreover, the enrichment of drought-associated elements (e.g. MYB and DRE motifs) in the promoter region of many up-regulated terpenoid genes suggests a major direct modulation of the terpenoid pathway at the transcriptional level, possibly via an ABA mediated stimulus. These elements were frequently associated with abiotic stress responses and particularly to drought and ABA regulation (Shinozaki and Yamaguchi-Shinozaki, 2007).

Conclusion

The stage when deficit is applied and the severity of deficit certainly impact the response of fruit metabolism (Ripoll et al., 2014). In grapes it is known that these factors strongly affect the physiological and metabolic response of the berry to water deficit (Chaves et al., 2010). In this study, large effects on fruit metabolism were observed only in 2012 when drought occurred from early stages of berry development to harvest and determined a lower yield and higher berry sugar concentration.

Recently it was hypothesized that an overproduction of key odorants such as terpenoids and the carotenoids-derived norisoprenoids might be part of the adaptation of these varieties to the environment in the absence of anthocyanin accumulation (Ferrandino and Lovisolo, 2014). Our transcript and metabolite analyses showed that, beside the flavonoid pathway, phenylpropanoid and terpenoid pathways can take part in the berry's response to water deficit in non-pigmented berries. A predicted gene-metabolite network containing strong correlations between terpenoid pathway genes, transcription factors, and monoterpenes, as well as significant enrichment of drought-responsive elements within promoter regions of transcript members suggests that an over-production of monoterpenes can be part of the fruit response to drought. These results indicate that water deficit conditions can potentially impact the quality of white wines by increasing the accumulation of flavour compounds (i.e., benzoic and cinnamic acid and monoterpenes) in the grapes; and they are pivotal to future studies that evaluate the impact of deficit irrigation strategies on wine quality.

Material & Methods

Field experiment, physiological measurements, and sample preparation

The field experiment was conducted in 2011 and 2012 in a vineyard at the University of Udine's (Italy) experimental farm (46°01'52.3"N 13°13'30.6"E). Climatological data were recorded during the experiment by an automated weather station located 100 m from the experimental site. Seven years old Tocai Friulano (also known as Sauvignon vert and Sauvignonasse in Chile and France, respectively) grapevines were grafted onto SO4, planted at 2.5 m x 1.0 m spacing in north–south oriented rows, and trained to a cane-pruned 'Guyot' system. Two irrigation treatments were established. Control (C) vines were irrigated in order to maintain midday stem water potential (Ψ_{Stem}) above -0.8 MPa. Deficit irrigated (D) vines were not irrigated unless the Ψ_{Stem} was measured lower than -1.5 MPa. Plant water status was monitored weekly by measuring Ψ_{Stem} using a Scholander pressure chamber (Herrera et al., 2015). Irrigation was supplied when rainfall in the preceding week was below 100% ETc or Ψ_{Stem} was measured lower than -0.8 MPa, as discussed above. A surface drip irrigation system with emitters (0.5 m x 2.5 m) set to an 8 L h^{-1} application rate was used. At the maximum rate, water was supplied at approximately 40 L per vine per week. In 2011, no irrigation was supplied to D plants until harvest; in 2012, due to a prolonged drought, irrigation (20 L per vine) was applied to D vines at 67, 70, 76 days after anthesis (DAA) in order to mitigate the severe water deficit. Each irrigation treatment was replicated on four plots of six vines each, arranged in a completely randomized design. No effect of the irrigation treatments was observed on the number of shoots and clusters per vine during both seasons.

Samplings were carried out at 32, 46, 62, 76, 89, 105 DAA and at 27, 41, 54, 68, 82, 93 DAA in 2011 and 2012, respectively. Two sets of berries were randomly collected from each plot. The first set, which consisted of 60 berries, was used to measure berry weight and total soluble solid concentration. The second set, which consisted of 40 berries, was used for transcript and metabolite analyses. Berries were carefully trimmed off the cluster at the pedicel with pair of scissors, quickly brought to the laboratory, and weighed and processed for soluble solids (Herrera et al., 2015), or immediately frozen at -80°C for transcript and metabolite analyses. Before metabolite and RNA extractions, pedicel was removed with a scalpel and berries were ground to a fine powder under liquid nitrogen using an analytical mill (IKA®-Werke GMbH & CO). One quality control (QC) sample was prepared by pooling an aliquot of all the samples and was used for QC runs in the metabolite analyses.

Grapes were harvested for commercial wine production at 105 and 93 DAA, in 2011 and 2012, respectively, when titratable acidity reached approximately 5 g/L (expressed as tartaric acid) in both treatments; yield per vine and cluster weight were recorded.

Targeted metabolite analyses

Phenolic compounds were determined accordingly to Vrhovsek et al. (2012). Briefly, 0.8 mL of chloroform and 1.2 mL of a mix of methanol and water (2:1) were added to one gram of frozen powder of ground berries. A 50 μL aliquot of *o*-coumaric acid solution (2 mg/mL in MeOH) was added as an internal standard. The extraction mixture was shaken for 15 min on an orbital

shaker (Grant-Bio Rotator PTR-60), then centrifuged for 10 min at 1,000 g. The upper aqueous-methanolic phase was collected. The extraction was repeated by adding 1.2 mL of methanol and water. The aqueous-methanolic phase was collected and combined with the previous one, brought to a final volume of 5 mL with Milli-Q water, and filtered with a 0.2 μm PTFE filter (Millipore). The chromatographic analysis was carried out using a Waters Acquity UPLC system (Milford) coupled to a Waters Xevo triple-quadrupole mass spectrometer detector (Milford). Compounds were identified based on their reference standard, retention time, and qualifier and quantifier ion, and were quantified by their calibration curve and expressed as mg/Kg of grapes.

Carotenoids and tocopherols were analyzed accordingly to Wehrens et al. (2013). Briefly, the chloroform phase of the extraction solution described above was collected. Twenty μL of trans-β-apo-8′-carotenal (25 μg/mL) was used as internal standard. Ten μL of a 0.1% triethylamine solution was added to prevent rearrangement of carotenoids. After extraction, samples were dried with N2, and stored at -80°C until analysis. Dried samples were suspended in 50 μL of ethyl acetate, and transferred to dark vials. The chromatographic analysis was performed in a 1290 Infinity Binary UPLC (Agilent) equipped with an RP C30 3 μm column coupled to a 20 x 4.6 mm C30 guard column. Spectra components and elution profiles were determined as in Wehrens et al. (2013). Compounds were quantified from linear calibration curves built with standard solutions and expressed as mg/Kg of grapes.

Free (non-glycosylated) VOCs were analyzed accordingly to Fedrizzi et al. (2012) with some modifications. On the day of analysis, four grams of frozen grape powder were weighed out in a 20 mL SPME dark-glass vial. Three grams of NaCl, 15 mg of citric acid, 15 mg of ascorbic acid, 50 μL of sodium azide, and 7 mL of milliQ water were added to the sample. Fifty μL of a solution containing five internal standards, d_{10}-4-methyl-3-penten-2-one (1 g/L), d_{11}-ethyl hexanoate (1 g/L), d_{16}-octanal (1 g/L), d_8-acetophenone (1 g/L), d_7-benzyl alcohol (1 g/L), was added to each sample. Prior to injection, the sample was pre-incubated at 60°C in a SMM Single Incubator (Chromtech) for 10 min stirring at 450 rpm. Next, the sample was incubated in the same conditions for 40 min with a DVB-CAR-PDMS 50/30 μm x 2 cm (Supelco) fiber in the headspace for absorption. Free VOCs were thermally desorbed in splitless mode for 4 min at 250°C. Extractions and injections were carried out with a CTC Combi-PAL autosampler (Zwingen). The analysis was performed with a Trace GC Ultra gas chromatograph (Thermo Scientific) coupled to a TSQ Quantum Tandem mass spectrometer. GC separation was performed on a 30 m Stabilwax (Restek Corporation) capillary column with an internal diameter of 0.25 mm and a film thickness of 0.25 μm with the conditions described in Fedrizzi et al. (2012). VOCs were identified by comparing the retention times of individual peaks with the retention times of their reference standards, and by identifying the mass spectra using the NIST library. The ratio of each VOC area to the d_{16}-octanal internal standard area was considered to reduce technical variability among extractions and chromatographic runs and VOCs quantity were expressed as μg/kg of berry of d_{16}-octanal equivalents.

Extractions and injections of the samples were performed in a random sequence and QC samples were injected at the beginning of the sequence and every six sample injections.
A list of the secondary metabolites analyzed in this study is reported in Table S2.

RNA extraction and RNA sequencing analysis

Samples collected at 41, 68 and 93 DAA in 2012 were selected for transcriptome analyses. Three biological replicates per treatment were considered. Total RNA was extracted with the 'Spectrum Plant total RNA' kit (Sigma-Aldrich) from 0.2 g of ground berries. The quantity and quality of the RNA were determined with a Caliper LabChip® GX (Perkin-Elmer).

Library preparation was performed using the TruSeq RNA Sample Prep Kit v2.0 according to the manufacturer's instructions (Illumina). Libraries were quantified using a 2100 Bioanalyzer (Agilent Technologies). Multiplexed cDNA libraries were pooled in equimolar amounts, and clonal clusters were generated using Cbot (Illumina). Sequencing was performed with an Illumina HiSeq 2000 platform (Illumina pipeline 1.8.2) at IGA Technology Services (Udine, Italy).

An average of 28.9M 50-nt single-end reads were generated per sample (Table 2). Trimming for quality and length, and filtering for mitochondria and chloroplast contamination were performed by the ERNE package version 1.2 tool ERNE-FILTER (Del Fabbro et al., 2013). The minimum PHRED score accepted for trimming was 20, and reads shorter than 40 bp were discarded. Reads were aligned against the reference grapevine genome PN40024 12x (Jaillon et al., 2007) using the software TopHat version 2.0.6 (Trapnell et al., 2012) with default parameters. Aligned reads were counted with a htseq-count (version 0.6.0), in intersection-non-empty mode for overlap resolution (Anders et al., 2015). Vitis vinifera annotation GTF-file (V1) was downloaded from Ensembl Plants website. Differentially expressed (DE) genes (false discovery rate less than 0.05) analysis was performed with the R package DeSeq2 (Love et al., 2014). Functional annotations of gene were retrieved from Grimplet et al. (2012) and VitisCyc (Naithani et al., 2014). Gene ontology analyses were carried out for each sampling. Overrepresented genes categories were identified with the BINGO app 3.0.2 of Cytoscape 3.1.1 (Maere et al., 2005). PlantGoSlim categories referred to biological processes were used to run the gene enrichment analysis, using a hypergeometric test with a significance threshold of 0.05 after Benjamini and Hochberg false discovery rate correction.

Quantitative real-time polymerase chain reaction

The validation of RNA-Seq data was carried out on a set of DE genes using the quantitative real-time polymerase chain reaction (qPCR) technique. The reverse transcription of RNA samples was performed with the QuantiTect Reverse Transcription Kit (Qiagen) and the Quantiscript Reverse Transcriptase (Qiagen). Specific primers for 15 selected genes were designed with Primer3web version 4.0.0 (Table 3). qPCR reactions, conditions, and calculation of relative expression values were carried out as in Falginella et al. (2012). The annealing temperature was 58°C for all primer pairs except the *VviUbiquitin* housekeeping gene pair, which annealed at 56°C. Correlation analysis based on the Pearson Correlation Coefficient (PCC) was carried out between the RNA-seq normalized counts and qPCR relative gene expression. qPCR was also carried out to determine the level of expression of selected structural genes of the phenylpropanoid, flavonoid, and terpenoid pathway during berry development in 2011 and 2012.

Statistical, network, and promoter analyses

A one-way ANOVA was performed using JMP 7 (SAS Institute Inc.) to detect significant differences ($P<0.05$) between irrigation treatments at each sampling point. Heatmaps representing $\log_2$ fold change ($\log_2$FC) of metabolite concentrations between treatments (D/C) and principal component analysis (PCA) on the entire transcriptome dataset were constructed and performed, respectively, using R software.

The metabolite correlation network was constructed for each condition (C and D) using all 74 metabolite accumulation profiles separately. The PCC was used as an index of similarity between any two variables (i.e. metabolites). Correlation pairs were deemed statistically significant when the $|PCC| > 0.8$ and P-value < 0.001 (2,000 permutations). The Cytoscape software (version 3.1.1) (Shannon et al., 2003) was used for network visualization and analysis of network properties such as the average node degree, clustering coefficient, and network density. Additionally, the two matrices (C and D) of metabolite and transcript datasets were merged and used for the construction of a global metabolite-transcript network focused on structural genes of phenylpropanoid, flavonoid, carotenoid, fatty acid, and terpenoid pathway. Selected networks were constructed for three monoterpenes (linalool, nerol, and α-terpineol) considering the top 100 correlating genes. All calculations and permutation tests were performed in R using the 'rsgcc' package (Ma and Wang, 2012).

Promoter motif enrichment analysis was conducted as described previously in Ma et al. (2013). A total of 29,839 grapevine promoter sequences (1 kb upstream of the 5′ UTR) based on the 12x grapevine genome assembly were retrieved from Gramene v45. Known *cis*-regulatory motifs of plants were retrieved from PLACE (Higo et al., 1999). Enrichment of motifs was validated using the hypergeometric distribution test. *Cis*-regulatory motifs were considered significantly enriched if the associated P value was < 0.01 and at least 10 promoters were associated with the given motif.

Abbreviations

4CL: 4-coumarate-CoA ligase; *ANR*: anthocyanidin reductase; *BCH*: β-carotene hydroxylase; *C*: control; *C3H*: *p*-coumaroyl shikimate 3'-hydroxylase; *C4H*: trans-cinnamate 4-monooxygenase; *CCD1*: (5,6) (5′,6′) (9,10) (9′,10′) cleavage dioxygenase; *CCD4*: (9,10) (9′,10′) cleavage dioxygenase; *CCoAMT*: caffeoyl-CoA 3-O-methyltransferase; *CHI*: chalcone isomerase; *CHS*: chalcone synthase; *CISO*: carotenoid isomerase; *COMT*: caffeic acid 3-O-metyltransferase; *D*: water deficit; *DAA*: days after anthesis; *DE*: differentially expressed; *DFR*: dihydroflavonol reductase; *DVB-CAR-PDMS*: divinylbenzene-carboxen-polydimethylsiloxane; *DXR*: 1-deoxy-D-xylulose-5-phosphate reductoisomerase; *DXS*: 1-deoxy-D-xylulose-5-phosphate synthase; *ETc*: crop evapotranspiration; *F3′5′H*: flavonoid-3′5′-hydroxylase; *F3H*: flavanone-3-hydroxylase; *FLS*: flavonol synthase; *GO*: gene ontology; *HCT*: hydroxycinnamoyl-CoA:shikimate/quinate hydroxycinnamoyltransferase; *HPLC-DAD*: high performance liquid chromatography-diode array detector; *HPT*: homogentisate phytyl transferase; *HS-SPME-GC-MS*: headspace-solid phase microextraction-gas chromatography-mass spectrometry; *LAR*: leucoanthocyanidin reductase; *LBCY*: lycopene β-cyclase; *LDOX*: leucoanthocyanidin dioxygenases; *LECY*: lycopene ε-cyclase; *LUT*: carotene hydroxylase; *MEP*: 2C-methyl-D-erythritol-4-phosphate; *MVA*:

mevalonate; *PAL*: phenylalanine ammonia lyase; *PCA*: principal component analysis; *PCC*: Pearson correlation coefficient; *PSY*: phytoene synthase; *QC*: quality control; *qPCR*: quantitative PCR; *RNA-seq*: RNA sequencing; *STS*: stilbene synthase; *TPS*: terpene synthase; *UFGT*: UDP-glucose:flavonoid 3-*O*-glucosyltransferase; *UHPLC-MS/MS*: ultra-high performance liquid chromatography-tandem mass spectrometer; *VOCs*: volatile organic compounds; *Vvi*: Vitis vinifera; *ZDS*: ζ-Carotene desaturase; Ψ_{Stem}: stem water potential.

Acknowledgement

This study was funded by the Italian Ministry of Agricultural and Forestry Policies (VIGNETO), the International Ph.D. Programme in the Genomics and Molecular Physiology of Fruit Plants (GMPF) of the Fondazione Edmund Mach International Research School Trentino (FEM-FIRS>T), the COST Action FA1106 Quality Fruit, the University of British Columbia (10R18459), and Natural Sciences and Engineering Research Council of Canada (10R23082).

References

Alonso R, Berli FJ, Bottini R, Piccoli P (2015) Acclimation mechanisms elicited by sprayed abscisic acid, solar UV-B and water deficit in leaf tissues of field-grown grapevines. Plant Physiol Biochem **91**: 56–60

Anders S, Pyl PT, Huber W (2015) HTSeq—a Python framework to work with high-throughput sequencing data. Bioinformatics **31**: 166–169

Battilana J, Emanuelli F, Gambino G, Gribaudo I, Gasperi F, Boss PK, Grando MS (2011) Functional effect of grapevine 1-deoxy-D-xylulose 5-phosphate synthase substitution K284N on Muscat flavour formation. J Exp Bot **62**: 5497–5508

Carbonell-Bejerano P, Diago MP, Martínez-Abaigar J, Martínez-Zapater JM, Tardáguila J, Núñez-Olivera E (2014) Solar ultraviolet radiation is necessary to enhance grapevine fruit ripening transcriptional and phenolic responses. BMC Plant Biol **14**: 183

Castellarin SD, Matthews MA, Di Gaspero G, Gambetta GA (2007a) Water deficits accelerate ripening and induce changes in gene expression regulating flavonoid biosynthesis in grape berries. Planta **227**: 101–112

Castellarin SD, Pfeiffer A, Sivilotti P, Degan M, Peterlunger E, Di Gaspero G (2007b) Transcriptional regulation of anthocyanin biosynthesis in ripening fruits of grapevine under seasonal water deficit. Plant Cell Environ **30**: 1381–1399

Cela J, Chang C, Munné-Bosch S (2011) Accumulation of γ- rather than α-tocopherol alters ethylene signaling gene expression in the vte4 mutant of *Arabidopsis thaliana*. Plant Cell Physiol **52**: 1389–1400

Chapman DM, Roby G, Ebeler SE, Guinard JX, Matthews MA (2005) Sensory attributes of Cabernet Sauvignon wines made from vines with different water status. Aust J Grape Wine Res **11**: 339–347

Chaves MM, Zarrouk O, Francisco R, Costa JM, Santos T, Regalado AP, Rodrigues ML, Lopes CM (2010) Grapevine under deficit irrigation: hints from physiological and molecular data. Ann Bot **105**: 661–676

Costantini L, Malacarne G, Lorenzi S, Troggio M, Mattivi F, Moser C, Grando MS (2015) New candidate genes for the fine regulation of the colour of grapes. J Exp Bot **66**: 4427–4440

Degu A, Hochberg U, Sikron N, Venturini L, Buson G, Ghan R, Plaschkes I, Batushansky A, Chalifa-Caspi V, Mattivi F, et al (2014) Metabolite and transcript profiling of berry skin during fruit development elucidates differential regulation between Cabernet Sauvignon and Shiraz cultivars at branching points in the polyphenol pathway. BMC Plant Biol **14**: 188

Degu A, Morcia C, Tumino G, Hochberg U, Toubiana D, Mattivi F, Schneider A, Bosca P, Cattivelli L, Terzi V, et al (2015) Metabolite profiling elucidates communalities and differences in the polyphenol biosynthetic pathways of red and white Muscat genotypes. Plant Physiol Biochem **86**: 24–33

Del Fabbro C, Scalabrin S, Morgante M, Giorgi FM (2013) An extensive evaluation of read trimming effects on Illumina NGS data analysis. PLoS ONE **8**: e85024

Deluc LG, Quilici DR, Decendit A, Grimplet J, Wheatley MD, Schlauch KA, Mérillon JM, Cushman JC, Cramer GR (2009) Water deficit alters differentially metabolic pathways affecting important flavor and quality traits in grape berries of Cabernet Sauvignon and Chardonnay. BMC Genomics **10**: 212

Demmig B, Winter K, Krüger A, Czygan FC (1988) Zeaxanthin and the heat dissipation of excess light energy in *Nerium oleander* exposed to a combination of high light and water stress. Plant Physiol **87**: 17–24

Falginella L, Di Gaspero G, Castellarin SD (2012) Expression of flavonoid genes in the red grape berry of "Alicante Bouschet" varies with the histological distribution of anthocyanins and their chemical composition. Planta **236**: 1037–1051

Fedrizzi B, Carlin S, Franceschi P, Vrhovsek U, Wehrens R, Viola R, Mattivi F (2012) D-optimal design of an untargeted HS-SPME-GC-TOF metabolite profiling method. Analyst **137**: 3725–3731

Ferrandino A, Lovisolo C (2014) Abiotic stress effects on grapevine (*Vitis vinifera* L.): Focus on abscisic acid-mediated consequences on secondary metabolism and berry quality. Environ Exp Bot **103**: 138–147

Gil M, Pontin M, Berli F, Bottini R, Piccoli P (2012) Metabolism of terpenes in the response of grape (*Vitis vinifera* L.) leaf tissues to UV-B radiation. Phytochemistry **77**: 89–98

Gómez-Plaza E, Mestre-Ortuño L, Ruiz-García Y, Fernández-Fernández JI, López-Roca JM (2012) Effect of benzothiadiazole and methyl jasmonate on the volatile compound composition of Monastrell grapes and wines. Am J Enol Vitic ajev.2012.12011

Griesser M, Weingart G, Schoedl-Hummel K, Neumann N, Becker M, Varmuza K, Liebner F, Schuhmacher R, Forneck A (2015) Severe drought stress is affecting selected primary metabolites, polyphenols, and volatile metabolites in grapevine leaves (*Vitis vinifera* cv. Pinot noir). Plant Physiol Biochem **88**: 17–26

Grimplet J, Hemert JV, Carbonell-Bejerano P, Díaz-Riquelme J, Dickerson J, Fennell A, Pezzotti M, Martínez-Zapater JM (2012) Comparative analysis of grapevine whole-genome gene predictions, functional annotation, categorization and integration of the predicted gene sequences. BMC Res Notes **5**: 213

Hannah L, Roehrdanz PR, Ikegami M, Shepard AV, Shaw MR, Tabor G, Zhi L, Marquet PA, Hijmans RJ (2013) Climate change, wine, and conservation. Proc Natl Acad Sci **110**: 6907–6912

Hartmann T (2007) From waste products to ecochemicals: Fifty years research of plant secondary metabolism. Phytochemistry **68**: 2831–2846

Herrera JC, Bucchetti B, Sabbatini P, Comuzzo P, Zulini L, Vecchione A, Peterlunger E, Castellarin SD (2015) Effect of water deficit and severe shoot trimming on the composition of *Vitis vinifera* L. Merlot grapes and wines. Aust J Grape Wine Res **21**: 254–265

Higo K, Ugawa Y, Iwamoto M, Korenaga T (1999) Plant cis-acting regulatory DNA elements (PLACE) database. Nucleic Acids Res **27**: 297–300

Hochberg U, Degu A, Toubiana D, Gendler T, Nikoloski Z, Rachmilevitch S, Fait A (2013) Metabolite profiling and network analysis reveal coordinated changes in grapevine water stress response. BMC Plant Biol **13**: 184

Hochberg U, Degu A, Cramer GR, Rachmilevitch S, Fait A (2015) Cultivar specific metabolic changes in grapevines berry skins in relation to deficit irrigation and hydraulic behavior. Plant Physiol Biochem **88**: 42–52

Höll J, Vannozzi A, Czemmel S, D'Onofrio C, Walker AR, Rausch T, Lucchin M, Boss PK, Dry IB, Bogs J (2013) The R2R3-MYB transcription factors MYB14 and MYB15 regulate stilbene biosynthesis in *Vitis vinifera*. Plant Cell **25**: 4135–4149

Jaillon O, Aury JM, Noel B, Policriti A, Clepet C, Casagrande A, Choisne N, Aubourg S, Vitulo N, Jubin C, et al (2007) The grapevine genome sequence suggests ancestral hexaploidization in major angiosperm phyla. Nature **449**: 463–467

Klee HJ, Giovannoni JJ (2011) Genetics and control of tomato fruit ripening and quality attributes. Annu Rev Genet **45**: 41–59

Kliebenstein DJ (2004) Secondary metabolites and plant/environment interactions: A view through *Arabidopsis thaliana* tinged glasses. Plant Cell Environ **27**: 675–684

Love MI, Huber W, Anders S (2014) Moderated estimation of fold change and dispersion for RNA-seq data with DESeq2. Genome Biol **15**: 550

Lund ST, Bohlmann J (2006) The molecular basis for wine grape quality-a volatile subject. Science **311**: 804–805

Ma C, Wang X (2012) Application of the GINI correlation coefficient to infer regulatory relationships in transcriptome analysis. Plant Physiol **160**: 192–203

Ma DM, Wang Z, Wang L, Alejos-Gonzales F, Sun MA, Xie DY (2015) A genome-wide scenario of terpene pathways in self-pollinated *Artemisia annua*. Mol Plant **8**: 1580–1598

Ma S, Shah S, Bohnert HJ, Snyder M, Dinesh-Kumar SP (2013) Incorporating motif analysis into gene co-expression networks reveals novel modular expression pattern and new signaling pathways. PLoS Genet **9**: e1003840

Maere S, Heymans K, Kuiper M (2005) BiNGO: A Cytoscape plugin to assess overrepresentation of gene ontology categories in biological networks. Bioinformatics **21**: 3448–3449

Malacarne G, Costantini L, Coller E, Battilana J, Velasco R, Vrhovsek U, Grando MS, Moser C (2015) Regulation of flavonol content and composition in (Syrah×Pinot Noir) mature grapes: integration of transcriptional profiling and metabolic quantitative trait locus analyses. J Exp Bot **66**: 4441–4453

Martin DM, Aubourg S, Schouwey MB, Daviet L, Schalk M, Toub O, Lund ST, Bohlmann J (2010) Functional annotation, genome organization and phylogeny of the grapevine (*Vitis vinifera*) terpene synthase gene family based on genome assembly, flcdna cloning, and enzyme assays. BMC Plant Biol **10**: 226

Mattivi F, Guzzon R, Vrhovsek U, Stefanini M, Velasco R (2006) Metabolite profiling of grape: flavonols and anthocyanins. J Agric Food Chem **54**: 7692–7702

Munné-Bosch S, Schwarz K, Alegre L (1999) Enhanced formation of α-tocopherol and highly oxidized abietane diterpenes in water-stressed rosemary plants. Plant Physiol **121**: 1047–1052

Munné-Bosch S, Alegre L (2002) The function of tocopherols and tocotrienols in plants. Crit Rev Plant Sci **21**: 31–57

Naithani S, Raja R, Waddell EN, Elser J, Gouthu S, Deluc LG, Jaiswal P (2014) VitisCyc: A metabolic pathway knowledgebase for grapevine (*Vitis vinifera*). Front Plant Sci. doi: 10.3389/fpls.2014.00644

Nisar N, Li L, Lu S, Khin NC, Pogson BJ (2015) Carotenoid metabolism in plants. Mol Plant **8**: 68–82

Reeves PH, Ellis CM, Ploense SE, Wu MF, Yadav V, Tholl D, Chételat A, Haupt I, Kennerley BJ, Hodgens C, et al (2012) A regulatory network for coordinated flower maturation. PLoS Genet **8**: e1002506

Reynolds AG, Wardle DA (1989) Impact of various canopy manipulation techniques on growth, yield, fruit composition, and wine quality of Gewürztraminer. Am J Enol Vitic **40**: 121–129

Ripoll J, Urban L, Staudt M, Lopez-Lauri F, Bidel LPR, Bertin N (2014) Water shortage and quality of fleshy fruits—making the most of the unavoidable. J Exp Bot **65**: 4097–4117

Robinson AL, Boss PK, Solomon PS, Trengove RD, Heymann H, Ebeler SE (2014) Origins of grape and wine aroma. Part 1. Chemical components and viticultural impacts. Am J Enol Vitic **65**: 1–24

Sánchez AM, Winterhalter P (2013) Carotenoid cleavage products in saffron (*Crocus sativus* L.). Carotenoid Cleavage Prod. American Chemical Society, pp 45–63

Selmar D, Kleinwächter M (2013) Stress enhances the synthesis of secondary plant products: The impact of stress-related over-reduction on the accumulation of natural products. Plant Cell Physiol **54**: 817–826

Shannon P, Markiel A, Ozier O, Baliga NS, Wang JT, Ramage D, Amin N, Schwikowski B, Ideker T (2003) Cytoscape: A software environment for integrated models of biomolecular interaction networks. Genome Res **13**: 2498–2504

Shinozaki K, Yamaguchi-Shinozaki K (2007) Gene networks involved in drought stress response and tolerance. J Exp Bot **58**: 221–227

Stitt M, Sulpice R, Keurentjes J (2010) Metabolic networks: how to identify key components in the regulation of metabolism and growth. Plant Physiol **152**: 428–444

Teixeira A, Eiras-Dias J, Castellarin SD, Gerós H (2013) Berry phenolics of grapevine under challenging environments. Int J Mol Sci **14**: 18711–18739

Trapnell C, Roberts A, Goff L, Pertea G, Kim D, Kelley DR, Pimentel H, Salzberg SL, Rinn JL, Pachter L (2012) Differential gene and transcript expression analysis of RNA-seq experiments with TopHat and Cufflinks. Nat Protoc **7**: 562–578

Vannozzi A, Dry IB, Fasoli M, Zenoni S, Lucchin M (2012) Genome-wide analysis of the grapevine stilbene synthase multigenic family: genomic organization and expression profiles upon biotic and abiotic stresses. BMC Plant Biol **12**: 130

Vrhovsek U, Masuero D, Gasperotti M, Franceschi P, Caputi L, Viola R, Mattivi F (2012) A versatile targeted metabolomics method for the rapid quantification of multiple classes of phenolics in fruits and beverages. J Agric Food Chem **60**: 8831–8840

Wehrens R, Carvalho E, Masuero D, De Juan A, Martens S (2013) High-throughput carotenoid profiling using multivariate curve resolution. Anal Bioanal Chem **405**: 5075–5086

Wong DC, Sweetman C, Drew DP, Ford CM (2013) VTCdb: a gene co-expression database for the crop species *Vitis vinifera* (grapevine). BMC Genomics **14**: 882

Young PR, Lashbrooke JG, Alexandersson E, Jacobson D, Moser C, Velasco R, Vivier MA (2012) The genes and enzymes of the carotenoid metabolic pathway in *Vitis vinifera* L. BMC Genomics **13**: 243

Zamboni A, Carli MD, Guzzo F, Stocchero M, Zenoni S, Ferrarini A, Tononi P, Toffali K, Desiderio A, Lilley KS, et al (2010) Identification of putative stage-specific grapevine berry biomarkers and omics data integration into networks. Plant Physiol **154**: 1439–1459

Zhao Q, Wang G, Ji J, Jin C, Wu W, Zhao J (2013) Over-expression of *Arabidopsis thaliana* β-carotene hydroxylase (chyB) gene enhances drought tolerance in transgenic tobacco. J Plant Biochem Biotechnol **23**: 190–198

Supplementary Data

Table S1*. Summary of differentially expressed genes (P<0.05) and associated information (12x V1 identification number, predicted annotation, fold change values, log_2 fold change and adjusted P value) identified between C and D at 41 (a), 68 (b), and 93 (c) days after anthesis (DAA). The 25 most represented transcription factors families in the DE genes (d). Plant gene ontology (GO) slim biological process categories enriched (P<0.05) within significantly up- and down-regulated genes at 41, 68, and 93 DAA between C and D (e) are represented as the relative (%) contribution of genes ascribed to that biological process over the total DE genes in each developmental stage. Detailed information concerning the various metabolite/transcript annotations, correlation relationships (PCC), and statistical significance (empirical P value) are depicted for the global (C and D) metabolite-metabolite network (f) and metabolite-transcript (structural) network in C (g) and D (h). Frequency tables for the significant metabolite-transcript correlations from (g) and (h) are summarized in (i). Correlation values (PCC, statistical significance of PCC, correlation ranks) for the predicted monoterpene (linalool, nerol, and α-terpineol)-transcript network reported in Figure 10a (j). Contingency tables containing enriched (P<0.01) PLACE cis-regulatory elements and associated information (e.g., motif description, occurrence of motif within promoter regions) identified in the combined monoterpene-transcript network presented in Figure 10b (k).

* Table S1 is the separate excel file

Table S2. List of phenolics, carotenoids, and free VOCs identified in this study using UHPLC-MS/MS, HPLC-DAD, and HS-SPME-GC-MS platforms.

Compound	Chemical Class	Analytical Platform
Ellagic acid	Benzoic and Cinnamic acids	UHPLC-MS/MS
Gallic acid	Benzoic and Cinnamic acids	UHPLC-MS/MS
Methyl gallate	Benzoic and Cinnamic acids	UHPLC-MS/MS
trans-Caftaric acid	Benzoic and Cinnamic acids	UHPLC-MS/MS
trans-Coutaric acid	Benzoic and Cinnamic acids	UHPLC-MS/MS
trans-Fertaric acid	Benzoic and Cinnamic acids	UHPLC-MS/MS
Astringin	Stilbenoids	UHPLC-MS/MS
Pallidol	Stilbenoids	UHPLC-MS/MS
cis-Piceid	Stilbenoids	UHPLC-MS/MS
trans-Piceid	Stilbenoids	UHPLC-MS/MS
trans-ε-Viniferin	Stilbenoids	UHPLC-MS/MS
Phlorizin	Hydrochalcones	UHPLC-MS/MS
Trilobatin	Hydrochalcones	UHPLC-MS/MS
Kaempferol-3-*O*-glucoside	Flavonols	UHPLC-MS/MS
Quercetin-3-*O*-glucoside	Flavonols	UHPLC-MS/MS
Quercetin-3-*O*-glucoronide	Flavonols	UHPLC-MS/MS
Rutin	Flavonols	UHPLC-MS/MS
(+)- Catechin	Flavan-3-ols	UHPLC-MS/MS
(-)- Epicatechin	Flavan-3-ols	UHPLC-MS/MS
(-)-Epicatechin gallate	Flavan-3-ols	UHPLC-MS/MS
(-)-Epigallocatechin	Flavan-3-ols	UHPLC-MS/MS
(-)-Epigallocatechin gallate	Flavan-3-ols	UHPLC-MS/MS
(+)-Gallocatechin	Flavan-3-ols	UHPLC-MS/MS
Procyanidin B1	Proanthocyanidins	UHPLC-MS/MS
Procyanidin B2+B4	Proanthocyanidins	UHPLC-MS/MS
Procyanidin B3	Proanthocyanidins	UHPLC-MS/MS
Caffeic acid + catechin condensation product	Others	UHPLC-MS/MS

Table S2. (continued)

Compound	Chemical Class	Analytical Platform
Antheraxanthin	Carotenoids	HPLC-DAD
β-Carotene	Carotenoids	HPLC-DAD
9-(Z)-β-Carotene	Carotenoids	HPLC-DAD
Lutein	Carotenoids	HPLC-DAD
Lutein, 5-6 epoxide	Carotenoids	HPLC-DAD
9-(Z) -Neoxanthin	Carotenoids	HPLC-DAD
Violaxanthin	Carotenoids	HPLC-DAD
Zeaxanthin	Carotenoids	HPLC-DAD
α-Tocopherol	Tocopherols	HPLC-DAD
γ-Tocopherol	Tocopherols	HPLC-DAD
Hexanoic acid	Acids	HS-SPME-GC-MS
Heptanol	Alcohols	HS-SPME-GC-MS
Hexanol	Alcohols	HS-SPME-GC-MS
2-Hexenol	Alcohols	HS-SPME-GC-MS
3-Hexenol	Alcohols	HS-SPME-GC-MS
Nonanol	Alcohols	HS-SPME-GC-MS
Octanol	Alcohols	HS-SPME-GC-MS
1-Octen-3-ol	Alcohols	HS-SPME-GC-MS
Benzaldehyde	Aldehydes	HS-SPME-GC-MS
(E,E) -2,4-Heptadienal	Aldehydes	HS-SPME-GC-MS
Heptanal	Aldehydes	HS-SPME-GC-MS
(E) -2-Heptenal	Aldehydes	HS-SPME-GC-MS
(E,E) -2,4-Hexadienal	Aldehydes	HS-SPME-GC-MS
Hexanal	Aldehydes	HS-SPME-GC-MS
(E) -2-Hexenal	Aldehydes	HS-SPME-GC-MS
Nonanal	Aldehydes	HS-SPME-GC-MS
(E) -2-Nonenal	Aldehydes	HS-SPME-GC-MS
(E) -2-Octenal	Aldehydes	HS-SPME-GC-MS
(E) -2-Pentenal	Aldehydes	HS-SPME-GC-MS
β-Damascenone	C13-Norisoprenoids	HS-SPME-GC-MS
β-Ionone	C13-Norisoprenoids	HS-SPME-GC-MS
β-Ionone-5-6-epoxide	C13-Norisoprenoids	HS-SPME-GC-MS
β-Cyclocitral	C10-Norisoprenoids	HS-SPME-GC-MS
3-Hexenyl acetate	Esters	HS-SPME-GC-MS
6-Methyl-5-hepten-2-one	Ketones	HS-SPME-GC-MS
1-Octen-3-one	Ketones	HS-SPME-GC-MS
trans -Caryophyllene	Terpenes	HS-SPME-GC-MS
Citronellol	Terpenes	HS-SPME-GC-MS
Geraniol	Terpenes	HS-SPME-GC-MS
Geranyl acetone	Terpenes	HS-SPME-GC-MS
Hotrienol	Terpenes	HS-SPME-GC-MS
α-Humulene	Terpenes	HS-SPME-GC-MS
Linalool	Terpenes	HS-SPME-GC-MS
Linalool oxA	Terpenes	HS-SPME-GC-MS
Linalool oxB	Terpenes	HS-SPME-GC-MS
Nerol	Terpenes	HS-SPME-GC-MS
α-Terpineol	Terpenes	HS-SPME-GC-MS

Figure S1. Trends of phenolic concentration in C and D berries during fruit development and ripening in 2011 (left hand panel) and 2012 (right hand panel). Data are expressed as mg/kg of fresh berries.

Benzoic and cinnamic acids

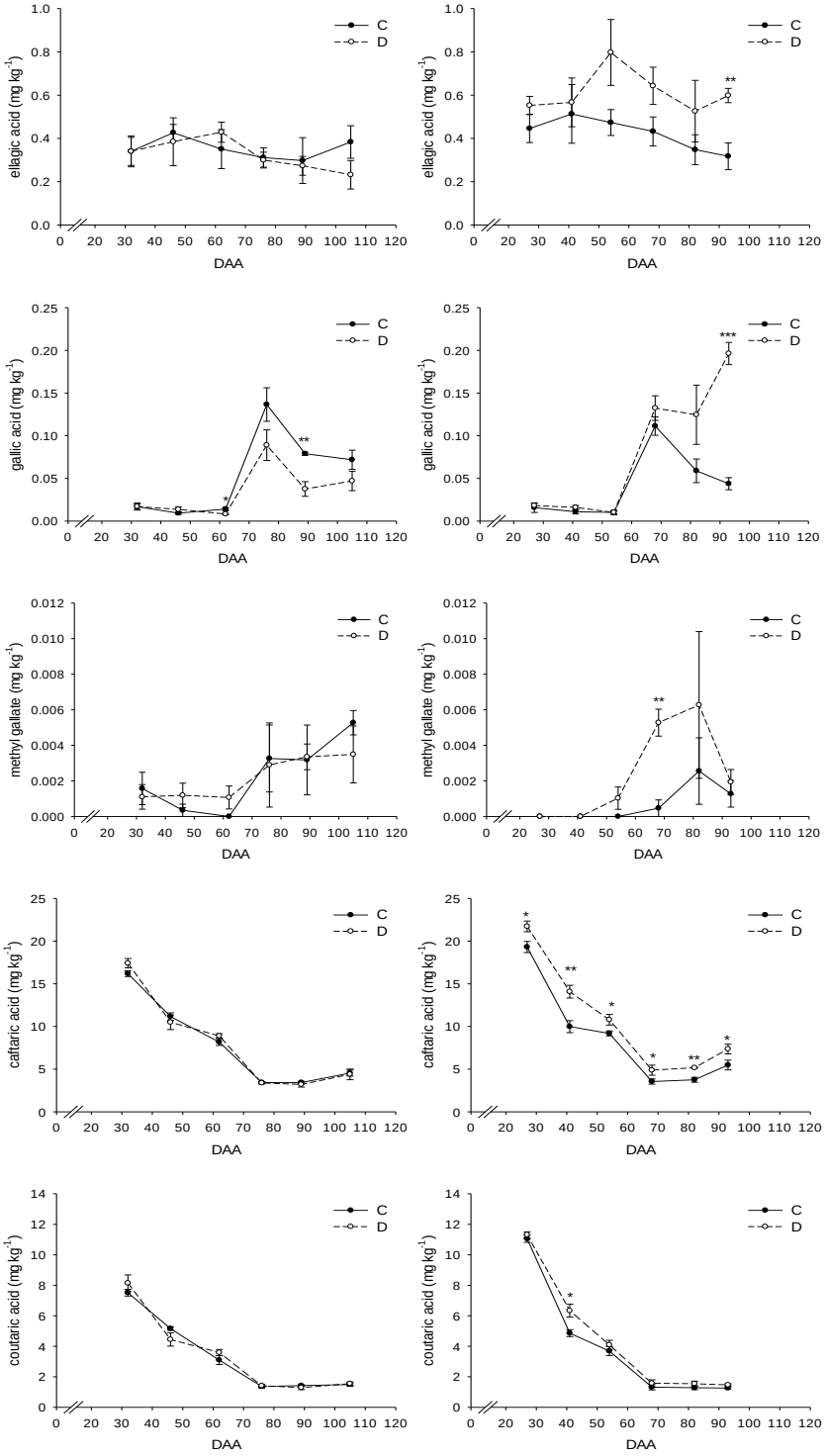

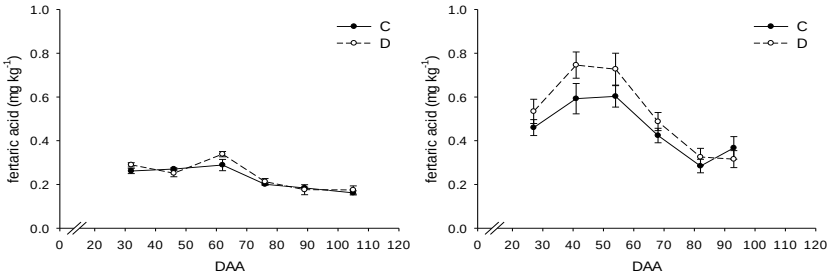

Stilbenoids

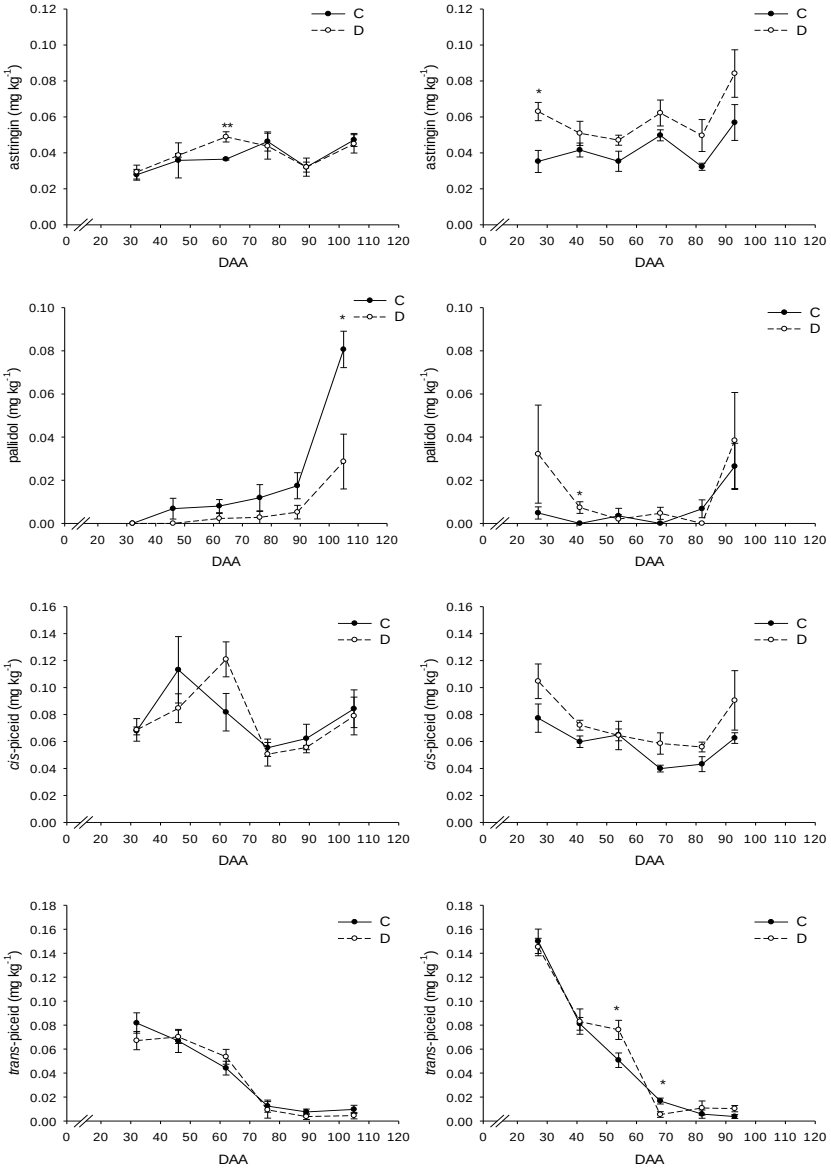

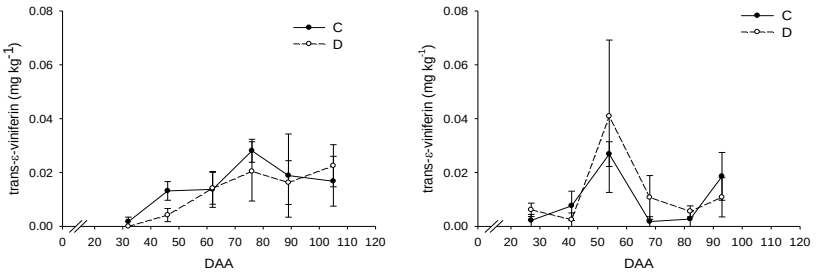

Hydroxychalcones

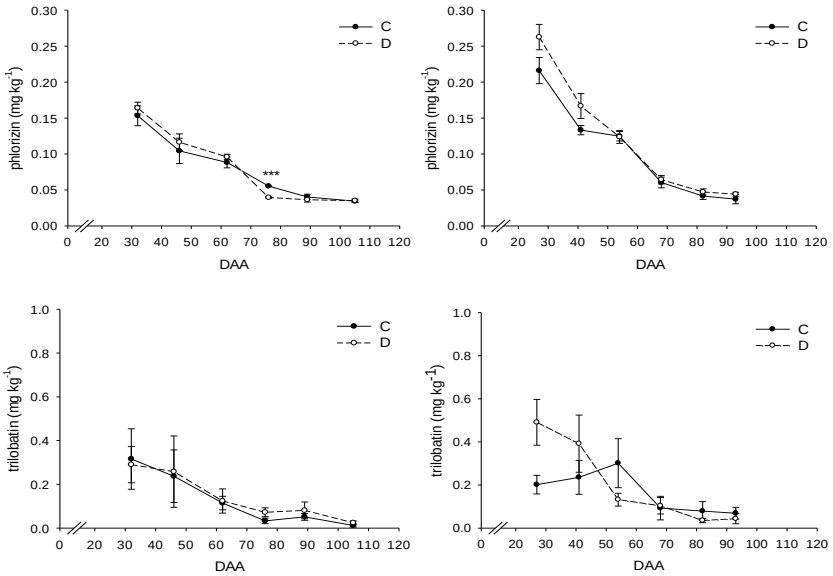

Flavonols

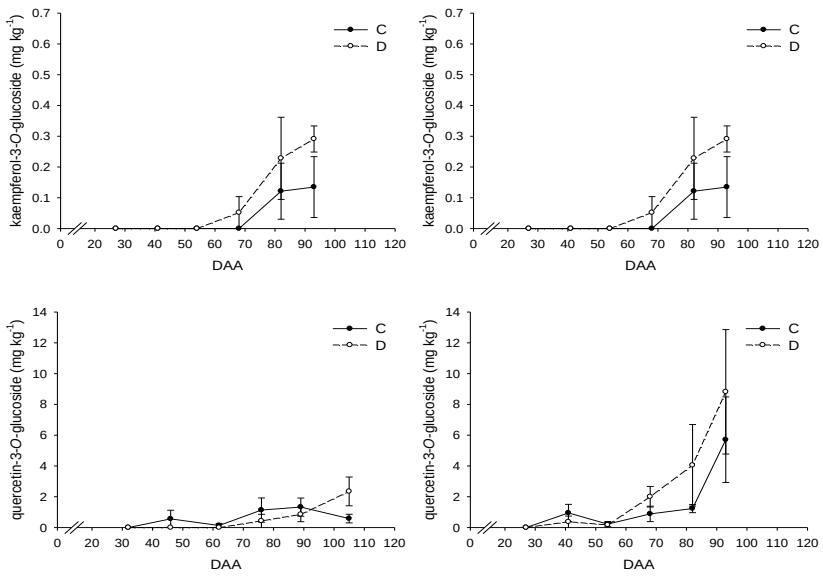

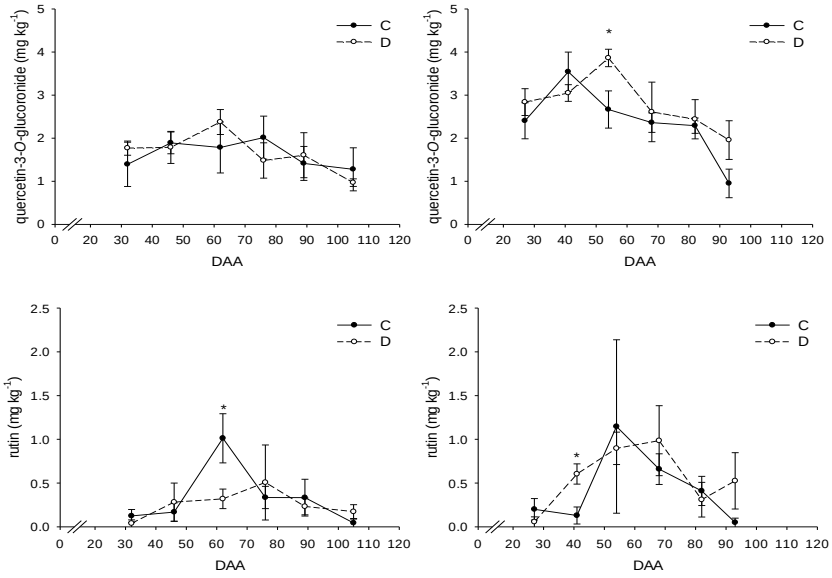
quercetin-3-O-glucoronide (mg kg-1)
rutin (mg kg-1)
DAA
C
D

Flavan-3-ols

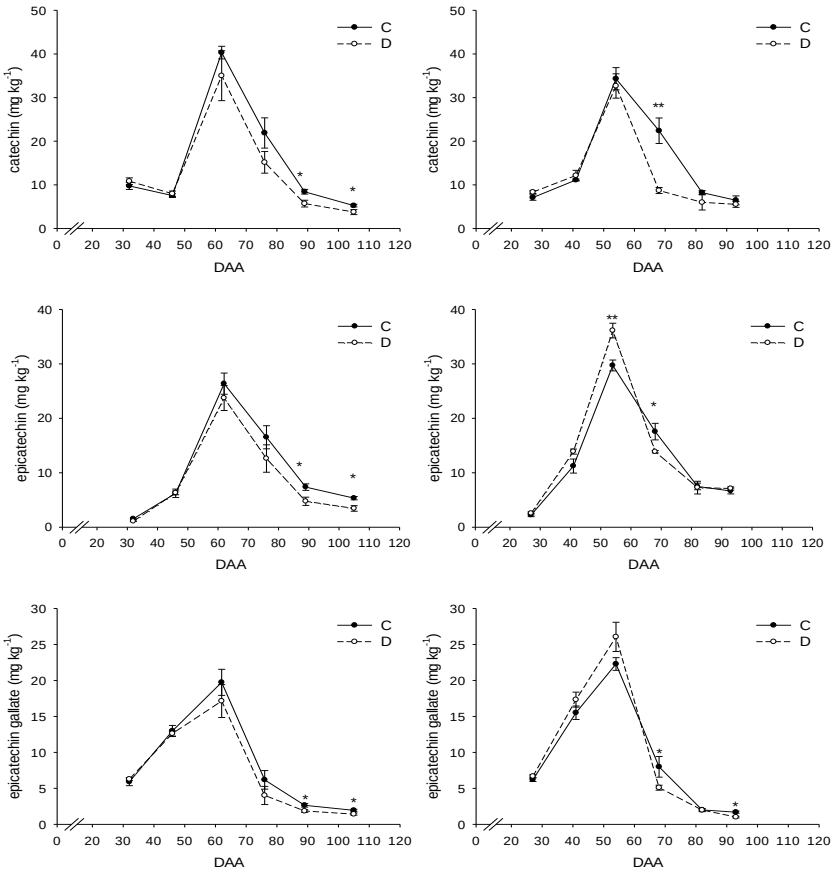
catechin (mg kg-1)
epicatechin (mg kg-1)
epicatechin gallate (mg kg-1)
DAA
C
D

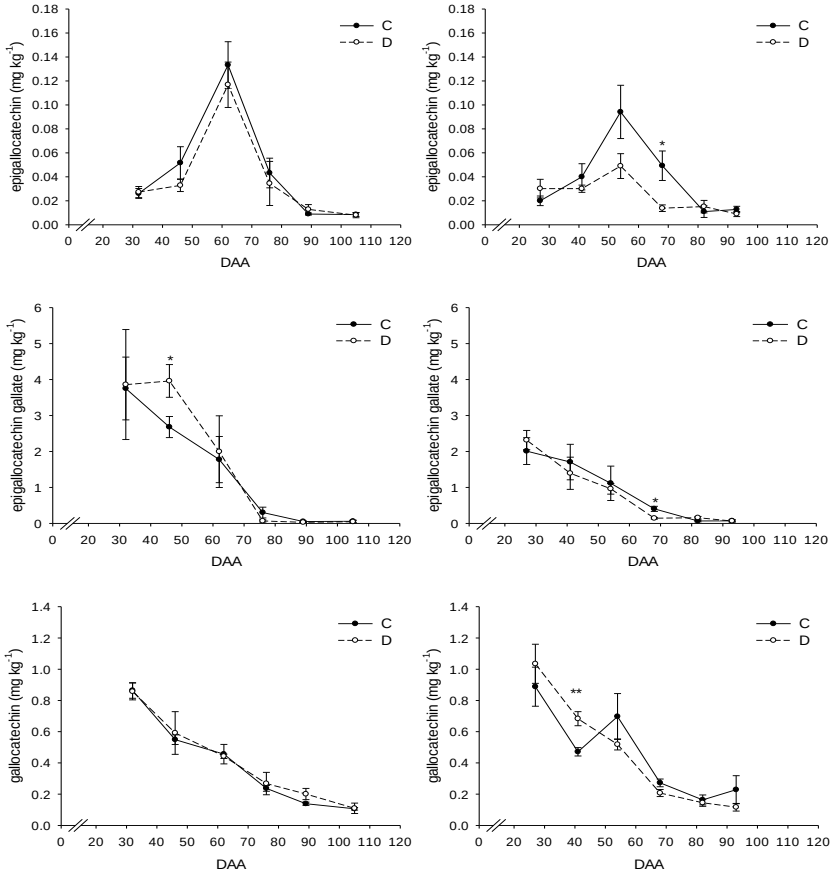

Proanthocyanidins

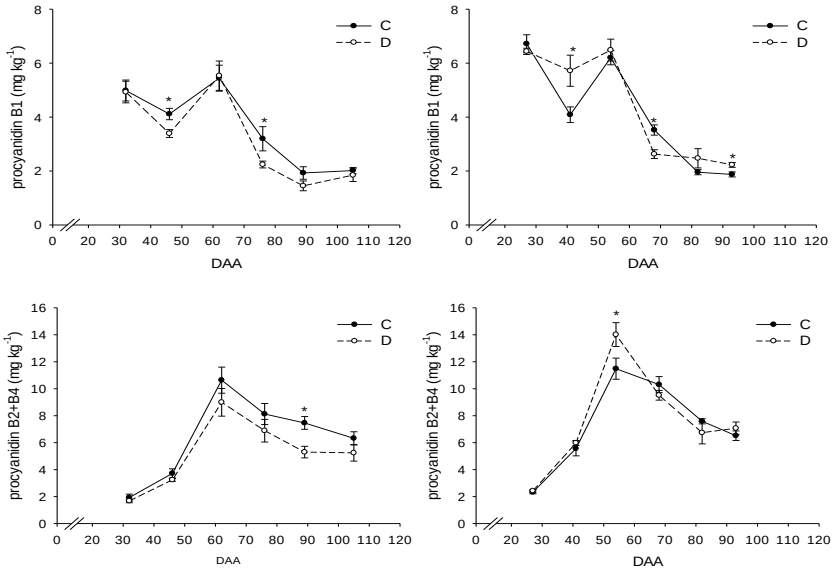

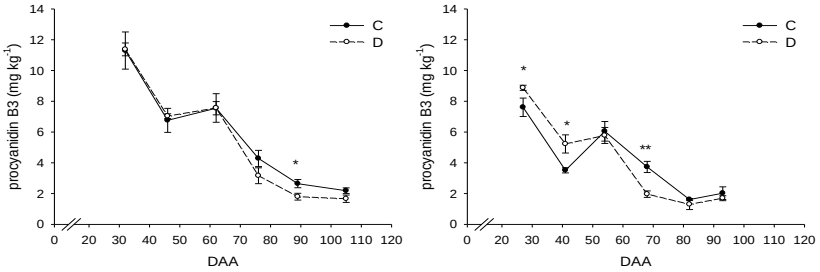
procyanidin B3 (mg kg-1)
DAA
C
D
*
*
*
**

Others

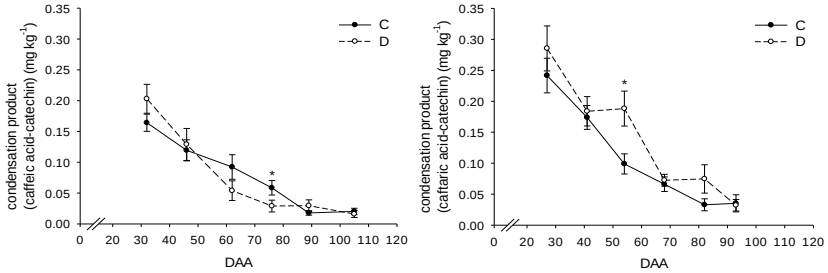
condensation product (caffeic acid-catechin) (mg kg-1)
condensation product (caftaric acid-catechin) (mg kg-1)
DAA
C
D
*
*

Figure S2. Trends of carotenoid and tocopherol concentration in C and D berries during fruit development and ripening in 2011 (left hand panel) and 2012 (right hand panel). Data are expressed as mg/kg of fresh berries.

Carotenoids

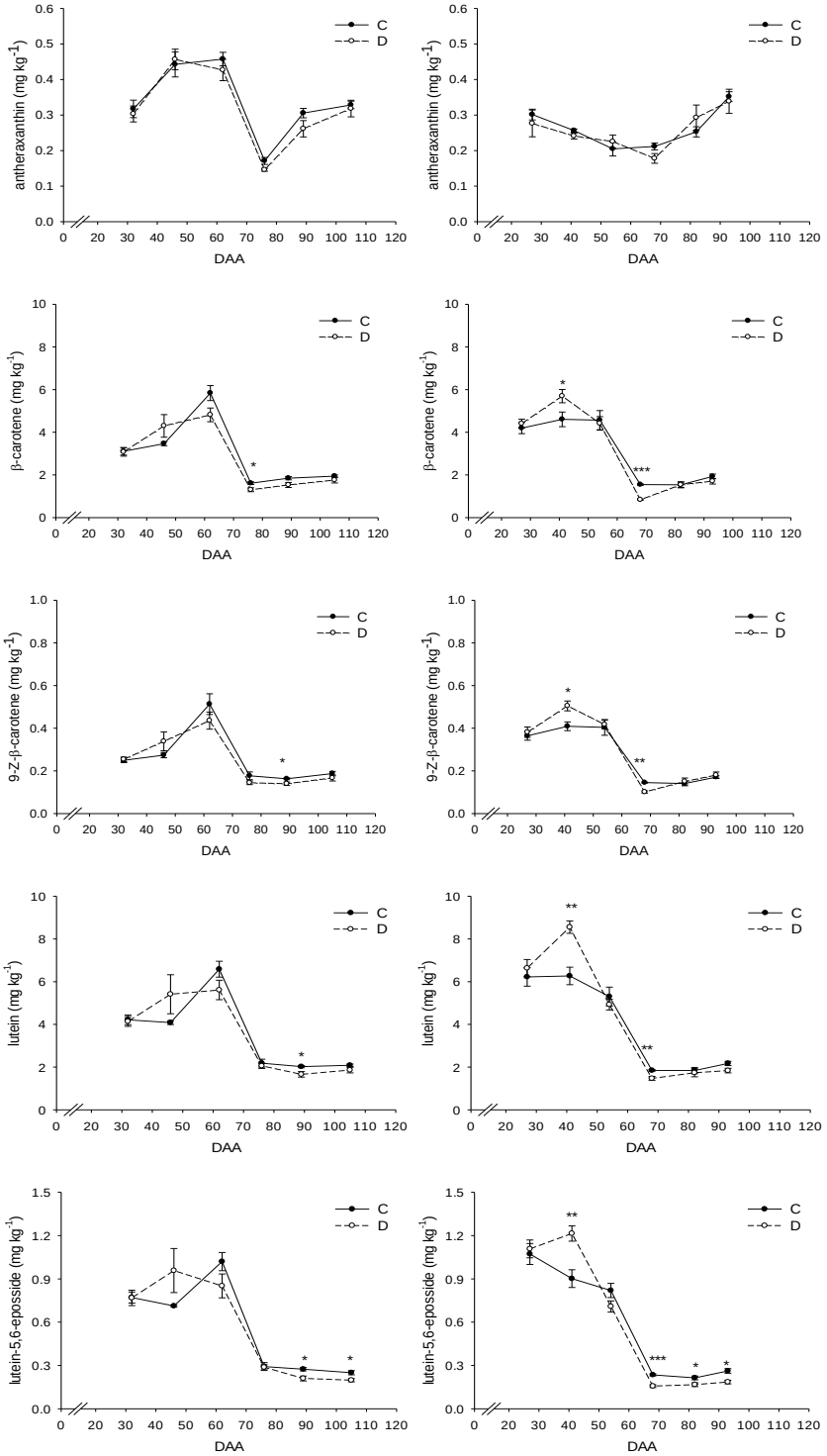

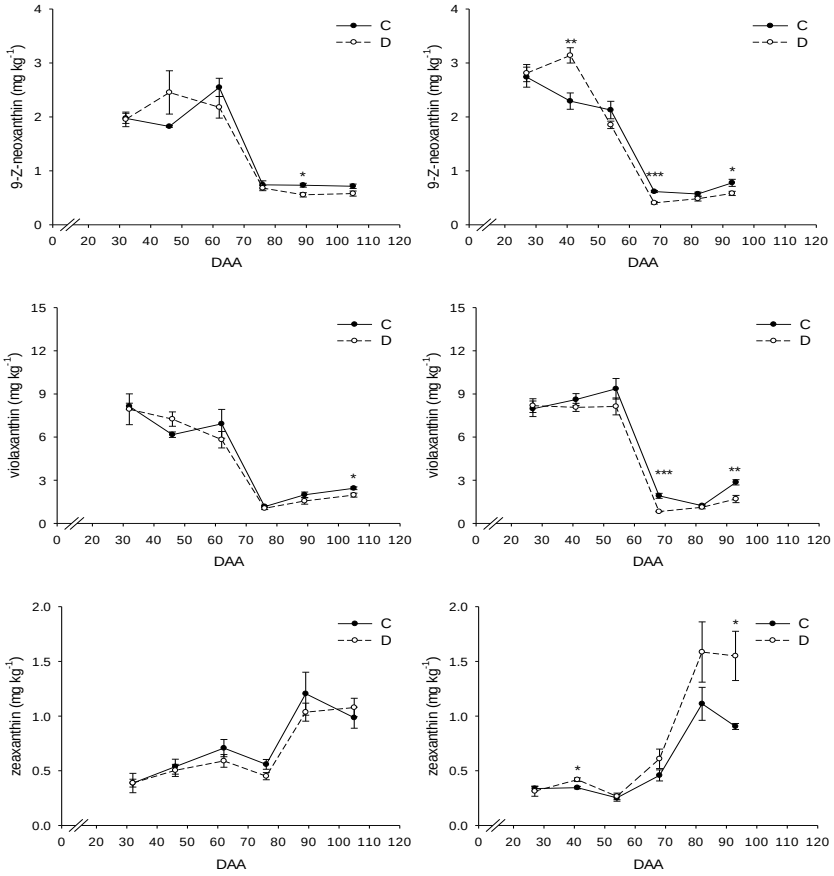

Tocopherols

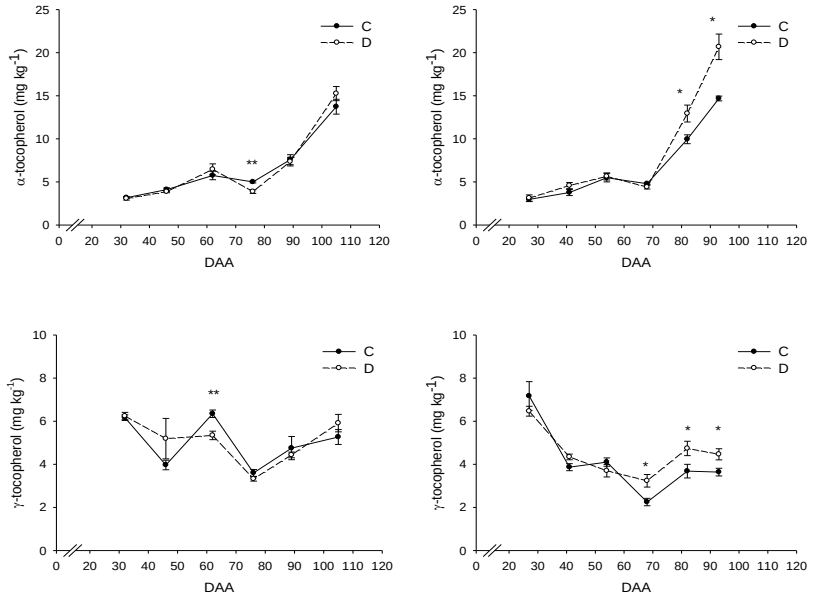

Figure S3. Trends of VOC concentration in C and D berries during fruit development and ripening in 2011 (left hand panel) and 2012 (right hand panel). Data are expressed as µg/kg of fresh berries.

Acids

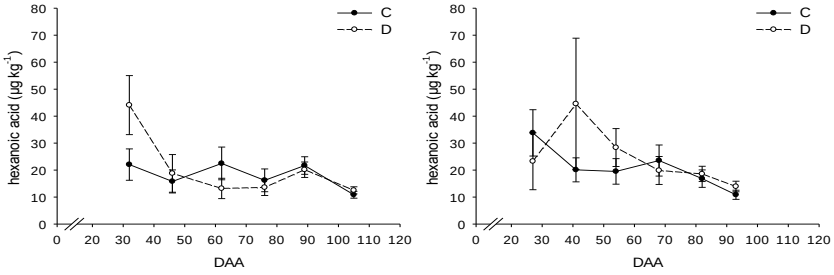

Alcohols

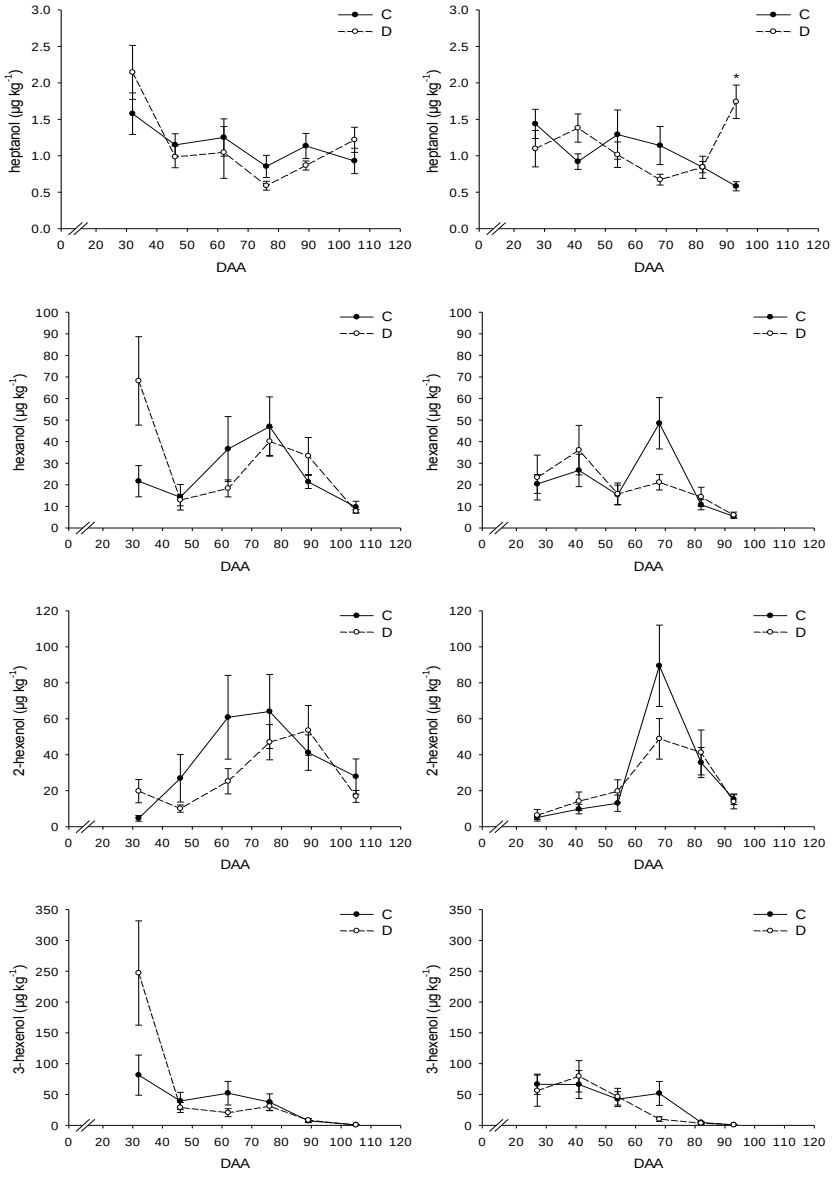

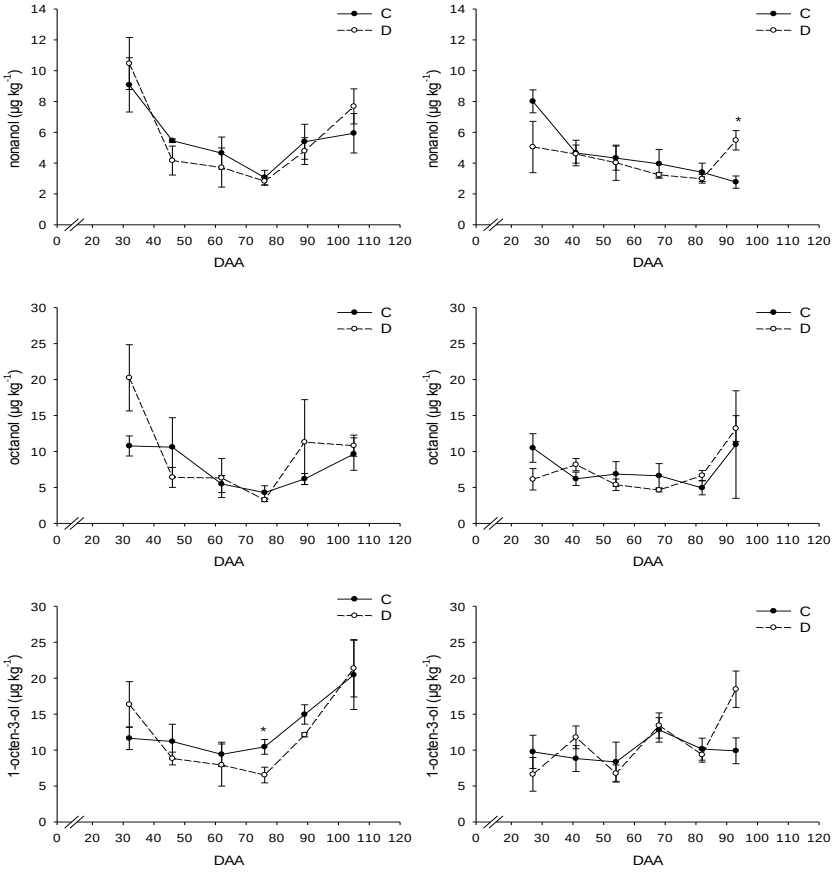
nonanol (µg kg-1)
octanol (µg kg-1)
1-octen-3-ol (µg kg-1)
DAA
C
D
*

Aldehydes

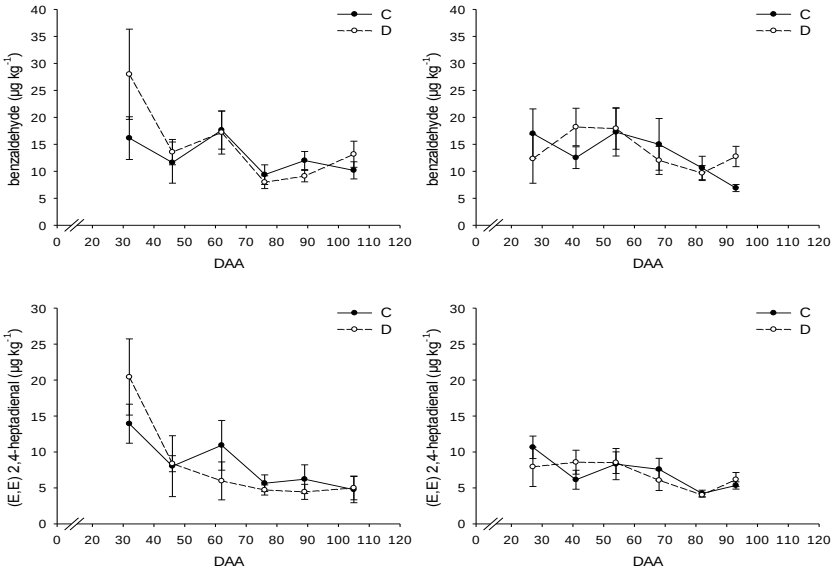
benzaldehyde (µg kg-1)
(E,E) 2,4-heptadienal (µg kg-1)
DAA
C
D

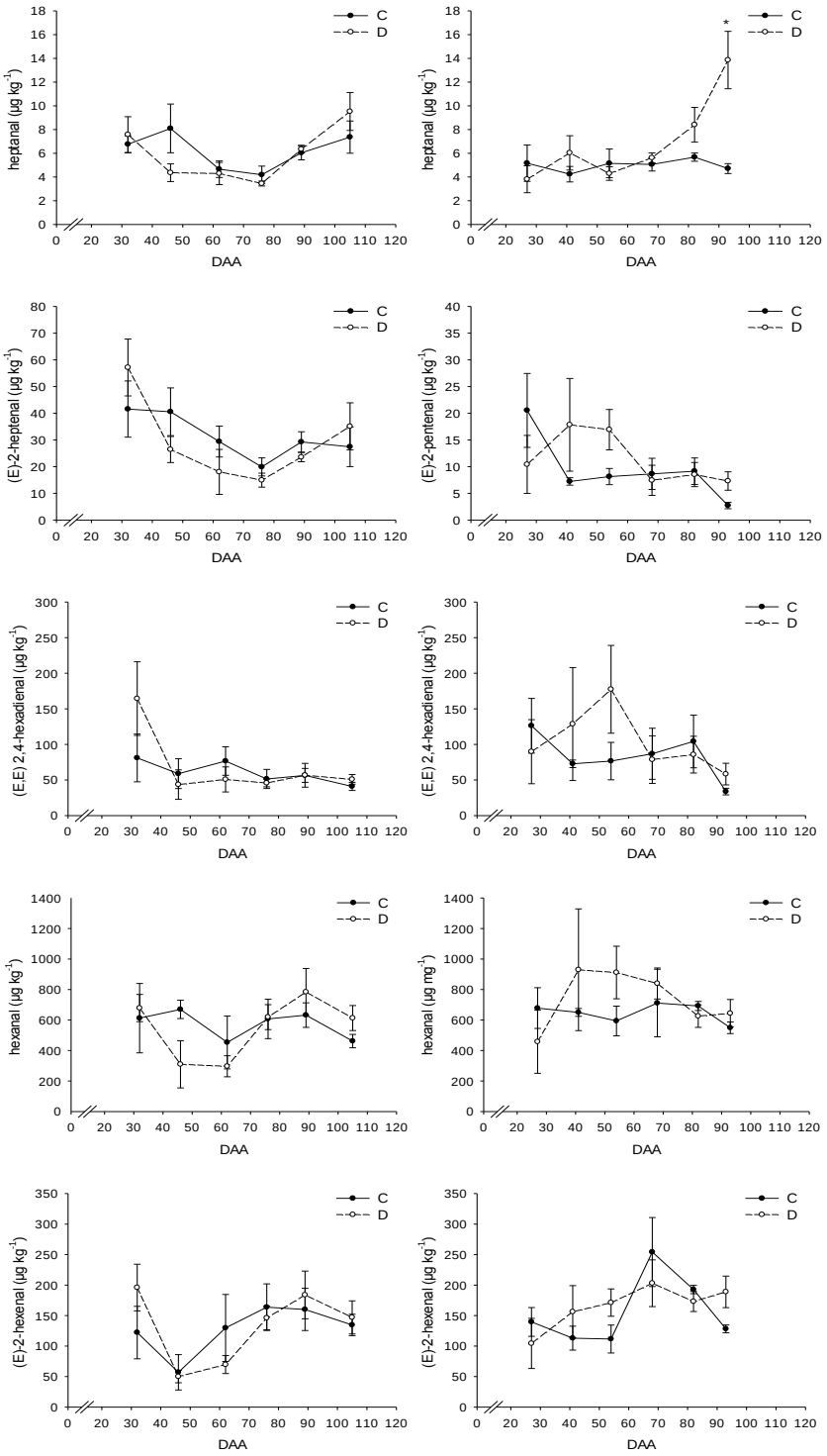
heptanal (µg kg-1)
heptanal (µg kg-1)
(E)-2-heptenal (µg kg-1)
(E)-2-pentenal (µg kg-1)
(E,E) 2,4-hexadienal (µg kg-1)
(E,E) 2,4-hexadienal (µg kg-1)
hexanal (µg kg-1)
hexanal (µg mg-1)
(E)-2-hexenal (µg kg-1)
(E)-2-hexenal (µg kg-1)
DAA
C
D
*

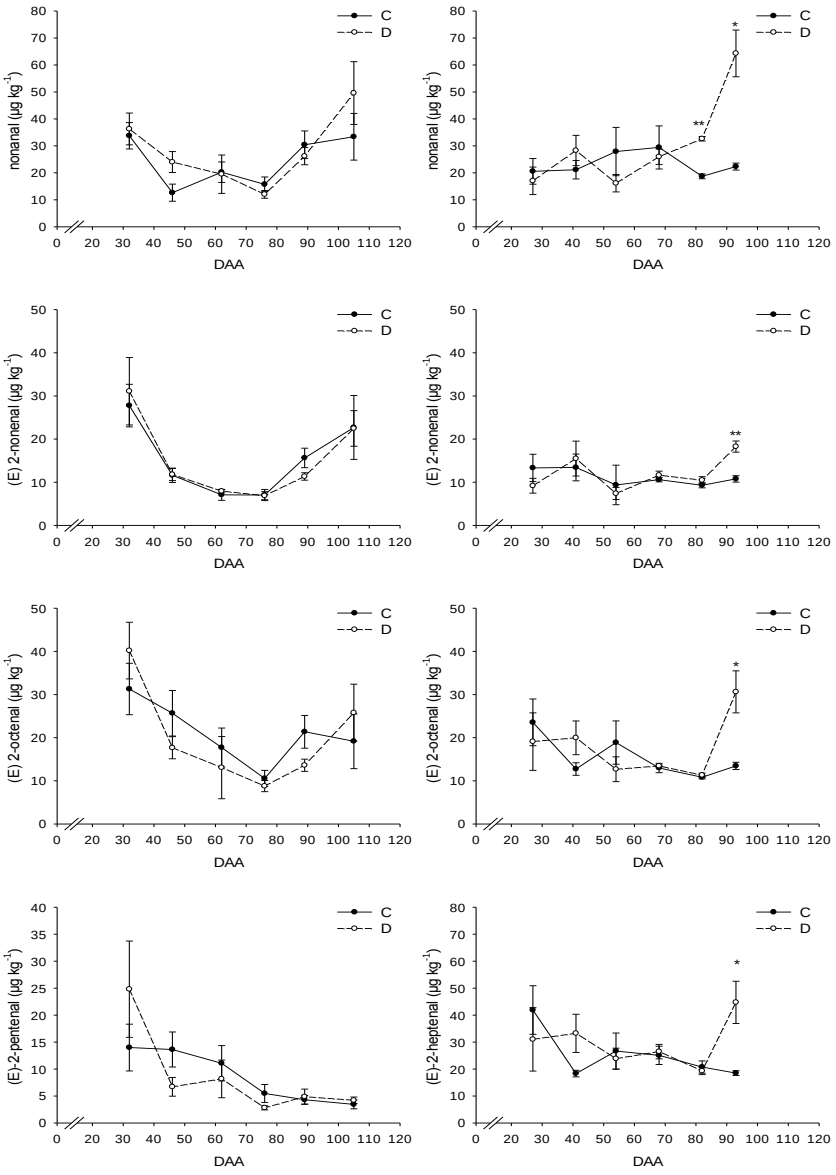

C_{10} & C_{13} Norisoprenoids

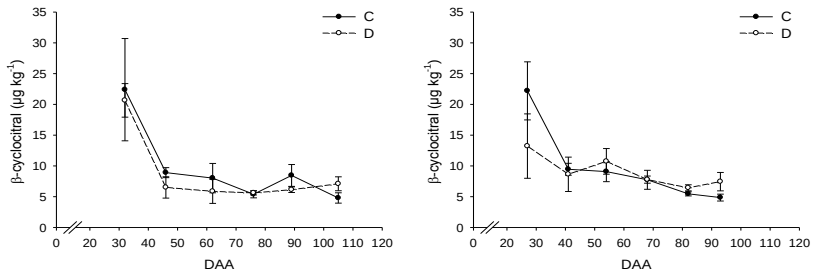

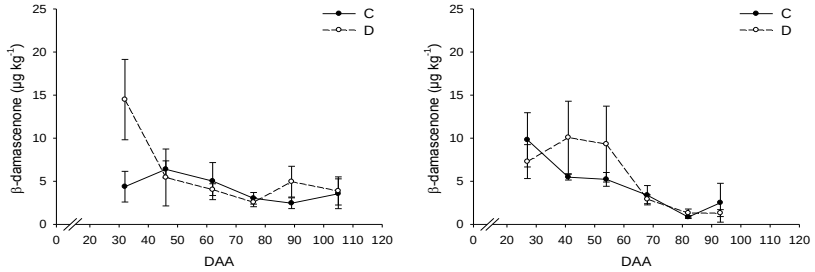

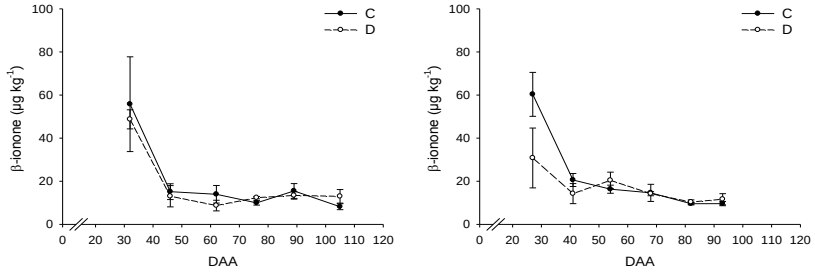

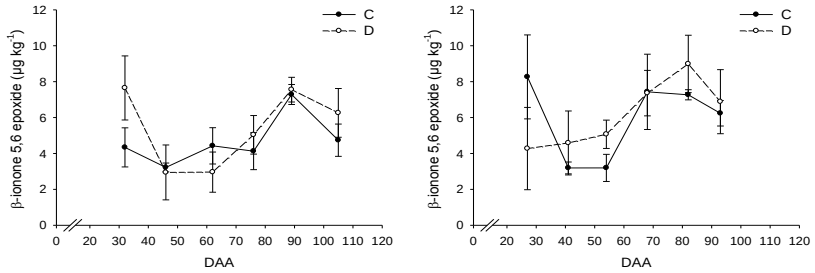

Esters

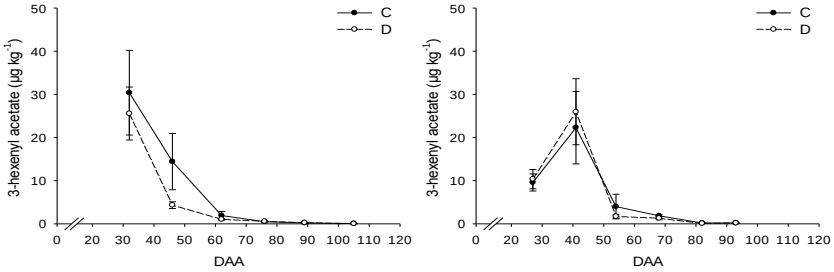

Ketones

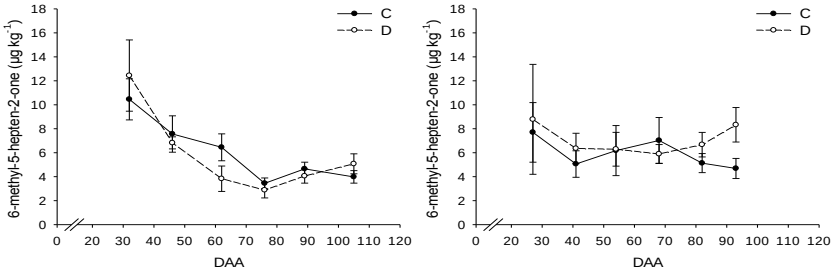

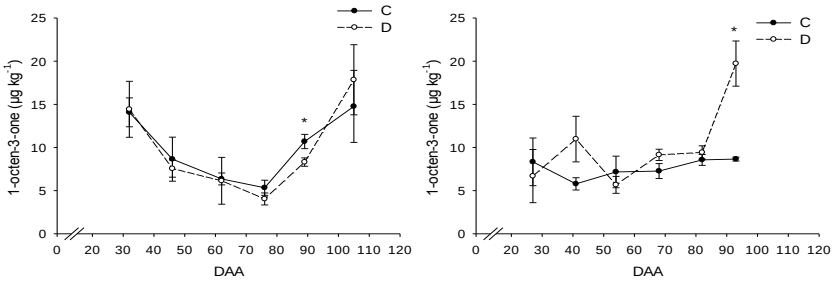
1-octen-3-one (µg kg-1)
DAA
C
D
*

Terpenes

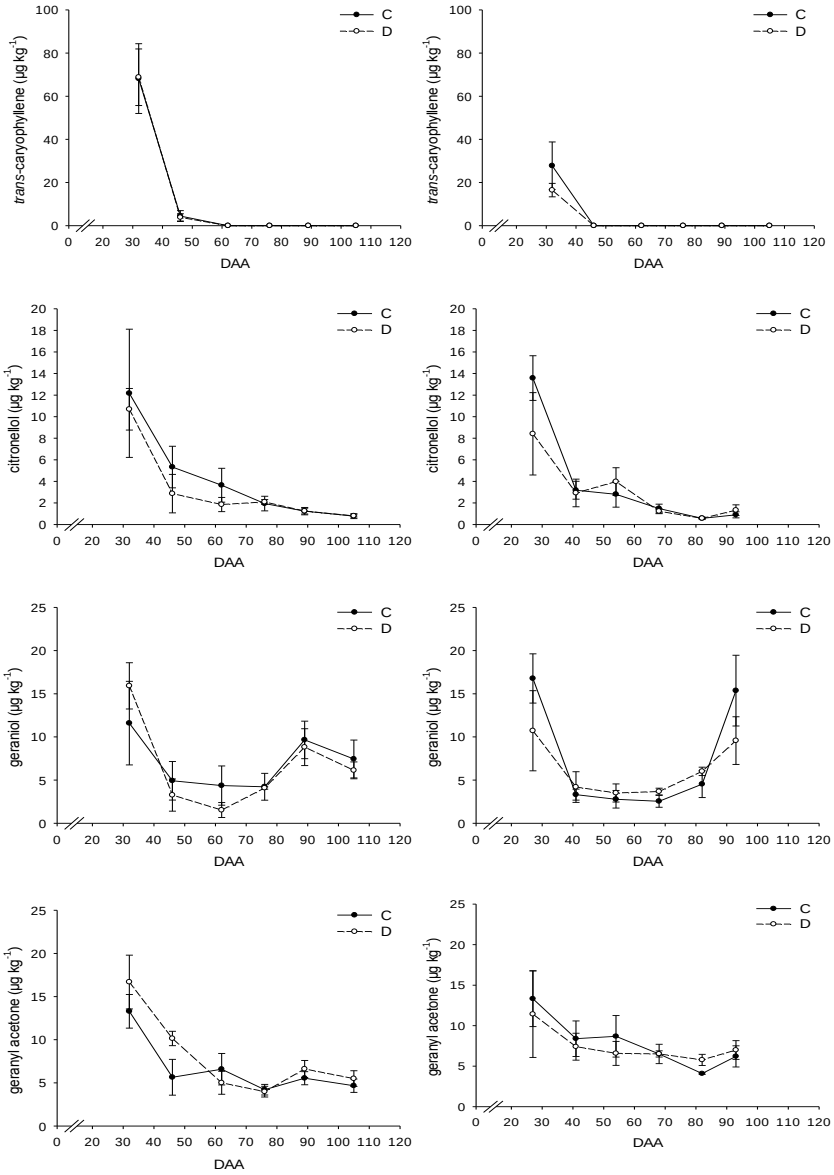
trans-caryophyllene (µg kg-1)
citronellol (µg kg-1)
geraniol (µg kg-1)
geranyl acetone (µg kg-1)
DAA
C
D

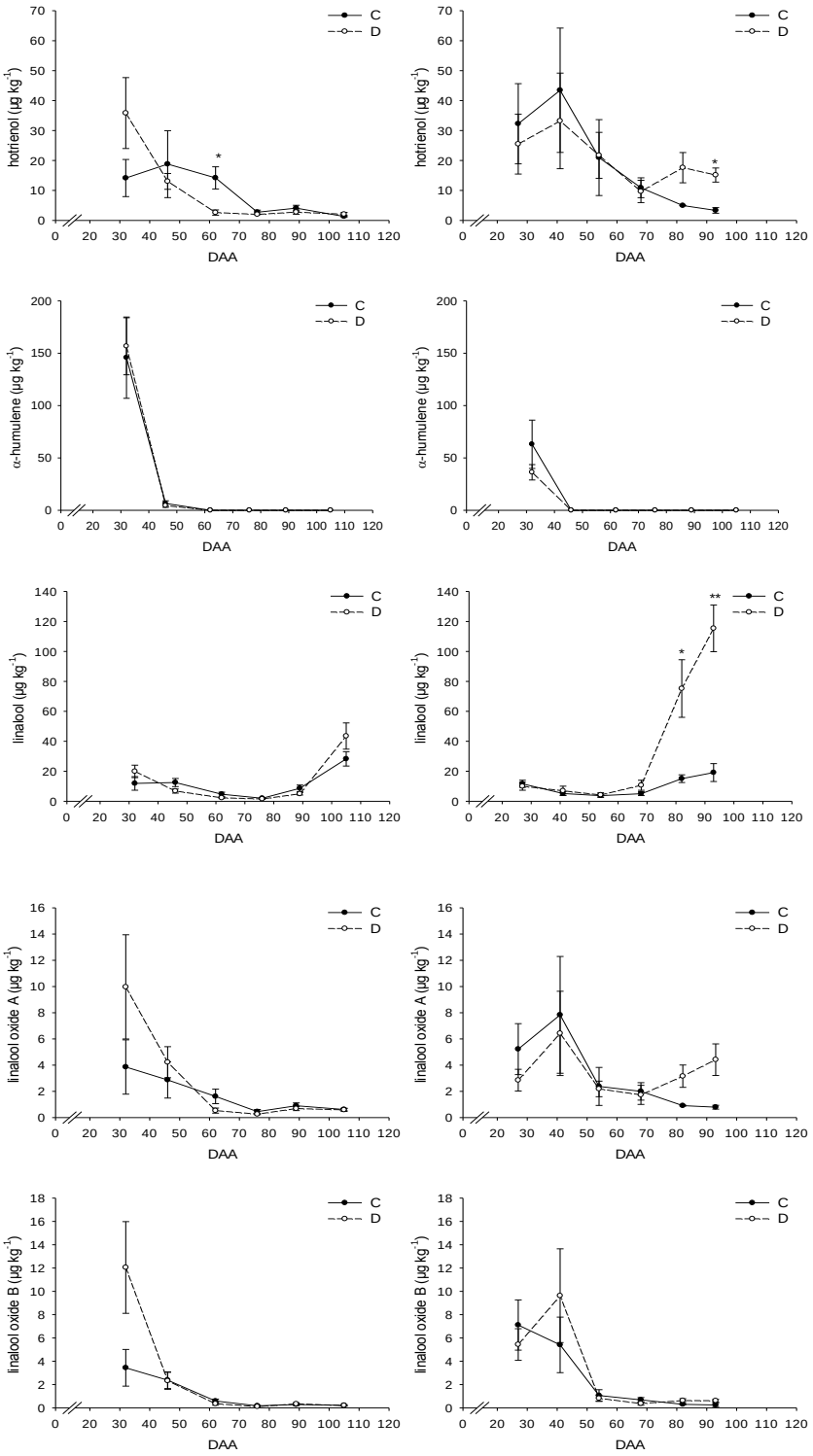
hotrienol (µg kg-1)
α-humulene (µg kg-1)
linalool (µg kg-1)
linalool oxide A (µg kg-1)
linalool oxide B (µg kg-1)
DAA
C
D
*
**

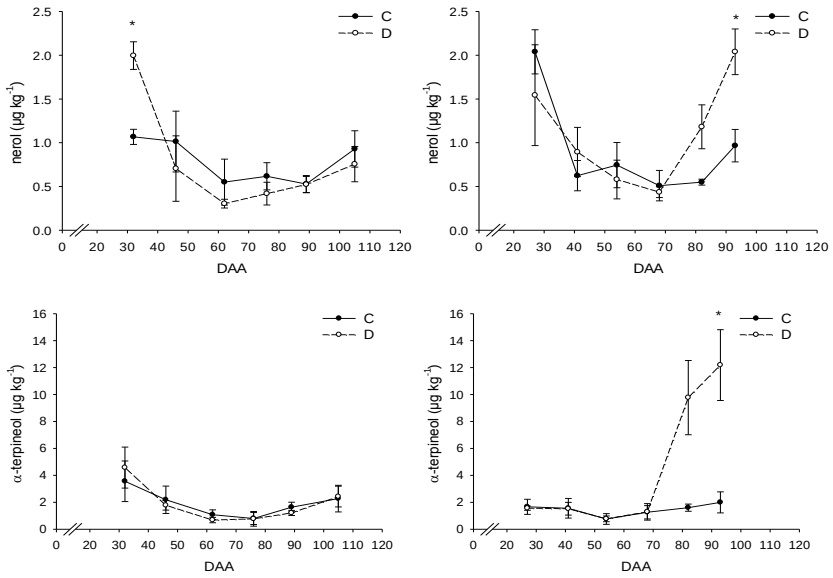
nerol (µg kg-1)
DAA
C
D
*
α-terpineol (µg kg-1)

Preface to chapter 3: Merlot

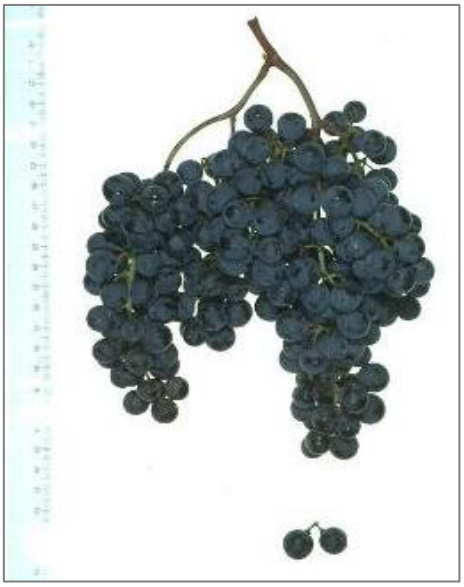

This vine originated in southwest France, mainly cultivated in the region of Bordeaux. From France it has spread all over the world. Many DOC wines are characterized by this grape, either as single varietal wines or blended with other grape varieties, such as Cabernet Sauvignon and Cabernet Franc.

The ampelographic features of the vine can be summarized in an expanded, cottony, white in color with crimson-red edges apex; in a medium mature leaf with three lobes, dark green in color.

The grape cluster is medium size with one or two wings more or less sparse; the grape berry is medium size, round with pruinose skin and blue-black in color.

The grape clusters are sensitive to downy mildew, and *Botrytis cinerea*. Vine is reasonable tolerant to drought.

Wine made purely from this grape is characterized by an intense ruby-red color and a bouquet of red fruit, in particular of wild berries and red flowers.

Information was retrieved from the *Vitis Rauscedo Catalogue – Variety Description Cards*.

Images of Merlot grape bunch and adaxial and abaxial leaf surfaces were retrieved from the *Vitis International Variety Catalogue – VIVC*.

The following chapter is part of a manuscript in preparation.

Chapter 3

INTEGRATIVE ANALYSIS OF TRANSCRIPTS AND METABOLITES MODULATED BY SEVERE WATER DEFICIT IN MERLOT (*VITIS VINIFERA* L.) BERRIES

Introduction

Environmental stresses such as drought, cold, heat, extreme light, excessive soil salinity, or their combinations are recognized to be the main responsible for the loss of crop yield worldwide. Depending on the severity and the timing of these constrains, different mechanisms are adopted by the plants to avoid or tolerate the stresses. These responses, in line with the genotype x environmental interaction, can be elastic i.e. reversible or plastic i.e. irreversible (Cramer et al., 2011). In fruit crops, fruit composition, besides yield, determines the economic sustainability of these crops in the different environments. Since secondary metabolites produced in the fruit are sensitive to the environmental cues, environmental stresses can affect fruit composition and the so called fruit "quality". For instance, in fleshy fruits, beside reducing growth and photosynthesis, drought can modulate fruit metabolism, increasing the production of quality related metabolites; hence, increasing the fruit economic value (reviewed in Ripoll et al., 2014).

Drought stress response has been studied in various plants and at various levels (physiological, metabolic, and molecular); however, the major achievements have been done so far investigating the molecular response of the model plant *Arabidopsis thaliana* (reviewed in Singh and Laxmi, 2015). The transcriptional response to water deficit is modulated by both a ABA-dependent and ABA-independent signal transduction pathways (Yamaguchi-Shinozaki and Shinozaki, 2006). In the ABA dependent pathway, the accumulation of ABA is sensed by PYR/PYL/RCAR-PP2C receptor complex, and activates a class III SnRK2s. This class, III SnRK2s, phosphorylates four transcription factors, ABA-responsive element (ABRE) binding protein 1 (AREB1), AREB2, ABRE binding factor 3 (ABF3), and ABF1. These transcription factors regulate several downstream genes by binding to the ABRE cis-regulatory element present in their promoter region. Beside this module, drought induced ABA also regulate the activity of MYB/MYCs, NACs, WRKYs, and NF-Y transcription factors that, in tour modulate the plant drought stress response and tolerance. In the ABA-independent signaling pathway, DREB2A plays a pivotal role in the gene expression regulation under drought stress. Additionally, some NAC transcription factors also regulate the drought response in an ABA independent manner. However, a cross-talk between ABA-dependent and ABA-independent pathways has been hypothesized under drought stress, with AREB/ABFs inducing DREB2A. Recently, the plant metabolic and molecular response to drought has been investigated in several organs of non-model systems such as *Medicago truncatula* (Zhang et al., 2014), *Oryza sativa* (Maruyama et al.,

2014), and *Zea mays* (Opitz et al., 2015). These studies encompassed RNA-sequencing and large scale metabolite analyses in order to reveal the major metabolic routes that modulate the response to drought in these field crops. These studies confirmed that transcription factors are highly enriched among the genes differentially regulated under water deficit. These groups of TFs included bHLH, bZIP, ERF, and HSF in *Zea mays*, and, among the others, MYB, AP2/EREBP, bHLH, NAC, bZIP, WRKY, and homeodomain contain proteins, C2C2 and C2H2 zinc finger proteins in *Medicago truncatula*. Despite the relevant role of fruit crops in agriculture, limited knowledge on the fruit response to drought is available. Recently Ripoll et al. (2016) reported that a moderate water deficit applied to tomato berries affected the fruit composition with an increased sugar accumulation and a reduced acidity together with a possible minor concentration of carotenoids. Among the fruit crops, grapevine has been used as a model plant for studying the ripening process in non-climacteric fruits, and due to its major economic role and the recent development of genomic tools, grapevine fruit is a valuable system for investigating the molecular and metabolic response of fruits to droughts.

Grapevine (*Vitis vinifera* L.) is one of the major fruit crop cultivated in the world; 7.1 million hectares are dedicated to grape production worldwide, which yielded to 77 million tons of grapes in 2013 (FAOSTAT). Most of the grapes harvested are dedicated to wine production. Generally classified as a drought tolerant plant, grapevine is often not irrigated, especially in Europe. Mediterranean climate, with warm and dry summers and cold and wet winters, is considered optimal for viticulture. However, as a consequence of the ongoing climate changes, heat waves and decreased precipitations in the Southern Europe is leading to transient drought events, in particular during the summer (Gao and Giorgi, 2008), affecting grapevine yield and composition. Remarkably, these climatic phenomena may decrease sustainability of viticulture in regions where grapes have been traditionally cultivated and shift the grape production onto new areas (Hannah et al., 2013). Understanding how drought affects fruit metabolism is a key step to development of new studies and irrigation strategies for optimizing irrigation treatments in vineyards.

The response of grapevine to water deficit has been widely studied. At the morphological and physiological level, vegetative development is reduced and the photosynthesis rate is impaired (Lovisolo et al., 2010) with different extent among isohydric, anisohydric, and near iso/anisohydric cultivars (Hochberg et al., 2013a). At the metabolic level, water deficit affect both the central and the specialized metabolism (Grimplet et al., 2009; Hochberg et al., 2015) and at the molecular level, gene expression is altered with several genes up- or down-regulated by water deficit (Castellarin et al., 2007a; Deluc et al., 2009). Specifically, major effects have been described in the amino acids, phenylpropanoid, flavonoid and terpenoid pathways.

In this study, we profiled the entire grape transcriptome, using high-throughput analysis, such as the RNA-sequencing, coupled to large-scale targeted metabolite analyses to evaluate the impact of water deficit on the berry metabolism of the red grape variety Merlot. Our study aimed to understand how water deficit modulates the major central and specialized metabolic pathways, identifying the key modulators of the molecular response of fruits to this abiotic stress in one of the major wine grapes varieties cultivated worldwide. An open field

experiment was conducted in a North Italian viticultural area characterized by transient drought events during the summer. Two different water regimes were applied to Merlot vines for two consecutive seasons, and the effect of water deficit on the central and specialized metabolism together with specific transcription factors families' activity was investigated at different stages of berry development and during ripening. Finally, a weighted gene co-expression network analysis was undertaken to investigate cluster of genes highly correlated during development and ripening of grape berries subjected to severe water deficit.

Results

Water deficit affects the agronomical parameters of grapes and impairs vine productivity

Two irrigation treatments were applied to the Merlot vines: control plants (C) were weekly irrigated and their stem water potential (Ψ_{Stem}) remained between -0.4 and -0.6 MPa; plants under deficit irrigation (D) were not irrigated from fruit set to harvest except in case of acute water deficit, i.e., when Ψ_{Stem} was measured lower than -1.4 MPa. Irrigation treatments affected the water status of the vines. Plants subjected to deficit irrigation showed a decrease in the Ψ_{Stem} throughout the seasons (Fig. 1a,b). In 2011, differences between treatments were observed from 50 days after anthesis (DAA) and the lowest value in D vines (-1.6 MPa) was measured at 110 DAA; whereas in 2012 Ψ_{Stem} differentiated between the treatments at 39 DAA and the minimum value (-1.5 MPa) in D vines was measured at 88 DAA. At the onset of ripening (veraison), 69 and 60 DAA in 2011 and 2012 respectively, the Ψ_{Stem} in D was -0.8 MPa in 2011 and -1.2 MPa in 2012. In both seasons, Ψ_{Stem} of D vines was consistently lower than -1.0 MPa for the entire ripening period. Deficit irrigated vines experienced similar level of water deficit between the two seasons; also, in both seasons, water deficit started at about 40-50 DAA and lasted until harvest.

Irrigation treatments significantly affected vine productivity and D reduced cluster weight and yield per vine in both seasons (Table 1). Furthermore, D significantly reduced berry weight during berry ripening at 74, 100, and 115 DAA in 2011 (Fig. 1c) and at 67, 81, 95, and 106 DAA in 2012 (Fig. 1d). On the contrary, total soluble solids (TSS) were increased by water deficit in 2012 both before (40 and 53 DAA) and after (95 and 106 DAA) veraison. Finally, the titratable acidity (TA) was lower and higher in D at 26 and 53 DAA, respectively (Fig. 1f). In 2011 water deficit did not affect TSS and TA (Fig. 1e).

Table 1. Effect of water deficit on crop production. Cluster per vine, cluster weight and yield per vine of fully irrigated (C, controls) and deficit irrigated (D, water deficit) grapevines in 2011 and 2012. Values are averages ± the standard error. Differences between treatments ($P<0.05$) were assessed with a one-way ANOVA. The level of significance is reported within the columns: * or ns, $P < 0.05$ or not significant, respectively

	Merlot			
Year	2011		2012	
Treatment	C	D	C	D
Cluster per Vine	22.9 ± 0.6	22.8 ± 1.2	20.1 ± 1.7	19.4 ± 1.4
	ns		ns	
Cluster Weight (g)	189.4 ± 11.5	142.4 ± 5.9	129.0 ± 4.2	101.5 ± 9.3
	*		*	
Yield per Vine (Kg)	4.29 ± 0.35	3.23 ± 0.22	2.62 ± 0.22	1.97 ± 0.19
	*		*	

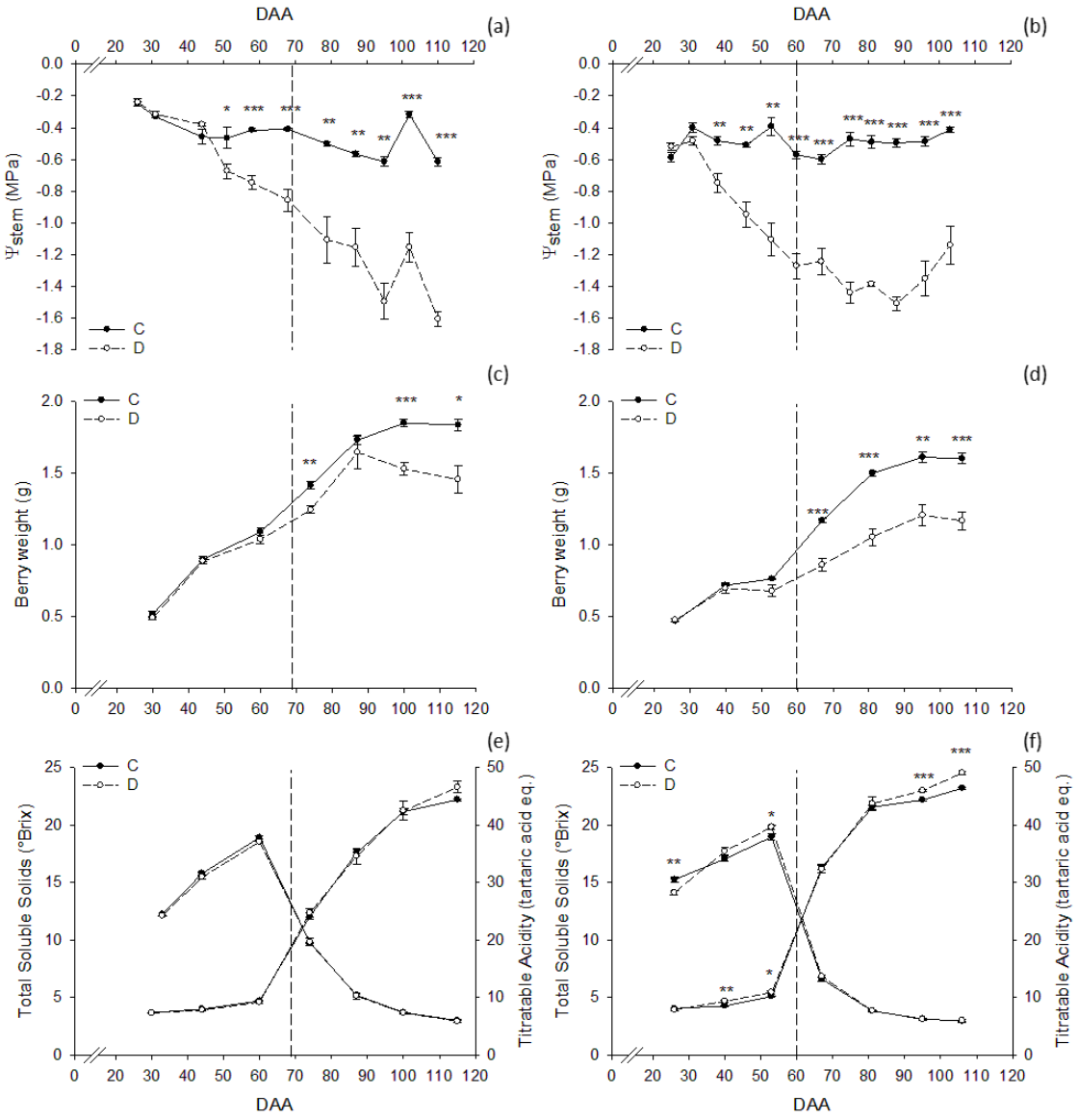

Figure 1. Measurement of stem water potential and physiological parameters in irrigated vines (C) and in plants under water deficit (D) in 2011 (left hand panels) and 2012 (right hand panels). Panel (a, b) stem water potential (Ψ_{Stem}), panel (c, d) berry weight (g), panel (e, f) total soluble solids (°Brix) and titratable acidity (tartaric acid equivalents). Dashed line indicates the onset of ripening (veraison). Bars represent ±SE. Asterisks indicate significant differences between treatments at P<0.05 (*), P<0.01 (**), P<0.001 (***) evaluated by one-way ANOVA.

Influence of water deficit on berry transcriptome

A transcriptomic analysis was undertaken at five developmental stages in the 2012 season. The fruit transcriptome was analyzed before veraison (26 and 53 DAA), at the onset of ripening (67 DAA) and during ripening (81 and 106 DAA).

After filtering for organelles contamination and quality trimming, the average number of unique reads that mapped the V1 version of the grape genome (Jaillon et al., 2007) was 27.1M (Table S2). Among the 29,971 genes of the grapevine genome, 23,253 (77.6%) genes were

expressed at 26 DAA, 23,220 (77.5%) at 53 DAA, 21,997 (73.4%) at 67 DAA, 22,453 (74.9%) at 81 DAA, and 22,162 (73.9%) at 106 DAA. No differences were detected in the number of expressed genes between C and D at any developmental stage analyzed.

A principal component analysis (PCA) was performed to compare the transcriptome profiles of the 30 samples analyzed (two treatments x five developmental stages x three biological replicates) (Fig. 2). The first three principal components explain 61.9%, 15.8%, 9.5% of the variance among samples, respectively. Berry transcriptomes were clearly separated accordingly to the developmental stage; however, within developmental stages, the berry transcriptome of D fruits grouped together and were slightly separated from the transcriptomes of C berries.

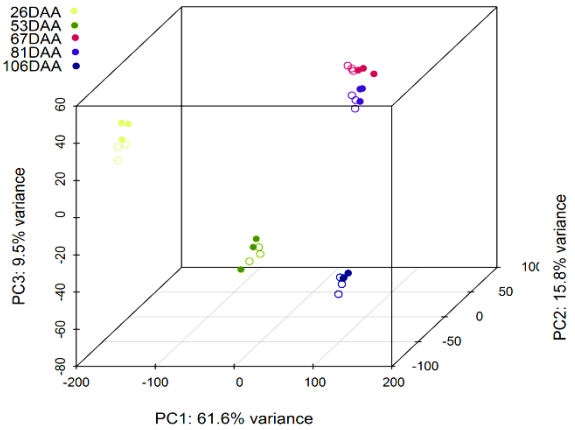

Figure 2. Analysis of the berry transcriptome in irrigated (C) and deficit irrigated (D) vines in 2012. Principal component analysis (PCA) of the berry transcriptome of 30 independent samples collected from C and D vines at 26, 53, 67, 81, and 106 DAA. Full and open symbols identify C and D berries, respectively.

The total number of differentially expressed (DE) genes between C and D in the five stages was 5,167 (Table S1 a,b,c,d,e). The number of DE genes changed during fruit development and ripening. D modulated the expression of 214 genes (175 up-regulated; 39 down-regulated) at 26 DAA, 90 genes (38 up-regulated; 52 down-regulated) at 53 DAA, 1,290 genes (662 up-regulated; 628 down-regulated) at 67 DAA, 2,900 genes (1,569 up-regulated; 1,331 down-regulated) at 81 DAA, and 2,925 genes (1,431 up-regulated; 1,494 down-regulated) at 106 DAA (Fig 3a). Several of them were differentially regulated at more than one developmental stage (Fig. 3b). Interestingly, one gene (*VIT_00s0265g00070*), annotated as 'Ubiquitin-conjugating enzyme E2O', was downregulated by D at all five developmental stages.

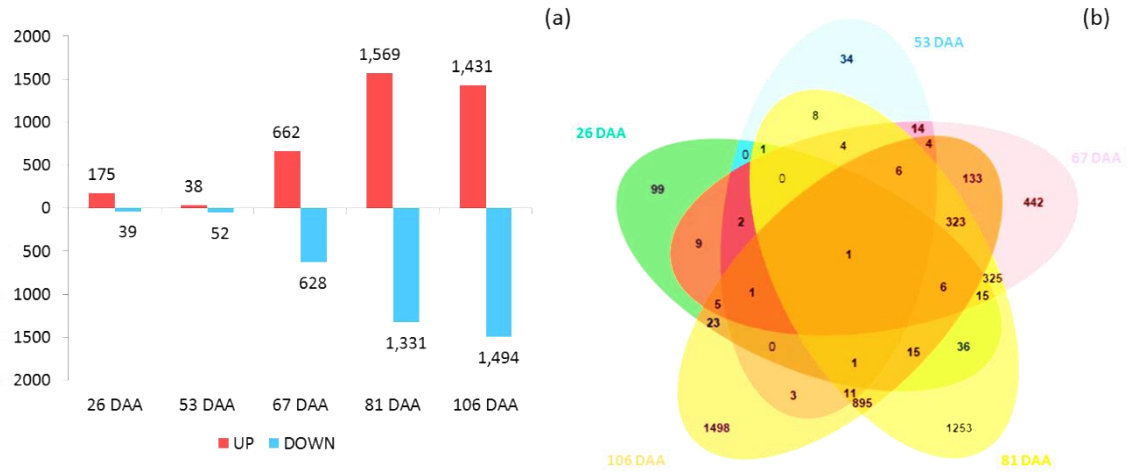

Figure 3. (a) Number of differently expressed (DE) genes at 26, 53, 67, 81, and 106 DAA. The numbers of genes up- or down regulated by water deficit are represented with red and blue bars, respectively. (b) Common and unique DE genes at 26, 53, 67, 81, and 106 DAA are represented in the Venn diagram drawn with the web tool jVenn.

Thirty GO categories (slim biological processes) were significantly overrepresented among the DE genes (Table S1f). Due to the low number of genes differently expressed at pre-veraison stages (26 and 53 DAA) few GO categories were represented at these stages. Emphasis was thus given to the stages of berry ripening (i.e., 67, 81, and 106 DAA). The five most consistently overrepresented categories in the up-regulated genes were '*Amino acid metabolic process*', '*Response to abiotic stress*', '*Response to endogenous stimulus*', '*Carbohydrate metabolic process*' and '*Secondary metabolic process*'. The five most consistently overrepresented categories in the down-regulated genes were '*Response to stress*', '*Transport*', '*Amino acid metabolic process*', '*Response to biotic stress*' and '*Secondary metabolic process*'.

Transcriptional regulatory networks of berry fruits under drought stress

Transcription factors (TFs) are central in regulating many plant biological processes; including developmental processes and response to the environment. A total of 447 *VviTFs*, of a possible 2,211 *VviTFs* encoded in the grapevine genome (Jaillon et al., 2007; Grimplet et al., 2012) were modulated in the berry in response to water deficit. Emphasis on the stages where pronounced water deficit was observed (67, 81, and 106 DAA) showed that large proportion of the drought-modulated *VviTFs* belong to the *VviMYB* (32 genes), *VvibHLH* (32 genes), *VviC2H2* (28 genes), *VviAP2-EREBP* (25 genes), *VviWRKY* (25 genes), *VviNAC* (23 genes), *VviC3H* (20 genes), *VviHB* (17 genes), *VviGRAS* (15 genes), and *VvibZIP* (14 genes) families. These TFs were significantly modulated by water deficit at one or more developmental stages (Fig. 4; Table S1g).

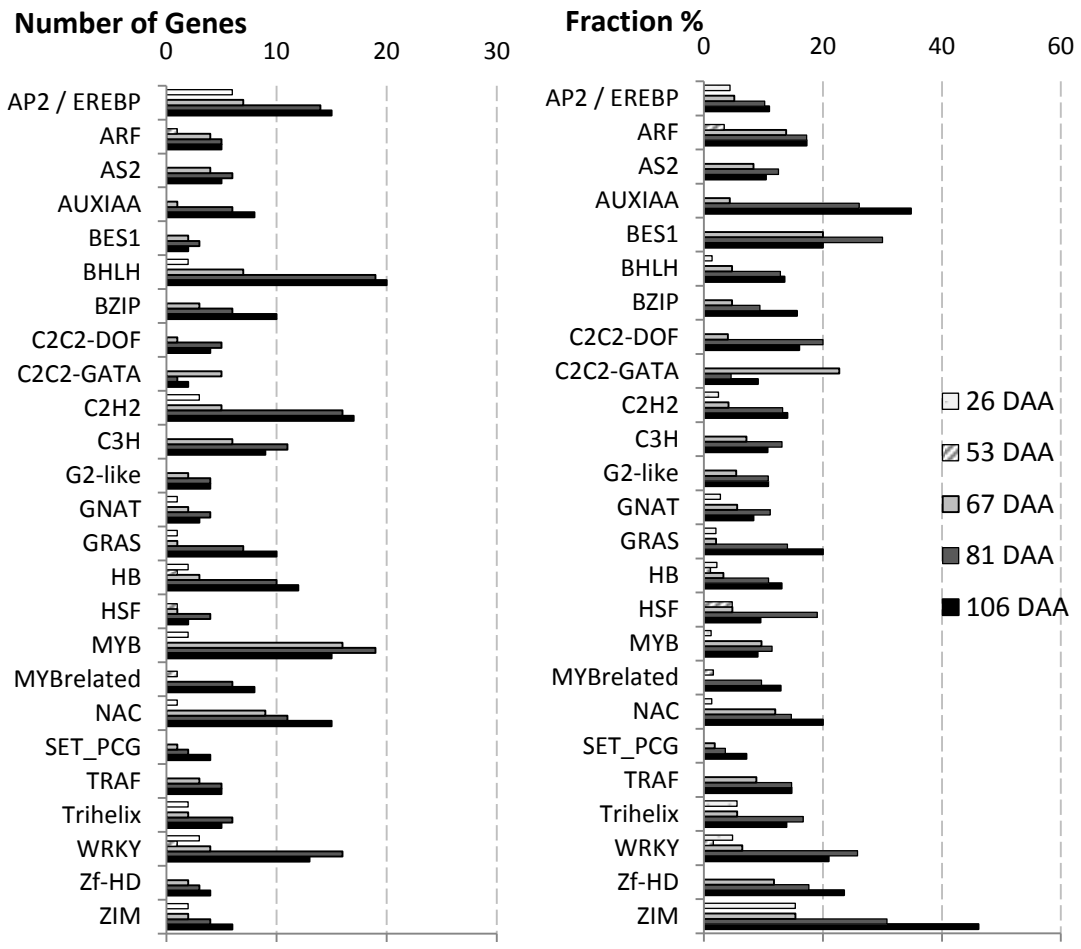

Figure 4. Modulation of the transcription factor (TF) family under water deficit. The TF genes, extracted from the list of the DE genes, are represented in the upper panel as percentage (%) found differently expressed at 26, 53, 67, 81, and 106 DAA compared to the whole list of TF genes present in grapevine. In the lower panel, the exact number of them at each point.

Modulation of specific families of transcription factors is also indicative of the activation of both ABA–dependent (i.e. *VvibZIP*, *VvibHLH/MYC*, *VviMYB*, and *VviNAC*) and ABA–independent (*VviAP2/ERF*, *VviHB/HD-ZIP*, and *VviNAC*) signal transduction pathways during drought stress (reviewed in Yoshida et al., 2014).

Central components of the ABA–dependent drought response pathway are the *cis*-element basic leucine zipper *(bZIP*) transcription factors known as *AREB/ABFs* acting in an ABA-responsive element binding (ABRE) mode. *VvibZIP45/AREB1/ABF2* (*VIT_18s0001g10450*) and *VvibZIP08/AREB2/ABF4* (*VIT_03s0063g00310*) were significantly up-regulated at 81 and 106 DAA, respectively. Interestingly, other *VvibZIP* transcription factors were also significantly up-regulated from 67 DAA onwards; these TF group include *VvibZIP09* (*VIT_04s0008g02750*) orthologous of *AtbZIP09*, *VvibZIP10* (*VIT_04s0008g05210*) orthologous of *AtbZIP56-HY5*, *VvibZIP14* (*VIT_05s0077g01140*) orthologous of *AtbZIP53*, *VvibZIP15* (*VIT_05s0020g01090*) orthologous of *AtbZIP64-HYN*, and *VvibZIP38* (*VIT_14s0030g02200*) orthologous of AtbZIP63 and AtbZIP10 (Jakoby et al., 2002; Liu et al., 2014). These proteins might be implicated in grape berry water deficit response.

Central components of the ABA–independent drought response pathway are the *cis*-element *AP2/ERF* transcription factors containing the dehydration-responsive element/C-repeat (DRE/CRT) and the DRE/CRT binding protein (DREB) (Sakuma et al., 2002). These genes were significantly modulated by water deficit. Specifically, *VviERF62/DREB-A6-4* (*VIT_05s0029g00140*) was significantly up-regulated at 81 and 106 DAA, while others were specifically up-regulated at 81 DAA (*VviCEJ1/DREB-A5-5*: *VIT_07s0031g00190*) or at 106 DAA (*VviDREB2D/DREB-A2-4*: *VIT_18s0001g13320*, *VviORA47/DREB-A5-2: VIT_11s0016g00670*, and *VviRAP2.4/DREB-A6-1: VIT_18s0001g05250*), respectively (Cramer et al., 2014). This highlights that also the ABA–independent pathway is unequivocally important in regulating the drought response in non-climacteric fruits subjected to water deficit. Interestingly, other TFs involved in the ABA–independent pathway may also be critical. For example, a gene (*VviHB12*: *VIT_16s0098g01170*) encoding for an orthologous of the *Arabidopsis thaliana* homeobox-leucine zipper protein (*AtHB12*) was significantly up-regulated from 53 DAA onwards, with the highest induction (1.39 log_2FC) at 81 DAA when water deficit reached the highest severity. Induction of *VviHB12* at 53 DAA highlights that this gene may also be involved in one of the earliest response to drought.

Glycolysis and tricarboxylic acid cycle (TCA) genes are modulated by water deficit during berry ripening

Water deficit affected the expression of genes involved in nine steps out of ten of the glycolysis metabolic pathway (Fig. 5). Among the DE genes, two hexokinases (*VIT_11s0016g03070* and *VIT_18s0001g14230*), two glucose-6P isomerases (*VIT_18s0001g07280* and *VIT_18s0001g12370*), and two phosphoglycerate mutases (*VIT_08s0056g00200* and *VIT_18s0001g05060*) were modulated by D. Within the two copies codifying for each enzymatic step, one was up-regulated and the other was down-regulated. A phosphofructokinase (*VIT_14s0108g00540*) was down-regulated at 81 DAA, while the gluconeogenic fructose 1,6-bisphosphatase (*VIT_18s0072g00770*) was up-regulated. Three fructose biphosphate aldolases (*VIT_03s0038g00670*, *VIT_04s0023g03010*, and *VIT_08s0007g03830*) and four glyceraldehyde-3P dehydrogenases (*VIT_01s0010g02460*, *VIT_14s0068g00680*, *VIT_18s0122g00960*, and *VIT_19s0085g00600*) were up-regulated during berry ripening. A triose phosphate isomerase (*VIT_06s0004g04800*) was down-regulated while an enolase (*VIT_16s0022g01770*) was up-regulated at 106 DAA. Three pyruvate kinases were modulated by D. Two of them (*VIT_00s0179g00350* and *VIT_06s0004g00130*) were up-regulated whereas another one (*VIT_16s0050g02660*) was down-regulated during ripening. Two pyruvate decarboxylases (*VIT_05s0062g00970* and *VIT_10s0003g00990*) were up-regulated at 26 DAA, whereas two phosphoenolpyruvate carboxykinases (*VIT_05s0049g00950* and *VIT_14s0036g00420*) were down-regulated during berry ripening in the gluconeogenesis pathway.

Conversely, few genes of the TCA cycle were differently expressed during berry development and ripening (Fig. 5). A citrate synthase (*VIT_12s0142g00610*), a 2-oxoglutarate dehydrogenase (*VIT_13s0019g00510*) and two succinate dehydrogenases (*VIT_04s0023g01650* and *VIT_14s0219g00150*) were up-regulated; whereas, an aconitate hydratase (*VIT_12s0059g02150*) and two isocitrate dehydrogenases (*VIT_12s0034g01080* and

VIT_19s0085g01150) were down-regulated during berry ripening. Malic acid is one of the two major organic acid accumulated in the grapes. For this reason malate metabolism in grape berry has been widely studied (reviewed in Sweetman et al., 2009). Three mitochondrial malate dehydrogenases were modulated by D at 106 DAA: two of them (*VIT_10s0003g01000* and *VIT_17s0000g06270*) were up-regulated, whereas the third one (*VIT_19s0014g01640*) was down-regulated. As part of malate metabolism, three cytosolic phosphoenolpyruvate carboxylases (*VIT_01s0011g02740*, *VIT_12s0028g02180*, and *VIT_19s0014g01390*) were modulated by D: the first one was up-regulated at 81 DAA while the other two were down-regulated at 106 DAA, and two cytosolic malate dehydrogenases (*VIT_07s0005g03350*, *VIT_15s0021g02410*) were down-regulated at 67 and 106 DAA respectively. Finally, a carrier involved in malate transport into the mitochondria (*VIT_08s0007g07270*) was down-regulated at 67 DAA.

Sugar metabolism is involved in the response to water deficit

Hexoses, glucose and fructose, are largely accumulated in the vacuoles of the fruit cells from the onset of ripening. Beside hexoses, we did also observe a large increase of sucrose during fruit ripening (see sections on metabolites below). Among the sugar transporters identified by Afoufa-Bastien et al. (2010), one sucrose transporter, *VviSUC27* (*VIT_18s0076g00250*) was up-regulated at 26 and 81 DAA by water deficit, as well as five hexose transporters (*VviHTs*) which were differently modulated by D. Water deficit down-regulated the expression of *VviHT1* (*VIT_00s0181g00010*), *VviHT2* (*VIT_18s0001g05570*), *VviHT5* (*VIT_05s0020g03140*), and *VviHT13* (*VIT_11s0016g03400*) during berry ripening. On the contrary, *VviHT3* (*VIT_11s0149g00050*) was up-regulated by D at 67 and 81 DAA. The plant *SWEET* family of sugar transporters is a protein family of sugar uniporters. Several *VviSWEET* genes known to be expressed in the berry (Chong et al., 2014) were modulated by D: *VviSWEET7* (*VIT_02s0025g02080*), *VviSWEET10* (*VIT_17s0000g00830*), and *VviSWEET11* (*VIT_07s0104g01340*) were up-regulated at 53 DAA, 81, and 106 DAA, respectively. On the contrary *VviSWEET15* (*VIT_01s0146g00260*) and *VviSWEET17d* (*VIT_14s0060g01910*) were down-regulated during berry ripening. Moreover, a cell wall invertase (*VIT_09s0002g02320*) was down-regulated at 81 DAA, three cytoplasmatic neutral invertases (*VIT_03s0038g01480*, *VIT_05s0077g00510*, and *VIT_13s0074g00720*) were instead up-regulated by D during berry ripening. Finally, two vacuolar invertases (*VviGINs*) were differently modulated. *VviGIN1* (*VIT_16s0022g00670*) was up-regulated at 26 and then down-regulated at 67 and 81 DAA, whereas *VviGIN2* (*VIT_02s0154g00090*) was up-regulated at 81 and 106 DAA. Furthermore, two tonoplast monosaccharide transporters were differently modulated by D: *VIT_03s0038g03940* was up-regulated while *VIT_18s0122g00850* was down-regulated during ripening. Lastly, two polyol monosaccharide transporters (*VviPTM2-4*: *VIT_11s0016g03920*, *VIT_12s0059g00250*) were differently modulated by D. *VviPTM2* was up-regulated at 67 and 81 DAA, whereas *VviPTM4* was down-regulated at 81 DAA. Several galactinol synthases were modulated by D: *VIT_14s0060g00810* was down-regulated at 106 DAA while *VIT_01s0127g00470*, *VIT_05s0077g00430*, *VIT_14s0060g00760*, *VIT_14s0060g00790*, and *VIT_14s0066g02350*, together with two raffinose synthases (*VviRAFS1-2*: *VIT_14s0066g00810* and *VIT_17s0000g08960*) were up-regulated during berry ripening.

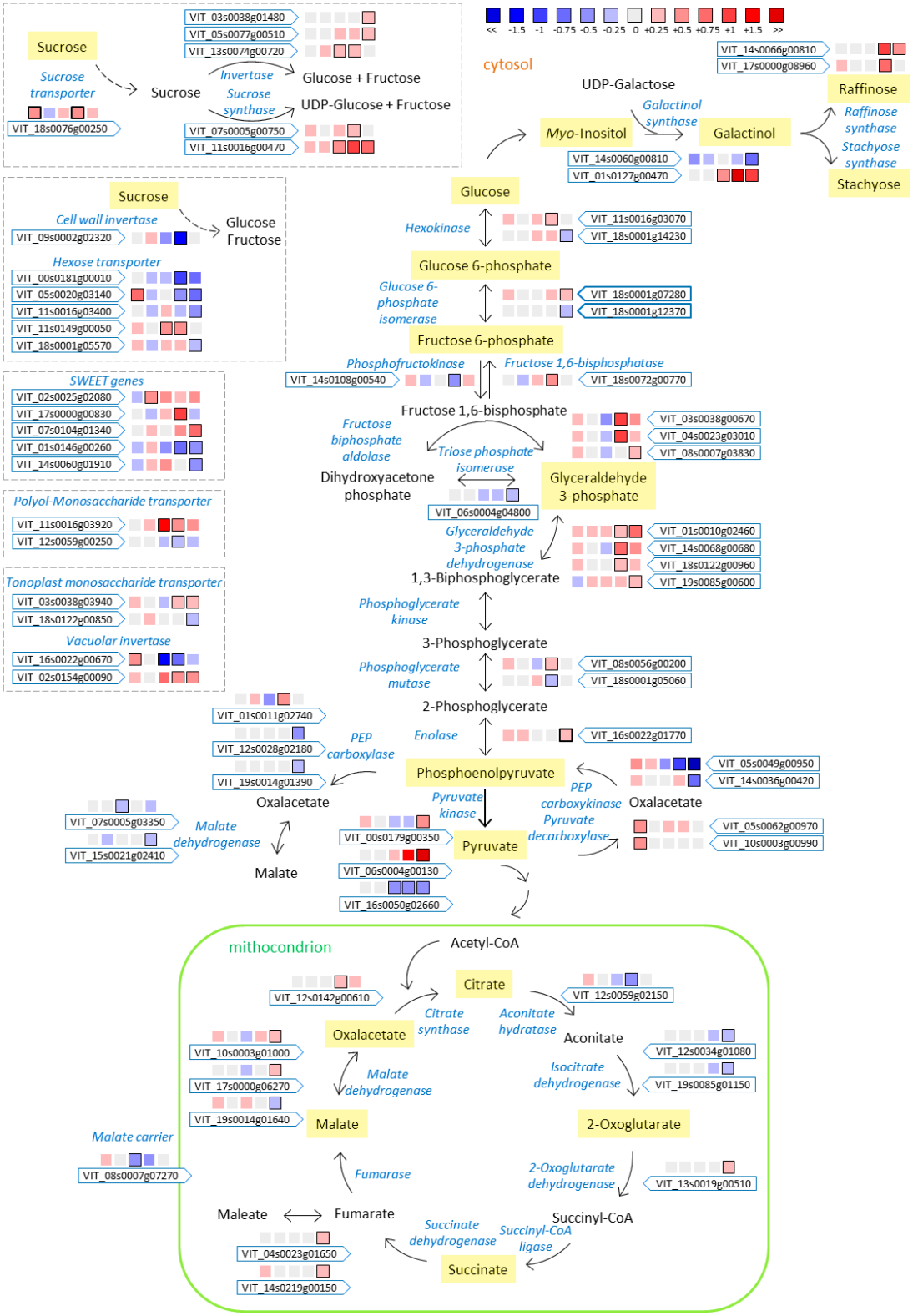

Figure 5. Effect of water deficit on, glycolysis, tricarboxylic acid cycle, and sugar import into the berry pathways during fruit development and ripening in 2011 and 2012. Heatmaps represent $\log_2$ fold change (D/C) at 26, 53, 67, 81, and 106 DAA from left to right. Blue and red boxes indicate lower and higher concentration in D, respectively (see figure legend). Bolded box border indicates significant differences ($P<0.05$) between treatments.

Biosynthesis of branched-chain amino acids and proline is hastened by water deficit

The biosynthesis of amino acids is linked to the glycolysis, TCA, and the pentose phosphate pathways (Fig. 6). Serine, glycine, and cysteine are produced from gliceraldehyde-3P, an intermediate of glycolysis. These reactions were barely modulated by D. A serine-glycine hydroxymethyltransferase (*VIT_05s0029g00310*) gene was up-regulated by D at 106, whereas another serine-glycine hydroxymethyltransferase (*VIT_18s0001g04340*) as well as a cysteine synthase (*VIT_14s0030g01520*) were down-regulated at 106 DAA. Pyruvate is the substrate of alanine and the branched-chain amino acids valine and leucine. Two alanine aminotransferases (*VIT_00s0225g00130*, *VIT_09s0002g00340*) were up-regulated at 67 and 81 DAA, respectively. Four genes involved in valine and leucine biosynthesis were modulated by D. An acetolactate synthase (*VIT_14s0068g01960*) was down-regulated at 67 and 81 DAA; a ketol-acid reductoisomerase (*VIT_12s0028g02340*) was up-regulated at 81 DAA; a dihydroxy-acid dehydratase (*VIT_05s0051g00830*) was up-regulated at 67, 81, and 106 DAA, and a branched-chain amino acid transaminase (*VIT_14s0128g00100*) was down-regulated at 81 and 106 DAA. Aromatic acids (phenylalanine, tyrosine and tryptophan) are synthetized through the shikimate pathway. A 3-deoxy-D-arabinoheptulosonate 7-phosphate synthase (*DAHP*: *VIT_00s0391g00070*) was up-regulated at 67 and 106 DAA while a 3-dehydroquinate dehydratase (*VIT_14s0030g00670*) was, instead, down-regulated at 106 DAA. Two shikimate dehydrogenases (*VIT_14s0030g00650* and *VIT_14s0030g00660*) were modulated by D: the first one was down-regulated at 81 DAA whereas the latter was up-regulated at 53 DAA. Three shikimate kinases (*VIT_07s0031g01600*, *VIT_16s0039g02500*, and *VIT_18s0001g01730*) were up-regulated during berry ripening and a chorismate synthase (*VIT_13s0019g04190*) was up-regulated at 106 DAA. An arogenate dehydrogenase (*VIT_09s0002g08070*) was up-regulated at 106 DAA, whereas a tryptophan synthase (*VIT_14s0083g00460*) and an arogenate dehydratase (*VIT_12s0059g00750*) were down-regulated at 81 and 106 DAA, and at 67 DAA, respectively. The intermediate of the TCA, 2-oxoglutarate, is the precursor for the synthesis of glutamate, glutamine, histidine, proline, and arginine. The synthesis of histidine and proline was enhanced by D. A pirroline 5-carboxylate synthase (*VIT_13s0019g02360*) and a histidinol dehydrogenase (*VIT_03s0063g00200*) were up-regulated during berry ripening. Furthermore, polyamines are deriving from the decarboxylation of arginine or ornithine. An arginine decarboxylase (*VIT_03s0038g00760*) was up-regulated at 67, 81, and 106 DAA. Lastly, another intermediate of TCA, the oxalacetate, is the precursor for the synthesis of aspartate, asparagine, lysine, methionine, threonine, and isoleucine. Methionine and threonine synthesis were enhanced by D. A cystathionine synthase (*VIT_14s0108g01110*), a cystathionine lyase (*VIT_02s0025g02560*), and three homocysteine S-methyltransferases (*VIT_05s0020g03860*, *VIT_06s0009g01080* and *VIT_07s0151g00520*) were up-regulated during berry ripening. Moreover, two threonine synthases (*VIT_04s0008g05990* and *VIT_11s0016g01720*) and a threonine deaminase (*VIT_08s0007g04310*) were upregulated at 81 DAA, and at 26 and 106 DAA, respectively.

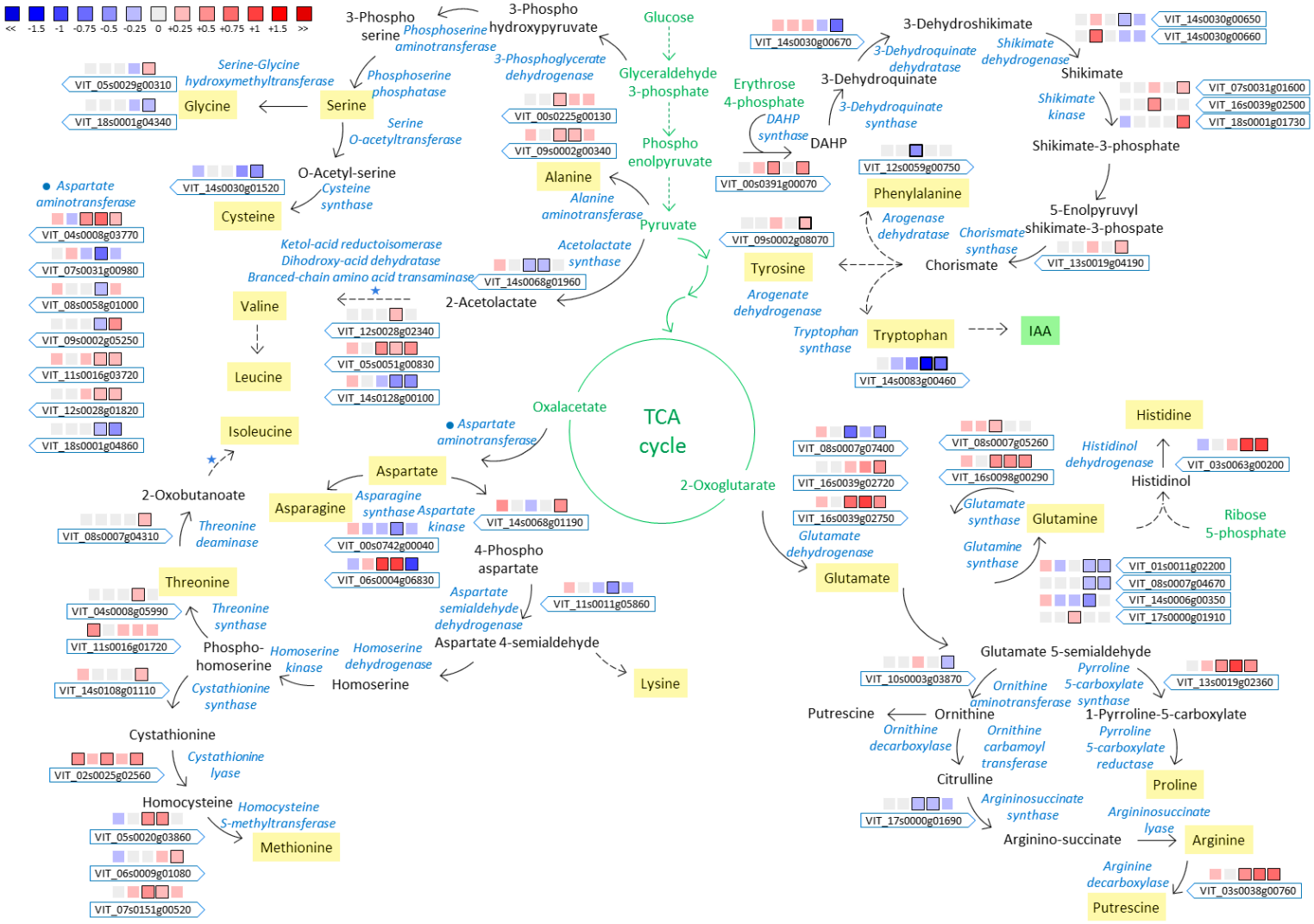

Figure 6. Effect of water deficit on the amino acid biosynthetic pathway during fruit development and ripening in 2011 and 2012. Heatmaps represent $\log_2$ fold change (D/C) at 26, 53, 67, 81, and 106 DAA from left to right. Blue and red boxes indicate lower and higher concentration in D, respectively (see figure legend). Bolded box border indicates significant differences ($P<0.05$) between treatments. Symbols identify commonly regulated steps of the pathway.

Phenylpropanoid and flavonoid pathways are boosted by water deficit while stilbenoids are lessened

Many genes belonging to the phenylpropanoid pathway were modulated by water deficit (Fig. 7).

Among the DE genes, two phenylalanine ammonia lyases (*VviPAL*: *VIT_06s0004g02620* and *VIT_13s0019g04460*) and one trans-cinnamate 4-monooxygenase (*VviC4H*: *VIT_06s0004g08150*) were up-regulated at 67 and 81 DAA. Conversely, other two *VviPALs* (*VIT_08s0040g01710* and *VIT_16s0039g01100*) and another *VviCH4* (*VIT_11s0065g00350*) were down-regulated during ripening. In addition, four 4-coumarate-CoA ligases were modulated at different developmental stages. *VIT_02s0025g03660* was up-regulated whereas *VIT_06s0061g00450* was down-regulated at 106 DAA; *VIT_11s0052g01090* was up-regulated at 67 DAA and then down-regulated at 81 DAA; *VIT_16s0050g00390* was up-regulated at 67, 81, and 106 DAA. Modifications of the intermediates of the phenylpropanoid pathway produce cinnamic acids. A p-coumaroyl shikimate 3'-hydroxylase (*VviC3H*: *VIT_11s0037g00440*), a hydroxycinnamoyl-CoA:shikimate/quinate hydroxycinnamoyltransferase (*VviHCT*: *VIT_08s0040g00780*), a caffeic acid 3-*O*-metyltransferase (*VviCOMT*: *VIT_02s0025g02920*) and two caffeoyl-CoA 3-*O*-methyltransferases (*VviCCoAOMT*: *VIT_01s0010g03460* and *VIT_07s0031g00350*) were up-regulated by D during berry ripening. An exception was a *VviCOMT* (*VIT_15s0048g02480*) that was down-regulated at 81 and 106 DAA.

The stilbenoid pathway was strongly down-regulated by D. Among the 45 stilbene synthases annotated in the genome of *Vitis vinifera* (Vannozzi et al., 2012), 28 were down-regulated by D during ripening. The two transcription factors that regulate the stilbene biosynthesis (Höll et al., 2013) (*VviMYB14-15*: *VIT_07s0005g03340*, *VIT_05s0049g01020*) were not consistently down-regulated by water deficit. *VviMYB14* was down-regulated at 67 and 81, and up-regulated at 106, while *VviMYB15* was up-regulated at 67 and 81 DAA.

Water deficit modulated the expression of many structural genes of the flavonoid pathway (Fig. 7). In particular, three chalcone synthases (*VviCHS*: *VIT_05s0136g00260*, *VIT_14s0068g00920* and *VIT_14s0068g00930*), two chalcone isomerases (*VviCHI*: *VIT_13s0067g03820* and *VIT_13s0067g02870*), four flavonoid 3’5’-hydroxylases (*VviF3’5’H: VIT_06s0009g02810*, *VIT_06s0009g02830*, *VIT_06s0009g02840* and *VIT_06s0009g03010*), two flavanone 3-hydroxylases (*VviF3H*: *VIT_04s0023g03370* and *VIT_18s0001g14310*), one dihydroflavonol reductase (*VviDFR*: *VIT_18s0001g12800*), and one leucoanthocyanidin dioxygenase (*VviLDOX*: *VIT_02s0025g04720*) were up-regulated by D at different developmental stages during berry ripening. An exception was a *VviLDOX* (*VIT_08s0105g00380*) that was down-regulated by D at 67 DAA.

Two flavonol synthases were differently modulated by D: *VIT_18s0001g03470* was up-regulated at 81 and 106 DAA while *VIT_18s0001g03430* was up-regulated at 53 DAA and then down-regulated at 67 and 81 DAA. Two genes annotated as flavonol-3-*O*-glycosyltransferases (*VviGT5-6*: *VIT_11s0052g01600*, *VIT_11s0052g01630*) (Ono et al., 2010) were up-regulated by D at 106 DAA. However, the major regulator of flavonol biosynthesis, *VviMYBF1*

(*VIT_07s0005g01210*) (Czemmel et al., 2009), was not differently expressed between C and D fruits.

As regards the structural genes that control the flavan-3-ol and proanthocyanidin biosynthesis, two leucoanthocyanidin reductases (*VviLAR1-2*: *VIT_01s0011g02960* and *VIT_17s0000g04150*) were up-regulated by D during berry ripening while *VviANR* (*VIT_00s0361g00040*) was up-regulated at 53 DAA. Three glycosyltransferases (*VvigGT1-3*: *VIT_03s0091g00040*, *VIT_03s0180g00200*, *VIT_03s0180g00320*) putatively involved in PA galloylation (Khater et al., 2012) were modulated by D. *VviGT1* and *VviGT2* were up-regulated at 53 and at 67DAA, and 81 and 106 DAA, respectively; while *VviGT3* was down-regulated at 81 DAA. Additionally, among the three transcription factors that control flavan-3-ol and PA biosynthesis, only *VviMYBPA1* (*VIT_15s0046g00170*) was affected by D and in particular it was down-regulated at 67 DAA.

Finally, among the anthocyanin specific genes, the UDP-glucose:flavonoid-3-*O*-glucosyltransferase (*VviUFGT*: *VIT_16s0039g02230*), two anthocyanin-*O*-methyltransferases (*VviAOMT*: *VIT_01s0010g03510* and *VIT_01s0010g03490*) (Fournier-Level et al., 2011) and an anthocyanin-3-*O*-glucoside-6''-*O*-acyltransferase (*Vvi3AT*: *VIT_03s0017g00870*) (Rinaldo et al., 2015) were up-regulated by D during ripening. The transcription factors regulating anthocyanins biosynthesis (*VviMYBA1-2*: *VIT_02s0033g00410* and *VIT_02s0033g00390*) were up-regulated at 67, 81 and 106 DAA.

Moreover, one transcription factors that control the expression of several genes of the flavonoid pathway (*VviMYB5b*: *VIT_06s0004g00570*) (Cavallini et al., 2014) was up-regulated at 67 DAA, while, *VviMYBC2-L1* (*VIT_01s0011g04760*) – a repressor of the proanthocyanidin and anthocyanins biosynthesis (Cavallini et al., 2015) – was up-regulated at 67 and 81 DAA.

Once formed, flavonols, proanthocyanidins and anthocyanidins are transported into the vacuoles. A proanthocyanidins transporter (*VviPAMATE1*: *VIT_12s0028g01160*) (Pérez-Díaz et al., 2014), a glycosylated-anthocyanins protein (*VviABCC1*: *VIT_16s0050g02480*) (Francisco et al., 2013) and an anthocyanin-acylglucosides transporter (*VviAnthoMATE2*: *VIT_16s0050g00910*) (Gomez et al., 2009) were differently expressed. *VviPAMATE1* was up-regulated at 67 DAA, *VviABCC1* was down-regulated at 67 DAA and up-regulated at 106 DAA, and *VviAnthoMATE2* was up-regulated at 67, 81, and 106 DAA.

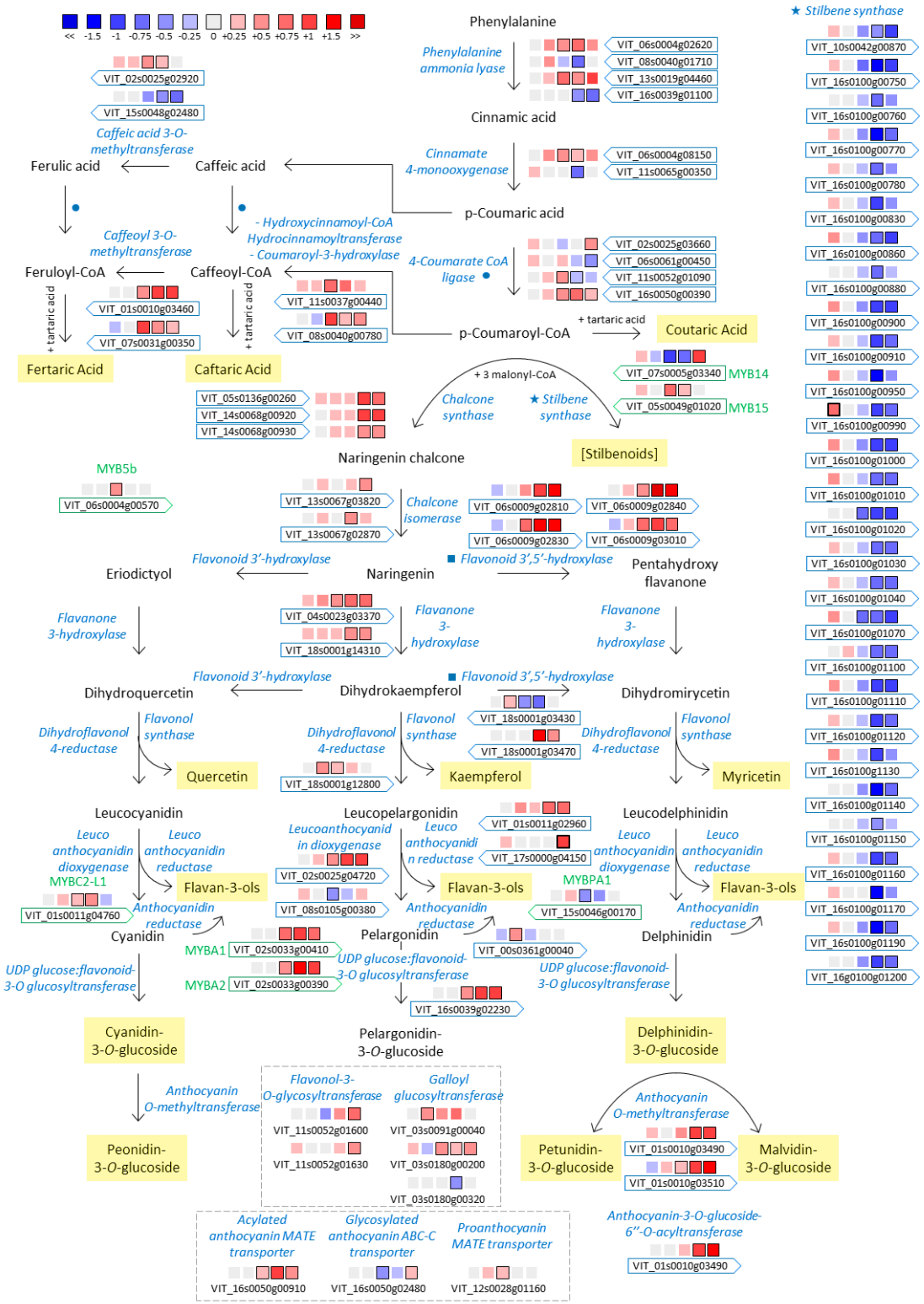

Figure 7. Effect of water deficit on phenylpropanoid and flavonoid pathways during fruit development and ripening in 2011 and 2012. Heatmaps represent $\log_2$ fold change (D/C) at 26, 53, 67, 81, and 106 DAA from left to right. Blue and red boxes indicate lower and higher concentration in D, respectively (see figure legend). Bolded box border indicates significant differences ($P<0.05$) between treatments. Symbols identify commonly regulated steps of the pathway.

Water deficit has a limited effect on the terpenoid pathway

Water deficit modulated the expression of few genes of the plastidial 2C-methyl-D-erythritol-4-phosphate (MEP) and the cytosolic mevalonate (MVA) pathways (Fig. 8). Three genes of the MEP pathway encoding for 1-deoxy-D-xylulose-5-phosphate synthases (*VviDXS*: *VIT_00s0218g00110*, *VIT_05s0020g02130*, and *VIT_11s0052g01730*) were down-regulated by D during ripening, with the exception of *VIT_11s0052g01730* that was also up-regulated at 106 DAA. Moreover, a 4-hydroxy-3-methylbut-2-enyl diphosphate synthase (*VviISPG*: *VIT_06s0004g02900*) was down-regulated at 81 and 106 DAA. Conversely, in the MVA pathway, an acetyl-CoA acetyltransferase (*VviAACT*: *VIT_00s0531g00050*) was up-regulated by D at 67 and 81 DAA, and down-regulated at 106 DAA. Three hydroxymethylglutaryl-CoA reductases (*VviHMGR*: *VIT_03s0038g04100*, *VIT_04s0044g01740*, and *VIT_18s0122g00610*) were up-regulated at 26 and 81 DAA, and *VIT_03s0038g04100* was down-regulated at 106 DAA. A phosphomevalonate decarboxylase (*VviPMD*: *VIT_13s0106g00790*) was down-regulated during ripening. Among the prenyltransferases, a farnesyl pyrophosphate synthase (*VviFPPS*: *VIT_19s0015g01010*) and two geranylgeranyl pyrophosphate synthases (*VviGPPSs*) were differently modulated. *VIT_18s0001g12000* was down-regulated by D at 81 DAA while *VIT_03s0038g03050* was up-regulated at the same stage.

Few genes of the terpene synthase gene family, recently characterized in *Vitis vinifera* by Martin et al. (2010), were modulated by D. In particular, two terpene synthases of the subfamily a (*VIT_18s0001g05290* and *VIT_19s0014g04930*), that control the production of sesquiterpenes, were down-regulated at 26 and at 67 DAA respectively; a terpene synthase of the subfamily b (*VIT_12s0134g00030*), that controls the production of monoterpenes, was down-regulated at 106 DAA and lastly, a terpene synthase of the subfamily c (*VIT_07s0151g01070*), that controls the production of diterpenes, was down-regulated at 81 and 106 DAA

The genes of the carotenoid pathway were recently characterized in *Vitis vinifera* (Young et al., 2012). Water deficit affected several genes of this pathway, mostly by up-regulating them (Fig. 8). A phytoene synthase (*VviPSY2*: *VIT_12s0028g00960*), a phytoene desaturase (*VviPDH1*: *VIT_04s0023g01790*), two ζ-carotene desaturases (*VviZDS*: *VIT_03s0038g02680* and *VIT_14s0030g01740*), two β-carotene hydroxylases (*VviBCH1-2*: *VIT_02s0025g00240* and *VIT_16s0050g01090*), two violaxanthin de-epoxidases (*VvVDE1-2*: *VIT_04s0043g01010* and *VIT_07s0031g01770*), and a neoxanthin synthase (*VviNSY1*: *VIT_14s0006g02880*) were up-regulated during ripening in one or two developmental stages. Exceptions were a carotenoid isomerase (*VviCISO1*: *VIT_08s0032g00800*) and a zeaxanthin epoxidase (*VviZEP1*: *VIT_07s0031g00620*) that were down-regulated. Both neoxanthin and violaxanthin can be cleaved by 11, 12 9-*cis*-epoxycarotenoid dioxygenase (*NCED*) and further modified to produce plant hormone abscisic acid (ABA). Three *VviNCEDs* (*VIT_05s0051g00670*, *VIT_10s0003g03750*, and *VIT_19s0093g00550*) were up-regulated by D during ripening. Furthermore, carotenoids can also be cleaved by specific carotenoid cleavage dioxygenases (*CCDs*) to produce apocarotenoids, with the aromatic norisoprenoids being the major class of apocarotenoids studied. Two *VviCCDs* (*VIT_02s0087g00910* and *VIT_02s0087g00930*) were modulated by D with the first one up-regulated and the latter down-regulated by D at 81 and 106 DAA.

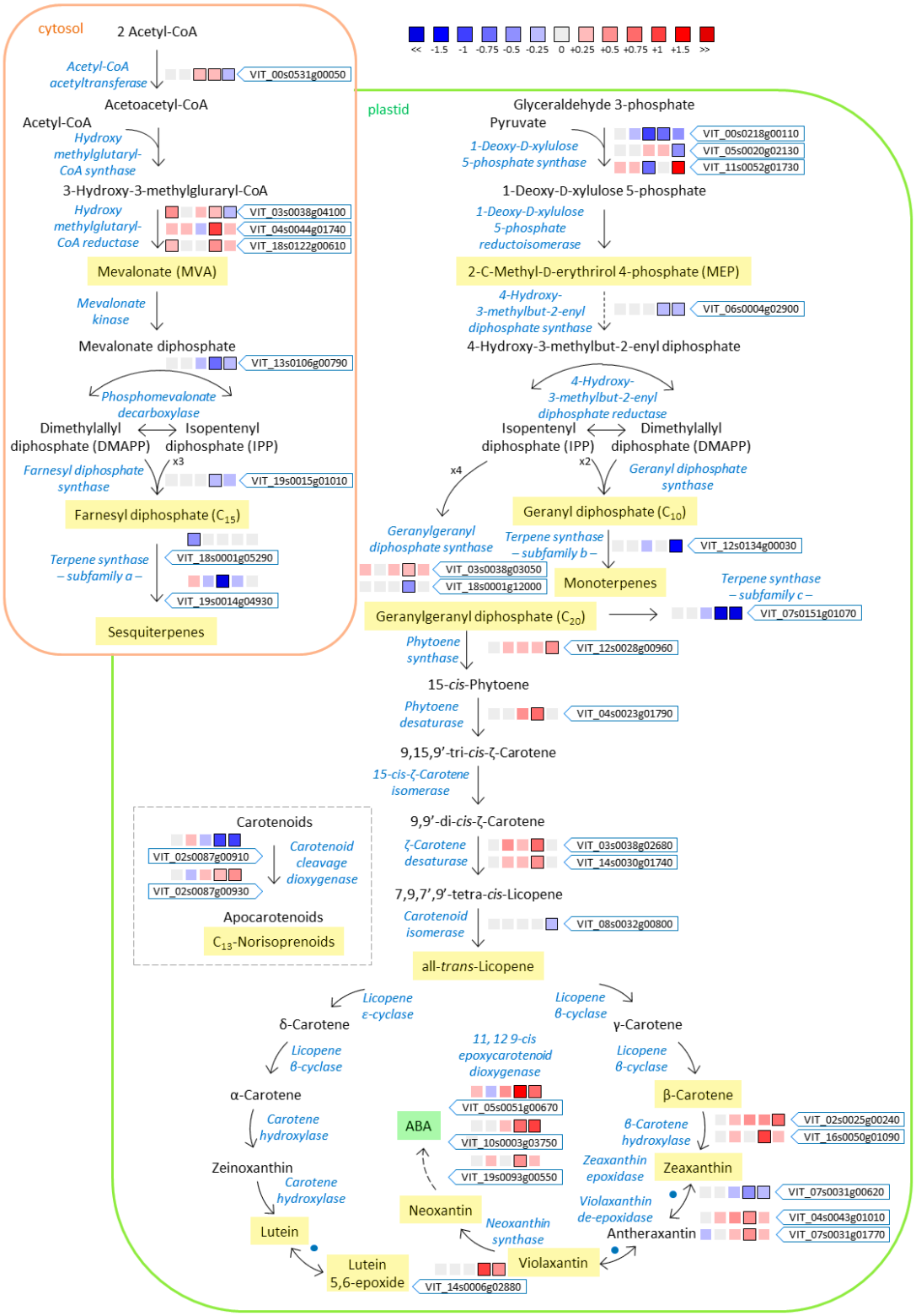

Figure 8. Effect of water deficit on terpenoid pathway during fruit development and ripening in 2011 and 2012. Heatmaps represent $\log_2$ fold change (D/C) at 26, 53, 67, 81, and 106 DAA from left to right. Blue and red boxes indicate lower and higher concentration in D, respectively (see figure legend). Bolded box border indicates significant differences ($P<0.05$) between treatments. Symbols identify commonly regulated steps of the pathway.

Other important fruit secondary metabolites are produced from the peroxidation of free C_{18} polyunsaturated fatty acid, such as linolenic and linoleic acids, which lead to the production of volatile organic compounds (VOCs), in particular, C_6 (Kalua and Boss, 2009) and putatively C_5 (Shen et al., 2014) volatile organic compounds. Among the genes involved in this pathway, three 9-lipoxygenases (*9-LOX*: *VIT_05s0020g03170*, *VIT_14s0128g00780*, and *VIT_14s0128g00790*) and three 13-lipoxygenases (*13-LOX*: *VIT_01s0010g02750*, *VIT_09s0002g01080*, and *VIT_13s0064g01480*) were down-regulated by D during berry ripening while a fourth *Vvi13-LOX* (*VIT_06s0004g01510*) was up-regulated at 53 and 106 DAA. A hydroperoxide lyase (*VIT_12s0059g01060*) was up-regulated at 26, 67, 81, and 106 DAA and five alcohol dehydrogenases (*VIT_04s0044g01120*, *VIT_04s0044g01130*, *VIT_17s0000g03280*, *VIT_18s0001g15410*, and *VIT_18s0001g15450*) were up-regulated by D during berry ripening (Table S1a,b,c,d,e).

Water deficit modulates primary and secondary metabolites

To gain further knowledge on the fruit metabolic response to water deficit and to relate the modulation observed in the transcriptome, targeted large-scale metabolite analyses were undertaken at all developmental stages sampled during 2011 and 2012 seasons. Therefore, berries were sampled for metabolite analyses seven times during each season: three times before veraison (30, 44, and 60 DAA in 2011, and 26, 40, and 53 DAA in 2012), one at onset of ripening (74 in 2011 and 67 in 2012), and three times during berry ripening (87, 100, and 115 in 2011, and 81, 95, and 106 in 2012) with the latest points of each season that coincided with the harvest date in the vineyard.

A total number of 100 compounds, belonging to the central (primary) and specialized (secondary) metabolism, were identified and quantified by gas chromatography-mass spectrometry (GC-MS), solid-phase microextraction gas chromatography-mass spectrometry (SPME-GC-MS), liquid chromatography with diode of array (HPLC-DAD) and liquid chromatography tandem mass spectrometry (UHPLC-MS/MS). A complete list of the compounds identified is reported in Table S3. Furthermore, the trend of the accumulation of these compounds in C and D grape berries during development and ripening in 2011 and 2012 is reported in Figure S1,2,3,4

Among the 33 primary compounds, encompassing amino acids and polyamine, organic acids, sugars and polyols, 11 in 2011 and 15 in 2012 were significantly modulated by water deficit at one or more developmental stages. Six of them were significantly modulated by D with the same trend between the two seasons; most of them were increased in concentration at harvest (Fig. 9). Amino acids and a polyamine, specifically leucine, valine, isoleucine, threonine, proline, and putrescine, were strongly increased by D during berry ripening in both seasons. At harvest, D decreased the concentration of some organic acids such as glycolate in 2011, citrate and maleate in 2012, and malate in both seasons. Among sugars and polyols, major effects of water deficit were recorded in 2012; sucrose was increased in D during berry ripening, whereas glucose-6P and fructose-6P were decreased at the onset of ripening. D decreased the concentration of raffinose before veraison in both seasons but increased the concentration of the same compound at harvest in 2012.

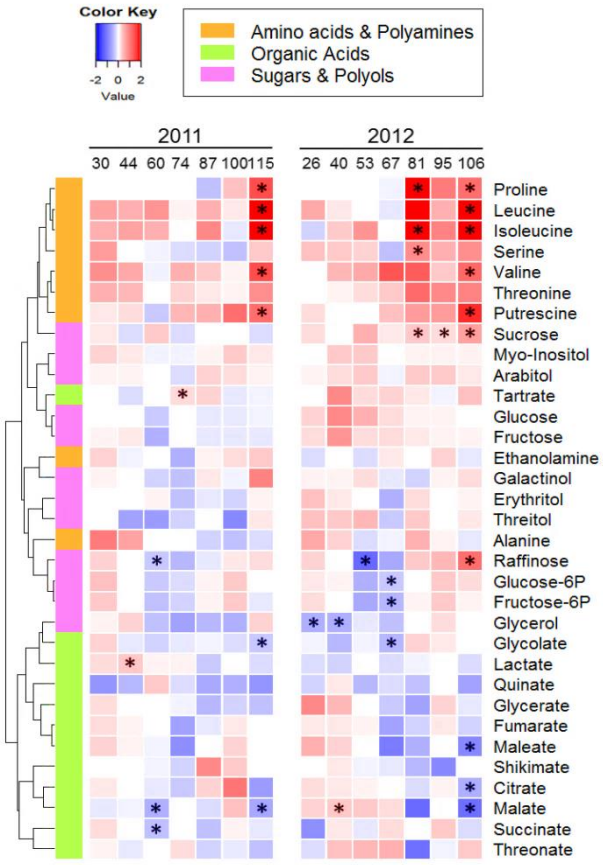

Figure 9. Effect of water deficit on central (primary) metabolism during fruit development and ripening in 2011 and 2012. Heatmaps represent $\log_2$ fold change (D/C) at all the developmental stages sampled. Blue and red boxes indicate lower and higher concentration in D, respectively. Asterisks indicate significant differences ($P<0.05$) between treatments. Metabolites were hierarchically clustered based on their response to water deficit. Color side bar on the left indicates the class of which each metabolite belongs.

Among the 39 phenylpropanoids, flavonoids, and stilbenoids detected 21 and 27 were significantly modulated by water deficit at one or more developmental stages in 2011 and 2012, respectively. Eighteen of them were significantly modulated by D with the same trend in the two seasons, in particular during berry ripening (Fig. 10). Water deficit mainly increased the concentration of benzoic and cinnamic acids: precisely, gallic acid was increased by D at harvest in both seasons while *trans*-caftaric, *trans*-coutaric and *trans*-fertaric acids were increased by D only in 2012 during berry ripening. Stilbenes such as *trans*-resveratrol, piceatannol and pallidol were decreased by D in both seasons at harvest, while *cis*- and *trans*-piceid were significantly decrease by D only in 2011 even though they had a similar trend but without significant differences in 2012. An exception within stilbenoids was isorhapontin that was increased by D at 95 and 106 DAA in 2012. Only one dihydrochalcone was detected and quantified: phlorizin, that at harvest was higher in concentration under water deficit. Monomeric flavan-3-ols such as catechin and epicatechin gallate were decreased by D in both seasons during berry ripening; however, the concentration of gallocatechin was increased at 95 and 106 DAA in 2012. Conversely, proanthocyanidins B1, B2+B4, and B3 were generally increased during berry

ripening. Among flavonols, only quercetin-3-*O*-rutinoside was significantly increase by D at 95 in 2012. However, the method used for detecting and quantifying flavonols was unable to detect the glycosylated myricetin, one of the main flavonols produced in red grapes (Mattivi et al., 2006). Water deficit significantly increased the concentration of anthocyanins during berry ripening in both seasons. All the anthocyanins produced in the grapes were increased by D but cyanidin, in its glycosylated and acylated forms, was not affected. Major effects of water deficit were observed for glycosylated and acylated malvidin. Overall, the coumaroyl form of anthocyanidins was the most significantly affected by D during berry ripening.

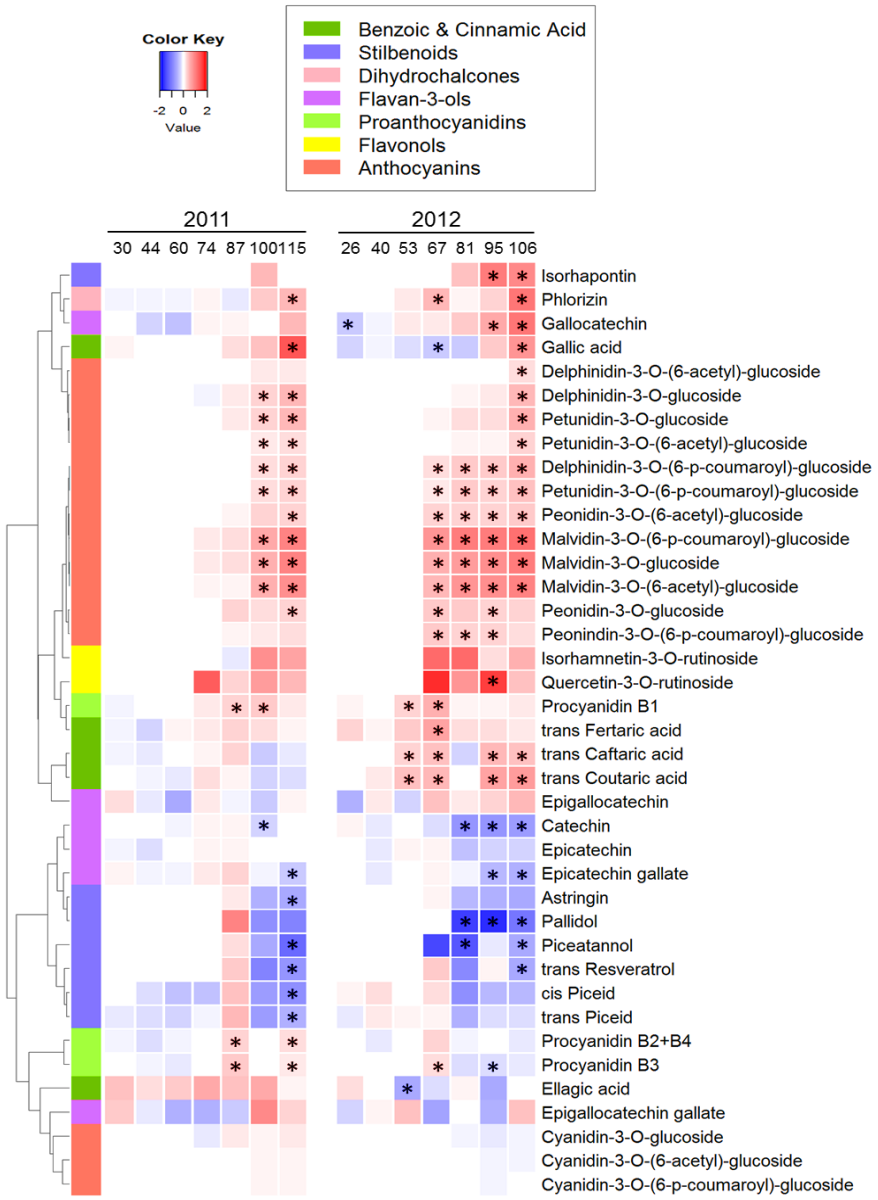

Figure 10. Effect of water deficit on the polyphenol compounds during fruit development and ripening in 2011 and 2012. Heatmaps represent $\log_2$ fold change (D/C) at all the developmental stages sampled. Blue and red boxes indicate lower and higher concentration in D, respectively. Asterisks indicate significant differences ($P<0.05$) between treatments. Metabolites were hierarchically clustered based on their response to water deficit. Color side bar on the left indicates the class of which each metabolite belongs.

Among the 28 carotenoids and volatile organic compounds analyzed in this study, 13 in 2011 and 13 in 2012 were significantly modulated by water deficit at one or more developmental stages. Eleven of them were significantly modulated by D with consistent trends between the two seasons (Fig. 11). Carotenoids such as violaxanthin, neoxanthin, and lutein 5-6-epoxide were decreased by water deficit during berry ripening in both seasons. Conversely, zeaxanthin was increased. The C_6 volatile organic compounds, *(E)*-2-hexenal, and 3-hexenol, were increased by D at the onset of ripening in both seasons, whereas hexanol was increased at the same stage in 2011, while it was decreased and increased by the same treatment at 26 and 40 DAA, respectively in 2012. Furthermore, the C_5, C_7, C_8 and C_9 volatile organic compounds such as 1-penten-3-ol, *(E)*-2-heptenal, *(E)*-2-octenal, 1-octen-3-ol, and nonanol were increased at harvest in both seasons; whereas, 1-octen-3-one was increased by D at harvest only in 2012, octanol was increased by D at the onset of ripening in 2012, and nonanal was increased by D at 100 DAA in 2011. Finally, terpenes and C_{13}-norisoprenoids were not affected by D in both seasons.

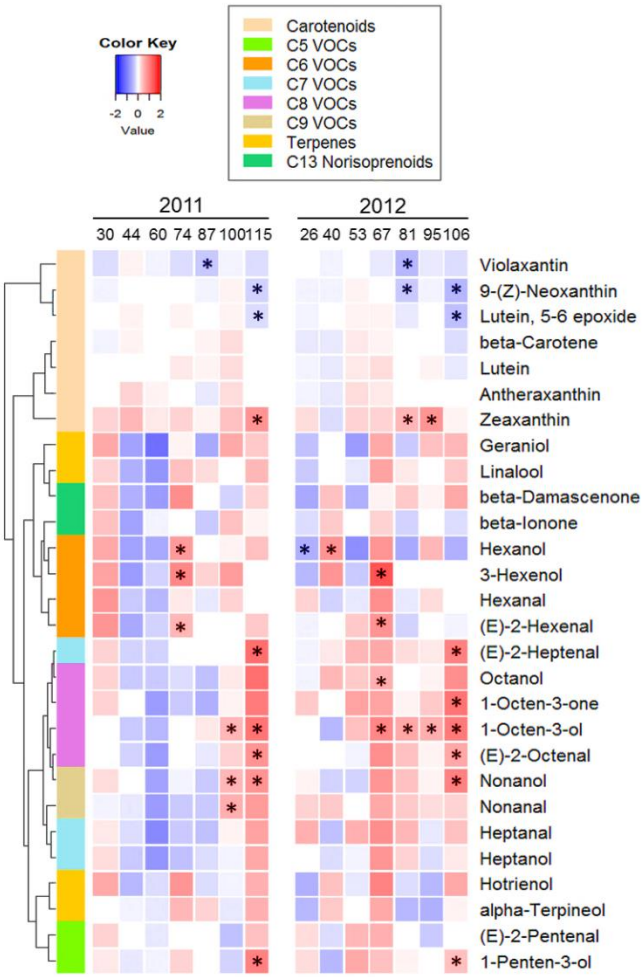

Figure 10. Effect of water deficit on the terpenoids and volatile organic compounds during fruit development and ripening in 2011 and 2012. Heatmaps represent $\log_2$ fold change (D/C) at all the developmental stages sampled. Blue and red boxes indicate lower and higher concentration in D, respectively. Asterisks indicate significant differences ($P<0.05$) between treatments. Metabolites were hierarchically clustered based on their response to water deficit. Color side bar on the left indicates the class of which each metabolite belongs.

Predicted drought-regulated modules link central players in metabolism

To determine the correlation pattern among DE genes and coordinated this regulation during berry development and ripening in response to water deficit, weighted gene co-expression network analysis (WGCNA) was performed (Langfelder and Horvath, 2008). Eleven co-response gene modules (clusters) of highly correlated genes based on the level of water deficit modulation were identified, with each module containing up to six generalized development-based accumulation patterns (Table S1h). The modules clearly indicated that large modulation of genes began from 67 DAA. In seven modules (named red, purple, yellow, blue, black, green-yellow, and magenta) we observed a general up-regulation; on the contrary in four modules (named pink, green, turquoise, and brown) we observed a general down-regulation. The possible developmental patterns of interests includes the ones which peak in expression at early and pre-veraison stages and decrease during ripening (sub-module 1, 4 , and 6), the ones which showed a steady increase in transcripts before peaking at harvest (sub-module 2), the ones which were generally highly expressed from mid-veraison to harvest (sub-module 3), and the one that peaked at veraison (sub-module 5).

Prioritizing on the yellow module, which showed a great proportion of genes up-regulated by deficit (Table S1h, dataset1) and on sub-modules 2, 3, and 5 with ripening-associated gene expression (Table S1h, dataset2), a subnetwork containing 390 nodes (genes) connected by 2079 edges (co-response correlations PCC > 0.9, P-value < 0.001) were extracted from the global network (Fig. 11). Many of these genes were highly interconnected, regardless of subtle differences in developmental expression, permitting the merging of these sub-modules. Many genes were involved in amino acid metabolism and its transport such as a threonine synthase (*VIT_04s0008g05990*), a pyrroline-5-carboxylate synthase (*VIT_13s0019g02360*), a homocysteine S-methyltransferase (*VIT_05s0020g03860*), and amino acid permeases (*VIT_18s0001g02020*, *VIT_19s0015g01300*). Moreover these modules included genes of the phenylpropanoid and flavonoid metabolism such as a 4-coumarate-CoA ligase (*VIT_16s0050g00390*), a chalcone synthases (*VIT_05s0136g00260*), three flavonoid 3',5'-hydroxylases (*VIT_06s0009g02860*, *VIT_06s0009g02920*, and *VIT_06s0009g03010*), the *VviMYBA1* and *VviMYBA2* transcription factors (*VIT_02s0033g00410*, *VIT_02s0033g00390*), and the acylated anthocyanin MATE transporter (*VIT_16s0050g00910*). Furthermore, also sugar derivatives metabolism genes (a sucrose synthase, three galactinol synthases, a trehalose synthase, and a trehalose-6P phosphatase) and 17 stress-related genes including four dehydration-responsive genes (*VIT_02s0033g01120*, *VIT_02s0109g00230*, *VIT_10s0003g04180*, and *VIT_16s0100g00570*) were also present. Interestingly, we observed that genes encoding transcriptional regulators (47 genes) from various TF families represented the 12% of the total sub-network. Meanwhile, hormone biosynthesis/signaling genes such as a 11,12 9-cis epoxycarotenoid dioxygenase (*VIT_05s0051g00670*), several protein phosphatase 2C, and four *cis*-zeatin-*O*-β-D-glucosyltransferase (*VIT_00s0324g00070*, *VIT_08s0040g01470*, *VIT_13s0019g02990*, and *VIT_18s0001g06120*) were also part of this module. Genes having high connectivity degree, referred as "hubs" in a network often play a central role under a given context (Jeong et al., 2001; Toubiana et al., 2013). The analysis of degree distribution revealed that 17 transcripts had degree greater than 39 genes (10% of the network size). Of note are genes encoding a sucrose

synthase (*VIT_11s0016g00470*), which had the second highest degree (66 genes); while others such as *VviERF62* (*VIT_05s0029g00140*), CBL-interacting protein kinase (*VIT_10s0003g01410*), and protein phosphatase 2C (*VIT_06s0004g05460*) have 47, 46, and 40, respectively; suggesting a central role of these genes in regulating the drought metabolic response in the fruit.

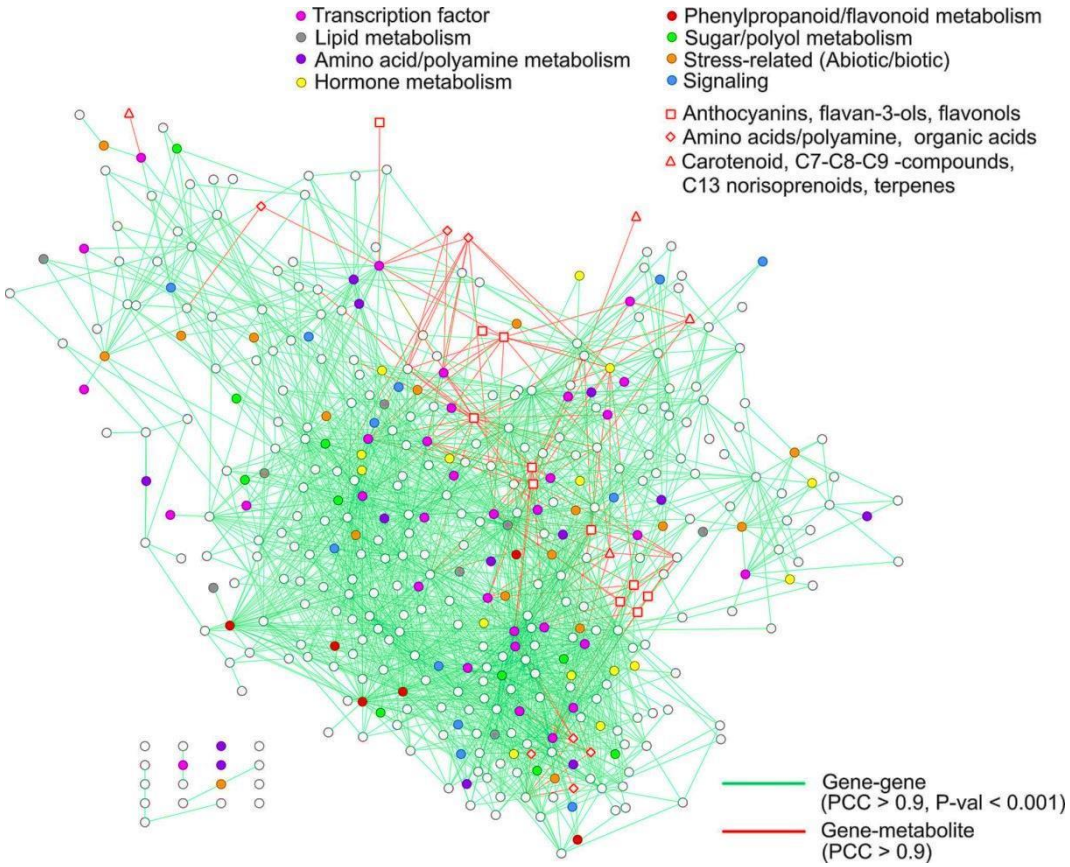

Figure 11. Network representation of the "yellow" module, sub-modules 2, 3, and 5. (a) Genes and metabolites are represented by circle and square nodes respectively. Green and red edges represent associations between gene-gene (PCC>0.9; P<0.001) and gene-metabolite (PCC>0.9). Different colors denote different categories, as reported in the legend.

Gene-metabolite co-response between transcriptional regulators and metabolites (Table S1i) were also searched in order to investigate the complex control of transcriptional regulation of metabolites or/and of the water deficit response, focusing on the two classes of metabolites: amino acids (osmoprotectants) and anthocyanins (wine quality). We observed that the co-responses of grapevine *VviERF62* (*VIT_05s0029g00140*), a predicted *DREB AP2/ERF* to drought stress across five time points had the highest degree (number) of correlations to amino acids namely proline, threonine, leucine, and isoleucine, compared to other transcription factors, implicating a role of this gene in amino acid metabolism during water deficit. Recent evidences have showed that overexpression of *AtERF1* significantly increase proline levels and conferred

tolerance to a myriad of abiotic stresses including drought (Cheng et al., 2013). For anthocyanin related metabolites, we observed that *VviMYBA1* (*VIT_02s0033g00410*), the regulator of anthocyanin biosynthesis (Walker et al., 2007) was only correlated to the responses of four anthocyanin compounds to drought. Nonetheless, transcription factors such as *VviNAC* (*VIT_08s0007g07640*) and *VviERFs* (*VIT_05s0029g00140*, *VIT_05s0049g00510*) were the TFs which shared the highest degree (number) of correlations to anthocyanin compounds indicating that they may direct/indirectly regulate anthocyanin levels during stress.

Cis-regulatory elements (CREs) were also analyzed within the promoter region of the yellow module genes independently and as a whole (Fig12a; TableS1j). Various ABA responsive elements (ABREs; core sequence ACGTGK) were consistently enriched across each developmental sub-network (yellow module 2, 3, and 5) and as a whole. Meanwhile, the drought-responsive element/C-repeat (DRE/CRT, core sequence: RCCGAC) involved in the regulation of osmotic stress–responsive gene expression (Yamaguchi-Shinozaki and Shinozaki, 2006) were enriched only in the whole network under strict significance (FDR<0.01). Nonetheless, ACGTGKC (FDR< 1.61E-09), CACGTGG (1.83E-09), MACCGMCW (FDR<2.59E-4), and TTGCGTG (FDR < 6.76E-4) motifs represents some examples of significantly enriched ABRE, bHLH, DRE, and NAC CREs present in 88, 65, 68, and 27 promoters, respectively. This observation reconciles the presence of many *VvibZIP*, *VvibHLH*, *VviAP2/ERF*, and *VviNAC* transcription factors present in the module. The presence of these transcription factors may be implicated in binding these motifs and driving transcriptional regulation of module members as well validating the role of this module-TF-gene network in drought response (Shinozaki and Yamaguchi-Shinozaki, 2007). In addition, we observed that the presence of these CREs is also common in gene promoters within the module, but several specific differences have also been identified (Fig. 12b; TableS1j). For example, large proportion of genes share the ABRE and bHLH CREs within their promoter region, while a ~30% of gene promoters where DRE and NAC CREs are present, also contain ABRE/bHLH CREs.

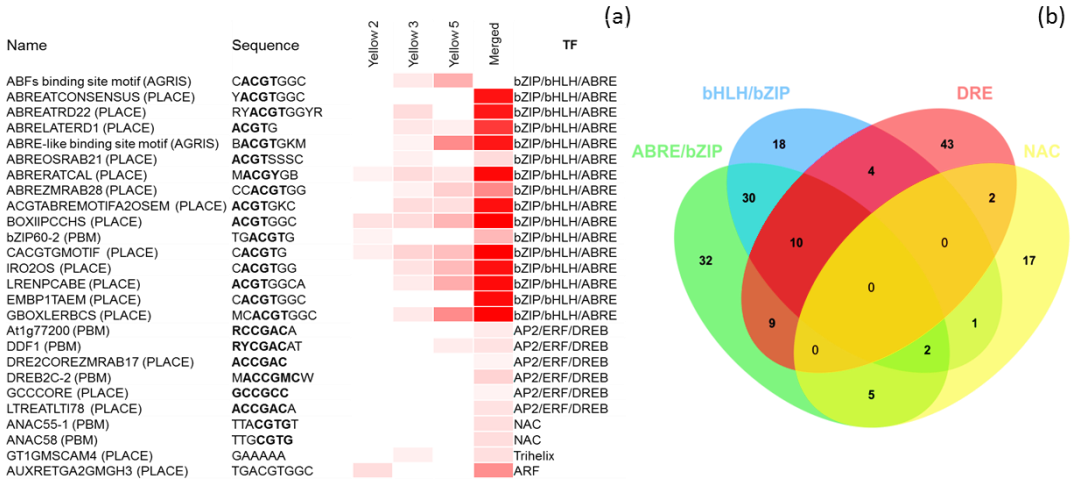

Figure 12. (a). Promoter enrichment analysis among the "yellow" module, sub-modules 2, 3, and 5 and the union of them. (b) The distribution of selected *cis*-regulatory elements (CRE), such as ACGTGKC (ABRE/bZIP), CACGTGG (bHLH/bZIP), MACCGMCW (DRE), and TTGCGTG (NAC) in promoter regions of genes within the module. Enrichment values are depicted as $\log_{10}$(FDR). Only selected CRE belonging to the ABRE-bZIP/bHLH-bZIP/DRE/NAC families are shown.

Discussion

The availability of the grapevine genome sequence and of high-throughput analysis (RNA-sequencing and large-scale metabolite analyses) coordinated with network analysis, provided a comprehensive picture of the mechanisms involved in the responses of fruit metabolism to water deficit. Our study revealed that severe water deficit affected fruit metabolism both at the transcriptional and metabolite level with major effects during the berry ripening process.

Signal transduction is mediated by transcription factors, which are the master regulation of gene expression. A great proportion of transcription factors (8.5 %), among the differently expressed genes identified in this study, were modulated by water deficit. We showed that both ABA-dependent and ABA-independent pathways were involved in this response. In the first case, several *VviAREBs/ABFs* and *VvibZIP* genes were modulated by water deficit in grapevine during berry ripening when deficit reached its highest severity. Overexpression of the *Arabidopsis thaliana AREB2/ABF4* resulted in plants with higher ABA sensitivity, reduced transpiration rate, and improved drought tolerance (Kang et al., 2002; Fujita et al., 2005). Also, basic leucine zipper TFs such as *AtbZIP10* and *AtbZIP53* were induced by osmotic stress (Weltmeier et al., 2006), and modulated the transcriptional activation of ABA-responsive genes such as proline, asparagine, and branched chain amino acid genes (Dietrich et al., 2011), or influenced the plants oxidative stress responses (Kaminaka et al., 2006). In the case of ABA-independent pathway, *VviAP2/ERF-DREB* transcription factors were highly induced by water deficit. These TFs can play critical roles in drought response by modulating a large suite of genes such as carbohydrate, amino acid, ROS detoxification, etc.. Furthermore, it has been reported that the *Arabidopsis thaliana AtHB12* was strongly induced by water deficit and ABA, and participates in the regulation of ABA signaling through the regulation of PP2C and ABA receptor gene expression (Olsson et al., 2004; Valdés et al., 2012). In our dataset, this gene was up-regulated at 53, 67, 81, and 106 DAA. The induction of *VviHB12* at 53 DAA, in pre-veraison, highlights that this gene may also be involved in one of the earliest response to drought.

Central or primary metabolism fulfils the essential needs of a plant and provides energy for growth, development and building blocks for the specialized or secondary metabolism. The respiratory metabolism is one of them and consist of glycolysis, tricarboxylic acid cycle (TCA) and electron transport chain (Fernie et al., 2004). Compared to other pathways studied here, genes and metabolites of the glycolysis and TCA were generally less affected by water deficit. On the contrary, amino acid biosynthesis was enhanced. In particular the genes involved in the synthesis of branched chain amino acids (valine, leucine, and isoleucine) and proline were up-regulated by water deficit together with an increased amount of these metabolites. Higher accumulation of branched-chain amino acids under water deficit was already reported in *Arabidopsis thaliana* (Urano et al., 2009) and *Oryza sativa* (Maruyama et al., 2014) leaves. These metabolites are thought to be regulated by ABA-dependent pathways in response to water deficit. Also the accumulation of the amino acid proline in response to water deficit has been reported in several tissues of plants such as *Arabidopsis thaliana* (Yoshiba et al., 1995), *Petunia hybrida* (Yamada et al., 2005), *Medicago sativa* (Girousse et al., 1996), *Triticum aestivum*

(Vendruscolo et al., 2007), and *Vitis vinifera* (Deluc et al., 2009). We observed that water deficit triggered the accumulation of free proline in the berry during ripening in parallel with an up-regulated of the pyrroline-5-carboxylate synthase (*VIT_13s0019g02360*) – a key regulatory biosynthetic gene. Proline is also involved in the response to other environmental stresses like salinity, low temperature, UV radiation, and heavy metal exposure (reviewed in Hayat et al., 2012). Proline, together with sugars and polyols, such as sucrose, mannitol, sorbitol, *myo*-inositol, galactinol, trehalose, and the raffinose family oligosaccharides (RFO), namely raffinose and stachyose, act as osmoprotectants in plant cells; contributing to the re- establishment of osmotic homeostasis, to turgor maintenance, and to ROS detoxification (Conde et al., 2011) and therefore they are accumulated in the cytosol at high concentration under moderate to severe water deficit. In particular, raffinose is synthetized through raffinose synthase (*RAFS*) from sucrose added of activated galactose moieties from galactinol, which derives from *myo*-inositol and UDP-galactose through galactinol synthase (*GOLS*). Five *VviGOLS* and two *VviRAFS* were up-regulated by D during berry ripening and the amount of raffinose present in the berry at harvest was higher in plants subjected to water deficit in 2012, although no differences were found for *myo*-inositol and galactinol. Higher concentration of raffinose as a response to water deficit was already reported in *Arabidopsis thaliana* (Taji et al., 2002) and *Oryza sativa* leaves (Maruyama et al., 2014).

Phenylpropanoid, stilbenoids, and flavonoid pathways were extensively affected by water deficit at both the transcript and metabolic level as already reported in other studies (Castellarin et al., 2007a; Deluc et al., 2009; Grimplet et al., 2009). Early steps of the phenylpropanoid pathway were both up- and down-regulated by water deficit. Transcript involved in benzoic and cinnamic acids were enhanced by D in parallel with a higher accumulation of *trans*-caftaric, *trans*-coutaric and gallic acids in 2012. Stilbene biosynthesis was down-regulated by water deficit in this study with 28 out of 45 stilbene synthases down-regulated by D together with the metabolites *trans*-resveratrol, piceatannol and pallidol present in lower concentration in the berries. Surprisingly, the two transcription factors designated to the regulation of stilbene biosynthesis in grapevine (*VviMYB14* and *VviMYB15* - Höll et al., 2013) were up-regulated at 106 and 67 and 81 DAA, respectively, indicating that the transcripts levels of these two TFs do not modulate the levels of transcripts of at least part of the stilbene synthases expressed in the fruit. The decrease in stilbenes concentration under water deficit is contrasting with what reported in Deluc et al. (2011) who described higher accumulation of *trans*-piceid together with some stilbene synthases in the red variety Cabernet Sauvignon under water deficit. Taken together, these data indicate a possible cultivar specificity on the effect of water deficit on stilbene biosynthesis, in particular, in our study *cis*- and *trans*- piceid were present in a lower amount in 2011 and 2012; however, differences were not significant in the latter season. Many, if not all, genes encoding for enzymes involved in the flavonoid pathway were up-regulated by D especially at veraison and during berry ripening. In particular structural genes such as chalcone synthases, chalcone isomerases, flavonoid-3'-5'-hydroxylases, flavanone-3-hydroxylases, dihydroflavonol reductases, and leucoanthocyanidin dioxygenases. Moreover, to add further strength on the entire up-regulation of the flavonoid pathway under water deficit, a general transcription factor of this pathway (*VviMYB5b* - Deluc et al., 2008; Cavallini et al., 2014) was up-regulated at veraison. As already reported (Castellarin et al.,

2007b), water deficit promoted the expression of the branch of the flavonoid pathway which leads to the production of tri-hydroxylated flavonoids. Four flavonoid-3'-5'-hydroxylases were up-regulated under water deficit, while no flavanoid 3'-hydroxylases were modulated in the same conditions. In agreement, the concentration of the try-hydroxylated anthocyanins namely delphinidin, petunidin and malvidin both in the glycosylated and acylated form, showed a higher accumulation under D. In general, key genes that control the anthocyanin biosynthesis such as *VviUFGT* and its regulators *VviMYBA1* and *VviMYBA2* were up-regulated under water deficit. Among the di-hydroxylated anthocyanins, only the peonidin based ones was positively affected by drought D. Interestingly, key genes for flavan-3-ols production (*VviLAR1*, *VviLAR2*, *VviANR*) were up-regulated by D: *VviLARs* during berry ripening while *VviANR* before veraison. This increase in the expression was not coupled with any increase of flavan-3-ol. Actually, catechin and epicatechin gallate were lower in D. However, flavan-3-ols polymers, proanthocyanidins, were more concentrated in D berries after veraison. This result can be explained with an increased rate of polymerization of flavan-3-ols during berry ripening under water deficit condition. Also, an higher galloylation of proanthocyanidins can be hypothesized based on the higher level of expression of two putative galloyl glucosyltransferases (Khater et al., 2012) under water deficit. Finally, two transcription factors related to flavan-3-ol and proanthocyanidin synthesis were modulated by D: *VviMYBPA1* that control *VviLAR1* was down-regulated at 67 DAA and the negative regulator *VviMYBC2-L1* was up-regulated at 67 and 81 DAA. Data in literature on the effect of water deficit on flavan-3-ols and proanthocyanidins are not consistent, with a little or no modulation of these compounds under water deficit (Castellarin et al., 2007a; Hochberg et al., 2015).

Free terpenes were barely present in Merlot berries and no differences were found between C and D on the accumulation of these metabolites. This is in agreement with what reported by Song et al. (2012) that found no differences in the free terpenoid content of Merlot grapes under different levels of irrigation. Recently, Battilana et al. (2011) characterized a 1-deoxy-D-xylulose-5-phosphate synthase, the rate limiting step in the MEP pathway, as the determinant of the monoterpenes concentration. In our dataset, this gene was down-regulated at harvest. Moreover, no specific prenyltransferases for monoterpenes production were modulated by D and only a prenyltransferase for sesquiterpenes (*VviFPPS*) was down-regulated. Only four terpene synthases out of sixty were modulated, all down-regulated during berry ripening. In the previous chapter, we studied the effect of water deficit during berry development and ripening in the white variety Tocai friulano and we putatively identify a transcription factor (*VviMYB24*, *VIT_14s0066g01090*) as a promising regulatory candidate for monoterpene and fatty acid biosynthetic pathways in grapevine. This gene in the Merlot dataset was down-regulated by D at 106 DAA indicating that the modulation of monoterpenes under water deficit is cultivar specific and that in Merlot it is strongly down-regulated. Carotenoids like violaxanthin, neoxanthin, and lutein 5,6-epoxide were generally reduced in concentration in D berries, while there were no differences between C and D in the amount of the other carotenoids identified in this study. Zeaxanthin was the only carotenoid that increased in concentration under water deficit. However, many genes of the carotenoids pathway were up-regulated. The interconversion of violaxanthin to zeaxanthin through violaxanthin de-epoxidase has a role in photoprotection in situation of high light due to changes in bunch

microclimate (Young et al., 2015). Two violaxanthin de-epoxidases (*VIT_04s0043g01010* and *VIT_07s0031g01770*) were up-regulated by D at 81 DAA. We also hypothesize that the up-regulation of the carotenoid pathway genes was toward a production of abscisic acid, which role in water deficit has been extensively studied (reviewed in Ferrandino and Lovisolo, 2014). Conversely to terpenoids, several VOCs were enhanced by water deficit. C_6 and C_9 VOCs are products of the fatty acid degradation and, recently, it has been demonstrated that also the C_5 volatile organic compound are products of this degradation (Shen et al., 2014). The fatty acid degradation involves lipoxygenase, hydroperoxide lyase, *(3Z)-(2E)* enal isomerase, and alcohol dehydrogenase (Schwab et al., 2008). We observed higher accumulation of C_5 and C_9 compounds together with C_7 and C_8 at harvest, while the C_6 compounds such as *(E)*-2-hexenal, hexanol, and 3-hexenol peaked at veraison. These compounds have been reported in several grapevine studies that aimed to investigate the volatile fraction of berries or leaves (Kalua and Boss, 2009; Song et al., 2012; Griesser et al., 2015). However, only C_6 compounds gained interest due to their green-leafy aroma. As far as we know, no information is available on the role of C_5, C_7, C_8, and C_9 VOCs in fruits and in the drought response. We detected for the first time a higher concentration of these compounds (1-penten-3-ol, *(E)*-2-heptenal, *(E)*-2-octenal, 1-octen-3-ol, 1-octen-3-one, and nonanol) in berries subjected to water deficit at harvest.

Gene co-expression networks can be employed to explore the relationship among highly-correlated genes and obtain information on their interactions and therefore on the structure of connected biological processes. Within a co-expression network, genes and similarity relationships (commonly represented by correlation coefficients) can be visualized as "nodes" and "edges" respectively. The connection of two nodes by an edge indicates a similar expression profile of the nodes according to a particular similarity metric. For a given set of genes, the collection of these nodes and edges forms a network. Visualization of the co-expression network enables the identification and description of densely connected gene clusters, referred to as modules, and an assessment of biological relevance can be achieved by investigating the functions of genes within each module (Saito et al., 2008). In the yellow modules, that was chosen because showed an high proportion of genes up-regulated by deficit, and in its sub-modules with ripening related genes, several pathways of the central and specialized metabolism were found connected. For instance, branched chain amino acids synthesis, phenylpropanoid and flavonoid, sugar derivatives metabolism genes were co-regulated with stress related genes and several transcriptional factors involved in the ABA-dependent and -independent pathways. These biological pathways are normally induced under water deficit as revealed by transcriptomic studies of *Arabidopsis thaliana* (Harb et al., 2010) and *Medicago truncatula* leaves (Zhang et al., 2014),and *Zea mays* roots (Opitz et al., 2015). Similarly, our network analysis revealed that regardless of tissue specificity, plants adopt a similar strategy by modulating osmoprotectant and anti-oxidant metabolites accumulation under drought stress to adapt and confer tolerance. Another strategy to cope with such stresses involves the coordinated regulation of genes involved in the perception, signaling, and transcriptional regulation during water deficit. Strong co-responses and co-regulation between structural and transcriptional regulatory genes during water deficit and berry development, enrichment of cis-regulatory element genes, and plausible gene-metabolite correlations implicates the role of this subnetwork and many of its members to be highly involved in

response to drought in grapevine berries at the molecular and biochemical level. However, functional validation of this regulatory module is necessary in future studies to confirm their role in the fruit response to drought.

Conclusion

In this study both the ABA-dependent and ABA-independent signal transduction pathways were activated by water deficit with several *VviAREB/ABFs*, *VvibZIP*, and *VviAP2/ERF-DREB* transcription factors that were up-regulated at one or more developmental stages of berry ripening. Analyses of the central and the specialized grapevine metabolism by investigating glycolysis and sugar accumulation, tricarboxylic acid cycle and amino acid biosynthesis, phenylpropanoid and flavonoid pathways, terpenes, carotenoids, and fatty acid degradation, both at the transcript and metabolite level, revealed that water deficit enhanced the accumulation of several osmoprotectants and secondary metabolite compounds. A weighted gene co-expression network analysis clustered in a single module several genes involved in the branched chain amino acids biosynthesis, phenylpropanoid and flavonoid pathways, and sugar derivatives metabolism together with the transcription factors involved in the drought-stress signal, indicating a putative role of these transcription factors on the regulation of the response of the fruit metabolism to drought in Merlot berries.

Materials & Methods

Field experiment, physiological measurements, and sample preparation

Field experiments were conducted during 2011 and 2012 at the University of Udine experimental farm on 18 years old Merlot (clone R3) vines, grafted on SO4 rootstock. Vines were planted with a 2.5 m x 1.0 m spacing and trained to spur cordon system. To ensure a proper management of the water regime during the experimental trial and ensure consistent treatments across seasons, four rows were covered with an ethylene-vinyl-acetate (EVA) film at the beginning of the seasons, as described in Herrera et al. (2015). Only the two middle rows of the vineyard and the plants located in the center of each row were considered for sampling to avoid any possible rainfall effect. Two irrigation treatments were imposed at approximately 25 days after anthesis (DAA): Control (C) vines where weekly irrigated maintaining the midday stem water potential (Ψ_{Stem}) above -0.6 MPa and deficit irrigated (D) vines were not irrigated from fruit set until Ψ_{Stem} was lower than -1.4 MPa, whereupon irrigation was managed to maintain Ψ_{Stem} between -1.0 and -1.4 MPa. Each treatment was replicated four times in plots of 12 vines each in a completely randomized design. Water was supplied by a sub-surface drip irrigation system as described in Herrera et al. (2015). Plant water status was monitored weekly by measuring midday Ψ_{Stem}. On each side of the row and for each experimental plot, two leaves from different vines were covered with aluminium foil coated plastic bags for 1 h. Leaves were then removed and Ψ_{Stem} was measured using a Scholander pressure chamber (Choné et al., 2001). Climatological data were recorded by an automated weather station located 100 m from the experimental site.

Berries were sampled at 30, 44, 60, 74, 87, 100, 115 DAA in 2011, and at 26, 40, 53, 67, 81, 95, 106 DAA in 2012. At each date, two sets of berries were randomly collected from each plot, for a total of four biological replicates per irrigation treatment. The first set of 60 berries was used for measurements of berry weight, total soluble solids (TSS), titratable acidity (TA), and pH. Samples were quickly brought to the laboratory in insulated cooler. Total soluble solids (TSS), titratable acidity (TA), and pH were analyzed as described in Herrera et al. (2015).The second set of 40 berries was used for the metabolite and transcript analyses.; samples were snap frozen with liquid nitrogen, and stored at -80 °C.

Whole berries, without pedicel, were grinded to a fine powder under liquid nitrogen using an analytical mill (IKA®-Werke GMbH & CO). The frozen powder was aliquoted for metabolite and RNA extraction. Moreover, a quality control (QC) sample for metabolite analysis was prepared by pooling together aliquots of all the samples.

RNA extractions and RNA sequencing analysis

Transcriptome analyses were performed on the samples collected at 26, 53, 67, 81, and 106 DAA in 2012. Three out of the four biological replicates per treatment were considered. Total RNA was extracted with the 'Spectrum Plant total RNA' kit (Sigma-Aldrich) from 0.2 g of ground berries. The quantity and quality of the RNA were determined with a Caliper LabChip® GX (Perkin-Elmer). Library preparation was performed using the TruSeq RNA Sample Prep Kit v2.0 according to the manufacturer's instructions (Illumina). Libraries were quantified using a

2100 Bioanalyzer (Agilent Technologies). Multiplexed cDNA libraries were pooled in equimolar amounts, and clonal clusters were generated using Cbot (Illumina). Sequencing was performed with an Illumina HiSeq 2000 platform (Illumina pipeline 1.8.2) at IGA Technology Services (Udine, Italy). Trimming for quality and length, and filtering for mitochondria and chloroplast contamination were performed by the ERNE package version 1.2 tool ERNE-FILTER (Del Fabbro et al., 2013). The minimum PHRED score accepted for trimming was 20, and reads shorter than 40 bp were discarded. Reads were aligned against the reference grapevine genome PN40024 12x (Jaillon et al., 2007) using the software TopHat version 2.0.6 (Trapnell et al., 2012) with default parameters. Aligned reads were counted with a htseq-count (version 0.6.0), in intersection-non-empty mode for overlap resolution (Anders et al., 2015). *Vitis vinifera* gene annotation GTF-file (V1) was downloaded from Ensembl Plants website. Differentially expressed (DE) genes (false discovery rate less than 0.05) analysis was performed with the R package DeSeq2 (Love et al., 2014). Annotation of gene functions was done according to Grimplet et al. (2012) and Naithani et al. (2014) and retrieved from recent literature. Gene ontology analyses were carried out for each sampling. Overrepresented genes categories were identified with the BINGO app 3.0.2 of Cytoscape 3.1.1 (Maere et al., 2005). PlantGoSlim categories referred to biological processes were used to run the gene enrichment analysis, using a hypergeometric test with a significance threshold of 0.05 after Benjamini and Hochberg false discovery rate correction.

Targeted metabolite analyses

Primary metabolites were analyzed accordingly to Degu et al. (2014). Briefly, 100 mg of frozen powder of ground berries were extracted in a methanol:chloroform:water solution (2.5:1:1 v/v). Internal standards were added (0.2 mg/mL ribitol in water, 1 mg/mL ampicillin in water and 1 mg/mL corticosterone in methanol). The mixture was vortexed and centrifuged for 2 min at 14,000 RPM and the supernatant collected. 300 μL of chloroform and water were respectively added to the supernatant and centrifuged at 14,000 RPM for 2 min. 100 μL of the upper aqueous-methanolic phase was dried in a vacuum concentrator for derivatization for GC–MS analysis (Lisec et al., 2006). Samples were redissolved and derivatized for 120 min at 37°C (in 40 μL of 20-mg/mL methoxyamine hydrochloride in pyridine) followed by a 30-min treatment with 70 μL N-methyl-N-(trimethylsilyl) trifluoroacetamide at 37°C as described in Hochberg et al. (2013). Eight microliters of a retention time standard mixture (0.029% v/v n-dodecane, n-pentadecane, n-nonadecane, n-docosane, n-octacosane, n-dotracontane and n-hexatriacontane dissolved in pyridine) was added prior to trimethylsilylation. The sample set also included a reference quality control of authentic metabolite standards (1 mg/mL each). One μL was injected on a 30-m VF-5 ms GC column with 0.25 mm i.d., film thickness of 0.25 μm, and + 10 m EZ-Guard (Agilent) in splitless and split mode (32:1) allowing a more accurate comparison of highly abundant metabolites (e.g., malate, tartrate, sucrose, glucose, fructose and threalose). The GC-MS system consisted of an AS 3000 autosampler, a TRACE GC ULTRA gas chromatograph, and a DSQII quadrupole mass spectrometer (Thermo-Fisher ltd). The run conditions are described in Hochberg et al. (2013). XCalibur software was used for the mass spectra identification using the NIST library (USA) and the RI libraries from the Max-Planck Institute for Plant Physiology (Germany). QC sample was used for data normalization.

Phenolic acids, stilbenes, flavonols, flavan-3-ols and proanthocyanidins were determined accordingly to Vrhovsek et al. (2012) with some modifications. Briefly, 0.8 mL of chloroform and 1.2 mL of a mix of methanol and water (2:1) were added to one gram of frozen powder of ground berries. A 50 μL aliquot of *o*-coumaric acid solution (2 mg/mL in MeOH) was added as an internal standard. The extraction mixture was shaken for 15 min on an orbital shaker (Grant-Bio Rotator PTR-60), and then centrifuged for 10 min at 1,000 g. The upper aqueous-methanolic phase was collected. The extraction was repeated by adding 1.2 mL of methanol and water. The aqueous-methanolic phase was collected and combined with the previous one, brought to a final volume of 5 mL with Milli-Q water, and filtered with a 0.2 μm PTFE filter (Millipore). The chromatographic analysis was carried out using a Waters Acquity UPLC system (Milford) coupled to a Waters Xevo triple-quadrupole mass spectrometer detector (Milford). Compounds were identified with TargetLynx software based on their reference standard, retention time, and qualifier and quantifier ion, and were quantified by their calibration curve and expressed as mg/Kg of grapes.

Carotenoids were analyzed accordingly to Wehrens et al. (2013). Briefly, the chloroform phase of the extraction solution described above was collected. Twenty μL of trans-β-apo-8'-carotenal (25 μg/mL) was used as internal standard. Ten μL of a 0.1% triethylamine solution was added to prevent rearrangement of carotenoids. After extraction, samples were dried with N2, and stored at -80°C until analysis. Dried samples were suspended in 50 μL of ethyl acetate, and transferred to dark vials. The chromatographic analysis was performed in a 1290 Infinity Binary UPLC (Agilent) equipped with an RP C30 3 μm column coupled to a 20 x 4.6 mm C30 guard column. The DAD signal was acquired from 200 to 600 nm at a frequency of 2.5 Hz. Spectra components and elution profiles were determined with the R package 'alsace' 3.0 using multivariate curve resolution with an orthogonal projection approach and alternative least squares (MRC-ALS). Compounds were quantified from linear calibration curves built with standard solutions and expressed as mg/Kg of grapes.

For the anthocyanins analysis an aliquot of 1.8 mL of methanol:water 1:1 was added to 0.18 g of frozen powder of ground berries. The extraction was performed at room temperature in an ultrasonic bath for 1 h. Samples were centrifuged at 15,000 rpm for 15 minutes, diluted and filtered using regenerated cellulose membranes with pore size of 0.2 μm (15mm syringe filter, Phenomenex). Anthocyanins were determined with an LC-20AT HPLC (Shimadzu, Japan) equipped with a diode array detector (SPD-M 20A, Shimadzu, Japan). Separation was performed using a C18 column (LiChroCART 250-4, Merck, Germany) maintained at 25°C. Solvent A was methanol and solvent B perchloric acid (0.3%) in water. Gradient of mobile phase A was as follows: 0-32 min 27%, 32-45 min 67.5%, 45-50min 100%, 50-60 min 27%. Individual anthocyanins were identified by comparing the retention time of each chromatographic peak with available data in the literature (Mazza et al., 1999). The concentration of individual anthocyanins was expressed in oenin chloride (Extrasynthese) equivalents and expressed as mg/Kg of grapes.

Free (non-glycosylated) VOCs were analyzed accordingly to Fedrizzi et al. (2012) with some modifications. On the day of analysis, four grams of frozen grape powder were weighed out in a 20 mL SPME dark-glass vial. Three grams of NaCl, 15 mg of citric acid, 15 mg of ascorbic acid,

50 μL of sodium azide, and 7 mL of milliQ water were added to the sample. Fifty μL of a solution containing five internal standards, d_{10}-4-methyl-3-penten-2-one (1 g/L), d_{11}-ethyl hexanoate (1 g/L), d_{16}-octanal (1 g/L), d_8-acetophenone (1 g/L), d_7-benzyl alcohol (1 g/L), was added to each sample. Prior to injection, the sample was pre-incubated at 60 °C in a SMM Single Incubator (Chromtech) for 10 min stirring at 450 rpm. Next, the sample was incubated in the same conditions for 40 min with a DVB-CAR-PDMS 50/30 μm x 2 cm (Supelco) fiber in the headspace for absorption. Free VOCs were thermally desorbed in splitless mode for 4 min at 250°C. Extractions and injections were carried out with a CTC Combi-PAL autosampler (Zwingen). The analysis was performed with a Trace GC Ultra gas chromatograph (Thermo Scientific) coupled to a TSQ Quantum Tandem mass spectrometer. GC separation was performed on a 30 m Stabilwax (Restek Corporation) capillary column with an internal diameter of 0.25 mm and a film thickness of 0.25 μm with the conditions described in Fedrizzi et al. (2012). XCalibur software was used for the peaks identification. VOCs were identified by comparing the retention times of individual peaks with the retention times of their reference standards, and by identifying the mass spectra using the NIST library. The ratio of each VOC area to the d_8-acetophenone internal standard area was considered to reduce technical variability among extractions and chromatographic runs and VOCs quantity were expressed as μg/Kg of grapes of d_8-acetophenone equivalents.

Extractions and injections of the samples were performed in a random sequence and QC samples were injected at the beginning of the sequence and every six sample injections.

Statistical and network analyses

A one-way ANOVA was performed using JMP 7 (SAS Institute Inc.) to detect significant differences ($P<0.05$) in the several parameters considered between irrigation treatments at each sampling date. Heatmaps representing the $\log_2$ fold change ($\log_2$FC) of metabolite concentrations between treatments (D/C) were drawn with R. Metabolites were clustered with Person correlation and a complete link. Principal component analysis (PCA) on the entire transcriptome dataset was performed, using R software. Co-expression analysis was performed using weighted correlation gene co-expression network analysis (WGCNA) package in R (Langfelder and Horvath, 2008) using the $\log_2$ fold change (D/C) [dataset1] and variance stabilized transformed (VST) counts [dataset2] of DE genes at 26, 53, 67, 81 and 106 DAA, separately to identify highly correlated genes sharing similar drought co-response and development accumulation patterns, respectively. Briefly, the Pearson's correlation coefficient (PCC) matrix for the genes were first calculated and transformed by raising the correlation values to a power of β, using the pickSoftThreshold function with a "signed" networkType. The resulting adjacency matrix is transformed into a topological overlap matrix (TOM) using the TOMsimilarity function with a "signed" TOMtype. The "signed" option ensures the direction (positive/negative correlations) of correlations are considered and not the absolute values. Finally, a hierarchal cluster tree is created from the TOM and dynamicTreeCut (Langfelder et al., 2008) prunes the branches to identify co-regulated modules. All these procedures can be called using blockwiseModules function in one step and parameters used in this study are power = 20 (determined by pickSoftThreshold), maxBlockSize = 30000, networkType = "signed",

TOMType = "signed", nThreads=23). Other parameters were kept at default; deepSplit at 2, mergeCutHeight at 0.25 while minModuleSize were set to 300 for the discovery of large modules. Empirical P-value of PCC values (statistical significance) of dataset1 and dataset2 were estimated by 1,000 permutations using the rsgcc package (Ma and Wang, 2012). WGCNA module assignments and PCC values were extracted visualization using Cytoscape software (version 3.1.1) (Shannon et al., 2003). Various networks were created using PCC threshold > 0.9 and p-value < 0.001.

Grapevine promoter sequences (1 kb upstream of the 5′ UTR) based on the 12xV1 predicted gene model coordinates were retrieved from the CRIBI genome repository. Known *cis*-regulatory element (CRE) from a compendia of known/characterized motif with ascribed functions (Higo et al., 1999; Yilmaz et al., 2011; Franco-Zorrilla et al., 2014) resulting in 552 non-redundant CREs were scanned in the gene promoters of each WGCNA co-response and developmental modules using a custom-made script in R. Enrichment of CREs in modules were validated with the hypergeometric test adjusted with false discovery for multiple testing correction using the R stat and fdrtool (Strimmer, 2008) packages. Putative CREs were deemed significantly enriched under FDR < 0.01.

Abbreviation

3AT: anthocyanin-3-*O*-glucoside-6′′-*O*-acyltransferase; *4CL*: 4-coumarate-CoA ligase; *AACT*: acetyl-CoA acetyltransferase; *ABA*: abscisic acid; *ABRE*: ABA-responsive element; *ANR*: anthocyanidin reductase; *AnthoMATE*: anthocyanin-acylglucosides transporter; *AOMT*: anthocyanin-O-methyltransferase; *BCH*: β-carotene hydroxylase; *C*: control; *C3H*: *p*-coumaroyl shikimate 3'-hydroxylase; *C4H*: trans-cinnamate 4-monooxygenase; *CCD*: carotenoid cleavage dioxygenase; *CCoAMT*: caffeoyl-CoA 3-O-methyltransferase; *CHI*: chalcone isomerase; *CHS*: chalcone synthase; *CISO*: carotenoid isomerase; *COMT*: caffeic acid 3-O-metyltransferase; *CREs*: *cis*-regulatory elements; *D*: water deficit; *DAA*: days after anthesis; *DAHP*: 3-deoxy-D-arabinoheptulosonate 7-phosphate synthase; *DE*: differentially expressed; *DFR*: dihydroflavonol reductase; *DRE/CRT* : dehydration-responsive element/C-repeat; *DREB*: DRE/CRT binding protein; *DVB-CAR-PDMS*: divinylbenzene-carboxen-polydimethylsiloxane; *DXS*: 1-deoxy-D-xylulose-5-phosphate synthase; *EVA*: ethylene-vinyl-acetate; *F3′5′H*: flavonoid-3′5′-hydroxylase; *F3H*: flavanone-3-hydroxylase; *FLS*: flavonol synthase; *FPPS*: farnesyl pyrophosphate synthase; *GC-MS*: gas chromatography-mass spectrometry; *GIN*: vacuolar invertase; *GO*: gene ontology; *GOLS*: galactinol synthase; *GPPS*: geranylgeranyl pyrophosphate synthase; *GT*: glycosyltransferases; *HCT*: hydroxycinnamoyl- CoA :shikimate / quinate hydroxycinnamoyltransferase; *HMGR*: hydroxymethylglutaryl-CoA reductases; *HPL*: hydroperoxide lyase; *HPLC-DAD*: high performance liquid chromatography-diode array detector; *HS-SPME-GC-MS*: headspace-solid phase microextraction-gas chromatography-mass spectrometry; *HT*: hexose transporter; *ISPG*: 4-hydroxy-3-methylbut-2-enyl diphosphate synthase; *LAR*: leucoanthocyanidin reductase; *LDOX*: leucoanthocyanidin dioxygenase; *LOX*: lipoxygenase; *MEP*: 2C-methyl-D-erythritol-4-phosphate; *MVA*: mevalonate; *NCED*: cis-epoxycarotenoid dioxygenase; *NSY*: neoxanthin synthase; *PAL*: phenylalanine ammonia lyase; *PCA*: principal component analysis; *PCC*: Pearson correlation coefficient; *PDH*: phytoene desaturase; *PMD*: phosphomevalonate decarboxylase; *PSY*: phytoene synthase; *PTM*: polyol monosaccharide transporter; *QC*: quality control; *RAFS*: raffinose synthase; *RFO*: raffinose family oligosaccharides; *RNA-seq*: RNA sequencing; *ROS*: reactive oxygen species; *STS*: stilbene synthase; *SUC*: sucrose transporter; *TA*: titratable acidity; *TCA*: tricarboxylic acid cycle; *TF*:

transcription factor; *TMT*: tonoplast monosaccharide transporter; *TPS*: terpene synthase; *TSS*: total soluble solids; *UFGT*: UDP-glucose:flavonoid 3-O-glucosyltransferase; *UHPLC-MS/MS*: ultra-high performance liquid chromatography-tandem mass spectrometer; *VDE*: violaxanthin de-epoxidase; *VOCs*: volatile organic compounds; *Vvi*: Vitis vinifera; *WGCNA* : weighted gene co-expression network analysis; *ZDS*: ζ-carotene desaturase; *ZEP*: zeaxanthin epoxidase; Ψ_{Stem}: stem water potential.

Acknowledgement

This study was funded by the Friuli-Venezia-Giulia Region (GISVI Project: "Gestione Integrata e Sostenibile Vite-Vino), the EU Cross-Border Cooperation Programme Italy-Slovenia 2007–2013 (VISO Project: Viticulture and Sustainable Development of Local Resources in the Wine Industry), the International Ph.D. Programme in the Genomics and Molecular Physiology of Fruit Plants (GMPF) of the Fondazione Edmund Mach International Research School Trentino (FEM-FIRS>T), the COST Action FA1106 Quality Fruit, the University of British Columbia (10R18459), and Natural Sciences and Engineering Research Council of Canada (10R23082).

References

Afoufa-Bastien D, Medici A, Jeauffre J, Coutos-Thévenot P, Lemoine R, Atanassova R, Laloi M (2010) The *Vitis vinifera* sugar transporter gene family: phylogenetic overview and macroarray expression profiling. BMC Plant Biol **10**: 245

Anders S, Pyl PT, Huber W (2015) HTSeq—a Python framework to work with high-throughput sequencing data. Bioinformatics **31**: 166–169

Battilana J, Emanuelli F, Gambino G, Gribaudo I, Gasperi F, Boss PK, Grando MS (2011) Functional effect of grapevine 1-deoxy-D-xylulose 5-phosphate synthase substitution K284N on Muscat flavour formation. J Exp Bot **62**: 5497–5508

Castellarin SD, Matthews MA, Di Gaspero G, Gambetta GA (2007a) Water deficits accelerate ripening and induce changes in gene expression regulating flavonoid biosynthesis in grape berries. Planta **227**: 101–112

Castellarin SD, Pfeiffer A, Sivilotti P, Degan M, Peterlunger E, Di Gaspero G (2007b) Transcriptional regulation of anthocyanin biosynthesis in ripening fruits of grapevine under seasonal water deficit. Plant Cell Environ **30**: 1381–1399

Cavallini E, Zenoni S, Finezzo L, Guzzo F, Zamboni A, Avesani L, Tornielli GB (2014) Functional diversification of grapevine MYB5a and MYB5b in the control of flavonoid biosynthesis in a Petunia anthocyanin regulatory mutant. Plant Cell Physiol **55**: 517–534

Cavallini E, Matus JT, Finezzo L, Zenoni S, Loyola R, Guzzo F, Schlechter R, Ageorges A, Arce-Johnson P, Tornielli GB (2015) The phenylpropanoid pathway is controlled at different branches by a set of R2R3-MYB C2 repressors in grapevine. Plant Physiol **167**: 1448–1470

Cheng MC, Liao P-M, Kuo WW, Lin TP (2013) The Arabidopsis ETHYLENE RESPONSE FACTOR1 regulates abiotic stress-responsive gene expression by binding to different cis-acting elements in response to different stress signals. Plant Physiol **162**: 1566–1582

Choné X, Leeuwen CV, Dubourdieu D, Gaudillère JP (2001) Stem water potential is a sensitive indicator of grapevine water status. Ann Bot **87**: 477–483

Chong J, Piron MC, Meyer S, Merdinoglu D, Bertsch C, Mestre P (2014) The SWEET family of sugar transporters in grapevine: VvSWEET4 is involved in the interaction with Botrytis cinerea. J Exp Bot **65**: 6589–6601

Conde A, Chaves MM, Gerós H (2011) Membrane transport, sensing and signaling in plant adaptation to environmental stress. Plant Cell Physiol **52**: 1583–1602

Conde A, Regalado A, Rodrigues D, Costa JM, Blumwald E, Chaves MM, Gerós H (2015) Polyols in grape berry: transport and metabolic adjustments as a physiological strategy for water-deficit stress tolerance in grapevine. J Exp Bot **66**: 889–906

Cramer GR, Ghan R, Schlauch KA, Tillett RL, Heymann H, Ferrarini A, Delledonne M, Zenoni S, Fasoli M, Pezzotti M (2014) Transcriptomic analysis of the late stages of grapevine (*Vitis vinifera* cv. Cabernet Sauvignon) berry ripening reveals significant induction of ethylene signaling and flavor pathways in the skin. BMC Plant Biol **14**: 1–21

Cramer GR, Urano K, Delrot S, Pezzotti M, Shinozaki K (2011) Effects of abiotic stress on plants: a systems biology perspective. BMC Plant Biol **11**: 163

Czemmel S, Stracke R, Weisshaar B, Cordon N, Harris NN, Walker AR, Robinson SP, Bogs J (2009) The grapevine R2R3-MYB transcription factor VvMYBF1 regulates flavonol synthesis in developing grape berries. Plant Physiol **151**: 1513–1530

Degu A, Hochberg U, Sikron N, Venturini L, Buson G, Ghan R, Plaschkes I, Batushansky A, Chalifa-Caspi V, Mattivi F, et al (2014) Metabolite and transcript profiling of berry skin during fruit development elucidates differential regulation between Cabernet Sauvignon and Shiraz cultivars at branching points in the polyphenol pathway. BMC Plant Biol **14**: 188

Del Fabbro C, Scalabrin S, Morgante M, Giorgi FM (2013) An extensive evaluation of read trimming effects on Illumina NGS data analysis. PLoS ONE **8**: e85024

Deluc L, Bogs J, Walker AR, Ferrier T, Decendit A, Merillon J-M, Robinson SP, Barrieu F (2008) The transcription factor VvMYB5b contributes to the regulation of anthocyanin and proanthocyanidin biosynthesis in developing grape berries. Plant Physiol **147**: 2041–2053

Deluc LG, Quilici DR, Decendit A, Grimplet J, Wheatley MD, Schlauch KA, Mérillon J-M, Cushman JC, Cramer GR (2009) Water deficit alters differentially metabolic pathways affecting important flavor and quality traits in grape berries of Cabernet Sauvignon and Chardonnay. BMC Genomics **10**: 212

Deluc LG, Decendit A, Papastamoulis Y, Mérillon J-M, Cushman JC, Cramer GR (2011) Water deficit increases stilbene metabolism in Cabernet Sauvignon berries. J Agric Food Chem **59**: 289–297

Dietrich K, Weltmeier F, Ehlert A, Weiste C, Stahl M, Harter K, Dröge-Laser W (2011) Heterodimers of the Arabidopsis transcription factors bZIP1 and bZIP53 reprogram amino acid metabolism during low energy stress. Plant Cell **23**: 381–395

Fedrizzi B, Carlin S, Franceschi P, Vrhovsek U, Wehrens R, Viola R, Mattivi F (2012) D-optimal design of an untargeted HS-SPME-GC-TOF metabolite profiling method. Analyst **137**: 3725–3731

Fernie AR, Carrari F, Sweetlove LJ (2004) Respiratory metabolism: glycolysis, the TCA cycle and mitochondrial electron transport. Curr Opin Plant Biol **7**: 254–261

Ferrandino A, Lovisolo C (2014) Abiotic stress effects on grapevine (*Vitis vinifera* L.): Focus on abscisic acid-mediated consequences on secondary metabolism and berry quality. Environ Exp Bot **103**: 138–147

Fournier-Level A, Hugueney P, Verriès C, This P, Ageorges A (2011) Genetic mechanisms underlying the methylation level of anthocyanins in grape (*Vitis vinifera* L.). BMC Plant Biol **11**: 179

Francisco RM, Regalado A, Ageorges A, Burla BJ, Bassin B, Eisenach C, Zarrouk O, Vialet S, Marlin T, Chaves MM, et al (2013) ABCC1, an ATP Binding Cassette protein from grape berry, transports anthocyanidin 3-*O*-glucosides. Plant Cell **25**: 1840–1854

Franco-Zorrilla JM, López-Vidriero I, Carrasco JL, Godoy M, Vera P, Solano R (2014) DNA-binding specificities of plant transcription factors and their potential to define target genes. Proc Natl Acad Sci **111**: 2367–2372

Fujita Y, Fujita M, Satoh R, Maruyama K, Parvez MM, Seki M, Hiratsu K, Ohme-Takagi M, Shinozaki K, Yamaguchi-Shinozaki K (2005) AREB1 is a transcription activator of novel ABRE-dependent ABA signaling that enhances drought stress tolerance in *Arabidopsis*. Plant Cell **17**: 3470–3488

Gao X, Giorgi F (2008) Increased aridity in the Mediterranean region under greenhouse gas forcing estimated from high resolution simulations with a regional climate model. Glob Planet Change **62**: 195–209

Girousse C, Bournoville R, Bonnemain JL (1996) Water deficit-induced changes in concentrations in proline and some other amino acids in the phloem sap of Alfalfa. Plant Physiol **111**: 109–113

Gomez C, Terrier N, Torregrosa L, Vialet S, Fournier-Level A, Verriès C, Souquet JM, Mazauric JP, Klein M, Cheynier V, et al (2009) Grapevine MATE-Type proteins act as vacuolar H+-Dependent acylated anthocyanin transporters. Plant Physiol **150**: 402–415

Griesser M, Weingart G, Schoedl-Hummel K, Neumann N, Becker M, Varmuza K, Liebner F, Schuhmacher R, Forneck A (2015) Severe drought stress is affecting selected primary metabolites, polyphenols, and volatile metabolites in grapevine leaves (*Vitis vinifera* cv. Pinot noir). Plant Physiol Biochem **88**: 17–26

Grimplet J, Hemert JV, Carbonell-Bejerano P, Díaz-Riquelme J, Dickerson J, Fennell A, Pezzotti M, Martínez-Zapater JM (2012) Comparative analysis of grapevine whole-genome gene predictions, functional annotation, categorization and integration of the predicted gene sequences. BMC Res Notes **5**: 213

Grimplet J, Wheatley MD, Jouira HB, Deluc LG, Cramer GR, Cushman JC (2009) Proteomic and selected metabolite analysis of grape berry tissues under well-watered and water-deficit stress conditions. PROTEOMICS **9**: 2503–2528

Hannah L, Roehrdanz PR, Ikegami M, Shepard AV, Shaw MR, Tabor G, Zhi L, Marquet PA, Hijmans RJ (2013) Climate change, wine, and conservation. Proc Natl Acad Sci **110**: 6907–6912

Harb A, Krishnan A, Ambavaram MMR, Pereira A (2010) Molecular and physiological analysis of drought stress in *Arabidopsis* reveals early responses leading to acclimation in plant growth. Plant Physiol **154**: 1254–1271

Hayat S, Hayat Q, Alyemeni MN, Wani AS, Pichtel J, Ahmad A (2012) Role of proline under changing environments. Plant Signal Behav **7**: 1456–1466

Herrera JC, Bucchetti B, Sabbatini P, Comuzzo P, Zulini L, Vecchione A, Peterlunger E, Castellarin SD (2015) Effect of water deficit and severe shoot trimming on the composition of *Vitis vinifera* L. Merlot grapes and wines. Aust J Grape Wine Res **21**: 254–265

Higo K, Ugawa Y, Iwamoto M, Korenaga T (1999) Plant cis-acting regulatory DNA elements (PLACE) database. Nucleic Acids Res **27**: 297–300

Hochberg U, Degu A, Fait A, Rachmilevitch S (2013a) Near isohydric grapevine cultivar displays higher photosynthetic efficiency and photorespiration rates under drought stress as compared with near anisohydric grapevine cultivar. Physiol Plant **147**: 443–452

Hochberg U, Degu A, Toubiana D, Gendler T, Nikoloski Z, Rachmilevitch S, Fait A (2013b) Metabolite profiling and network analysis reveal coordinated changes in grapevine water stress response. BMC Plant Biol **13**: 184

Hochberg U, Degu A, Cramer GR, Rachmilevitch S, Fait A (2015) Cultivar specific metabolic changes in grapevines berry skins in relation to deficit irrigation and hydraulic behavior. Plant Physiol Biochem **88**: 42–52

Höll J, Vannozzi A, Czemmel S, D'Onofrio C, Walker AR, Rausch T, Lucchin M, Boss PK, Dry IB, Bogs J (2013) The R2R3-MYB transcription factors MYB14 and MYB15 regulate stilbene biosynthesis in *Vitis vinifera*. Plant Cell **25**: 4135–4149

Jaillon O, Aury J-M, Noel B, Policriti A, Clepet C, Casagrande A, Choisne N, Aubourg S, Vitulo N, Jubin C, et al (2007) The grapevine genome sequence suggests ancestral hexaploidization in major angiosperm phyla. Nature **449**: 463–467

Jakoby M, Weisshaar B, Dröge-Laser W, Vicente-Carbajosa J, Tiedemann J, Kroj T, Parcy F (2002) bZIP transcription factors in *Arabidopsis*. Trends Plant Sci **7**: 106–111

Jeong H, Mason SP, Barabási A-L, Oltvai ZN (2001) Lethality and centrality in protein networks. Nature **411**: 41–42

Kalua CM, Boss PK (2009) Evolution of volatile compounds during the development of Cabernet Sauvignon grapes (*Vitis vinifera* L.). J Agric Food Chem **57**: 3818–3830

Kaminaka H, Näke C, Epple P, Dittgen J, Schütze K, Chaban C, Holt BF, Merkle T, Schäfer E, Harter K, et al (2006) bZIP10-LSD1 antagonism modulates basal defense and cell death in *Arabidopsis* following infection. EMBO J **25**: 4400–4411

Kang J, Choi H, IM M, Kim SY (2002) *Arabidopsis* basic leucine zipper proteins that mediate stress-responsive abscisic acid signaling. Plant Cell **14**: 343–357

Khater F, Fournand D, Vialet S, Meudec E, Cheynier V, Terrier N (2012) Identification and functional characterization of cDNAs coding for hydroxybenzoate/hydroxycinnamate glucosyltransferases co-expressed with genes related to proanthocyanidin biosynthesis. J Exp Bot **63**: 1201–1214

Langfelder P, Horvath S (2008) WGCNA: an R package for weighted correlation network analysis. BMC Bioinformatics **9**: 559

Langfelder P, Zhang B, Horvath S (2008) Defining clusters from a hierarchical cluster tree: the Dynamic Tree Cut package for R. Bioinformatics **24**: 719–720

Lisec J, Schauer N, Kopka J, Willmitzer L, Fernie AR (2006) Gas chromatography mass spectrometry–based metabolite profiling in plants. Nat Protoc **1**: 387–396

Liu J, Chen N, Chen F, Cai B, Santo SD, Tornielli GB, Pezzotti M, Cheng Z-M (Max) (2014) Genome-wide analysis and expression profile of the bZIP transcription factor gene family in grapevine (*Vitis vinifera*). BMC Genomics **15**: 1–18

Love MI, Huber W, Anders S (2014) Moderated estimation of fold change and dispersion for RNA-seq data with DESeq2. Genome Biol **15**: 550

Lovisolo C, Perrone I, Carra A, Ferrandino A, Flexas J, Medrano H, Schubert A (2010) Drought-induced changes in development and function of grapevine (Vitis spp.) organs and in their hydraulic and non-hydraulic interactions at the whole-plant level: a physiological and molecular update. Funct Plant Biol **37**: 98–116

Ma C, Wang X (2012) Application of the gini correlation coefficient to infer regulatory relationships in transcriptome analysis. Plant Physiol **160**: 192–203

Maere S, Heymans K, Kuiper M (2005) BiNGO: a Cytoscape plugin to assess overrepresentation of Gene Ontology categories in Biological Networks. Bioinformatics **21**: 3448–3449

Martin DM, Aubourg S, Schouwey MB, Daviet L, Schalk M, Toub O, Lund ST, Bohlmann J (2010) Functional annotation, genome organization and phylogeny of the grapevine (*Vitis vinifera*) terpene synthase gene family based on genome assembly, flcdna cloning, and enzyme assays. BMC Plant Biol **10**: 226

Maruyama K, Urano K, Yoshiwara K, Morishita Y, Sakurai N, Suzuki H, Kojima M, Sakakibara H, Shibata D, Saito K, et al (2014) Integrated analysis of the effects of cold and dehydration on rice metabolites, phytohormones, and gene transcripts. Plant Physiol **164**: 1759–1771

Mattivi F, Guzzon R, Vrhovsek U, Stefanini M, Velasco R (2006) Metabolite profiling of grape: flavonols and anthocyanins. J Agric Food Chem **54**: 7692–7702

Mazza G, Fukumoto L, Delaquis P, Girard B, Ewert B (1999) Anthocyanins, phenolics, and color of Cabernet Franc, Merlot, and Pinot Noir wines from British Columbia. J Agric Food Chem **47**: 4009–4017

Naithani S, Raja R, Waddell EN, Elser J, Gouthu S, Deluc LG, Jaiswal P (2014) VitisCyc: a metabolic pathway knowledgebase for grapevine (*Vitis vinifera*). Front Plant Sci. doi: 10.3389/fpls.2014.00644

Olsson A, Engström P, Söderman E (2004) The homeobox genes ATHB12 and ATHB7encode potential regulators of growth in response to water deficit in Arabidopsis. Plant Mol Biol **55**: 663–677

Ono E, Homma Y, Horikawa M, Kunikane-Doi S, Imai H, Takahashi S, Kawai Y, Ishiguro M, Fukui Y, Nakayama T (2010) Functional differentiation of the glycosyltransferases that contribute to the chemical diversity of bioactive flavonol glycosides in grapevines (vitis vinifera). Plant Cell **22**: 2856–2871

Opitz N, Marcon C, Paschold A, Malik WA, Lithio A, Brandt R, Piepho H-P, Nettleton D, Hochholdinger F (2015) Extensive tissue-specific transcriptomic plasticity in maize primary roots upon water deficit. J Exp Bot erv453

Pérez-Díaz R, Ryngajllo M, Pérez-Díaz J, Peña-Cortés H, Casaretto JA, González-Villanueva E, Ruiz-Lara S (2014) VvMATE1 and VvMATE2 encode putative proanthocyanidin transporters expressed during berry development in *Vitis vinifera* L. Plant Cell Rep **33**: 1147–1159

Rinaldo A, Cavallini E, Jia Y, Moss SMA, McDavid DAJ, Hooper LC, Robinson SP, Tornielli GB, Zenoni S, Ford CM, et al (2015) A grapevine anthocyanin acyltransferase, transcriptionally regulated by VvMYBA, can produce most acylated anthocyanins present in grape skins. Plant Physiol pp.01255.2015

Ripoll J, Urban L, Staudt M, Lopez-Lauri F, Bidel LPR, Bertin N (2014) Water shortage and quality of fleshy fruits—making the most of the unavoidable. J Exp Bot **65**: 4097–4117

Ripoll J, Urban L, Brunel B, Bertin N (2016) Water deficit effects on tomato quality depend on fruit developmental stage and genotype. J Plant Physiol **190**: 26–35

Saito K, Hirai MY, Yonekura-Sakakibara K (2008) Decoding genes with coexpression networks and metabolomics – "majority report by precogs." Trends Plant Sci **13**: 36–43

Sakuma Y, Liu Q, Dubouzet JG, Abe H, Shinozaki K, Yamaguchi-Shinozaki K (2002) DNA-Binding specificity of the ERF/AP2 domain of *Arabidopsis* DREBs, transcription factors involved in dehydration- and cold-inducible gene expression. Biochem Biophys Res Commun **290**: 998–1009

Schwab W, Davidovich-Rikanati R, Lewinsohn E (2008) Biosynthesis of plant-derived flavor compounds. Plant J **54**: 712–732

Shannon P, Markiel A, Ozier O, Baliga NS, Wang JT, Ramage D, Amin N, Schwikowski B, Ideker T (2003) Cytoscape: a software environment for integrated models of biomolecular interaction networks. Genome Res **13**: 2498–2504

Shen J, Tieman D, Jones JB, Taylor MG, Schmelz E, Huffaker A, Bies D, Chen K, Klee HJ (2014) A 13-lipoxygenase, TomloxC, is essential for synthesis of C5 flavour volatiles in tomato. J Exp Bot **65**: 419–428

Shinozaki K, Yamaguchi-Shinozaki K (2007) Gene networks involved in drought stress response and tolerance. J Exp Bot **58**: 221–227

Singh D, Laxmi A (2015) Transcriptional regulation of drought response: a tortuous network of transcriptional factors. Front Plant Sci. doi: 10.3389/fpls.2015.00895

Song J, Shellie KC, Wang H, Qian MC (2012) Influence of deficit irrigation and kaolin particle film on grape composition and volatile compounds in Merlot grape (*Vitis vinifera* L.). Food Chem **134**: 841–850

Strimmer K (2008) A unified approach to false discovery rate estimation. BMC Bioinformatics **9**: 303

Sweetman C, Deluc LG, Cramer GR, Ford CM, Soole KL (2009) Regulation of malate metabolism in grape berry and other developing fruits. Phytochemistry **70**: 1329–1344

Taji T, Ohsumi C, Iuchi S, Seki M, Kasuga M, Kobayashi M, Yamaguchi-Shinozaki K, Shinozaki K (2002) Important roles of drought- and cold-inducible genes for galactinol synthase in stress tolerance in Arabidopsis thaliana. Plant J **29**: 417–426

Toubiana D, Fernie AR, Nikoloski Z, Fait A (2013) Network analysis: tackling complex data to study plant metabolism. Trends Biotechnol **31**: 29–36

Trapnell C, Roberts A, Goff L, Pertea G, Kim D, Kelley DR, Pimentel H, Salzberg SL, Rinn JL, Pachter L (2012) Differential gene and transcript expression analysis of RNA-seq experiments with TopHat and Cufflinks. Nat Protoc **7**: 562–578

Urano K, Maruyama K, Ogata Y, Morishita Y, Takeda M, Sakurai N, Suzuki H, Saito K, Shibata D, Kobayashi M, et al (2009) Characterization of the ABA-regulated global responses to dehydration in Arabidopsis by metabolomics. Plant J **57**: 1065–1078

Valdés AE, Övernäs E, Johansson H, Rada-Iglesias A, Engström P (2012) The homeodomain-leucine zipper (HD-Zip) class I transcription factors ATHB7 and ATHB12 modulate abscisic acid signalling by regulating protein phosphatase 2C and abscisic acid receptor gene activities. Plant Mol Biol **80**: 405–418

Vannozzi A, Dry IB, Fasoli M, Zenoni S, Lucchin M (2012) Genome-wide analysis of the grapevine stilbene synthase multigenic family: genomic organization and expression profiles upon biotic and abiotic stresses. BMC Plant Biol **12**: 130

Vendruscolo ECG, Schuster I, Pileggi M, Scapim CA, Molinari HBC, Marur CJ, Vieira LGE (2007) Stress-induced synthesis of proline confers tolerance to water deficit in transgenic wheat. J Plant Physiol **164**: 1367–1376

Vrhovsek U, Masuero D, Gasperotti M, Franceschi P, Caputi L, Viola R, Mattivi F (2012) A versatile targeted metabolomics method for the rapid quantification of multiple classes of phenolics in fruits and beverages. J Agric Food Chem **60**: 8831–8840

Walker AR, Lee E, Bogs J, McDavid DAJ, Thomas MR, Robinson SP (2007) White grapes arose through the mutation of two similar and adjacent regulatory genes. Plant J **49**: 772–785

Wehrens R, Carvalho E, Masuero D, Juan A de, Martens S (2013) High-throughput carotenoid profiling using multivariate curve resolution. Anal Bioanal Chem **405**: 5075–5086

Weltmeier F, Ehlert A, Mayer CS, Dietrich K, Wang X, Schütze K, Alonso R, Harter K, Vicente-Carbajosa J, Dröge-Laser W (2006) Combinatorial control of Arabidopsis proline dehydrogenase transcription by specific heterodimerisation of bZIP transcription factors. EMBO J **25**: 3133–3143

Yamada M, Morishita H, Urano K, Shiozaki N, Yamaguchi-Shinozaki K, Shinozaki K, Yoshiba Y (2005) Effects of free proline accumulation in petunias under drought stress. J Exp Bot **56**: 1975–1981

Yamaguchi-Shinozaki K, Shinozaki K (2006) Transcriptional regulatory networks in cellular responses and tolerance to dehydration and cold stresses. Annu Rev Plant Biol **57**: 781–803

Yilmaz A, Mejia-Guerra MK, Kurz K, Liang X, Welch L, Grotewold E (2011) AGRIS: the Arabidopsis Gene Regulatory Information Server, an update. Nucleic Acids Res **39**: D1118–D1122

Yoshiba Y, Kiyosue T, Katagiri T, Ueda H, Mizoguchi T, Yamaguchi-Shinozaki K, Wada K, Harada Y, Shinozaki K (1995) Correlation between the induction of a gene for Δ1-pyrroline-5-carboxylate synthetase and the accumulation of proline in Arabidopsis thaliana under osmotic stress. Plant J **7**: 751–760

Yoshida T, Mogami J, Yamaguchi-Shinozaki K (2014) ABA-dependent and ABA-independent signaling in response to osmotic stress in plants. Curr Opin Plant Biol **21**: 133–139

Young P, Eyeghe-Bickong HA, Plessis K du, Alexandersson E, Jacobson DA, Coetzee ZA, Deloire A, Vivier MA (2015) Grapevine plasticity in response to an altered microclimate: Sauvignon Blanc modulates specific metabolites in response to increased berry exposure. Plant Physiol pp.01775.2015

Young PR, Lashbrooke JG, Alexandersson E, Jacobson D, Moser C, Velasco R, Vivier MA (2012) The genes and enzymes of the carotenoid metabolic pathway in Vitis vinifera L. BMC Genomics **13**: 243

Zhang J-Y, Cruz de Carvalho MH, Torres-Jerez I, Kang Y, Allen SN, Huhman DV, Tang Y, Murray J, Sumner LW, Udvardi MK (2014) Global reprogramming of transcription and metabolism in *Medicago truncatula* during progressive drought and after rewatering. Plant Cell Environ **37**: 2553–2576

Supplementary Data

Table S1*. Summary of differentially expressed genes (P<0.05) and associated information (12x V1 identification number, predicted annotation, fold change values, log_2 fold change and adjusted P value) identified between C and D at 26 (a), 53 (b), 67 (c), 81 (d), and 106 (e) days after anthesis (DAA). (f) Plant gene ontology (GO) slim biological process categories enriched (P<0.05) within significantly up- and down-regulated genes at 26, 53, 67, 81, and 106 DAA between C and D are represented in a heatmap where red and blue colors denote the overrepresented categories in the up- or down regulated genes, respectively. (g) Summary of the transcription factors differentially expressed genes (P<0.05) and associated information (12x V1 identification number, predicted annotation, TF family name, log_2FC at 26, 53, 67, 81 and 106 DAA and their respectively adjusted p-value). Blue and red colors denote lower and higher concentration in D, respectively. Cell colored in green denote significance in that specific developmental stage. (h) Weighted correlation gene co-expression network analysis (WGCNA). In column b-f, log_2FC (D/C) of the differently expressed genes at 26, 53, 67, 81, and 106 (dataset1) with blue and red cell colors indicating up- or down-regulation; in column g-k, variance stabilized transformed (VST) counts at 26, 53, 67, 81, and 106 (dataset2) with blue and green colors indicating the lower or higher level of expression. Modules, sub-modules, functional annotation, network, and bin information are reported for each gene. (i) Correlation values (PCC, type of network, statistical significance of PCC, and degree of correlation) for the gene-gene and gene-metabolite network. (h). Detailed information on the *cis*-regulatory elements enrichment analysis among the "yellow" module, sub-modules 2, 3, and 5.

***** Table S1 is the separate excel file

Table S2. RNA sequencing analysis metrics. From 2012 samples, transcriptome analyses were performed in C and D berries at five selected berry developmental stages (26 DAA and 53 DAA, before veraison; 67 DAA, beginning of ripening; 81 and 106 DAA, during ripening) using an Illumina HiSeq platform.

Sampling (DAA)	Treatment	Biol. Rep.	Sequenced Reads	Trimmed and Filtered Reads	Mapped Reads	Unique Reads	Expressed Genes
26	C	1	32,282,090	27,285,970	25,243,216	24,173,521	22,949
26	C	2	23,218,489	22,903,285	20,935,341	20,020,535	23,576
26	C	3	18,987,430	18,756,732	17,497,629	16,763,590	23,214
26	D	1	38,030,560	32,117,022	29,449,144	28,148,361	22,829
26	D	2	21,823,539	21,554,999	20,080,109	19,207,041	23,298
26	D	3	26,975,517	26,651,368	24,776,353	23,663,710	23,654
53	C	1	48,502,153	41,329,184	36,962,611	35,181,638	23,334
53	C	2	32,683,299	31,833,552	26,901,141	25,540,691	23,021
53	C	3	33,287,117	32,513,137	28,120,305	26,644,501	23,155
53	D	1	35,861,125	34,996,173	30,361,145	28,905,599	23,243
53	D	2	32,371,631	31,790,674	28,156,175	26,746,733	23,156
53	D	3	31,895,415	31,177,159	27,397,806	26,058,126	23,411
67	C	1	29,986,521	29,562,710	27,225,348	25,908,529	22,098
67	C	2	29,979,931	29,554,286	27,175,999	25,813,402	22,140
67	C	3	26,456,360	26,061,866	24,057,180	22,879,874	22,180
67	D	1	28,029,734	27,594,638	25,227,554	23,570,934	21,530
67	D	2	31,262,847	30,798,680	28,119,560	26,615,329	22,069
67	D	3	30,934,072	30,494,505	28,192,068	26,644,349	21,963

Table S2. (continued)

Sampling (DAA)	Treatment	Biol. Rep.	Sequenced Reads	Trimmed and Filtered Reads	Mapped Reads	Unique Reads	Expressed Genes
81	C	1	56,213,525	44,149,321	41,653,412	39,672,979	22,813
81	C	2	41,388,889	40,728,237	37,824,937	36,009,744	22,715
81	C	3	20,751,950	20,405,881	18,550,887	17,634,540	21,760
81	D	1	41,321,398	40,656,157	37,710,401	35,847,981	22,603
81	D	2	37,894,910	37,305,935	34,633,903	32,943,905	22,615
81	D	3	28,343,487	27,893,814	25,611,214	24,362,357	22,209
106	C	1	24,799,483	24,431,124	22,611,345	21,613,028	21,964
106	C	2	44,340,639	43,707,436	40,246,983	38,392,957	22,752
106	C	3	33,374,833	29,502,167	27,184,432	25,977,126	21,066
106	D	1	29,059,685	28,620,355	26,418,924	25,190,721	21,961
106	D	2	32,545,793	32,087,904	29,760,625	28,365,623	22,352
106	D	3	40,625,594	40,038,315	36,845,815	35,126,958	22,878

Table S3. List of compounds identified in this study using GC-MS, UHPLC-MS/MS, HPLC-DAD, and HS-SPME-GC-MS platforms.

Compound	Chemical Class	Analytical Platform
Leucine	Amino acids	GC-MS
Valine	Amino acids	GC-MS
Isoleucine	Amino acids	GC-MS
Serine	Amino acids	GC-MS
Ethanolamine	Amino acids	GC-MS
Alanine	Amino acids	GC-MS
Threonine	Amino acids	GC-MS
Proline	Amino acids	GC-MS
Putrescine	Polyamine	GC-MS
Glycerate	Organic Acids	GC-MS
Lactate	Organic Acids	GC-MS
Glycolate	Organic Acids	GC-MS
Quinate	Organic Acids	GC-MS
Shikimate	Organic Acids	GC-MS
Citrate	Organic Acids	GC-MS
Succinate	Organic Acids	GC-MS
Fumarate	Organic Acids	GC-MS
Maleate	Organic Acids	GC-MS
Malate	Organic Acids	GC-MS
Threonate	Organic Acids	GC-MS
Tartrate	Organic Acids	GC-MS
Sucrose	Sugars	GC-MS
Glucose	Sugars	GC-MS
Fructose	Sugars	GC-MS

Table S3. (continued)

Compound	Chemical Class	Analytical Platform
Glucose-6-phosphate	Sugars	GC-MS
Fructose-6-phosphate	Sugars	GC-MS
Myo -Inositol	Polyols	GC-MS
Raffinose	Polyols	GC-MS
Galactinol	Polyols	GC-MS
Arabitol	Polyols	GC-MS
Erythritol	Polyols	GC-MS
Threitol	Polyols	GC-MS
Glycerol	Polyols	GC-MS
Gallic acid	Benzoic acids	UHPLC-MS/MS
Ellagic Acid	Benzoic acids	UHPLC-MS/MS
trans -Caftaric acid	Cinnamic acids	UHPLC-MS/MS
trans -Coutaric acid	Cinnamic acids	UHPLC-MS/MS
trans -Fertaric acid	Cinnamic acids	UHPLC-MS/MS
trans -Resveratrol	Stilbenes	UHPLC-MS/MS
cis -Piceid	Stilbenes	UHPLC-MS/MS
trans -Piceid	Stilbenes	UHPLC-MS/MS
Piceatannol	Stilbenes	UHPLC-MS/MS
Astringin	Stilbenes	UHPLC-MS/MS
Pallidol	Stilbenes	UHPLC-MS/MS
Isorhapontin	Stilbenes	UHPLC-MS/MS
Phlorizin	Dihydrochalcones	UHPLC-MS/MS
(+) -Catechin	Flavan-3-ols	UHPLC-MS/MS
(-) -Epicatechin	Flavan-3-ols	UHPLC-MS/MS
(-) -Epicatechin gallate	Flavan-3-ols	UHPLC-MS/MS
(+) -Gallocatechin	Flavan-3-ols	UHPLC-MS/MS
(-) -Epigallocatechin	Flavan-3-ols	UHPLC-MS/MS
(-) -Epigallocatechin gallate	Flavan-3-ols	UHPLC-MS/MS
Procyanidin B1	Proanthocyanidins	UHPLC-MS/MS
Procyanidin B2+B4	Proanthocyanidins	UHPLC-MS/MS
Procyanidin B3	Proanthocyanidins	UHPLC-MS/MS
Quercetin-3-*O* -rutinoside	Flavonols	UHPLC-MS/MS
Isorhamnetin-3-*O* -rutinoside	Flavonols	UHPLC-MS/MS
Cyanidin-3-*O* -glucoside	Amino acids	HPLC-DAD
Peonidin-3-*O* -glucoside	Amino acids	HPLC-DAD
Delphinidin-3-*O* -glucoside	Amino acids	HPLC-DAD
Petunidin-3-*O* -glucoside	Amino acids	HPLC-DAD
Malvidin-3-*O* -glucoside	Amino acids	HPLC-DAD
Cyanidin-3-*O* -(6''-acetyl)-glucoside	Amino acids	HPLC-DAD
Peonidin-3-*O* -(6''-acetyl)-glucoside	Amino acids	HPLC-DAD
Delphinidin-3-*O* -(6''-acetyl)-glucoside	Amino acids	HPLC-DAD
Petunidin-3-*O* -(6''-acetyl)-glucoside	Amino acids	HPLC-DAD
Malvidin-3-*O* -(6''-acetyl)-glucoside	Amino acids	HPLC-DAD
Cyanidin-3-*O* -(6''-p-coumaroyl)-glucoside	Amino acids	HPLC-DAD
Peonindin-3-*O* -(6''-p-coumaroyl)-glucoside	Amino acids	HPLC-DAD

Table S3. (continued)

Compound	Chemical Class	Analytical Platform
Delphinidin-3-*O*-(6''-p-coumaroyl)-glucoside	Amino acids	HPLC-DAD
Petunidin-3-*O*-(6''-p-coumaroyl)-glucoside	Amino acids	HPLC-DAD
Malvidin-3-*O*-(6''-p-coumaroyl)-glucoside	Amino acids	HPLC-DAD
β-Carotene	Carotenoids	HPLC-DAD
Zeaxanthin	Carotenoids	HPLC-DAD
Antheraxanthin	Carotenoids	HPLC-DAD
Violaxanthin	Carotenoids	HPLC-DAD
9-*(Z)*-Neoxanthin	Carotenoids	HPLC-DAD
Lutein	Carotenoids	HPLC-DAD
Lutein, 5-6 epoxide	Carotenoids	HPLC-DAD
Hexanal	C6 Compounds	HS-SPME-GC-MS
(E)-2-Hexenal	C6 Compounds	HS-SPME-GC-MS
Hexanol	C6 Compounds	HS-SPME-GC-MS
3-Hexenol	C6 Compounds	HS-SPME-GC-MS
(E)-2-Pentenal	C5 Compounds	HS-SPME-GC-MS
1-Penten-3-ol	C5 Compounds	HS-SPME-GC-MS
Heptanal	C7 Compounds	HS-SPME-GC-MS
(E)-2-Heptenal	C7 Compounds	HS-SPME-GC-MS
Heptanol	C7 Compounds	HS-SPME-GC-MS
Octanol	C8 Compounds	HS-SPME-GC-MS
(E)-2-Octenal	C8 Compounds	HS-SPME-GC-MS
1-Octen-3-ol	C8 Compounds	HS-SPME-GC-MS
1-Octen-3-one	C8 Compounds	HS-SPME-GC-MS
Nonanal	C9 Compounds	HS-SPME-GC-MS
Nonanol	C9 Compounds	HS-SPME-GC-MS
Linalool	Terpenes	HS-SPME-GC-MS
Geraniol	Terpenes	HS-SPME-GC-MS
Hotrienol	Terpenes	HS-SPME-GC-MS
α-Terpineol	Terpenes	HS-SPME-GC-MS
β-Ionone	C13 Norisoprenoids	HS-SPME-GC-MS
β-Damascenone	C13 Norisoprenoids	HS-SPME-GC-MS

Figure S1. Trends of primary metabolites concentration in C and D berries during fruit development and ripening in 2011 (left hand panel) and 2012 (right hand panel).

Amino acids and Polyamine

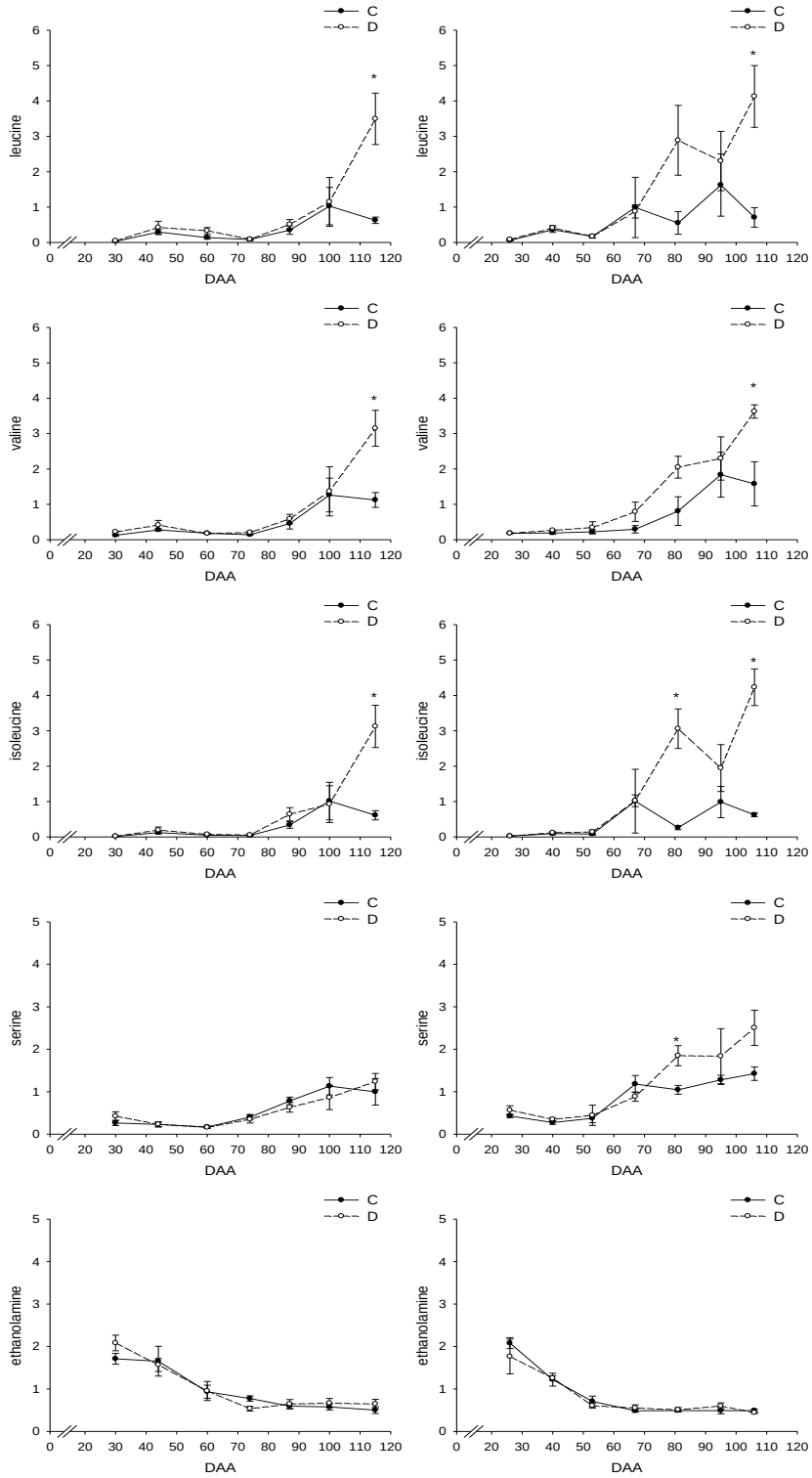

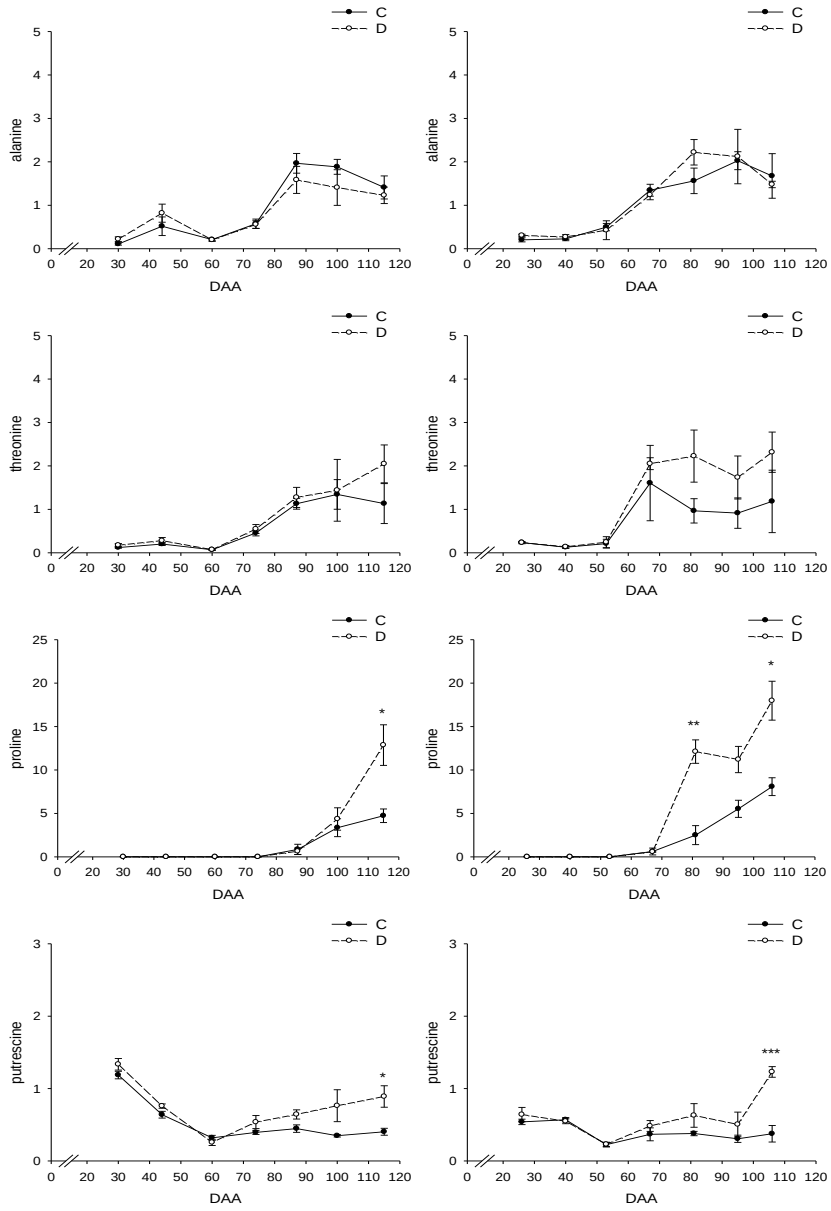

Organic Acids

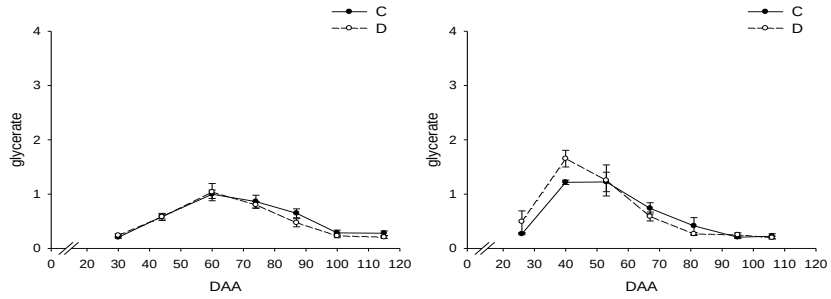

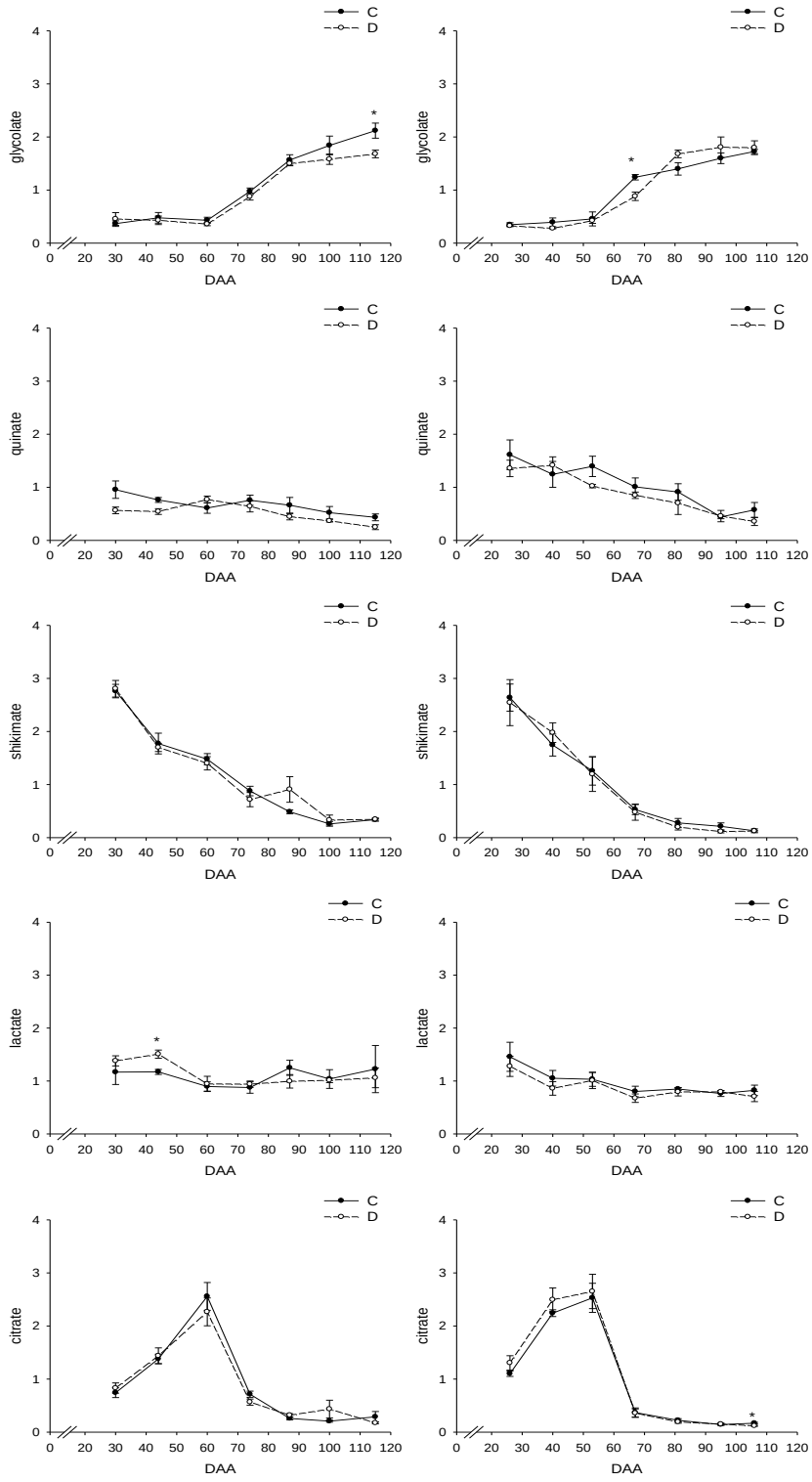
C
D
glycolate
quinate
shikimate
lactate
citrate
DAA
*

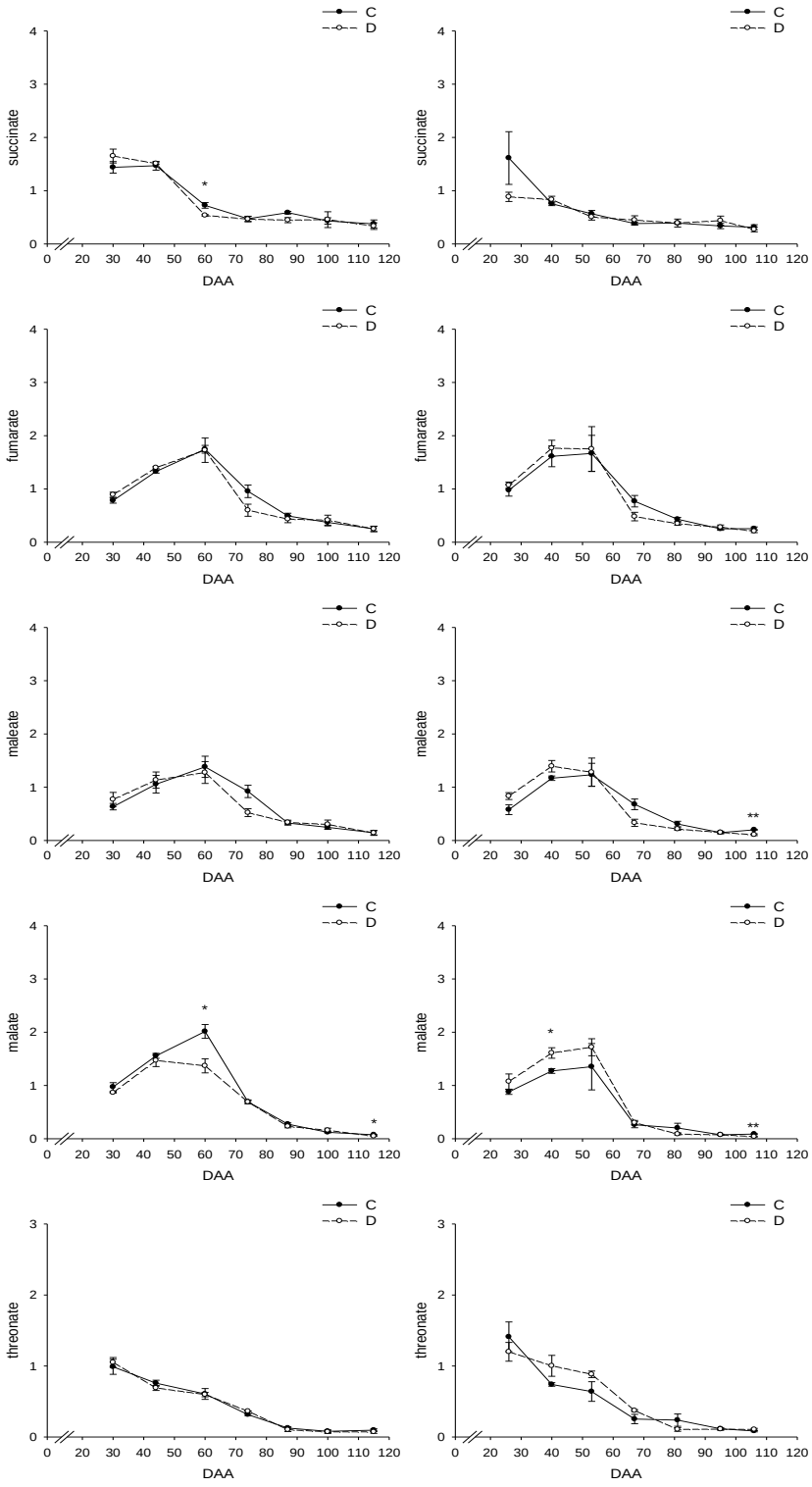
C
D
succinate
fumarate
maleate
malate
threonate
DAA
*
**

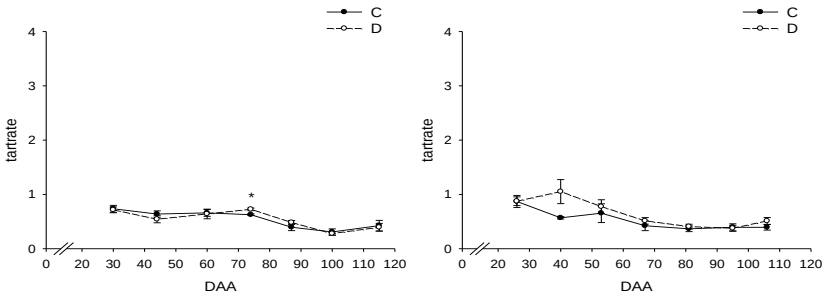

Sugars and Polyols

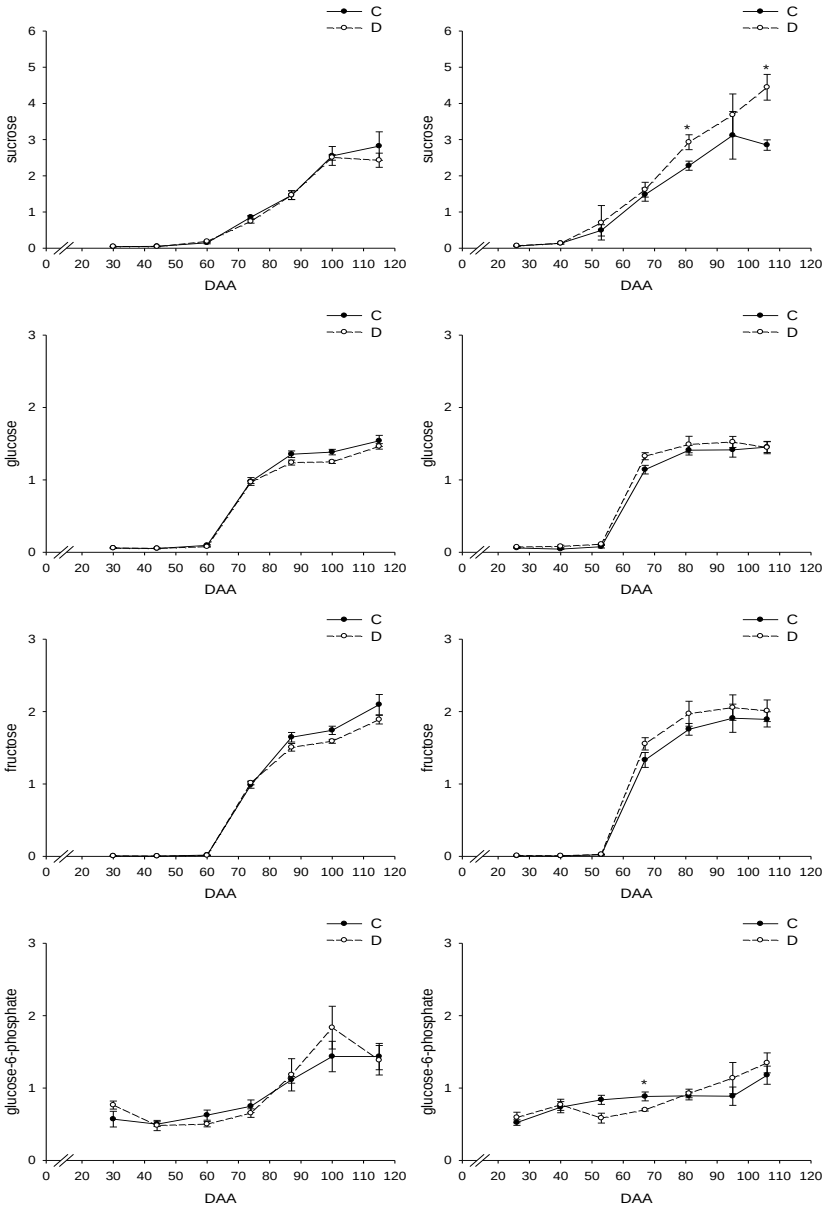

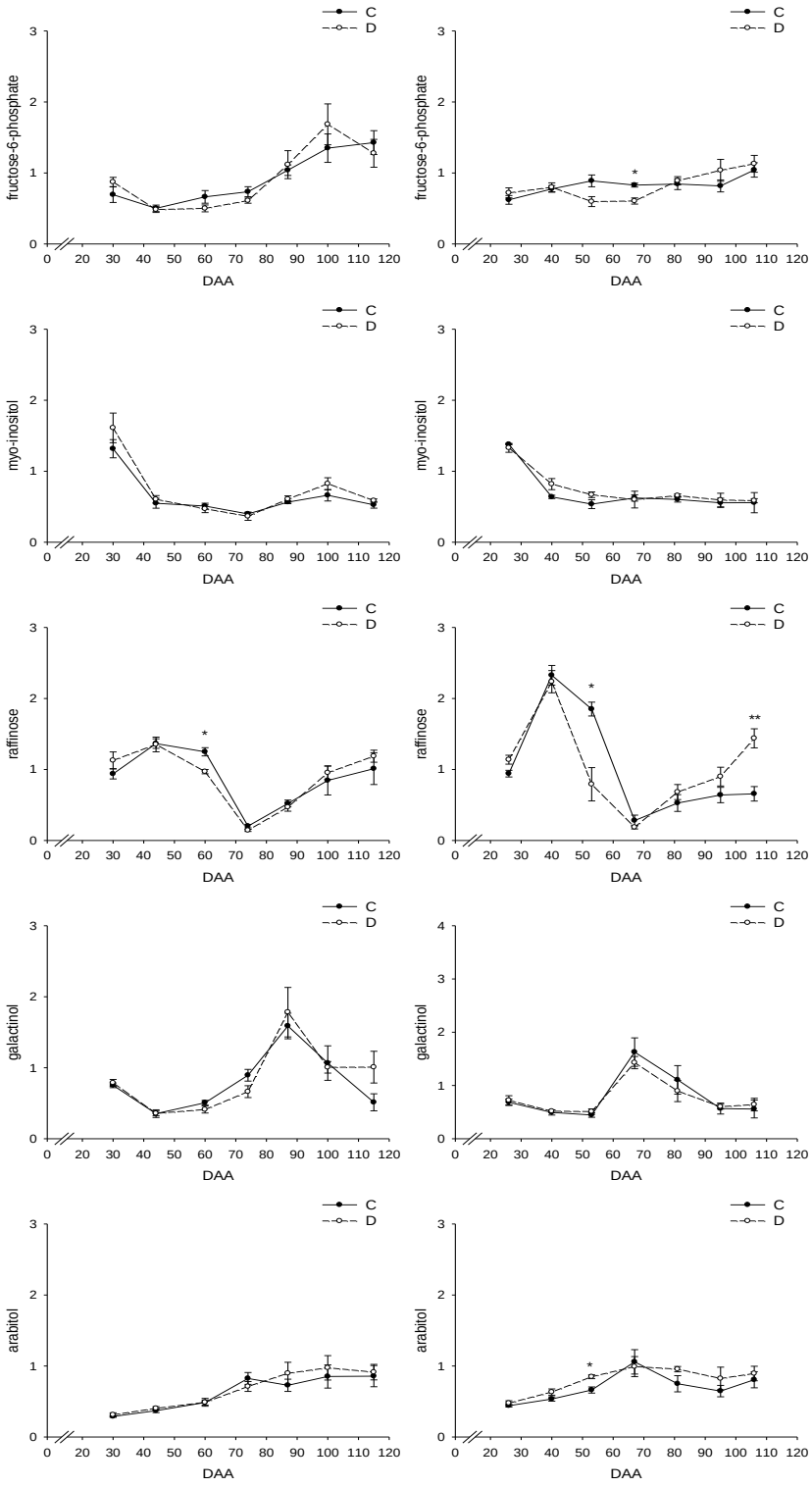
C
D
fructose-6-phosphate
myo-inositol
raffinose
galactinol
arabitol
DAA
*
**

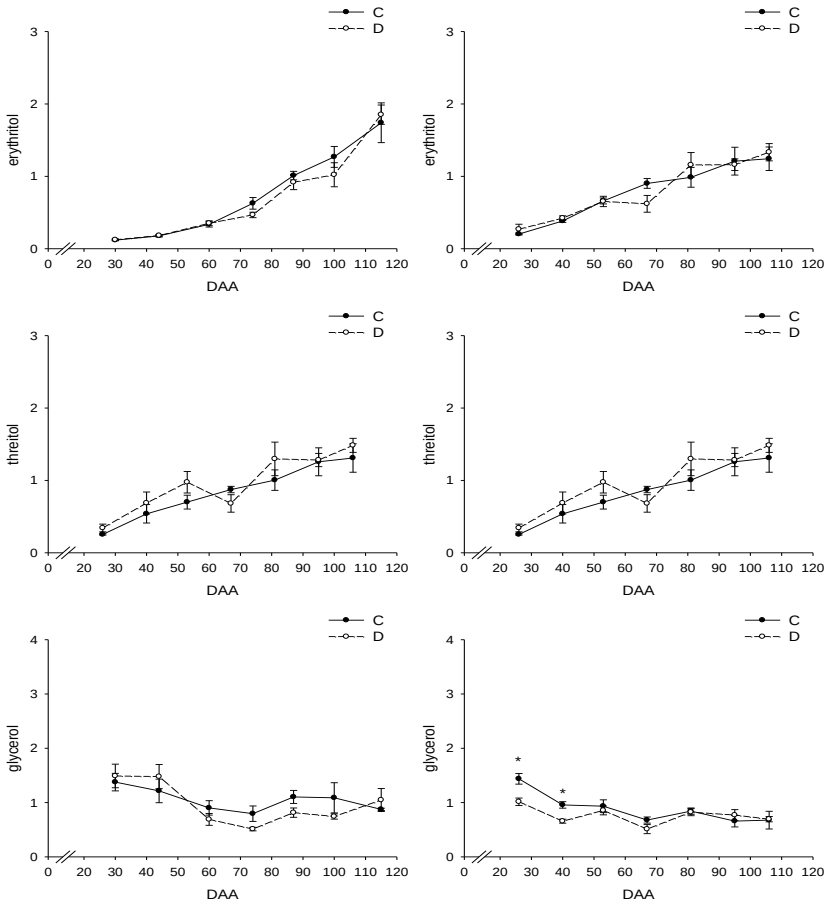
C
D
erythritol
threitol
glycerol
DAA
0
20
30
40
50
60
70
80
90
100
110
120
*

Figure S2. Trends of phenolic concentration in C and D berries during fruit development and ripening in 2011 (left hand panel) and 2012 (right hand panel). Data are expressed as mg/kg of fresh berries.

Benzoic and cinnamic acid

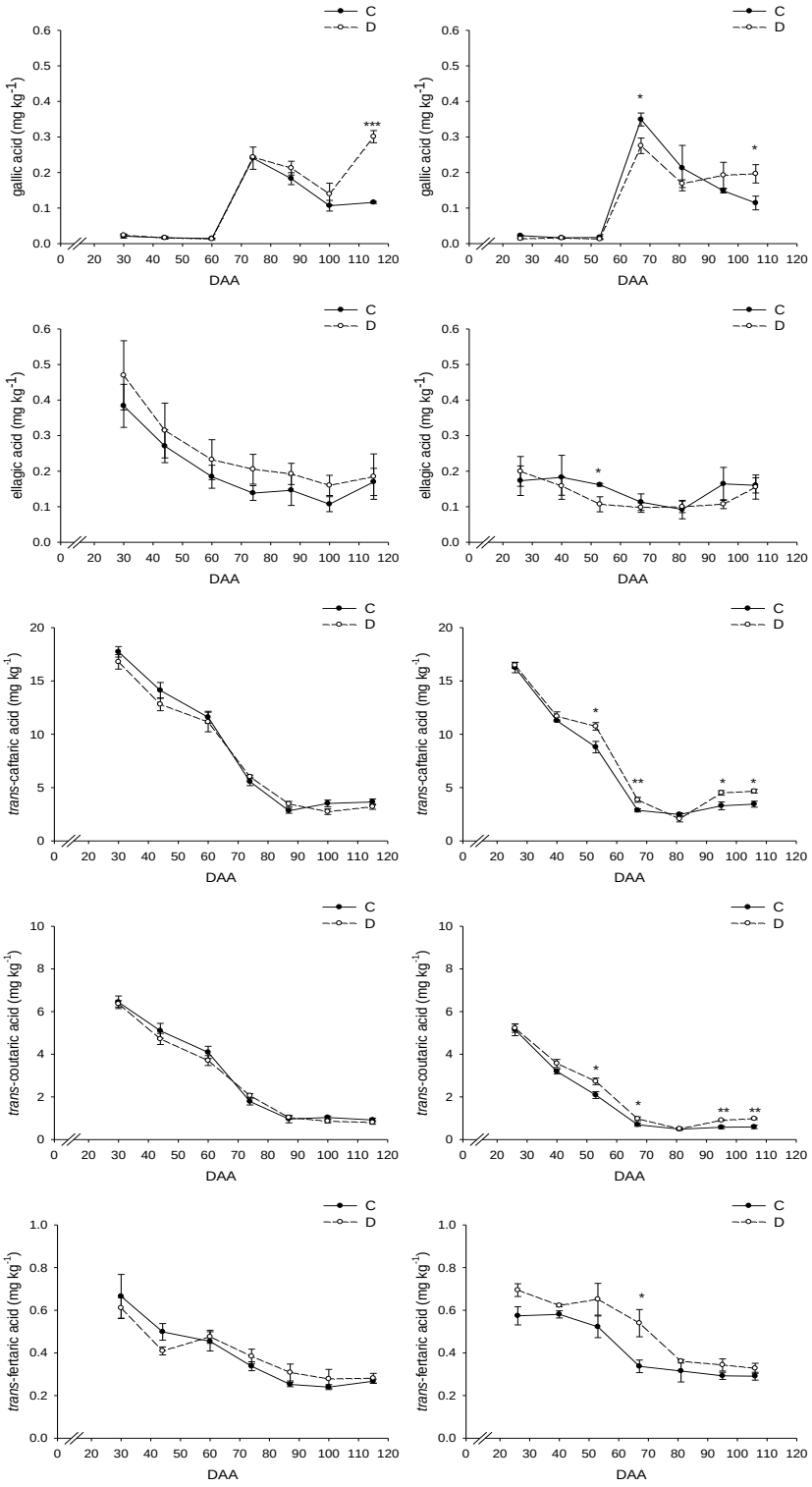

Stilbenoids

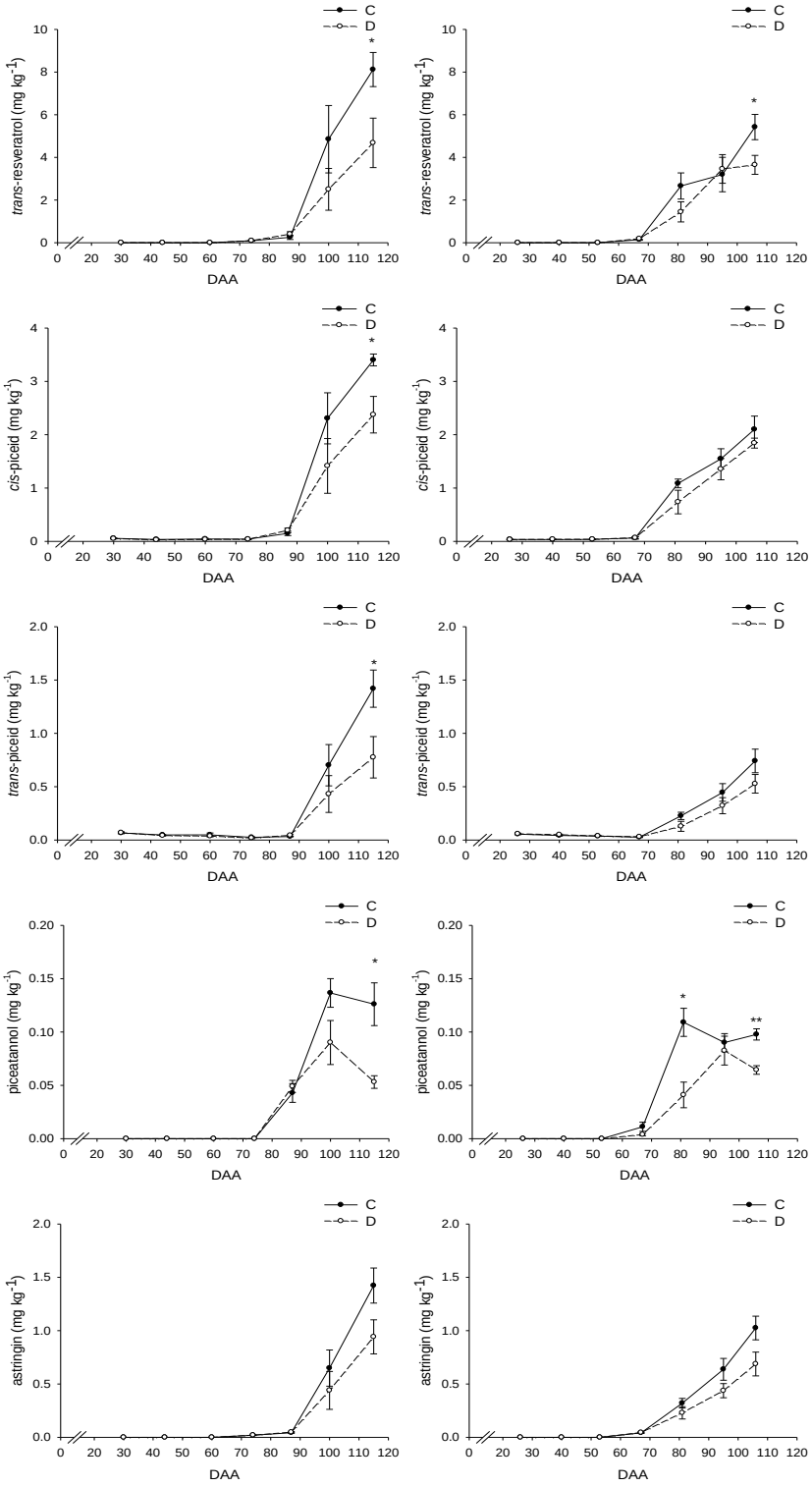

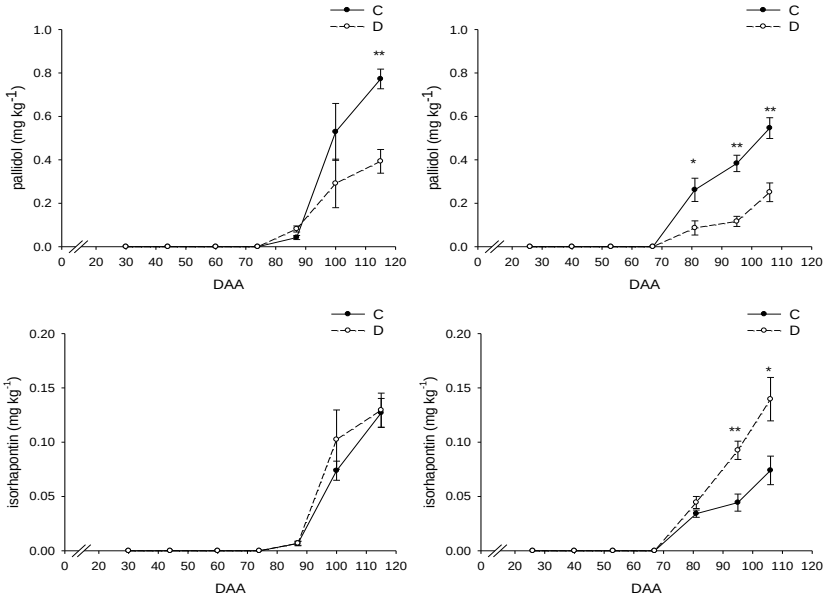

Dihydrochalcones

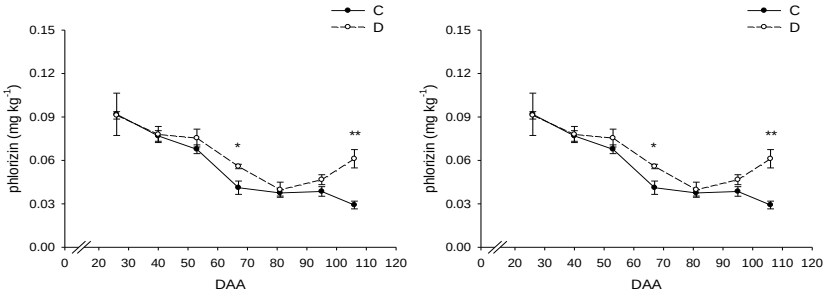

Flavan-3-ols

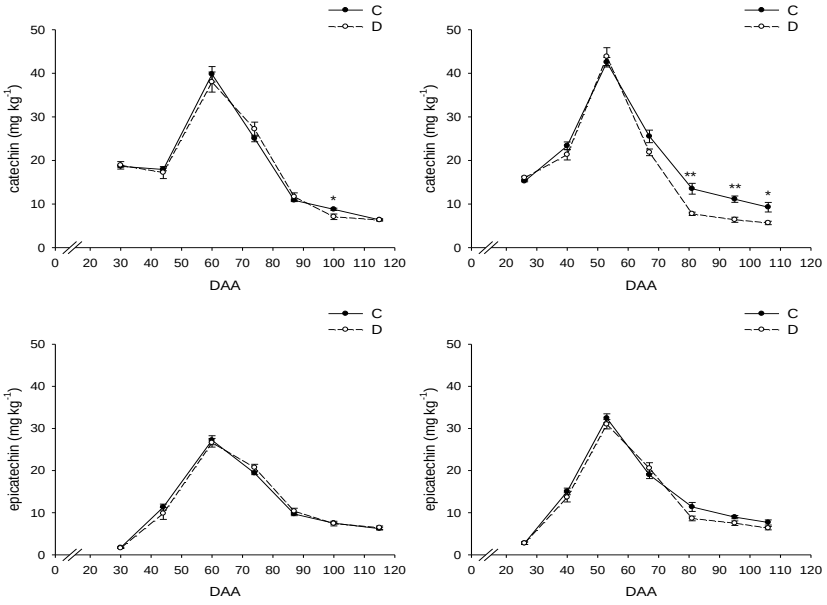

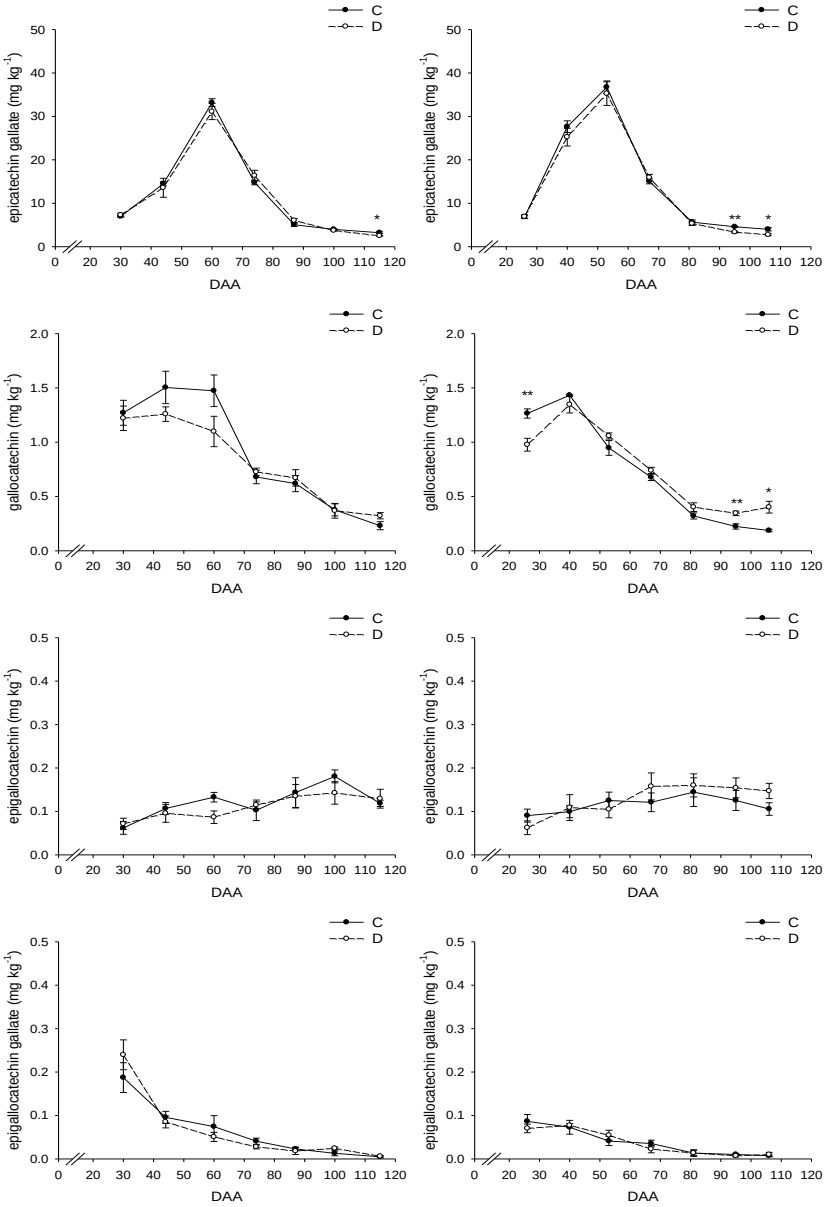

Proanthocyanidins

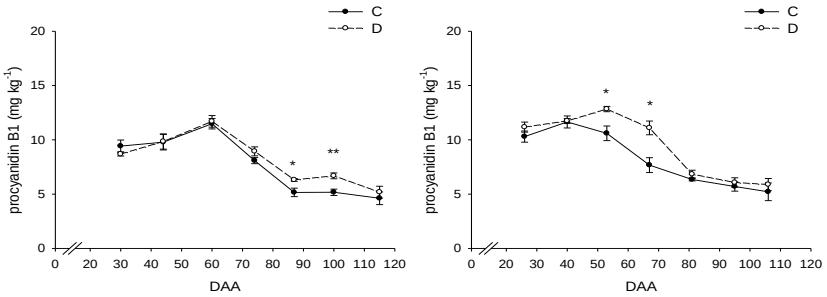

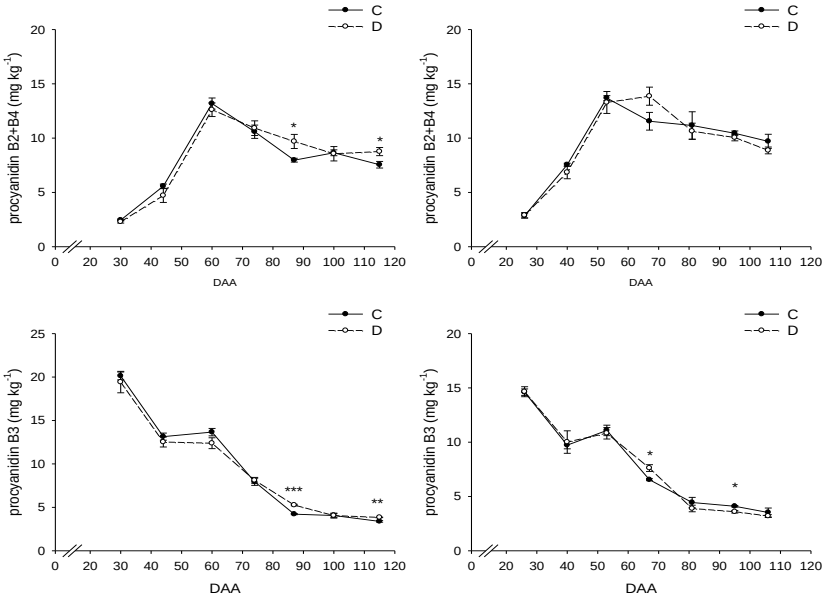

Flavonols

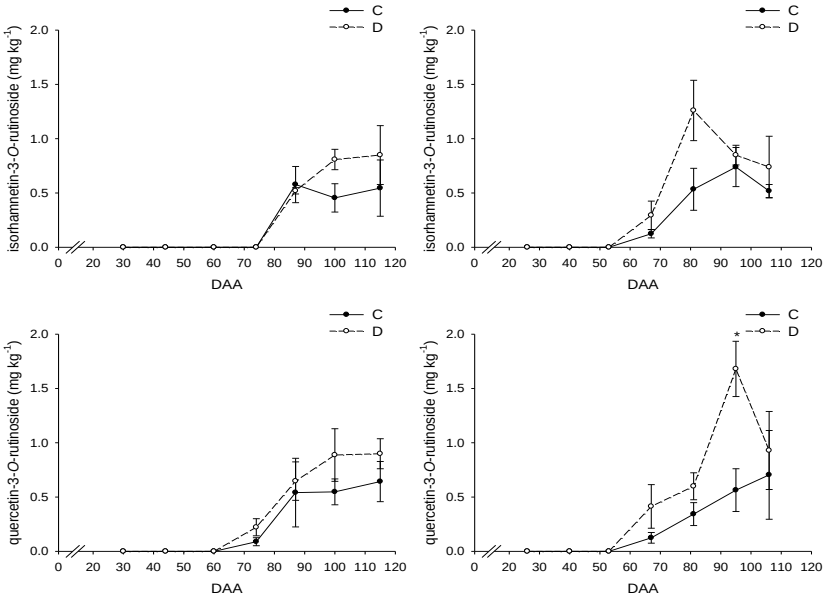

Anthocyanins

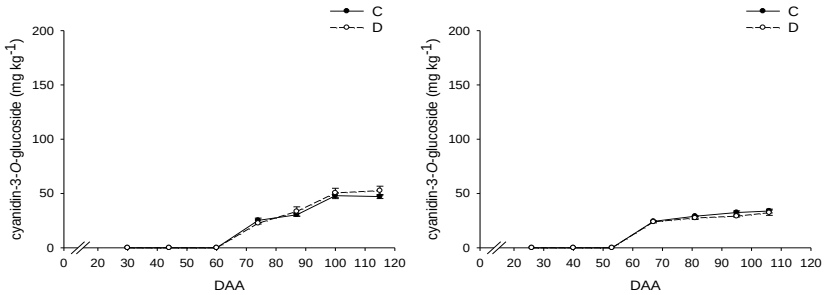

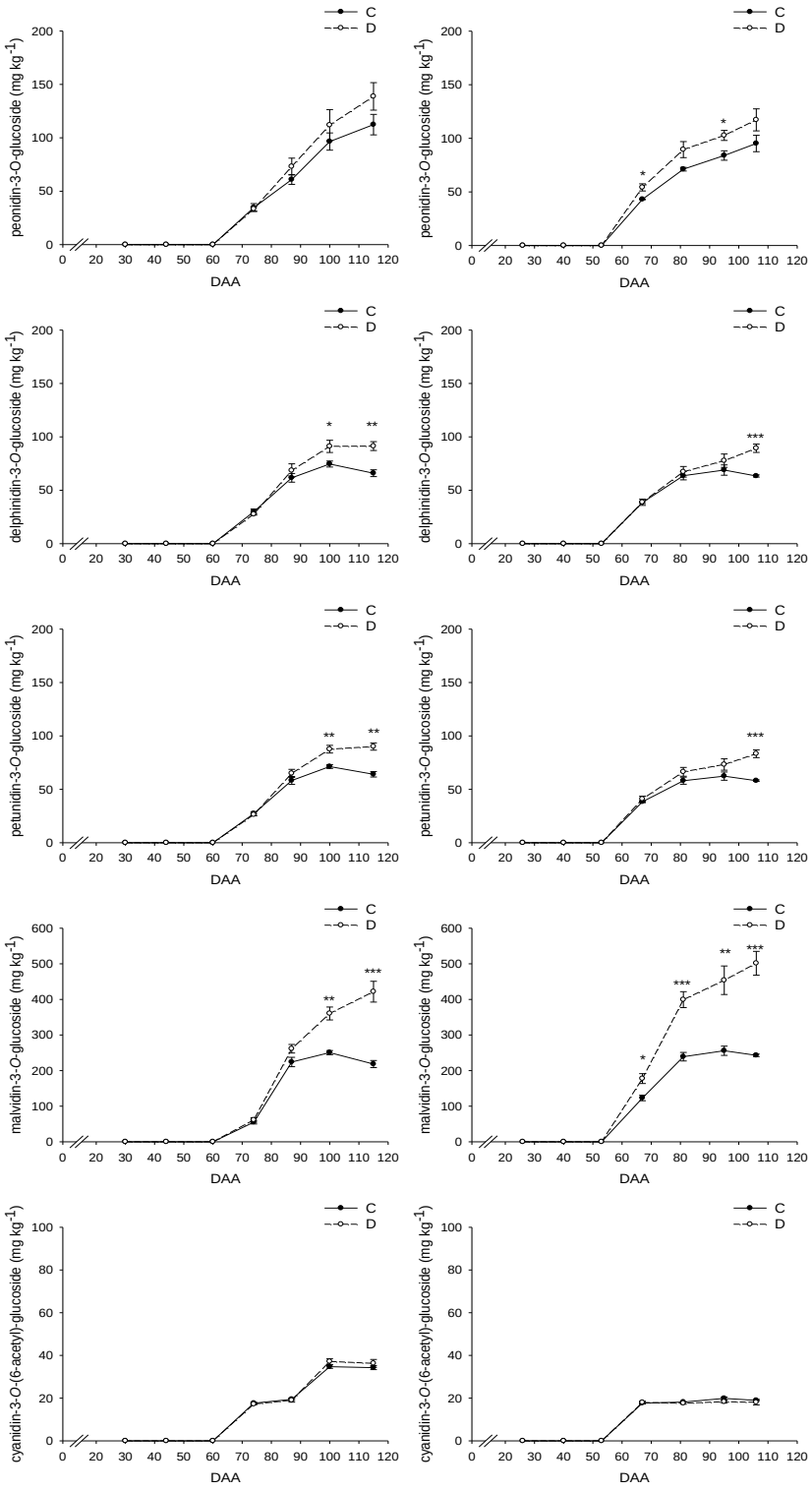
C
D
peonidin-3-O-glucoside (mg kg-1)
delphinidin-3-O-glucoside (mg kg-1)
petunidin-3-O-glucoside (mg kg-1)
malvidin-3-O-glucoside (mg kg-1)
cyanidin-3-O-(6-acetyl)-glucoside (mg kg-1)
DAA

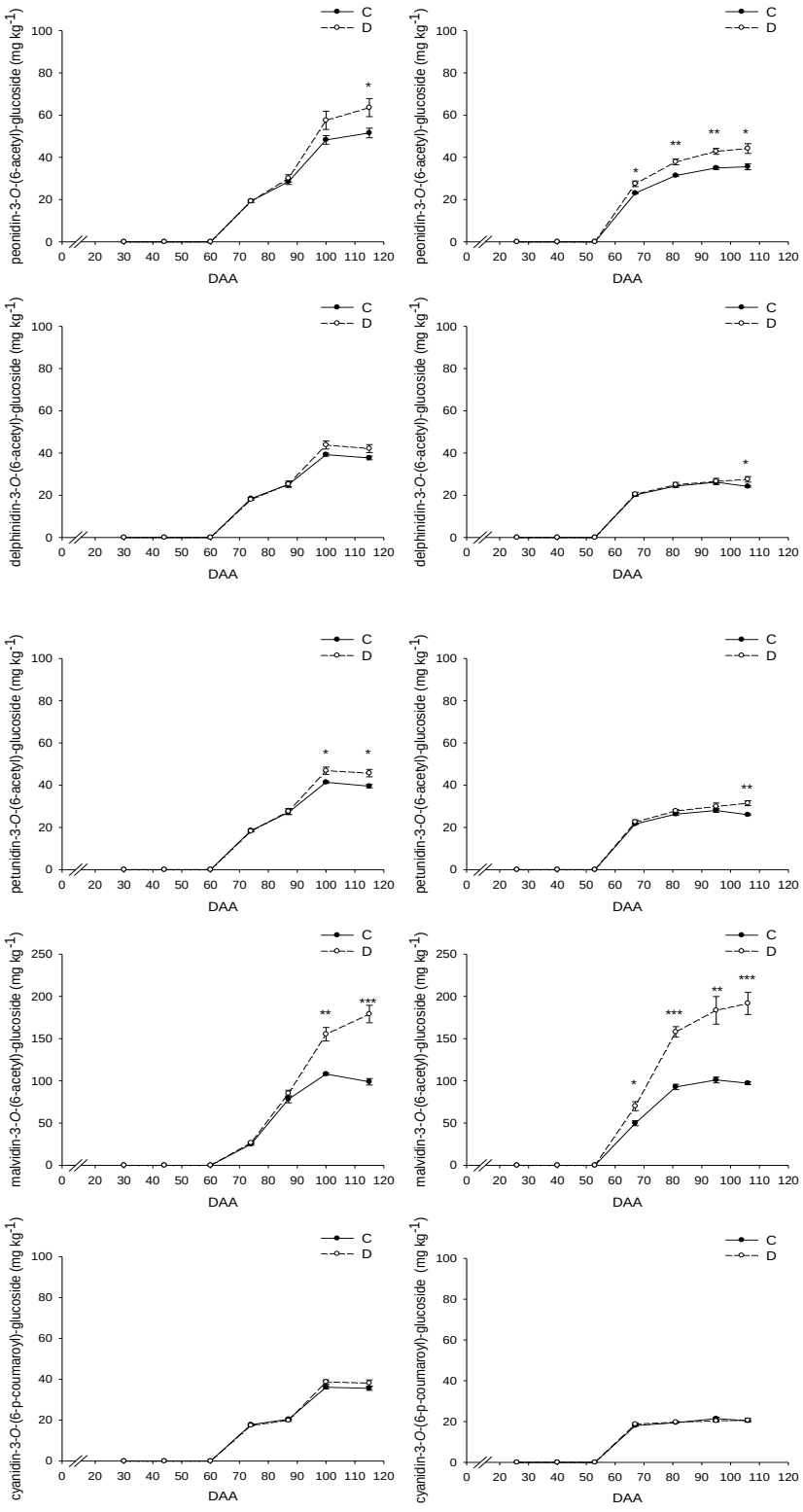
C
D
peonidin-3-O-(6-acetyl)-glucoside (mg kg-1)
delphinidin-3-O-(6-acetyl)-glucoside (mg kg-1)
petunidin-3-O-(6-acetyl)-glucoside (mg kg-1)
malvidin-3-O-(6-acetyl)-glucoside (mg kg-1)
cyanidin-3-O-(6-p-coumaroyl)-glucoside (mg kg-1)
cyanidin-3-O-(6-p-coumaroyl)-glucoside (mg kg-1)
DAA

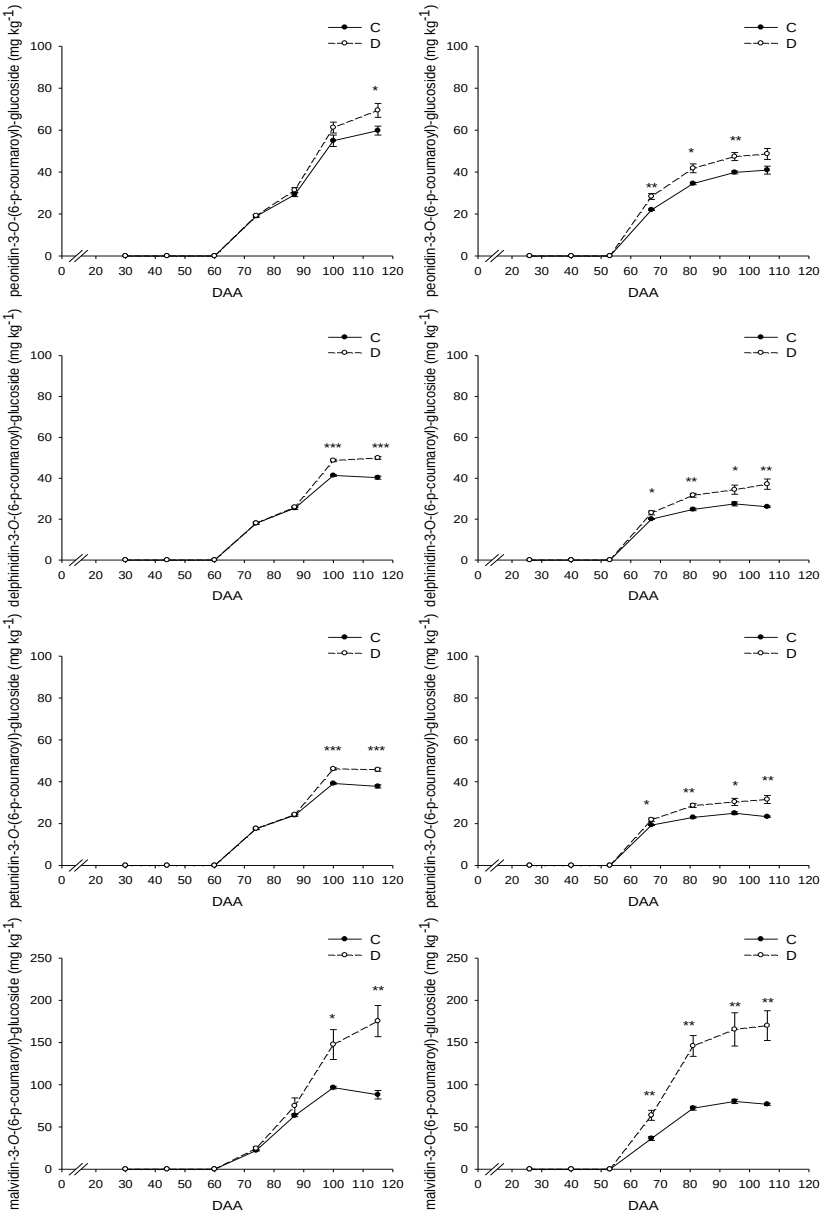
C
D
DAA
peonidin-3-O-(6-p-coumaroyl)-glucoside (mg kg-1)
delphinidin-3-O-(6-p-coumaroyl)-glucoside (mg kg-1)
petunidin-3-O-(6-p-coumaroyl)-glucoside (mg kg-1)
malvidin-3-O-(6-p-coumaroyl)-glucoside (mg kg-1)

Figure S3. Trends of carotenoid concentration in C and D berries during fruit development and ripening in 2011 (left hand panel) and 2012 (right hand panel). Data are expressed as mg/kg of fresh berries.

Carotenoids

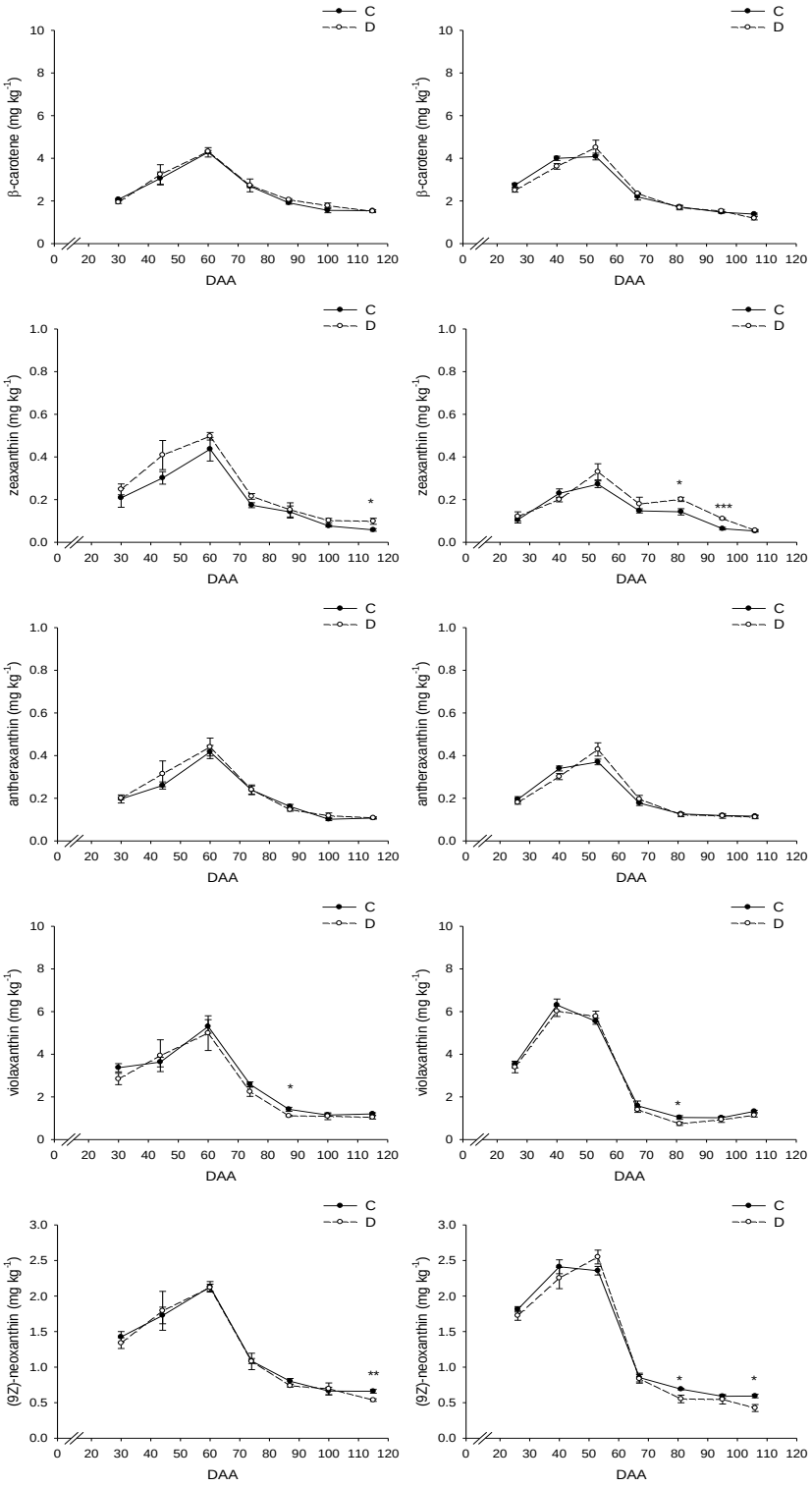

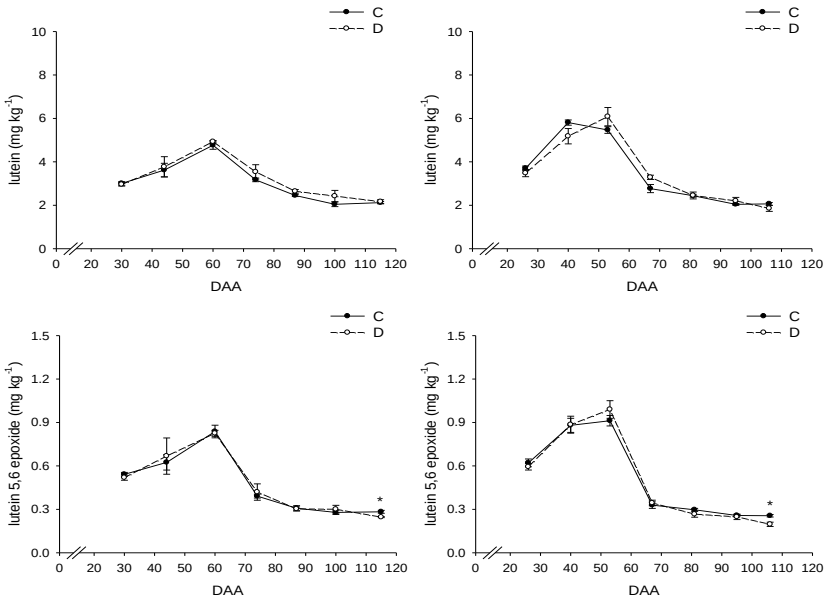
C
D
lutein (mg kg-1)
lutein 5,6 epoxide (mg kg-1)
DAA
*

Figure S4. Trends of volatile organic compounds concentration in C and D berries during fruit development and ripening in 2011 (left hand panel) and 2012 (right hand panel). Data are expressed as µg/kg of fresh berries.

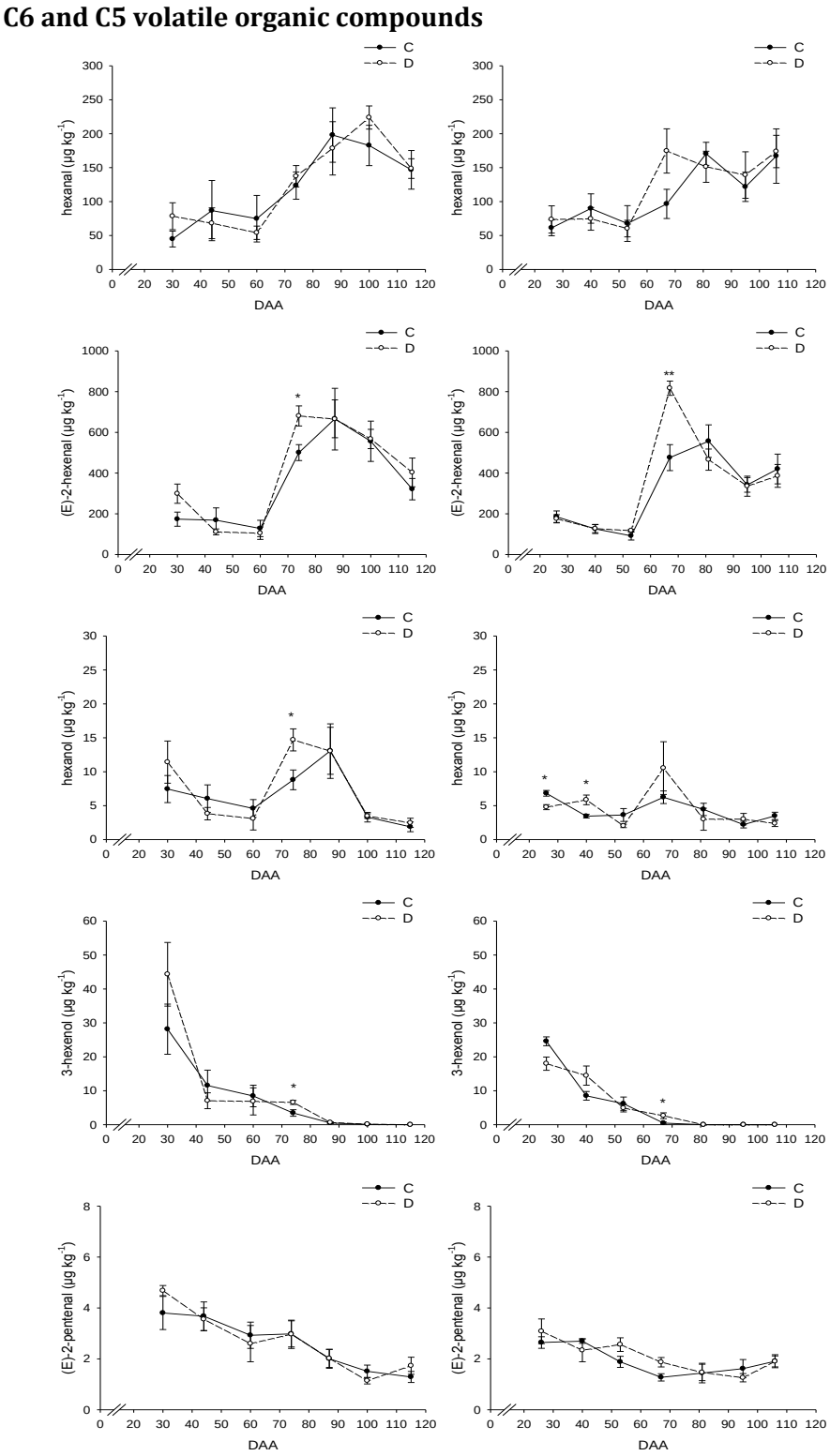

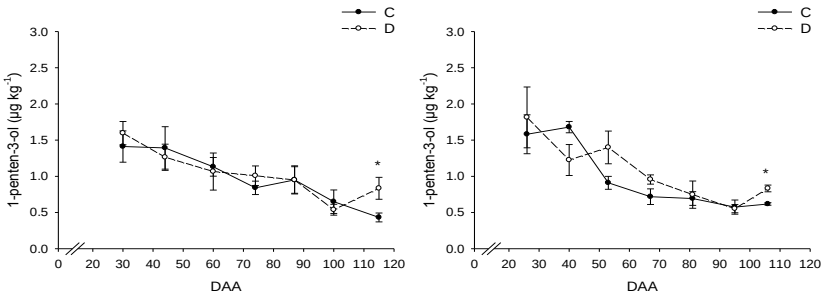

C7, C8 and C9 volatile organic compounds

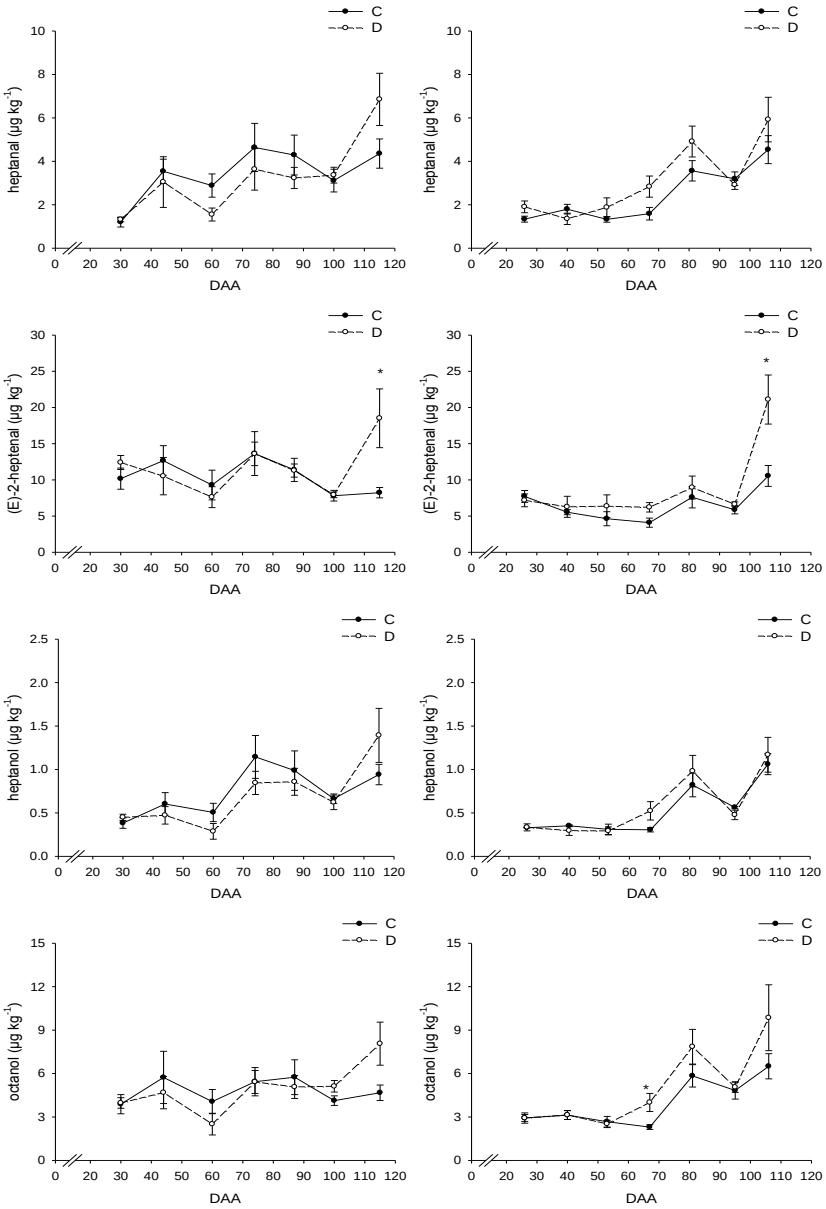

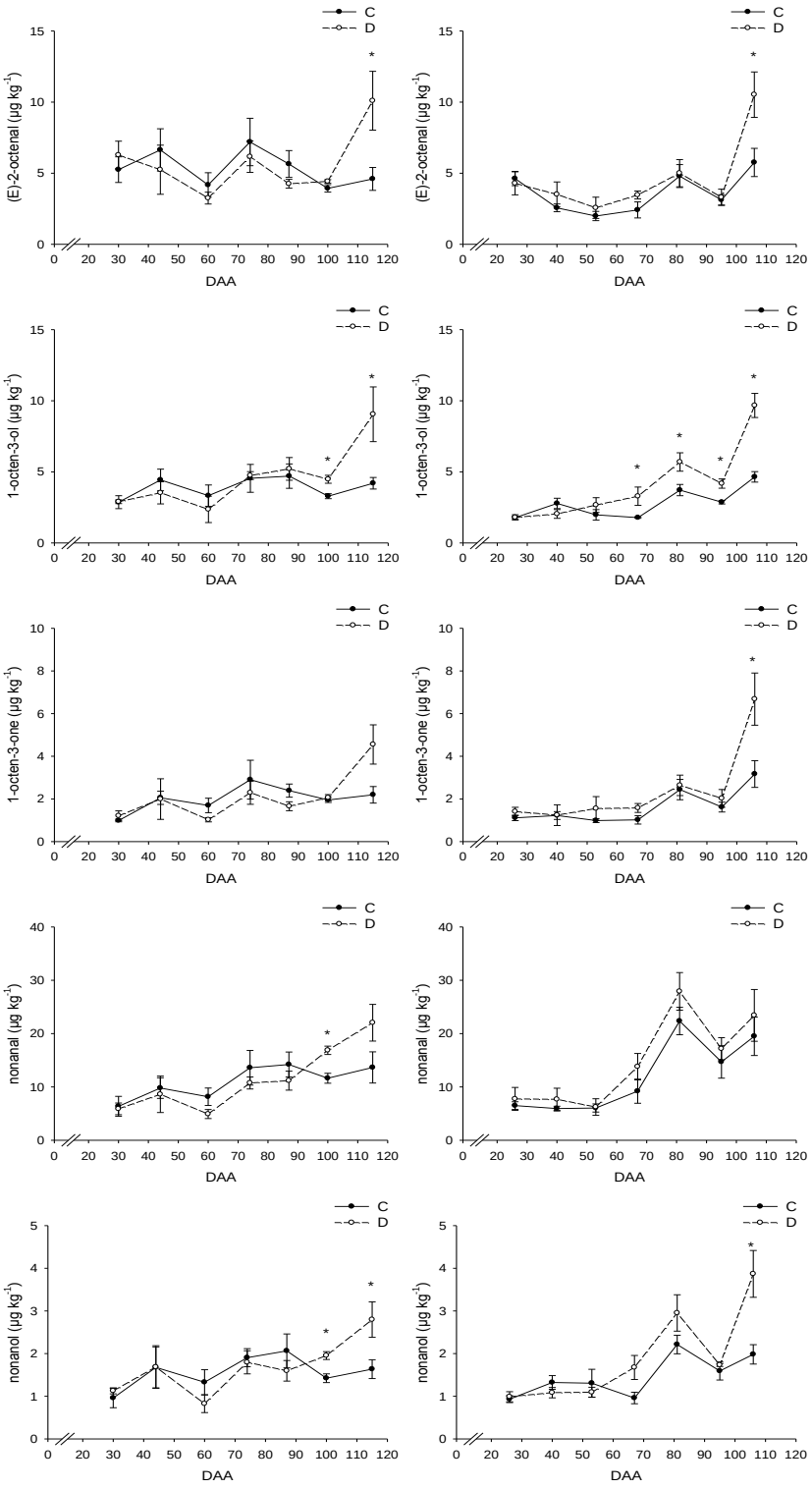
C
D
(E)-2-octenal (µg kg-1)
1-octen-3-ol (µg kg-1)
1-octen-3-one (µg kg-1)
nonanal (µg kg-1)
nonanol (µg kg-1)
DAA
*

C13 Norisoprenoids

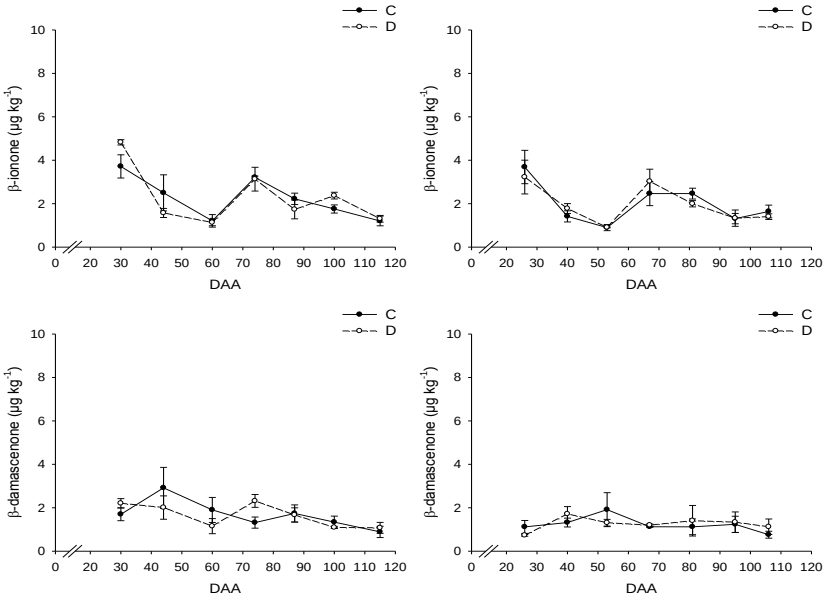

Terpenes

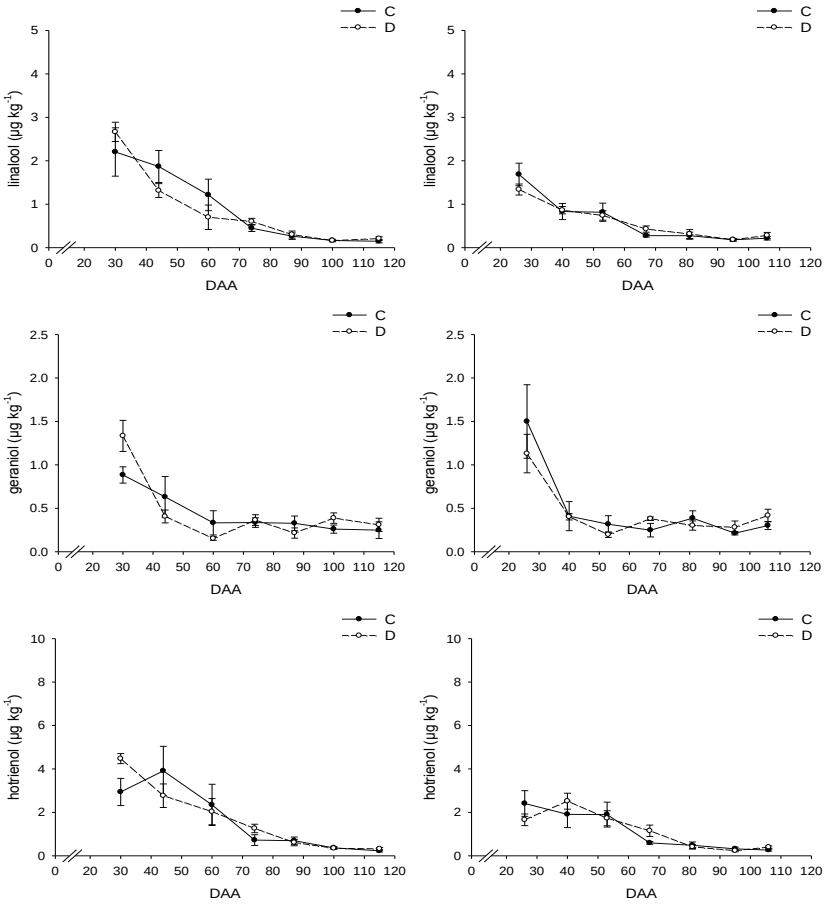

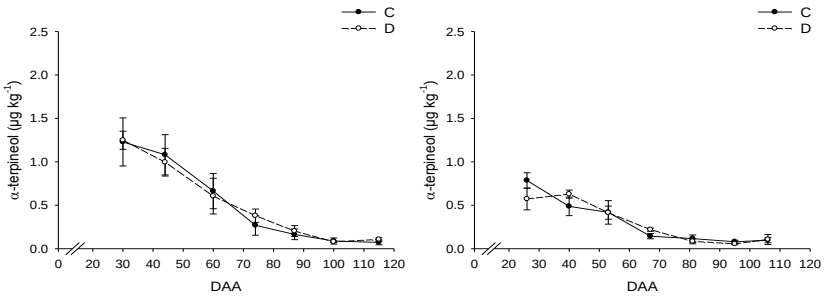
C
D
α-terpineol (µg kg-1)
2.5
2.0
1.5
1.0
0.5
0.0
0 20 30 40 50 60 70 80 90 100 110 120
DAA
C
D
α-terpineol (µg kg-1)
2.5
2.0
1.5
1.0
0.5
0.0
0 20 30 40 50 60 70 80 90 100 110 120
DAA

Chapter 4

EFFECT OF WATER DEFICIT ON THE FRUIT METABOLISM OF TOCAI FRIULANO AND MERLOT: COMMONALITIES AND DIFFERENCES

In order to better understand the differences in the response to water deficit between white and red grapes, the Tocai friulano (chapter 2) and Merlot (chapter 3) results has been compared. In this chapter, the major commonalities and the differences between the two genotypes disclosed by the transcriptome and metabolite analyses performed will be highlighted.

The comparison of the two genotypes is possible only for the data collected in 2012, when the timing and severity of the environmental constrain were similar in Tocai friulano and Merlot vineyards. In particular, deficit occurred from about 40 days after anthesis (DAA) and lasted until the end of ripening with significant differences between control and unirrigated vines.

The common developmental stages where both transcriptome and metabolite analyses were performed are three: one before ripening (41 DAA for Tocai friulano and 53 DAA for Merlot), one at the beginning of ripening (68 DAA for Tocai friulano and 67 DAA for Merlot), and one at end of ripening (93 DAA for Tocai friulano and 106 DAA for Merlot). Before ripening the physiological parameters measured (sugar accumulation and titratable acidity) in control vines were 4.8 °Brix and 32.6 g/L of tartaric equivalent for Tocai friulano and 5.1 °Brix and 38.0 g/L of tartaric equivalents for Merlot; at the beginning of ripening 15.1 °Brix and 11.9 g/L of tartaric equivalent and 16.4 °Brix and 16.2 g/L of tartaric equivalent for Tocai friulano and Merlot respectively; lastly at the end of ripening 21.5 °Brix and 5.1 g/L of tartaric equivalent for Tocai friulano and 23.2 °Brix and 5.9 g/L of tartaric equivalent for Merlot. Taking into account the peculiarity of white and red grape varieties, these values are similar between genotypes across developmental stage allowing the comparison.

The genes differentially expressed (DE) in Tocai friulano were 1,016 at 41 DAA, 2,448 at 68 DAA, and 2,446 at 93 DAA, while in Merlot they were 90 at 53 DAA, 1,290 at 67 DAA, and 2,925 at 106 DAA. The DE genes in common for both genotypes in the three developmental stages were 20 before ripening, 630 at the beginning of ripening, and 870 at the end of ripening. Furthermore, a high percentage of them showed the same response (either genes were up-regulated or were down-regulated) under water deficit in the two genotypes. Precisely the 80, 96, and 85 % of DE genes had the same behavior before ripening, at the beginning of ripening, and at the end of ripening, respectively (Fig. 1).

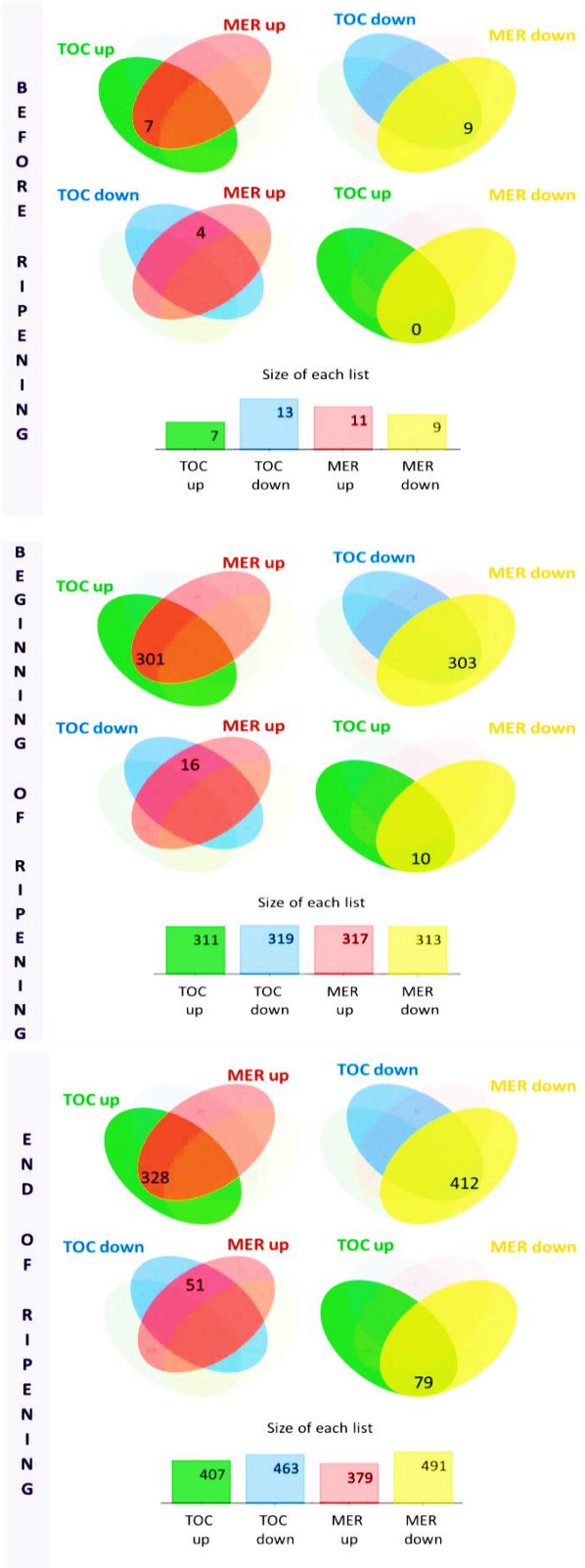

Figure 1. Differentially expressed genes in common between Tocai friulano and Merlot in 2012. The number of genes in common is represented with a Venn Diagram. The number of genes with the same or opposite trend before ripening (graph on the top), at the beginning of ripening (graph in the middle), and at the end of ripening (graph at the bottom) is specified; *TOC* means Tocai friulano, *MER* means Merlot; *up* means genes up-regulated; *down* means genes down-regulated.

Thirteen plant GO categories (slim biological processes) were significantly overrepresented among the DE common genes (Fig. 2). Before ripening, only *amino acid metabolic process* was the category significantly overrepresented. At the beginning of ripening, *amino acid metabolic process, carbohydrate metabolic process*, *catabolic process*, *cell growth*, *development*, *lipid metabolic process, response to abiotic stress*, *response to biotic stress*, *response to stress*, *response to endogenous stimulus*, *response to external stimulus*, and *transport* were the major represented GO categories. At the end of ripening *amino acid metabolic process*, *carbohydrate metabolic process*, *catabolic process*, *cell growth*, *response to abiotic stress*, *response to endogenous stimulus*, *secondary metabolic process*, and *transport* were the main represented GO categories.

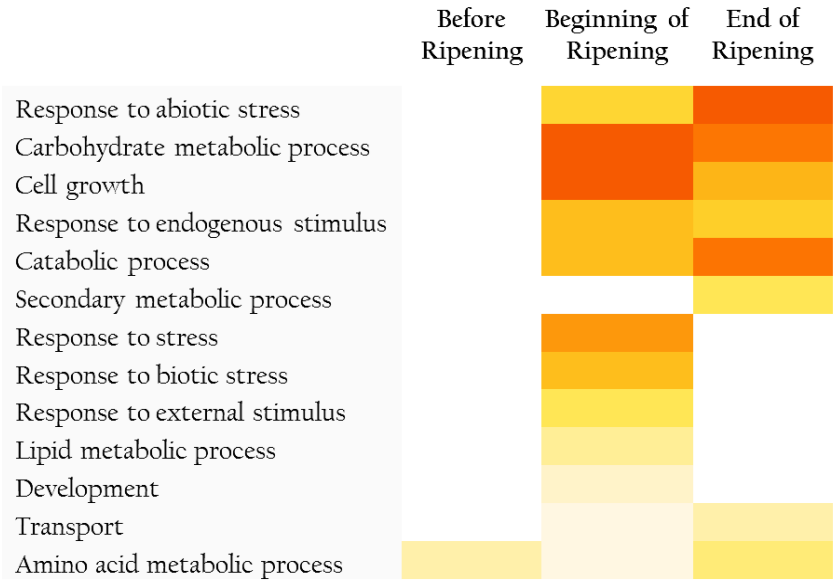

Figure 2. Plant gene ontology (GO) slim biological process categories enriched (P<0.05) within differentially expressed genes in common between Tocai friulano and Merlot before ripening, at the beginning of ripening, and at the end of ripening. The colors in the heatmap denote the level of significance from white (no significance) to light-orange - dark-orange increased level of significance.

Regarding the secondary biosynthetic pathways analyzed in both genotypes in the previous chapters, before ripening water deficit up-regulated key genes of the flavonoid pathway such as a flavonol synthase (*VviFLS*, *VIT_18s0001g03430*), a dihydroflavonol 4-reductase (*VviDFR, VIT_18s0001g12800*), an anthocyanidin reductase *(VviANR, VIT_00s0361g00040),* and a galloyl glucosyltransferase (*VvigGT1, VIT_03s0091g00040*). At the beginning of ripening, two genes of the phenylpropanoid pathway annotated as caffeic acid 3-*O*-methyltransferase (*VviCOMT, VIT_02s0025g02920)* and caffeoyl-CoA acid 3-*O*-methyltransferase (*VviCCoAMT, VIT_07s0031g00350*) were commonly up-regulated by deficit. In the flavonoid pathway, a flavonol synthase (*VviFLS, VIT_18s0001g03430*), a leucoanthocyanidin dioxygenase (*VviLDOX, VIT_08s0105g00380*), and *VviMYBPA1* (*VIT_15s0046g00170*) were down-regulated. On the contrary another leucoanthocyanidin dioxygenase (*VviLDOX, VIT_02s0025g04720*), a proanthocyanidin MATE transporter (*VIT_12s0028g01160*), *VviMYB5b* (*VIT_06s0004g00570*), and *VviMYBC2-L1*

(*VIT_01s0011g04760*) were instead up-regulated. At the end of ripening the DE genes of the phenylpropanoid and flavonoid pathways in common between Tocai friulano and Merlot were a 4-coumarate-CoA ligase (*Vvi4CL, VIT_02s0025g03660*), a p-coumaroyl shikimate 3'-hydroxylase (*VviC3H, VIT_08s0040g00780*), a caffeoyl-CoA acid 3-*O*-methyltransferase (*VviCCoAMT, VIT_07s0031g00350*), the chalcone synthases 1 and 2 (*VviCHS, VIT_14s0068g00920, VIT_14s0068g00930*), a chalcone isomerase (*VviCHI, VIT_13s0067g03820*), a flavanone-3-hydroxylase (*VviF3H, VIT_18s0001g14310*), a flavonol synthase (*VviFLS, VIT_18s0001g03470*), a leucoanthocyanidin dioxygenase (*VviLDOX, VIT_02s0025g04720*), a leucoanthocyanidin reductase (*VviLAR, VIT_17s0000g04150*) and two flavonol-3-*O*-glycosyltransferases (*VviGT5-6, VIT_11s0052g01600, VIT_11s0052g01630*). All these genes were up-regulated by water deficit. For the carotenoid pathway, only two genes (a carotenoid isomerase, *VIT_08s0032g00800*, and a carotenoid cleavage dioxygenase 4 (9,10) (9`,10`), *VIT_02s0087g00910*) were commonly modulated by water and they were both down-regulated. Terpenoid pathway showed an opposite behavior in grapes exposed to water deficit: only a terpene synthase (*VIT_12s0134g00030*) was modulated between the two genotypes but in Tocai friulano was up-regulated while in Merlot was down-regulated.

Transcription factors are important in modulating the transcriptome response to deficit and the ripening process in general. Before ripening, only two transcription factors (a *VviHB/HD-ZIP* and a *VviMYB*) were modulated in common between Tocai friulano and Merlot. At the beginning of ripening they were 50 and at the end of ripening 81. The majority of them showed the same response for both genotypes. The five main classes represented at the beginning of ripening were the *VviMYB*, the *VvibHLH/MYC*, the *VviAP2-EREBP*, the *VviARF*, and the *VviAS2*, while the five main classes represented at the end of ripening were the *VvibHLH/MYC*, the *VviC2H2*, the *VviGRAS*, the *VviHB-HD-ZIP*, and the *VviNAC*. The unique modulation of these specific families of transcription factors in both genotypes is likewise suggestive of the activation of both ABA–dependent (i.e. *VvibZIP*, *VvibHLH/MYC*, *VviMYB*, and *VviNAC*) and ABA–independent (*VviAP2/ERF*, *VviHB/HD-ZIP*, and *VviNAC*) signal transduction pathways under water deficit condition.

The metabolites differentially accumulated under deficit conditions in common for both genotypes in the three developmental stages were: 3 before ripening, 3 at the beginning of ripening, and 8 at the end of ripening (Fig. 3). Before ripening, caftaric acid, coutaric acid and procyanidin B1 were commonly up-regulated by water deficit. At the beginning of ripening, only caftaric acid was the metabolite, which shared a common up-regulation between Tocai friulano and Merlot; on the contrary, other two compounds (procyanidin B1 and procyanidin B3) were modulated by water deficit with an opposite trend between the two genotypes. At the end of ripening several metabolites such as 1-octen-3-one, caftaric acid, (E)-2-heptenal, (E)-2-octenal, gallic acid, and nonanol were up-regulated by water deficit; instead lutein 5,6 epoxide and neoxanthin were down-regulated.

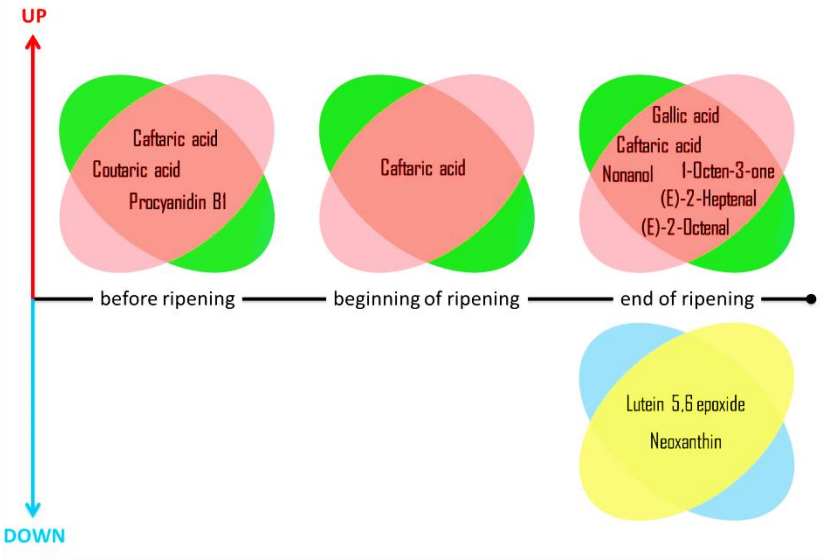

Figure 3. Differentially expressed metabolites in common between Tocai friulano and Merlot in 2012. The metabolites in common are represented with a Venn Diagram. The compounds with the same trend before ripening (graph on the left), at the beginning of ripening (graph in the middle), and at the end of ripening (graph on the right) are specified.

Overall, the phenylpropanoid and flavonoid pathways were activated by water deficit. Several key genes were up-regulated by water deficit and accordingly several metabolites were accumulated in higher amount in both genotypes. Interestingly, the phenylpropanoid genes and the derivatives of benzoic and cinnamic acids were up-regulated and increased in concentration, respectively, by water deficit in the two genotypes. The flavonoids anthocyanins were intensely modulated by water deficit only in the red grape variety. An higher expression of the flavonoid 3',5' hydroxylases was consistent with a major production of trihydroxylated anthocyanins, such as delphinidin, petunidin and malvidin in the glycosylated and acylated forms. The carotenoid pathway was repressed by water deficit with only an exception detected in both genotypes: the compound zeaxanthin was up-regulated during berry ripening, indicating a possible role of this compound in plant drought tolerance. The terpenoid pathway was differently modulated by water deficit: in the white variety, it was enhanced with an up-regulation of several key genes of the terpene pathway and an over-production of monoterpenes, while in the red variety none of the terpene synthases were activated under water deficit as well as the production of terpenes was not affected. Lastly, the analysis of the transcription factor families revealed a pivotal role of the ABA signal transduction with the activation in the two genotypes of both the ABA-dependent and ABA-independent pathways. ABA is a well know ripening and water deficit related hormone. Our data confirm the role of ABA in the modulation of fruit development and composition under water deficit conditions.

Taken together, these data confirm a large effect of water deficit not only at the morphological and physiological level but also at the metabolic and molecular level with several aspects shared between white and red grape varieties.

Chapter 5

WATER DEFICIT ENHANCES THE ACCUMULATION OF GLYCOSYLATED SECONDARY METABOLITES IN MERLOT AND TOCAI FRIULANO WINES

Introduction

The quality of fruits, and hence the value of the wines in the specific case of grape, is tightly linked with the accumulation of secondary metabolites, such as polyphenols and volatiles which contribute to the final color, taste and aroma. Furthermore, secondary metabolites play a pivotal role in the adaptation of plants to the environment acting as a defense mechanism (Ferrandino and Lovisolo, 2014). Many experiments revealed that plants subjected to water deficit accumulate higher concentrations of several classes of secondary metabolites, such as phenolics and terpenes as well as alkaloids and glucosinolates (reviewed in Selmar and Kleinwächter, 2013).

Polyphenols biosynthesis and accumulation in grape has been widely studied, having special consideration for the environmental effects on these compounds (reviewed in Downey et al., 2006 and in Teixeira et al., 2013). Three are the classes of flavonoids commonly detected in grapes and wines: anthocyanins, flavonols, and tannins. Anthocyanins are present in the skins of the grape berry, they start to be accumulated at the onset of ripening and they are responsible of the color of the red grape varieties. Different level of hydroxylation, methylation and acylation of the five most commonly detected anthocyanins can impact the color intensity and hue of wines. It has been reported that water deficit enhances the biosynthesis and accumulation of the try-hydroxylated anthocyanins, namely delphinidin, and the methylated try-hydroxylated anthocyanins, namely petunidin and malvidin, shifting thus the anthocyanin profile towards an enrichment of purple/blue pigments (Castellarin et al., 2007b). Flavonols are yellow pigments and they act as UV protectants; their synthesis occur in the berry skins and is highly correlated with the level of sunlight exposure (Downey et al., 2004). Furthermore, they take part to the co-pigmentation process forming complexes with anthocyanins and thus they stabilize the color of red wines (Boulton, 2001). Condensed tannins are complex polymers of flavan-3-ols and they are synthesized in pre-veraison primarily in the skins and in the seeds of the grape berry. They have a role in determining the taste components of wines, such as astringency, bitterness mouthfeel and body; moreover they contribute to the color stability forming polymeric complexes with anthocyanins. Previous grapevine water deficit studies reported a little or no modulation of flavan-3-ols and condensed tannins (Castellarin et al., 2007a; Hochberg et al., 2015).

Volatile aromatic compounds are commonly present in plants in the free form, contributing directly to the odor, or glycosidically bound to sugar moieties. The latter are

present in higher concentration in the berry as non-volatile and odorless compounds (Hjelmeland and Ebeler, 2014). In grape, theses sugar moieties are often a disaccharide with preponderance of α-L-arabinofuranosyl-β-D-glucopyranosides, α-L-rhamnopyranosyl-β-D-glucopyranosides, β-D-xylopyranosyl-β-D-glucopyranosides, β-D-apiofuranosyl-β-D-glucopyranosides (Robinson et al., 2014). The glycosylation process occurs through the activity of specific glycosyltransferases (*VviGTs*). In the grapevine genome (Jaillon et al., 2007), more than one hundred putative *VviGTs* have been identified but up to now only three of them (*VviGT7*, *VviGT14* and *VviGT15*: *VIT_16s0050g01580*, *VIT_18s0001g06060* and *VIT_06s0004g05780*) have been functionally characterized with specificity toward terpenes (Bönisch et al., 2014a; Bönisch et al., 2014b). The hydrolysis of these glycoconjugates by acids or enzymes can release the odor-active aglycones. Glycosidically bound volatile compounds can thus be liberated either by slow chemical acid hydrolysis or by means of endogenous grape-derived glycosidases and exogenous yeast-derived glycosidases. However, grape and yeast glycosidases showed low activity under fermentation conditions due to low pH and temperature, and they were also inhibited by ethanol and glucose concentration (Robinson et al., 2014). Nevertheless, it is possible to enhance the wine flavor through the addition of exogenous fungal glycosidases (Cabaroglu et al., 2003). The main grape-deriving aromatic compounds are the terpenes and the C_{13}-norisoprenoids. Terpenes largely contribute to the aroma of white wines developing floral scents. Among the forty main monoterpenes compounds found in grape, the most odoriferous are linalool and its oxides, α-terpineol, nerol, geraniol, citronellol and hotrienol. The detection thresholds of each of them are quite low (few μg/L) and furthermore together they play a synergistic action toward a significant decreasing of this threshold. C_{13}-norisoprenoids are the products of the oxidative degradation of carotenoids. They have very low olfactory perception thresholds and therefore a high sensorial impact on wine aroma (Mendes-Pinto, 2009). The main compounds found in grapes and wines are β-damascenone, with reminiscent of tropical fruits, β-ionone with violet scent, 3-oxo-α-ionol with tobacco flavour, 3-hydroxy-β-damascone with tea and tobacco reminiscent, β-damascone with tobacco and fruity aroma, TDN (1,1,6-trimethyl-1,2-dihydronaphthalene) which has a petroleum aroma, and vitispirane with camphor/woody nuances (Winterhalter and Schreier, 1994; Darriet et al., 2012). It has been reported that water deficit enhances the biosynthesis and accumulation of C_{13}-norisoprenid compounds in grape (Deluc et al., 2009; Song et al., 2012).

In this study, we evaluated the impact of water deficit on the red cultivar Merlot and on the white cultivar Tocai friulano wine compositions mainly focusing on the secondary metabolites that largely contribute to the visual, olfactory and gustative properties. We hypothesized that wines produced from grapes subject to water deficit may accumulate higher amount of glycosylated secondary metabolites. An open field experiment was conducted in a North Italian viticultural area characterized by transient drought events during the summer. Two different water regimes were applied to Merlot and Tocai friulano vines for two consecutive seasons. The harvested grapes were microvinificated with a standard protocol and the effect of water deficit on anthocyanins, tannins, and free and glycosidically-bound aromatic compounds accumulation was investigated in the wines produced from fully-irrigated grapes and grapes subjected to water deficit. Finally, a descriptive sensory test was undertaken to investigate the final color, aroma, taste and mouthfeel sensory attributes.

Results

Effect of water deficit on Merlot and Tocai friulano grape and wine composition

In order to understand the effect of water deficit on the grape at harvest and as a consequence in the wines produced from those grapes, two water treatments were applied to the plants during the seasons. Irrigated vines (defined as C) were weekly irrigated with the aim of keeping their stem water potential (Ψ_{Stem}) above -0.8 MPa, whereas vines under deficit irrigation (defined as D) were not irrigated from fruit set until harvest, unless they suffered of extreme water deficit.

Stem water potential (Ψ_{Stem}) is a sensitive indicator of grapevine water status (Choné et al., 2001) and in these trials Ψ_{Stem} was significantly affected by D in both seasons for both cultivars showing experimental reliability (Table 1). However, higher effects were recorded in 2011 compared to 2012 when Ψ_{Stem} at harvest was consistently lower than -0.6 / -1.0 MPa in D due to a second part of the season particularly dry (Fig. S1a). In 2012, some rainfalls occurred during the second part of the season, decreasing the temperatures and increasing humidity (Fig. S1b). This lead to a slight increase of Ψ_{Stem} at harvest with differences between treatments of about -0.3 / -0.7 MPa. It is important to highlight that Merlot vines were sheltered with an open-sided transparent cover at the beginning of the seasons, while Tocai friulano vines were in an open-field and hence subjected to the natural precipitations. Thus, for Merlot we have data with similar level of water deficit, which occurred at about 40-50 DAA and lasted until harvest. For Tocai friulano we are witnessing a season (2011) with a late deficit, which occurred at about 80-90 DAA, and a season (2012) with a deficit that occurred early at about 30-40 DAA and lasted until harvest.

Water deficit significantly affected cluster weight and yield, reducing both of them by 25% in 2011 and in 2012 in Merlot, while water deficit reduced by 18% and 23% cluster weight and yield in Tocai friulano only in 2012 (Table 1).

Table 1. Effect of water deficit on crop production in Merlot and Tocai friulano vines. Stem water potential, cluster per vine, cluster weight, and yield per vine of fully irrigated (C, control) and deficit irrigated (D, water deficit) grapevines in 2011 and 2012. Values are averages ± the standard error. Differences between treatments was assessed with a one-way ANOVA. The level of significance is reported within the columns: *, **, *** or ns, P<0.05, P<0.01, P<0.001 or not significant, respectively

	Merlot				**Tocai friulano**			
Year	2011		2012		2011		2012	
Treatment	C	D	C	D	C	D	C	D
Stem Water Potential (Ψ_{stem})	-0.62 ± 0.03	-1.61 ± 0.05 ***	-0.41 ± 0.01	-1.14 ± 0.12 ***	-0.99 ± 0.07	-1.64 ± 0.06 ***	-0.61 ± 0.02	-0.93 ± 0.06 **
Cluster per Vine	22.9 ± 0.6	22.8 ± 1.2 ns	20.1 ± 1.7	19.4 ± 1.4 ns	13.9 ± 2.2	14.9 ± 2.3 ns	20.1 ± 2.6	18.4 ± 2.0 ns
Cluster Weight (g)	189.4 ± 11.5	142.4 ± 5.9 *	129.0 ± 4.2	101.5 ± 9.3 *	228.1 ± 24.5	210.3 ± 27.3 ns	170.5 ± 10.8	139.4 ± 15.5 *
Yield per Vine (Kg)	4.29 ± 0.35	3.23 ± 0.22 *	2.62 ± 0.22	1.97 ± 0.19 *	3.18 ± 0.60	3.08 ± 0.48 ns	3.27 ± 0.25	2.52 ± 0.26 *

Water deficit affected Merlot berry weight, significantly reducing it by a 21% and a 27% in 2011 and 2012 respectively, while no significant effects were recorded for Tocai friulano. Furthermore, in 2012, total soluble solids were increased in D berries by a 5% in Merlot and by an 8% in Tocai friulano. Titratable acidity and pH were not influenced by D in Merlot neither in 2011 nor in 2012; conversely, TA was reduced in 2011 and pH was increased in 2012 in Tocai friulano (Table 2).

Table 2. Effect of water deficit on physiological parameters of Merlot and Tocai friulano grape berry. Berry weight, total soluble solids, titratable acidity and pH of fully irrigated (C, control) and deficit irrigated (D, water deficit) grape berry in 2011 and 2012. Values are averages ± the standard error. Differences between treatments was assessed with a one-way ANOVA. The level of significance is reported within the columns: *, **, *** or ns, P<0.05, P<0.01, P<0.001 or not significant, respectively

	Merlot				**Tocai friulano**			
Year	2011		2012		2011		2012	
Treatment	C	D	C	D	C	D	C	D
Berry Weight (g)	1.87 ± 0.05	1.47 ± 0.11 *	1.61 ± 0.05	1.17 ± 0.07 **	1.82 ± 0.05	1.70 ± 0.03 ns	1.45 ± 0.07	1.28 ± 0.10 ns
Total Soluble Solids (°Brix)	22.2 ± 0.10	23.3 ± 0.51 ns	23.2 ±0.10	24.6 ± 0.17 ***	22.0 ± 0.60	20.4 ± 0.34 ns	21.5 ± 0.22	23.4 ± 0.47 *
Titratable Acidity (g/L)	6.00 ± 0.04	5.88 ± 0.24 ns	5.93 ± 0.19	6.00 ± 0.12 ns	5.57 ± 0.14	4.89 ± 0.13 *	5.10 ± 0.32	4.35 ± 0.09 ns
pH	3.49 ± 0.01	3.48 ± 0.04 ns	3.53 ± 0.02	3.63 ± 0.03 ns	3.61 ± 0.02	3.67 ± 0.02 ns	3.65 ± 0.04	3.81 ± 0.04 *

The grapes were manually harvested at technological maturity and then microvinificated using a standard protocol.

Merlot wines showed no differences in the alcohol content. Water deficit decreased wine pH in both seasons, and increased titratable acidity in 2011. Dry extract was higher in D wines only in 2012 (Table 3).

Tocai friulano wines showed higher alcohol content only in 2012 and an increased pH in 2011. No effects of D were recorded in titratable acidity and dry extract in 2011 and 2012 (Table 3).

Table 3. Effect of water deficit on Merlot and Tocai friulano wine composition. Alcohol content, titratable acidity, pH and dry extract of fully irrigated (C, control) and deficit irrigated (D, water deficit) grape berry in 2011 and 2012. Values are averages ± the standard error. Differences between treatments was assessed with a one-way ANOVA. The level of significance is reported within the columns: *, **, *** or ns, P<0.05, P<0.01, P<0.001 or not significant, respectively

	Merlot				**Tocai friulano**			
Year	2011		2012		2011		2012	
Treatment	C	D	C	D	C	D	C	D
Alcohol (%)	12.8 ± 0.15	13.1 ± 0.46 ns	13.4 ± 0.02	13.8 ± 0.21 ns	13.0 ± 0.46	12.2 ± 0.05 ns	13.4 ± 0.08	14.4 ± 0.29 *
Titratable Acidity (g/L)	5.70 ± 0.11	6.13 ± 0.13 *	6.85 ± 0.10	6.65 ± 0.05 ns	5.28 ± 0.28	4.70 ± 0.04 ns	5.33 ± 0.28	4.73 ± 0.03 ns
pH	3.54 ± 0.02	3.39 ± 0.03 **	3.58 ± 0.02	3.47 ± 0.01 **	3.55 ± 0.02	3.63 ± 0.02 *	3.69 ± 0.06	3.66 ± 0.04 ns
Dry extract (g/L)	27.1 ± 0.53	28.9 ± 0.73 ns	32.6 ± 0.71	36.0 ± 1.01 *	20.1 ± 0.19	20.0 ± 0.30 ns	23.1 ± 0.38	27.5 ± 2.08 ns

Additional analyses, such as anthocyanins, tannins and small and large polymeric pigments content were carried out for the red cultivar Merlot on grapes and wines (Table 4).

Skin grape anthocyanins content and as well as total anthocyanins present in wines were strongly affected by D showing an average increase of 45% in 2011 and 2012, both in grape and in wine. Color intensity and hue of red wines reflect the contribution of red and yellow colors among the others. Therefore, the spectrum of red wines has a maximum at 520 nm and a minimum at 420 nm. Merlot wines had significant higher color intensity (OD420 +OD520) and lower hue (OD420/OD520).

Tannins from grape skins and seeds during winemaking and aging can combine with anthocyanins and form polymeric pigments. By joining a protein precipitation assay with the bisulfite bleaching method, it is possible to discriminate the level of monomeric anthocyanins from small and large polymeric pigments (Harbertson et al., 2003). Both small and large polymeric pigments showed an average increase of 57% and 34% respectively in D wines in both seasons. Furthermore, grape skin tannins content showed an average increase of 28% in D in 2011 and 2012. Neither grape seed tannins nor wine tannins were significantly affected by D.

Table 4. Effect of water deficit on Merlot grapes and wines composition in 2011 and 2012. Grape skin anthocyanins content, grape skin and seed tannins content, wine anthocyanins and tannins content, wine small and large polymeric pigment content, and wine color intensity and hue of fully irrigated (C, control) and deficit irrigated (D, water deficit) grape berry in 2011 and 2012. Values are averages ± the standard error. Differences between treatments was assessed with a one-way ANOVA. The level of significance is reported within the columns: *, **, *** or ns, P<0.05, P<0.01, P<0.001 or not significant, respectively

		Merlot			
Year		2011		2012	
Treatment		C	D	C	D
GRAPE	**Skin Anthocyanins (mg/g FM)**	0.74 ± 0.03	1.33 ± 0.04 ***	0.80 ± 0.03	1.49 ± 0.11 ***
	Skin Tannins (mg/g FM)	1.05 ± 0.05	1.37 ± 0.03 **	0.95 ± 0.06	1.43 ± 0.09 **
	Seed Tannins (mg/g FM)	2.49 ± 0.23	1.98 ± 0.05 ns	3.09 ± 0.05	3.41 ± 0.18 ns
WINE	**Anthocyanins (mg/L)**	145.6 ± 3.34	279.9 ± 41.35 *	119.2 ± 3.70	299.4 ± 34.70 **
	Tannins (mg/L)	236.8 ± 17.16	282.5 ± 45.97 ns	302.2 ± 32.52	221.6 ± 31.09 ns
	Small Polymeric Pigments (AU)	0.83 ± 0.08	1.99 ± 0.14 ***	1.17 ± 0.09	2.65 ± 0.21 ***
	Large Polymeric Pigments (AU)	0.67 ± 0.05	1.08 ± 0.07 **	2.02 ± 0.30	2.91 ± 0.10 *
	Color Intensity (AU)	0.54 ± 0.03	1.08 ± 0.06 ***	0.56 ± 0.06	1.00 ± 0.02 ***
	Hue (AU)	0.78 ± 0.02	0.63 ± 0.03 **	0.95 ± 0.03	0.75 ± 0.02 **

Free and glycosidically-bound volatiles

The free and the glycosidically-bound volatiles were identified in wines produced with the fully irrigated grapes and in wines produced with grapes subjected to water deficit. Because the goal of this trial was the identification of the possible compounds affected by water deficit and not by the vinification process, which is tightly dependent by the yeast strain used and by the specific fermentative technique, we mainly focused our attention to the grape-derived aroma compounds, such as terpenes and C_{13}-norisoprenoids giving thus less attention to the fermentative compounds, such as fusel alcohols, esters, carbonyl compounds, and fatty acid and phenylpropanoid derivatives (Robinson et al., 2014).

A total number of 52 volatile compounds were identified and quantified in the free fraction by gas chromatography-mass spectrometry (GC-MS). They encompass alcohols, esters, carbonyl compounds, fatty acid and phenylpropanoids derivatives, and monoterpenes; no free C_{13}-norisoprenoids were identified (Table S1). Merlot and Tocai friulano are cultivars defined as not-aromatic and hence they contain a minor level of free monoterpenes compared for example to the highly aromatic Muscat cultivars; moreover, red cultivar are typically regarded as having lower amount of these compounds compared to the white ones. Monoterpenes are known for their floral and fruity aroma. Specifically, in Merlot only few monoterpenes were significantly modulated by D but without a clear trend. For example, citronellol and *p*-cymene were decreased by D only in 2011 and the concentration of geranic acid was decreased in 2011 but increased in 2012. Remarkably different was the effect that water deficit had on Tocai friulano especially in 2012, the season characterized by an early and prolonged deficit. Therefore, the concentration of linalool, *cis* and *trans* linalool oxide, α-terpineol and diendiol I were strongly increased by D.

A total number of 34 volatile compounds were identified and quantified by gas chromatography-mass spectrometry (GC-MS) in the glycosidically-bound fraction after enzymatic hydrolysis (Table S2). They encompass alcohols, fatty acid and phenylpropanoids derivatives, monoterpenes and C_{13}-norisoprenoids. D wines were highly enriched of glycosylated monoterpenes and C_{13}-norisoprenoids. Specifically, Merlot D wines showed higher concentration of *cis* and *trans* 8-hydroxylinalool, 7-hydroxygerianol and geranic acid in both seasons. As seen before for the free fraction, a higher number of glycosylated monoterpenes were accumulated in Tocai friulano grapes subjected to water deficit in 2012, and hence in those wines. Higher concentration were recorder for linalool, *cis* and *trans* linalool oxide, *cis* and *trans* 8-hydroxylinalool, 7-hydroxygerianol and geranic acid. C_{13}-norisoprenoids are deriving from the degradation of carotenoids and they have a strong impact on wine aroma. Compounds like 3-hydroxy-β-damascone, 3-oxo-α-ionol and 3-hydroxy-7,8-dihydro-β-ionol were present in higher amount in the D wines of Merlot in 2011 and 2012 and in the D wines of Tocai friulano in 2012.

The grape-derived volatile compounds identified in the free and glycosidically bound fraction were hierarchically clustered with Pearson method and complete link and they were represented in a heatmap as $\log_2$ fold change of D versus C (Fig. 1). Interesting to note, three monoterpenes were not increased by D. Among them, free *p*-cymene and free geranic acid were

present in a lower amount only in Merlot wines while free geraniol was detected only in Tocai friulano wines in lower concentration in both seasons. Conversely, the concentration of the glycosidically bound C_{13}-norisoprenoid were the most consistently affected by D showing a higher accumulation in the D wines in both cultivars and in the two seasons. These compounds were clustered all together. A conspicuous number of both free and glycosidically bound monoterpenes, with particularly emphasis on linalool and its derivatives, were strongly increased by D only in Tocai friulano 2012 wines.

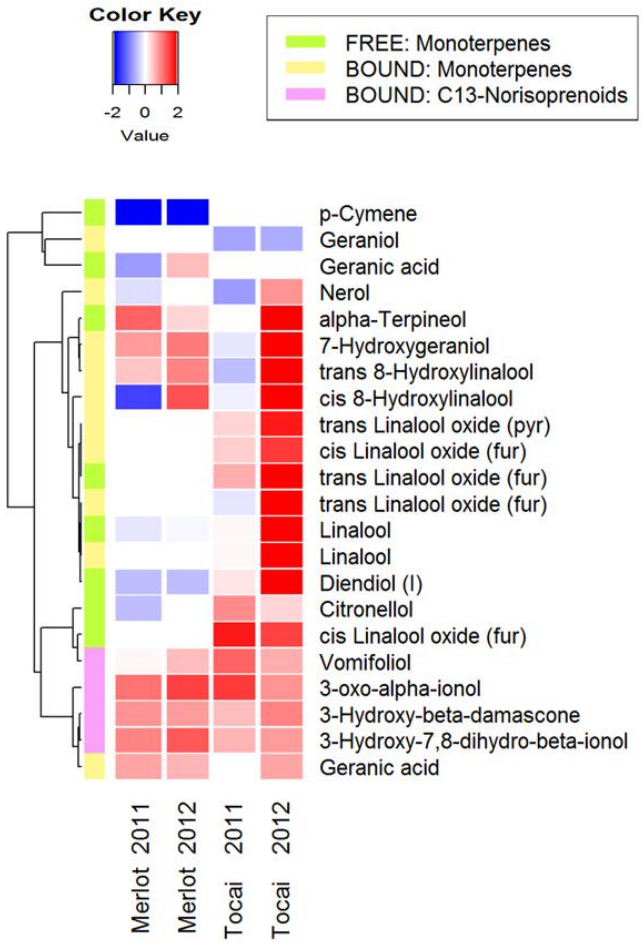

Figure 1. Effect of water deficit on free and glycosidically bound volatile compounds in Merlot and Tocai friulano wines in 2011 and 2012. Heatmaps represent $\log_2$ fold change (D/C) of the grape-derived aroma namely monoterpenes and C_{13}-norisoprenoids under water deficit conditions. Blue and red boxes indicate lower and higher concentration in D, respectively. Metabolites were hierarchically clustered based on their response to water deficit.

Sensory attributes of Merlot and Tocai friulano wines

Descriptive sensory tests, assessed by skilled panelists on Merlot and Tocai friulano wines in 2011 and 2012, revealed that water irrigation significantly affected several sensory attributes for Merlot wines (Fig. 2) but surprisingly only one in Tocai friulano wines (Fig. 3).

Merlot water deficit wines showed in both seasons higher visual attributes, such as *color intensity* and *color hue*, higher aroma attributes, such as *aroma intensity*, *aroma red fruits*, and *aroma jam*, higher retronasal attributes, such as *retronasal red fruits*, and among the taste attributes *body* was significantly higher in both seasons. Moreover, *retronasal intensity* and *retronasal persistence* were higher in D in 2011 and 2012 respectively, and *aroma spicy* was higher only in 2012.

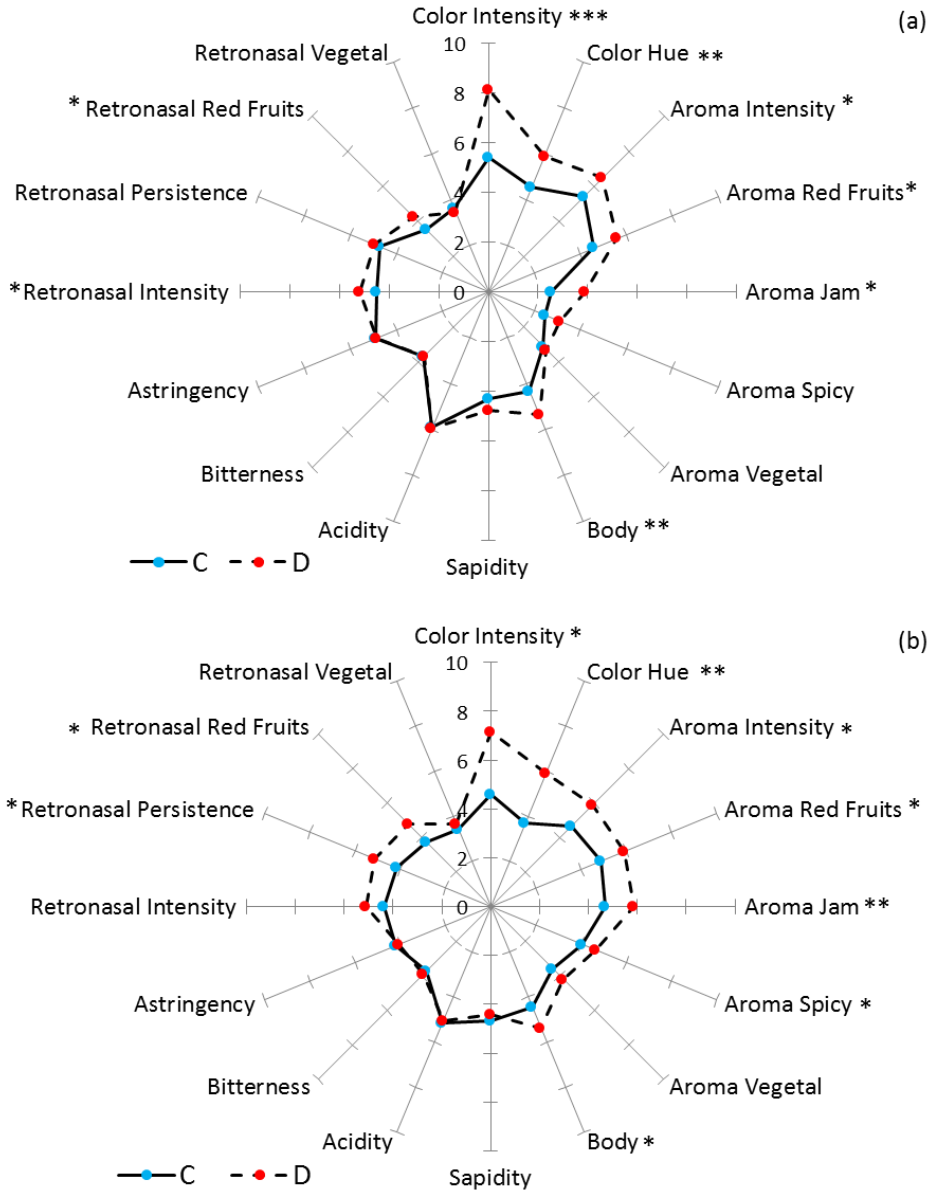

Figure 2. Descriptive sensory test results of Merlot fully irrigated (C) and deficit irrigated (D) wines in 2011 (a) and 2012(b) are represented in a radar chart. Blue dots with continuous line represent the average observations among C wines. Red dots with dashed line represent the average observations among D wines. Asterisks placed near each attribute indicate significant differences (*, ** or ***: P<0.05, P<0.01 or P<0.001) between treatments.

Tocai friulano water deficit wines showed only in 2012 higher visual attributes, such as *color intensity*.

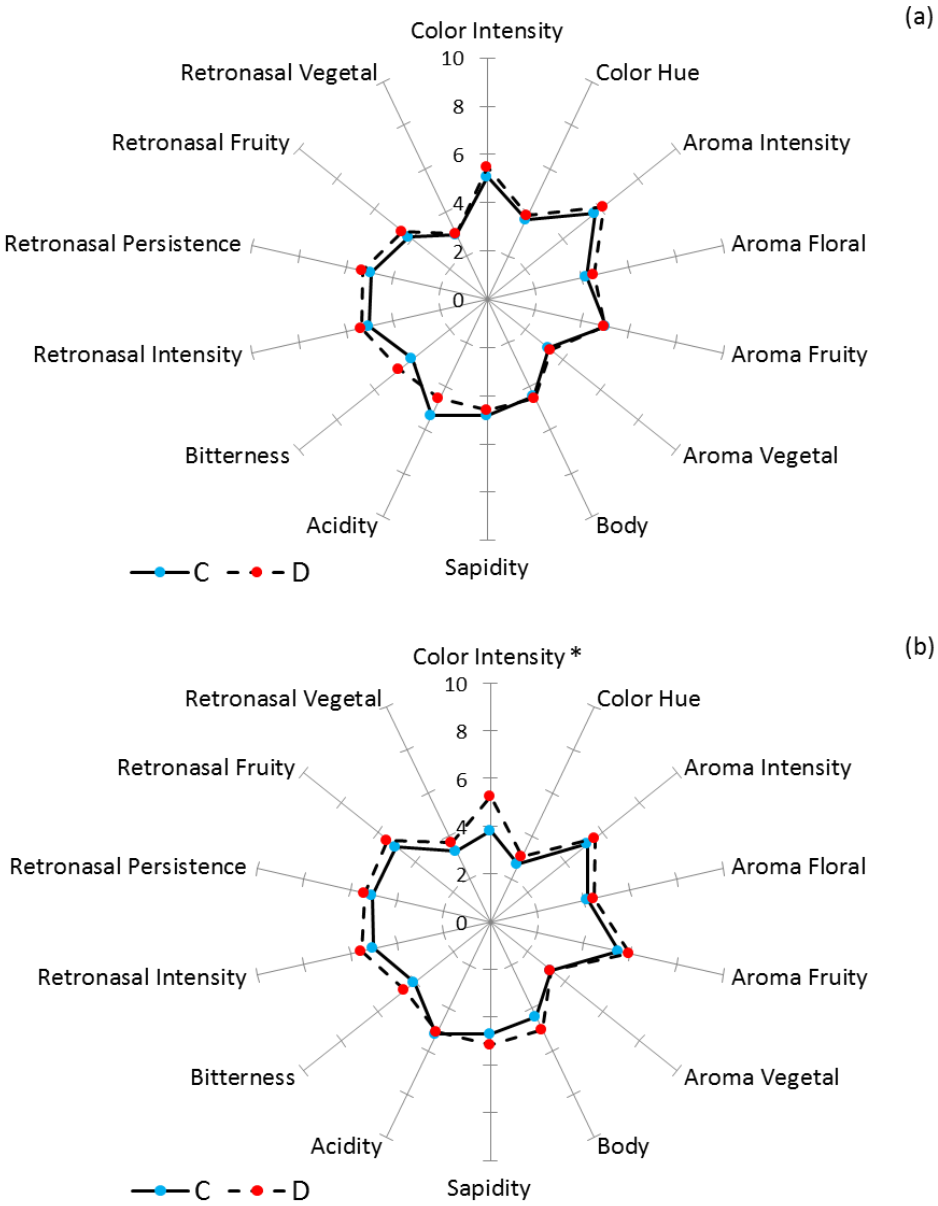

Figure 3. Descriptive sensory test results of Tocai friulano fully irrigated (C) and deficit irrigated (D) wines in 2011 (a) and 2012(b) are represented in a radar chart. Blue dots with continuous line represent the average observations among C wines. Red dots with dashed line represent the average observations among D wines. Asterisks placed near each attribute indicate significant differences (*, ** or ***: P<0.05, P<0.01 or P<0.001) between treatments.

Discussion

Water deficit modulated the accumulation of anthocyanins, small and large polymeric pigments, and free and glycosidically-bound aromatic compounds in the wine; however the modulation of the secondary metabolism varied between cultivars and seasons, indicating an interaction between genotype and environment and moreover that the severity and the timing of the drought impacts this response.

Our study indicates that in the red Merlot variety anthocyanins concentration responds to water deficit affecting not only the concentration of anthocyanins but also their composition. Therefore, together with a higher total amount of anthocyanins in wines, we observed higher wine color intensity and hence as consequence lower hue (Table 4). This means that in the grapes try-hydroxylated anthocyanins were highly accumulated leading to an enrichment of purple/blue pigments as already reported in Merlot (Castellarin et al., 2007b; Herrera et al., 2015) and in Cabernet Sauvignon (Castellarin et al., 2007a). Furthermore, also small and large polymeric pigments were increased by water deficit. According to Harbertson et al. (2003), the color due to small polymeric pigments is mostly contributed by the grape berry content and hence refers to the concentration of anthocyanins and tannins present in the grape skins. Both were increased by water deficit. Conversely, the large polymeric pigments are formed during fermentation and aging and they highly contribute in stabilizing the color of the finished wine. These results were confirmed by the sensory evaluations which highlighted higher visual properties of D red wines.

The profiling of the free and glycosidically-bound aromatic compounds revealed a more pronounced accumulation of monoterpenes in the white cultivar Tocai friulano in the season when drought occurred from early stages of development to harvest with, among all, higher accumulation of free and glycosidically-bound linalool and its oxide. This result was not confirmed by the sensory evaluations which do not highlighted higher aroma properties of D white wines. However, these compounds were found in greater amount in the glycosidically-bound fraction in its odor-inactive form. These reservoir of compounds can potentially improve, when released, the aromatic properties of the wines Interesting to note, the glycosidically-bound *cis* 8-hydroxylinalool was the highest compounds detected. On the contrary in Merlot wines, there were few free and glycosidically-bound monoterpenes detected and they were accumulated in a low amount and hence it was challenging determine the effect of water deficit of these compounds. Ou et al. (2010) reported that Merlot wines produced from vines under water deficit contained higher amounts of citronellol, nerol, geraniol, but linalool was not affected by deficit irrigation. We could not totally confirm their results because we did not detect linalool, both in the free and in glycosidically-bound volatile fraction, but we found higher concentration of *trans* 8-hydroxylinalool in both seasons and *cis* 8-hydroxylinalool in 2012. Glycosidically-bound geraniol and nerol were not affected by water deficit in our experiments and citronellol was slightly decreased by water deficit in 2011. These results are partially in agreement on what reported by Qian et al. (2009) who performed quantitative analysis of linalool, geraniol, and citronellol without detecting significant differences in these compounds in Merlot wines produced from grape under different water deficit treatments. The

different outputs on Merlot terpenes composition found in literature and in comparison to our data could be due to the low concentration of these compounds in Merlot grapes and wines. Several C_{13} norisoprenoids, which derive from the degradation of carotenoids through the activity of specific carotenoid cleavage dioxygenases, were detected only in the glycosidically-bound fraction. They are important compounds in wine greatly contributing to the aroma. Their accumulation was strongly enhanced by water deficit in both cultivars and seasons as already reported by Bindon et al. (2007). This can be due to an over-production of the carotenoid precursors under water deficit either because of an increased synthesis in response to higher sunlight bunch exposure which affects the xanthophylls cycle (Young et al., 2015) or because the carotenoid pathway is also the route of synthesis of the hormone abscisic acid which is the water stress-related hormone par excellence and its synthesis is increased upon drought. It has also been reported that water deficit can up-regulated the carotenoid cleavage dioxygenases genes (VviCCDs) in grape (Deluc et al., 2009).

Conclusion

It was hypothesized that glycosylation of secondary metabolites may have an important function in plant defense and stress tolerance maintaining metabolic homeostasis. The addition of a sugar moiety to low-molecular-weight compounds has a wide range of effects such as improving chemical stability, increasing water solubility, and reducing chemical reactivity (Vogt and Jones, 2000; Jones and Vogt, 2001). Our metabolite analyses showed that red and white cultivars have specific strategies to cope with water deficit: glycosylation of specific classes of secondary metabolites is one of them. In the red cultivars, there is a predominance of glycosylated anthocyanins while the white cultivars are enriched of glycosylated aromatic compounds. These results indicate that drought events can potentially impact the quality of red and white wines by increasing the accumulation of color and aromatic compounds in the grapes, and hence in the wine, contributing to the well appreciated visual, olfactory and gustative properties.

Material & Methods

Experimental design

The field experiment was conducted in 2011 and 2012 in a vineyard at the University of Udine's experimental farm (North-Eastern Italy) on Merlot and Tocai friulano vines. Merlot vines were covered with an ethylene-vinyl-acetate (EVA) open-sided film at the beginning of the seasons, as described in Herrera et al. (2015) while Tocai friulano vines were in the open field without any coverage. Two different irrigation treatments (fully irrigated grapevine i.e. control, C and deficit irrigated grapevine, D) were established at approximately 25 days after anthesis (DAA) and applied until harvest, as explained in the previous chapters. Each irrigation treatment was replicated on four plots arranged in a completely randomized design. Plant water status was monitored weekly by measuring Ψ_{Stem} using a Scholander pressure chamber (Herrera et al., 2015). In 2011, irrigation was supplied to Merlot D plants three times while no irrigation was supplied to Tocai friulano D plants until harvest due to abundant rainfalls occurred during the first part of the season and during the week preceding the onset of fruit ripening (Fig. S1a). In 2012, irrigation was applied four times to Merlot D vines and three times to Tocai friulano D vines in order to mitigate the severe water deficit (Fig. S1b). Vines were harvest at 115 and 106 DAA for Merlot and at 105 and 93 DAA for Tocai friulano in 2011 and 2012, respectively. Two sets of 30 berries were harvested separately from each plot and quickly brought to the laboratory. Measure of juice total soluble solids (TSS), pH and titratable acidity (TA) for Merlot and Tocai friulano berries, and analysis of anthocyanins and tannins for Merlot berries were carried on as described in Herrera et al. (2015).

Microvinification and wine analysis

Wines were produced for each of the two growing seasons with a standard microvinification protocol developed by the Viticulture and Enology Research Group at the University of Udine, Italy.

An average of 18 kg of Merlot and Tocai friulano grapes from each experimental plot were harvested manually and transported to the experimental winery of the University of Udine. Grapes from single plots were kept separately except in 2012, when the yield per plot was low and the grapes of the fourth plot were distributed among the others within the same treatment to reach the desired mass for fermentation; thus, four and three replicates for each irrigation treatment were microvinificated in 2011 and 2012, respectively.

For Merlot, eight and six independent fermentations were carried out in 2011 and 2012, respectively. Each lot was mechanically de-stemmed and crushed (Delta, Toscana Enologica Mori, Italy), transferred to a 20-L glass fermentation container, 35 mg/kg of sulfur dioxide (SO_2) were added and then inoculated with 0.2 g/L of a commercial yeast strain (Lalvin EC-1118, Lallemand Inc., Canada). Grapes and juice were fermented at 18°C for 10 days on the skins and punched down twice daily. After alcoholic fermentation, the wines were pressed and 25 mg/L of SO_2 added. Wines were racked twice, at 10 and 30 days after the end of fermentation, and then bottled in 0.5-L bottles closed with synthetic stoppers. Malolactic fermentation was not carried out.

For Tocai friulano, eight and six independent fermentations were carried out in 2011 and 2012 respectively. Each lot was mechanically de-stemmed, crushed and pressed. Solids (skins, seeds and rachis) were separated and clean must transferred to a 20-L glass fermentation container, 50 mg/L of sulfur dioxide (SO_2) added and inoculated with 0.2 g/L of a commercial yeast strain (Lalvin EC-1118, Lallemand Inc., Canada) and fermented at 18°C for 10 days. After alcoholic fermentation, the wines were racked twice, at 10 and 30 days after the end of fermentation; then 50 mg/L of SO_2 were added to wine and bottled in 0.5-L bottles closed with synthetic stoppers.

Bottles were stored at 10°C for 4 months, at which time chemical and sensory analyses were undertaken. Alcohol content, titratable acidity, pH and dry extract were determined as described in Herrera et al. (2015) for both Merlot and Tocai friulano wines. Wine color intensity (OD420nm + OD520nm), color hue (OD420nm/ OD520nm) and the concentration of anthocyanins, tannins and small and large polymeric pigments (SPP and LPP) were determined for Merlot wines by spectrophotometric analyses as described in Herrera et al. (2015).

Extraction and analysis of the wine free and glycosidically-bound volatiles

Sample preparation and extraction was performed according to Boido et al. (2003) with some modifications as reported in Vrhovsek et al. (2014). Briefly, solid phase extraction was performed using Isolute ENV+ cartridges, 1 g (Biotage, Sweden). The cartridge was pre-conditioned with 15 mL methanol followed by 20 mL of milliQ water. Fifty mL of wine, diluted with 50 mL of milli-Q water and added of 0.1 mL of internal standard n-heptanol (250 mg/L), were loaded onto the cartridge, which was then washed with 15 mL of milli-Q water to remove possible impurities. The free volatile compounds were eluted from the cartridge with 30 mL of dichloromethane; the solution was added with 60 mL of pentane, dried with sodium sulfate anhydrous (Na_2SO_4) and concentrated to 1 mL on a Vigreux column. The glycosidically-bound volatile precursors were eluted with 30 mL of methanol and evaporated to dryness by using a rotary vacuum evaporator (Rotavapor RE121, Buchi). The flasks were washed with a solution of pentane-dichloromethane (2:1 v/v) to remove any residual traces of free volatile compounds. The bound fraction was then redissolved in 4 mL of citrate buffer at pH 5; 200 μL of enzyme AR2000 (70 mg/mL) was added and tubes were kept in a 40 °C water bath at dark for 24 h. After the addition of 10 μL of internal standard (n-heptanol), the compounds were extracted three times with 2 mL of pentane/dichloromethane (2:1 v/v). The organic phase containing the free released volatiles was collected, dried with Na_2SO_4 anhydrous and then concentrated to 0.5 mL on Vigreux column. GC analysis was performed using a Trace GC Ultra gas chromatograph coupled with a TSQ Quantum Tandem mass spectrometer (Thermo Scientific) equipped with a CTC Combi-PAL autosampler (Zwingen). GC separation was performed on a 30 m VF-WAXms capillary column injecting a volume of 1 μL. Run conditions are reported in Vrhovsek et al. (2014). Data acquisition and analyses were performed using the XCalibur software. Compounds were identified by comparing the retention times of individual peaks with the retention times of their reference standards when available or by identifying the mass spectra using the NIST library with the retention index. The response of the internal standard n-heptanol was used for compounds normalization. Compounds were then expressed as μg/L of n-heptanol equivalents.

Sensory analysis

The wines were subjected to a descriptive sensory test in duplicate, as described in Herrera et al. (2015). Briefly, the panel was composed of 12 expert persons. In the first session were defined the scorecard by tasting a subset of experimental wines describing them by a series of attributes and scoring each attribute on a scale one-to-ten.
Merlot scorecard was as follow: *color intensity* and *color hue* (visual attributes); *aroma intensity*, *aroma red fruits*, *aroma jam*, *aroma spicy* and *aroma vegetal* (aroma attributes); *body*, *sapidity*, *acidity* and *bitterness* (taste attributes); *retronasal intensity*, *retronasal persistence*, *retronasal red fruits* and *retronasal vegetal* (retronasal attributes).
Tocai friulano scorecard was as follow: *color intensity* and *color hue* (visual attributes); *aroma intensity*, *aroma floral*, *aroma fruity* and *aroma vegetal* (aroma attributes); *body*, *sapidity*, *acidity* and *bitterness* (taste attributes); *retronasal intensity*, *retronasal persistence*, *retronasal fruity* and *retronasal vegetal* (retronasal attributes).
These scorecards were used in the second session. Wine samples were randomly labelled and 50 mL were served to each member of the panel. To the participants were asked to taste the wines, scoring each attribute on a 1 (low) to 10 (high) intensity scale, with the exception of the attribute '*color hue*', for which 1 represented red-brown hue and 10 red-violet hue for Merlot and for which 1 represented yellow hue and 10 green hue for Tocai friulano.

Statistical analyses

A one-way ANOVA was performed using JMP 7 (SAS Institute Inc.) to detect significant differences ($P<0.05$) between irrigation treatments in vine productivity, grape and wine composition, and sensory properties. Heatmaps representing $\log_2$ fold change ($\log_2$FC) of metabolite concentrations between treatments (D/C) were constructed using R software. Descriptive sensory test results were represented with radar charts.

Abbreviations

C: control; *CCD*: carotenoid cleavage dioxygenase; *D*: water deficit; *DAA*: days after anthesis; *GC-MS*: gas chromatography-mass spectrometry; *GT*: glycosyltransferase; *Vvi*: Vitis vinifera; Ψ_{Stem}: stem water potential.

Acknowledgement

This study was funded by the Italian Ministry of Agricultural and Forestry Policies (VIGNETO), by the Friuli-Venezia-Giulia Region (GISVI Project: "Gestione Integrata e Sostenibile Vite-Vino), the EU Cross-Border Cooperation Programme Italy-Slovenia 2007–2013 (VISO Project: Viticulture and Sustainable Development of Local Resources in the Wine Industry), the International Ph.D. Programme in the Genomics and Molecular Physiology of Fruit Plants (GMPF) of the Fondazione Edmund Mach International Research School Trentino (FEM-FIRS>T)

References

Bindon KA, Dry PR, Loveys BR (2007) Influence of plant water status on the production of C_{13}-norisoprenoid precursors in *Vitis vinifera* L. cv. Cabernet Sauvignon grape berries. J Agric Food Chem **55**: 4493–4500

Boido E, Lloret A, Medina K, Fariña L, Carrau F, Versini G, Dellacassa E (2003) Aroma composition of *Vitis vinifera* cv. Tannat: The typical red wine from Uruguay. J Agric Food Chem **51**: 5408–5413

Bönisch F, Frotscher J, Stanitzek S, Rühl E, Wüst M, Bitz O, Schwab W (2014a) Activity-based profiling of a physiologic aglycone library reveals sugar acceptor promiscuity of family 1 UDP-glucosyltransferases from grape. Plant Physiol **166**: 23–39

Bönisch F, Frotscher J, Stanitzek S, Rühl E, Wüst M, Bitz O, Schwab W (2014b) A UDP-glucose:monoterpenol glucosyltransferase adds to the chemical diversity of the grapevine metabolome. Plant Physiol **165**: 561–581

Boulton R (2001) The copigmentation of anthocyanins and its role in the color of red wine: A critical review. Am J Enol Vitic **52**: 67–87

Cabaroglu T, Selli S, Canbas A, Lepoutre J-P, Günata Z (2003) Wine flavor enhancement through the use of exogenous fungal glycosidases. Enzyme Microb Technol **33**: 581–587

Castellarin SD, Matthews MA, Di Gaspero G, Gambetta GA (2007a) Water deficits accelerate ripening and induce changes in gene expression regulating flavonoid biosynthesis in grape berries. Planta **227**: 101–112

Castellarin SD, Pfeiffer A, Sivilotti P, Degan M, Peterlunger E, Di Gaspero G (2007b) Transcriptional regulation of anthocyanin biosynthesis in ripening fruits of grapevine under seasonal water deficit. Plant Cell Environ **30**: 1381–1399

Choné X, Van Leeuwen C, Dubourdieu D, Gaudillère JP (2001) Stem water potential is a sensitive indicator of grapevine water status. Ann Bot **87**: 477–483

Darriet P, Thibon C and Dubourdieu D (2012) Aroma and aroma precursors in grape berry. In: The Biochemistry of the Grape Berry, edited by Gerós H, Chavez MM, and Delrot S. Bentham Science Publishers. pp: 111–136

Deluc LG, Quilici DR, Decendit A, Grimplet J, Wheatley MD, Schlauch KA, Mérillon J-M, Cushman JC, Cramer GR (2009) Water deficit alters differentially metabolic pathways affecting important flavor and quality traits in grape berries of Cabernet Sauvignon and Chardonnay. BMC Genomics **10**: 212

Downey MO, Dokoozlian NK, Krstic MP (2006) Cultural practice and environmental impacts on the flavonoid composition of grapes and wine: A review of recent research. Am J Enol Vitic **57**: 257–268

Downey MO, Harvey JS, Robinson SP (2004) The effect of bunch shading on berry development and flavonoid accumulation in Shiraz grapes. Aust J Grape Wine Res **10**: 55–73

Ferrandino A, Lovisolo C (2014) Abiotic stress effects on grapevine (*Vitis vinifera* L.): Focus on abscisic acid-mediated consequences on secondary metabolism and berry quality. Environ Exp Bot **103**: 138–147

Harbertson JF, Picciotto EA, Adams DO (2003) Measurement of polymeric pigments in grape berry extracts and wines using a protein precipitation assay combined with bisulfite bleaching. Am J Enol Vitic **54**: 301–306

Herrera JC, Bucchetti B, Sabbatini P, Comuzzo P, Zulini L, Vecchione A, Peterlunger E, Castellarin SD (2015) Effect of water deficit and severe shoot trimming on the composition of *Vitis vinifera* L. Merlot grapes and wines. Aust J Grape Wine Res **21**: 254–265

Hjelmeland AK, Ebeler SE (2014) Glycosidically bound volatile aroma compounds in grapes and wine: A review. Am J Enol Vitic ajev.2014.14104

Hochberg U, Degu A, Cramer GR, Rachmilevitch S, Fait A (2015) Cultivar specific metabolic changes in grapevines berry skins in relation to deficit irrigation and hydraulic behavior. Plant Physiol Biochem **88**: 42–52

Jaillon O, Aury JM, Noel B, Policriti A, Clepet C, Casagrande A, Choisne N, Aubourg S, Vitulo N, Jubin C, et al (2007) The grapevine genome sequence suggests ancestral hexaploidization in major angiosperm phyla. Nature **449**: 463–467

Jones P, Vogt T (2001) Glycosyltransferases in secondary plant metabolism: tranquilizers and stimulant controllers. Planta **213**: 164–174

Mendes-Pinto MM (2009) Carotenoid breakdown products the —norisoprenoids— in wine aroma. Arch Biochem Biophys **483**: 236–245

Ou C, Du X, Shellie K, Ross C, Qian MC (2010) Volatile compounds and sensory attributes of wine from cv. Merlot (*Vitis vinifera* L.) grown under differential levels of water deficit with or without a kaolin-based, foliar reflectant particle film. J Agric Food Chem **58**: 12890–12898

Qian MC, Fang Y, Shellie K (2009) Volatile composition of Merlot wine from different vine water status. J Agric Food Chem **57**: 7459–7463

Robinson AL, Boss PK, Solomon PS, Trengove RD, Heymann H, Ebeler SE (2014) Origins of grape and wine aroma. Part 1. Chemical components and viticultural impacts. Am J Enol Vitic **65**: 1–24

Selmar D, Kleinwächter M (2013) Stress enhances the synthesis of secondary plant products: the impact of stress-related over-reduction on the accumulation of natural products. Plant Cell Physiol **54**: 817–826

Song J, Shellie KC, Wang H, Qian MC (2012) Influence of deficit irrigation and kaolin particle film on grape composition and volatile compounds in Merlot grape (*Vitis vinifera* L.). Food Chem **134**: 841–850

Teixeira A, Eiras-Dias J, Castellarin SD, Gerós H (2013) Berry phenolics of grapevine under challenging environments. Int J Mol Sci **14**: 18711–18739

Vogt T, Jones P (2000) Glycosyltransferases in plant natural product synthesis: characterization of a supergene family. Trends Plant Sci **5**: 380–386

Vrhovsek U, Lotti C, Masuero D, Carlin S, Weingart G, Mattivi F (2014) Quantitative metabolic profiling of grape, apple and raspberry volatile compounds (VOCs) using a GC/MS/MS method. J Chromatogr B **966**: 132–139

Winterhalter P, Schreier P (1994) C_{13}-Norisoprenoid glycosides in plant tissues: An overview on their occurrence, composition and role as flavour precursors. Flavour Fragr J **9**: 281–287

Young P, Eyeghe-Bickong HA, Plessis KD, Alexandersson E, Jacobson DA, Coetzee ZA, Deloire A, Vivier MA (2015) Grapevine plasticity in response to an altered microclimate: Sauvignon Blanc modulates specific metabolites in response to increased berry exposure. Plant Physiol pp.01775.2015

Supplementary data

Table S1. Effect of water deficit on the free volatile compounds in Merlot and Tocai friulano fully irrigated (C, control) and deficit irrigated (D, water deficit) wines in 2011 and 2012. The average concentration of each compounds ± the standard error is represented as µl/L of n-heptanol equivalents. The difference between treatments was assessed with a one-way ANOVA. The level of significance is reported within the columns: *, **, *** or ns, P<0.05, P<0.01, P<0.001 or not significant, respectively

	Merlot							
Year	2011			2012				
Treatment	C		D	C		D		
Alcohols								
3-Methylthiopropanol	2204.6 ± 106.7	ns	2779.6 ± 246.7	1718.3 ± 142.9	ns	1568.2 ± 211.3		
2,3-Butanediol	511.0 ± 45.3	*	698.9 ± 55.7	1395.4 ± 121.1	ns	1931.2 ± 282.5		
Isoamyl alcohol	12937 ± 1950	ns	18393 ± 3051	12733 ± 618	ns	11388 ± 542		
2-Hexenol	12.9 ± 0.4	*	8.1 ± 1.4	8.5 ± 3.2	ns	3.5 ± 0.9		
***trans* 3-Hexanol**	15.0 ± 0.8	ns	13.7 ± 0.4	27.6 ± 2.2	ns	23.1 ± 1.4		
***cis* 3-Hexanol**	3.6 ± 0.2	*	4.6 ± 0.3	4.2 ± 0.4	ns	4.0 ± 0.3		
1-Hexanol	588.5 ± 23.9	**	772.2 ± 21.3	1232.4 ± 99.1	ns	1250.8 ± 97.4		
1-Octen-3-ol	49.0 ± 2.2	ns	40.7 ± 3.6	61.7 ± 5.4	**	26.9 ± 1.9		
Fatty acid derivatives								
Acetic acid	16.7 ± 1.6	***	42.9 ± 3.3	40.3 ± 2.2	ns	41.6 ± 8.0		
Butyric acid	303.7 ± 16.0	**	377.9 ± 7.2	352.2 ± 8.1	ns	385.7 ± 23.5		
Isobutyric acid	561.3 ± 27.6	ns	477.4 ± 31.6	1184.3 ± 49.0	**	588.4 ± 54.4		
Isovaleric acid	1830.5 ± 82.3	ns	1586.8 ± 137.6	2633.0 ± 157.9	**	1416.3 ± 139.7		
Hexanoic acid	835.0 ± 30.7	ns	915.3 ± 36.5	895.9 ± 44.1	ns	952.0 ± 68.3		
Octanoic acid	801.6 ± 42.3	ns	745.5 ± 33.4	668.6 ± 11.9	ns	802.0 ± 88.5		
Decanoic acid	87.5 ± 5.6	ns	77.1 ± 3.6	125.3 ± 7.7	ns	147.5 ± 12.3		
Esters								
Ethyl lactate	4058.2 ± 343.9	ns	6045.0 ± 1878	2284.1 ± 1233.3	ns	3100.1 ± 2059.2		
Ethyl butyrate	57.0 ± 11.2	ns	87.0 ± 5.1	53.4 ± 2.8	ns	63.7 ± 5.9		

	Tocai friulano							
Year	2011			2012				
Treatment	C		D	C		D		
Alcohols								
3-Methylthiopropanol	109.7 ± 13.8	ns	128.2 ± 22.4	88.6 ± 14.2	ns	94.6 ± 8.7		
2,3-Butanediol	1121.6 ± 52.4	ns	1046.3 ± 42.3	1948.3 ± 240.5	ns	2291.2 ± 557.1		
Isoamyl alcohol	10994 ± 1226	ns	10775 ± 1045	12665 ± 563	ns	13368 ± 2975		
2-Hexenol	--- ---		--- ---	--- ---		--- ---		
***trans* 3-Hexanol**	57.9 ± 17.1	ns	90.5 ± 15.1	91.5 ± 1.6	ns	97.7 ± 5.5		
***cis* 3-Hexanol**	24.9 ± 4.4	ns	16.2 ± 2.0	36.3 ± 10.7	ns	11.8 ± 2.4		
1-Hexanol	546.3 ± 49.3	*	707.9 ± 28.4	995.5 ± 74.3	ns	1032.1 ± 13.1		
1-Octen-3-ol	19.9 ± 3.8	ns	18.1 ± 4.9	29.5 ± 3.8	**	55.8 ± 3.4		
Fatty acid derivatives								
Acetic acid	16.4 ± 1.5	ns	13.9 ± 1.9	9.4 ± 0.7	ns	11.3 ± 0.8		
Butyric acid	649.8 ± 28.4	ns	594.3 ± 41.0	490.0 ± 46.8	ns	495.5 ± 6.2		
Isobutyric acid	167.2 ± 18.3	ns	174.8 ± 24.2	186.0 ± 26.5	ns	181.8 ± 3.5		
Isovaleric acid	290.1 ± 20.5	ns	331.4 ± 30.3	312.5 ± 21.6	ns	317.3 ± 13.8		
Hexanoic acid	3134.9 ± 190.2	ns	3035.1 ± 265.4	2179.6 ± 6.5	ns	2160.8 ± 188.1		
Octanoic acid	2972.8 ± 128.9	ns	3241.8 ± 408.2	3697.0 ± 57.8	ns	3643.8 ± 149.7		
Decanoic acid	242.9 ± 16.0	ns	249.9 ± 27.8	795.7 ± 69.0	*	1103.1 ± 57.4		
Esters								
Ethyl lactate	1230.2 ± 161.9	ns	2811.5 ± 1477.1	561.6 ± 151.0	ns	595.3 ± 74.7		
Ethyl butyrate	189.3 ± 8.9	ns	199.7 ± 14.8	286.0 ± 11.6	ns	291.0 ± 36.8		

Table S1. (continued)

	Merlot						Tocai friulano					
Year	2011			2012			2011			2012		
Treatment	C		D	C		D	C		D	C		D
Esters												
Methyl-4-hydroxybutyrate	48.6 ± 3.3	ns	44.2 ± 6.6	112.2 ± 3.0	***	56.6 ± 4.2	--- ---		--- ---	--- ---		--- ---
Ethyl 4-hydroxybutyrate	7467.3 ± 297.3	ns	6325.2 ± 1386	12978.3 ± 439.9	ns	9593.6 ± 1487.2	2019.4 ± 256.8	ns	2018.4 ± 205.0	2384.0 ± 290.0	ns	2741.9 ± 389.4
Ethyl-3-hydroxybutyrate	197.6 ± 13.0	ns	253.5 ± 24.3	124.4 ± 2.8	*	194.2 ± 20.3	378.0 ± 37.0	ns	299.1 ± 25.3	290.3 ± 19.2	*	393.7 ± 15.3
Ethyl hydrogen succinate	36100 ± 3204	*	83848 ± 17699	27700 ± 2635	ns	23206 ± 1640	21209 ± 2235	ns	23491 ± 7315	6989 ± 1257	ns	8607 ± 531
Isoamyl acetate	142.2 ± 10.1	ns	139.1 ± 13.8	196.8 ± 20.1	*	133.7 ± 4.1	995.4 ± 58.5	ns	850.9 ± 156.8	4513.5 ± 302.1	ns	5441.2 ± 636.7
Diethyl succinate	2807.7 ± 199.9	ns	8886.5 ± 2686.3	970.0 ± 32.3	ns	1198.4 ± 162.6	2141.1 ± 227.7	ns	2919.0 ± 1197.2	591.0 ± 12.3	***	871.6 ± 36.5
Diethyl malate	450.1 ± 47.6	ns	554.4 ± 138.7	123.9 ± 17.4	ns	112.8 ± 42.1	1678.7 ± 290.5	*	668.7 ± 172.4	169.0 ± 32.1	ns	123.8 ± 4.7
Hexyl acetate	9.4 ± 1.0	ns	6.1 ± 1.3	7.8 ± 0.3	ns	4.0 ± 1.6	33.6 ± 2.7	ns	32.9 ± 3.8	281.0 ± 13.8	ns	255.4 ± 29.6
Ethyl hexanoate	200.6 ± 10.7	ns	226.1 ± 12.0	193.7 ± 8.5	ns	217.6 ± 21.8	630.0 ± 11.0	ns	615.5 ± 45.0	710.0 ± 18.6	*	762.7 ± 1.3
Ethyl octanoate	164.3 ± 9.5	ns	162.9 ± 12.2	142.3 ± 7.6	ns	179.5 ± 24.6	487.8 ± 14.2	ns	487.7 ± 68.4	678.9 ± 64.1	ns	698.8 ± 17.9
Ethyl decanoate	15.7 ± 0.6	ns	12.9 ± 1.8	28.9 ± 2.4	ns	36.4 ± 5.0	20.5 ± 3.7	ns	20.8 ± 3.7	100.6 ± 17.9	ns	156.2 ± 15.4
Ethyl-2-phenyl acetate	8.0 ± 0.2	*	6.7 ± 0.5	8.8 ± 0.7	**	4.3 ± 0.4	--- ---		--- ---	--- ---		--- ---
2-Phenylethyl acetate	--- ---		--- ---	--- ---		--- ---	158.2 ± 20.4	ns	150.0 ± 14.0	599.9 ± 57.0	ns	751.3 ± 85.0
Lactones												
γ-Butyrolactone	476.3 ± 32.6	ns	551.8 ± 29.7	340.7 ± 5.7	ns	381.8 ± 42.6	142.0 ± 11.4	*	100.0 ± 3.4	64.2 ± 5.7	ns	67.4 ± 6
4-Ethoxy-γ-butyrolactone	202.2 ± 11.6	ns	265.9 ± 43.2	217.5 ± 27.5	ns	275.3 ± 25.1	71.1 ± 10.3	ns	84.2 ± 30.2	58.8 ± 0.1	ns	67.7 ± 9.0
Pantolactone	98.3 ± 2.9	ns	91.8 ± 7.8	140.1 ± 5.3	**	91.0 ± 5.0	49.3 ± 3.9	ns	59.7 ± 1.7	52.0 ± 2.0	*	44.3 ± 1.7
Ketones												
Acetoin	59.6 ± 21.5	ns	179.9 ± 98.2	63.0 ± 10.1	ns	74.4 ± 27.1	84.0 ± 13.5	ns	164.0 ± 67.4	143.3 ± 45.1	**	786.7 ± 84.2
Phenylpropanoid derivatives												
Benzyl alcohol	1507.7 ± 104.6	***	539.5 ± 80.7	1890.5 ± 199.2	**	403.2 ± 50.7	65.3 ± 14.6	*	110.4 ± 6.8	38.8 ± 8	ns	36.1 ± 3.1

Table S1. (continued)

	Merlot						Tocai friulano					
Year	2011			2012			2011			2012		
Treatment	C		D	C		D	C		D	C		D
Phenylpropanoid derivatives												
Benzaldehyde	8.0 ± 2.8	ns	4.0 ± 0.4	5.4 ± 0.5	ns	4.2 ± 0.1	13.6 ± 6.7	ns	9.8 ± 6.9	9.6 ± 2.8	ns	8.0 ± 1.2
2-Phenylethanol	59466 ± 4547	ns	68460 ± 4795	58217 ± 364	**	43482 ± 1923	20502 ± 2002	ns	22345 ± 1652	18994 ± 957	ns	22744 ± 1725
Tryptophol	3432.1 ± 334.8	ns	5654.8 ± 1376.7	3325.7 ± 189.5	**	9175.7 ± 1168.6	274.1 ± 77.0	ns	358.9 ± 85.3	153.4 ± 58.4	*	418.9 ± 54.9
Vanillin	51.2 ± 9.1	ns	45.7 ± 14.1	24.4 ± 3.8	ns	35.1 ± 1.8	11.5 ± 2.9	ns	10.6 ± 1.2	11.2 ± 0.5	ns	10.3 ± 1.2
Isovanillic acid	1665.0 ± 139.6	ns	1897.8 ± 70.7	1930.5 ± 36.7	ns	1550.1 ± 157.0	--- ---		--- ---	--- ---		--- ---
Acetovanillone	125.3 ± 7.9	**	81.2 ± 6.6	105.1 ± 1.1	***	83.7 ± 1.2	10.9 ± 1.1	ns	11.7 ± 0.6	11.6 ± 0.3	ns	11.6 ± 1.2
Tyrosol	17880 ± 2615	ns	22432 ± 2378	13975 ± 881	ns	10077 ± 1548	5589 ± 956	*	9303 ± 1095	9202 ± 1433	ns	12291 ± 1141
Guaiacol	11.8 ± 2.7	ns	17.7 ± 9.0	5.5 ± 1.2	ns	6.5 ± 0.0	--- ---		--- ---	--- ---		--- ---
4-Vinylguaiacol	19.9 ± 3.3	ns	27.5 ± 6.6	43.7 ± 8.9	ns	21.9 ± 3.4	25.7 ± 7	ns	28.4 ± 3.1	25.4 ± 2.8	ns	23.2 ± 2.5
Monoterpenes												
Linalool	5.3 ± 0.4	ns	5.0 ± 0.1	5.0 ± 0.7	ns	4.9 ± 0.4	10.7 ± 2.0	ns	11.0 ± 1.3	9.0 ± 1.9	*	33.5 ± 6.0
***trans* Linalool oxide (furanoid)**	--- ---		--- ---	--- ---		--- ---	5.5 ± 0.4	ns	7.0 ± 0.8	6.2 ± 0.9	*	12.9 ± 1.2
***cis* Linalool oxide (furanoid)**	--- ---		--- ---	--- ---		--- ---	1.8 ± 0.2	ns	3.3 ± 0.6	1.0 ± 0.2	*	1.7 ± 0.2
α-Terpineol	2.3 ± 0.2	ns	3.5 ± 0.5	2.1 ± 0.3	ns	2.4 ± 0.2	5.8 ± 0.5	ns	5.9 ± 0.8	3.5 ± 0.6	*	9.8 ± 1.3
Citronellol	16.8 ± 0.3	*	14.1 ± 0.9	22.1 ± 0.4	ns	21.9 ± 1.8	5.4 ± 0.5	*	7.3 ± 0.5	6.8 ± 1.3	ns	7.6 ± 0.8
Diendiol (I)	15.9 ± 1.9	ns	13.1 ± 1.3	22.1 ± 1.3	ns	18.6 ± 1.2	80.2 ± 19.1	ns	85.9 ± 3.5	337.5 ± 105.9	*	1153.7 ± 204.6
Geranic acid	5.6 ± 0.3	*	4.3 ± 0.3	7.6 ± 0.1	*	9.1 ± 0.5	--- ---		--- ---	--- ---		--- ---
p-Cymene	5.1 ± 0.2	*	2.4 ± 0.6	2.4 ± 1.1	ns	0.7 ± 0.1	--- ---		--- ---	--- ---		--- ---

Table S2. Effect of water deficit on the glycosidically-bound volatile compounds in Merlot and Tocai friulano fully irrigated (C, control) and deficit irrigated (D, water deficit) wines in 2011 and 2012. The average concentration of each compounds ± the standard error is represented as µl/L of n-heptanol equivalents. The difference between treatments was assessed with a one-way ANOVA. The level of significance is reported within the columns: *, **, *** or ns, P<0.05, P<0.01, P<0.001 or not significant, respectively

	Merlot						**Tocai friulano**					
Year	2011			2012			2011			2012		
Treatment	C		D	C		D	C		D	C		D
Alcohols												
2-Hexenol	32.0 ± 2.8	**	68.4 ± 8.3	12.9 ± 1.3	**	35.3 ± 2.8	--- ---		--- ---	--- ---		--- ---
***trans* 3-Hexanol**	3.9 ± 0.2	ns	4.5 ± 0.3	2.6 ± 0.2	***	5.0 ± 0.1	--- ---		--- ---	--- ---		--- ---
***cis* 3-Hexanol**	2.7 ± 0.2	**	4.3 ± 0.3	2.4 ± 0.2	**	4.4 ± 0.3	2.8 ± 0.1	ns	2.5 ± 0.4	8.5 ± 1.1	*	4.6 ± 0.2
1-Hexanol	81.4 ± 3.9	**	107.3 ± 4.9	57.3 ± 4.5	**	122.9 ± 10.5	21.3 ± 4.7	ns	21.3 ± 5.0	16.5 ± 0.5	**	34.2 ± 2.2
1-Octanol	7.0 ± 0.4	ns	8.3 ± 0.5	5.7 ± 0.2	*	8.9 ± 0.7	4.6 ± 0.6	ns	3.3 ± 0.1	4.2 ± 0.0	***	6.1 ± 0.2
Fatty acid derivatives												
Hexanoic acid	2.9 ± 0.4	ns	3.3 ± 0.2	3.2 ± 0.3	ns	4.4 ± 0.4	2.4 ± 0.4	ns	2.8 ± 0.4	2.0 ± 0.2	ns	3.0 ± 0.8
Octanoic acid	10.7 ± 0.8	***	42.1 ± 5.0	31.7 ± 4.6	ns	48.8 ± 5.0	11.6 ± 1.8	ns	8.6 ± 1.4	9.2 ± 1.5	ns	14.8 ± 3.0
Decanoic acid	8.7 ± 0.8	*	15.2 ± 1.8	17.5 ± 4.2	ns	25.8 ± 1.6	10.0 ± 1.7	ns	6.4 ± 0.8	10.0 ± 1.1	ns	15.0 ± 2.5
Palmitic acid	79.6 ± 15.9	ns	63.3 ± 7.0	112.3 ± 32.4	ns	86.3 ± 24.1	64.2 ± 19.4	ns	63.9 ± 10.0	108.0 ± 22.3	ns	101.2 ± 23.6
Phenylpropanoid derivatives												
Benzyl alcohol	3963.4 ± 259.5	***	2025.8 ± 183.0	3365.3 ± 46.7	***	1693.2 ± 42.1	229.2 ± 15.4	ns	205.0 ± 19.7	303.1 ± 8.0	ns	284.8 ± 5.4
Benzaldehyde	17.3 ± 2.4	*	9.9 ± 1.1	20.3 ± 3.8	ns	10.9 ± 1.3	1.3 ± 0.2	ns	1.3 ± 0.1	1.3 ± 0.1	ns	1.7 ± 0.2
2-Phenylethanol	581.8 ± 11.7	ns	642.7 ± 27.7	999.6 ± 39.6	ns	1239.6 ± 81.7	161.1 ± 7.3	ns	177.6 ± 20.5	229.9 ± 15.7	*	296.2 ± 7.9
Tryptophol	34.0 ± 2.6	ns	59.5 ± 12.8	47.5 ± 3.9	ns	89.6 ± 19.8	1.9 ± 0.3	ns	2.9 ± 0.5	3.4 ± 0.6	ns	10.7 ± 1.2
Vanillin	41.0 ± 6.4	ns	32.7 ± 3.9	23.0 ± 2.0	ns	18.3 ± 0.5	3.0 ± 0.5	ns	2.3 ± 0.4	3.2 ± 0.4	ns	3.8 ± 0.7
Vanillyl acetone	27.8 ± 2.6	ns	35.2 ± 6.2	21.7 ± 0.8	***	35.8 ± 0.5	1.5 ± 0.3	ns	1.7 ± 0.4	0.9 ± 0.1	ns	1.6 ± 0.4
Tyrosol	220.9 ± 61.0	ns	278.4 ± 25.6	153.9 ± 39.4	ns	206.3 ± 35.2	124.8 ± 47.6	ns	56.1 ± 13.6	70.6 ± 34.1	ns	85.8 ± 35.5
4-Vinylphenol	8.4 ± 0.5	ns	10.8 ± 1.4	6.5 ± 0.8	ns	10.8 ± 2.9	5.7 ± 0.8	ns	3.8 ± 0.4	3.9 ± 0.2	**	5.7 ± 0.2

Table S2. (continued)

	Merlot						Tocai friulano					
Year	2011			2012			2011			2012		
Treatment	C		D	C		D	C		D	C		D
Phenylpropanoid derivatives												
Guaiacol	1.7 ± 0.2	**	2.5 ± 0.1	2.4 ± 0.2	ns	2.6 ± 0.3	0.6 ± 0.1	ns	0.5 ± 0.1	0.5 ± 0.1	ns	0.6 ± 0.1
4-Vinylguaiacol	3.0 ± 0.2	*	18.3 ± 5.5	3.7 ± 0.3	*	40.2 ± 10.3	1.7 ± 0.2	ns	2.0 ± 0.1	2.0 ± 0.1	ns	2.1 ± 0.2
Eugenol	1.2 ± 0.1	ns	1.5 ± 0.2	1.2 ± 0.1	ns	1.5 ± 0.1	1.2 ± 0.1	ns	1.3 ± 0.2	2.1 ± 0.2	ns	2.2 ± 0.3
Monoterpenes												
Linalool	--- ---		--- ---	--- ---		--- ---	2.6 ± 1.2	ns	2.7 ± 0.6	12.1 ± 5.3	*	50.4 ± 12.5
***trans* Linalool oxide (furanoid)**	--- ---		--- ---	--- ---		--- ---	3.8 ± 1.0	ns	3.5 ± 0.4	12.0 ± 4.0	*	40.5 ± 5.6
***cis* Linalool oxide (furanoid)**	--- ---		--- ---	--- ---		--- ---	1.3 ± 0.1	ns	1.5 ± 0.2	1.6 ± 0.2	*	2.7 ± 0.3
***trans* Linalool oxide (pyranoid**	--- ---		--- ---	--- ---		--- ---	4.0 ± 0.3	ns	4.5 ± 0.3	6.8 ± 1.1	*	12.5 ± 1.5
***trans* 8-Hydroxylinalool**	8.3 ± 0.2	*	9.7 ± 0.5	7.1 ± 0.5	**	10.0 ± 0.3	8.9 ± 1.6	ns	7.5 ± 1.5	28.8 ± 6.9	*	86.9 ± 11.4
***cis* 8-Hydroxylinalool**	5.3 ± 0.2	***	3.2 ± 0.2	3.2 ± 0.4	*	5.1 ± 0.4	43.7 ± 12	ns	41.3 ± 13.7	190.9 ± 59.7	*	528.1 ± 46.3
Geraniol	10.4 ± 0.2	ns	10.5 ± 0.1	15.0 ± 1.0	ns	15.3 ± 0.9	10.4 ± 1.4	ns	8.1 ± 1.4	74.3 ± 3.1	ns	59.8 ± 4.6
7-Hydroxygeraniol	7.0 ± 0.5	**	9.2 ± 0.2	8.6 ± 0.4	*	12.2 ± 1.0	8.3 ± 1.2	ns	7.7 ± 1.6	32.0 ± 6.4	*	63.5 ± 4.3
Nerol	3.6 ± 0.2	ns	3.3 ± 0.1	4.4 ± 0.2	ns	4.3 ± 0.3	2.7 ± 0.5	ns	2.1 ± 0.4	12.4 ± 1.0	ns	16.5 ± 1.4
Geranic acid	5.9 ± 0.1	*	7.7 ± 0.5	7.5 ± 0.4	*	9.3 ± 0.3	0.6 ± 0.1	ns	0.6 ± 0.1	3.4 ± 0.2	*	4.4 ± 0.3
C_{13}-Norisoprenoids												
3-Hydroxy-β-damascone	94.1 ± 3.6	*	126.9 ± 10.8	99.7 ± 5.2	**	131.1 ± 3.6	70.6 ± 15.7	ns	84.5 ± 23.1	160.4 ± 17.4	*	224.3 ± 13.2
3-oxo-α-ionol	48.5 ± 0.4	*	70.4 ± 8.5	57.6 ± 3.7	**	96.8 ± 4.8	33.9 ± 8.2	ns	58.2 ± 8.2	72.5 ± 6.1	*	96.8 ± 2.5
3-Hydroxy-7,8-dihydro-β-ionol	37.3 ± 1.4	*	52.7 ± 4.7	39.8 ± 2.3	**	61.8 ± 2.6	13.7 ± 2.9	ns	16.8 ± 3.4	39.2 ± 3.0	*	51.6 ± 2.6
Vomifoliol	9.8 ± 1.2	ns	10.1 ± 0.9	8.6 ± 1.1	ns	10.4 ± 1.7	12.6 ± 4.6	ns	19.2 ± 3.6	17.4 ± 1.8	ns	22.0 ± 2.9

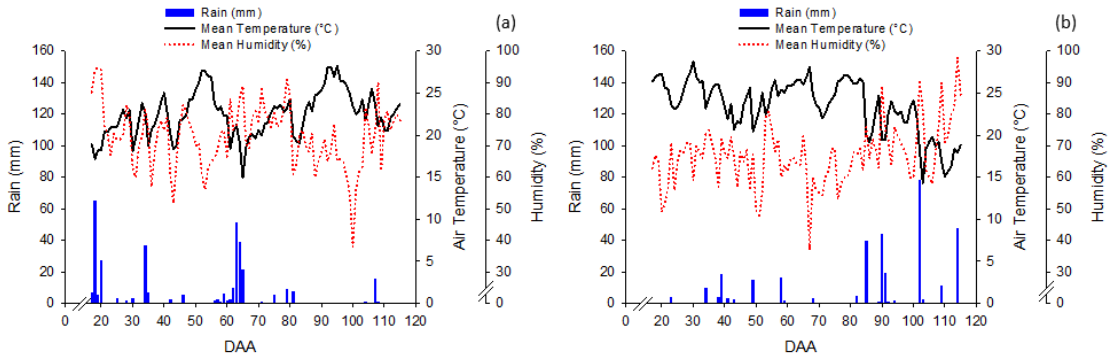

Figure S1. Weather conditions at the experimental site during the 2011 (left hand panel) and 2012 (right hand panel) season. Measurement of rain (mm), mean air temperature (°C), and mean humidity (%) were recorded by an automated weather station located 100 m from the experimental site.

Conclusion

The effect of water deficit on fruit metabolism was assessed in a white (Tocai friulano) and a red (Merlot) grape variety over two consecutive seasons (2011 and 2012) in a North-Italian viticultural area. For both varieties, two different irrigation treatments, full irrigation and deficit irrigation, were applied in an experimental vineyard and the profile of the entire transcriptome and of primary and secondary metabolites was investigated in the grapes. Transcriptome and metabolites datasets were combined with integrated network analyses.

In the white variety Tocai friulano, the transcript and metabolite analyses highlighted an up-regulation of the terpenoid pathway together with an over-production of monoterpenes such as linalool, α-terpineol, and nerol under a prolonged and severe water deficit. An integrate gene-metabolite network emphasized a higher co-regulation between terpenoid pathway genes, and monoterpenes, and a significant enrichment of drought-responsive elements in the promoter regions of such transcripts. This prompts that monoterpenes can be part of the fruit response to drought in white varieties with a possible enhanced production of these flavour components in grapes. The white wines produced from these grapes subjected to water deficit were characterized by a higher amount of monoterpenes and C_{13}-norisoprenoids, especially in the glycosidically-bound form, with a potential effect on wine composition and sensory features. However, this response was observed only in the season when the deficit started early during fruit development and not when it occurred during the last part of fruit ripening.

In the red variety Merlot, a deeper analysis over the primary and secondary metabolism highlighted an up-regulation and accumulation of osmoprotectants such as proline, sucrose, and raffinose, and secondary metabolites such as the trihydroxylated anthocyanins. Both the ABA-dependent and the ABA-independent signal transduction pathways were triggered by water deficit with several *VviAREB/ABFs*, *VvibZIP*, and *VviAP2/ERF-DREB* transcription factors up-regulated during berry ripening. A weighted gene co-expression network analysis clustered in a single module genes involved in amino acids biosynthesis, phenylpropanoid and flavonoid pathways, and sugar derivatives metabolism together with the transcription factors involved in the drought-stress signal, highlighting a possible role of these transcription factors as master regulators of the response of fruit metabolism to drought in red grapes. The red wines produced from the grapes subjected to water deficit were characterized by a higher concentration of anthocyanins, higher color intensity and bluer coloration.

Taken together, the implementation of the deficit irrigation strategies in commercial vineyards might lead to an improved quality of grapes and wines with an enhanced accumulation of aromatic compounds and pigments in white and red grape varieties, respectively. However, the deficit irrigations strategies adopted in this study also determined a significant loss of production, which, in commercial settings, might reduce the revenue of vineyards. Our study sheds new light into the metabolic mechanisms of fruit response to drought events but more studies are necessary to better understand how the timing of deficit application and the confounding effects of other seasonal components impact the plant and fruit response to these events.

Summary of PhD. experiences

This PhD. project is included in the International Ph.D. Programme in the Genomics and Molecular Physiology of Fruit Plants (GMPF) of the Fondazione Edmund Mach International Research School Trentino (FEM-FIRS>T) with partner institution the University of Udine. I was selected through an international call in June 2012 and awarded of a Ph.D. scholarship to undertake research in "Effect of genotype and environment on fruit metabolism of the grapevine" starting from September 2012. At the beginning of 2013, I was enrolled as s PhD student in the School in Agricultural Science and Biotechnology at the University of Udine.

My supervisors are Dr. Fulvio Mattivi of the Department of Food Quality and Nutrition, Research and Innovation Center, of the Fondazione Edmund Mach (San Michele all'Adige, Italy), Prof. Enrico Peterlunger of the Department of Agronomical and Environmental Sciences of the University of Udine (Italy), and Dr. Simone Diego Castellarin, previously, of the Department of Agronomical and Environmental Sciences of the University of Udine (Italy) and, currently, of the Wine Research Center at the University of British Columbia (Vancouver, Canada).

During the period of the PhD., I spent approximately one year in each institution and in addition, I have got access to several linked facilities. The field experiments were conducted at the experimental farm A. Servadei of the University of Udine. Microvinifications were done in collaboration with the Viticulture and Enology Research Group at the University of Udine. Transcriptomic analyses were performed in the laboratories at the University of Udine and at the Applied Genomics Institute (IGA) in Udine. Metabolomic analyses were carried out at the Metabolomics platform, managed by Dr. Urska Vrhovsek, at the Fondazione Edmund Mach. Primary metabolites were analyzed in cooperation with the researchers of Dr. Aaron Fait's group at the Jacob Blaustein Institutes for Desert Research (Ben-Gurion University of the Negev, Israel). Network analyses were accomplished in the laboratories of the Wine Research Center in Vancouver, Canada. Although here it is not the right place, I wish to express to all my sincere gratitude and appreciation.

During the past three years, I attended the training school on RNA-Seq data analysis held at ENSAT Toulouse (France) organized by the COST action FA1106 Quality Fruit and the national school in Analytical and Bioanalytical Techniques in Mass Spectrometry held in Parma (Italy) organized by the Società Chimica Italiana. Furthermore, I attended dedicated courses on the R environment and a summer school on bioinformatics tools for genomics and network analysis, both organized by the Fondazione Edmund Mach.

I actively participated to international and local symposia and events, such as the 3rd Ms Food Day (Trento, 2013, 9-11 October), the IX In Vino Analytica Scientia Symposium –IVAS– (Mezzocorona, 2015, 14-17 July), and the final conference of the VISO project (EU Cross-Border Cooperation Programme Italy-Slovenia 2007–2013: Viticulture and Sustainable Development of Local Resources in the Wine Industry) held in Vipava, Slovenia (March, 2015).

Thanks